University of Alberta

Peroxisome Dynamics in the Yeast *Saccharomyces cerevisiae*

By

Franco Joseph Vizeacoumar

A thesis submitted to the Faculty of Graduate Studies and Research in partial fulfillment of the requirements for the degree of Doctor of Philosophy

Department of Cell Biology

Edmonton, Alberta

Fall 2005

Library and Archives Canada

Published Heritage Branch

395 Wellington Street
Ottawa ON K1A 0N4
Canada

Bibliothèque et Archives Canada

Direction du Patrimoine de l'édition

395, rue Wellington
Ottawa ON K1A 0N4
Canada

0-494-08748-X

Your file *Votre référence*
ISBN:
Our file *Notre reference*
ISBN:

NOTICE:
The author has granted a non-exclusive license allowing Library and Archives Canada to reproduce, publish, archive, preserve, conserve, communicate to the public by telecommunication or on the Internet, loan, distribute and sell theses worldwide, for commercial or non-commercial purposes, in microform, paper, electronic and/or any other formats.

The author retains copyright ownership and moral rights in this thesis. Neither the thesis nor substantial extracts from it may be printed or otherwise reproduced without the author's permission.

AVIS:
L'auteur a accordé une licence non exclusive permettant à la Bibliothèque et Archives Canada de reproduire, publier, archiver, sauvegarder, conserver, transmettre au public par télécommunication ou par l'Internet, prêter, distribuer et vendre des thèses partout dans le monde, à des fins commerciales ou autres, sur support microforme, papier, électronique et/ou autres formats.

L'auteur conserve la propriété du droit d'auteur et des droits moraux qui protège cette thèse. Ni la thèse ni des extraits substantiels de celle-ci ne doivent être imprimés ou autrement reproduits sans son autorisation.

In compliance with the Canadian Privacy Act some supporting forms may have been removed from this thesis.

While these forms may be included in the document page count, their removal does not represent any loss of content from the thesis.

Conformément à la loi canadienne sur la protection de la vie privée, quelques formulaires secondaires ont été enlevés de cette thèse.

Bien que ces formulaires aient inclus dans la pagination, il n'y aura aucun contenu manquant.

Canada

UNIVERSITY OF ALBERTA

LIBRARY RELEASE FORM

NAME OF THE AUTHOR	:	**Franco Joseph Vizeacoumar**
TITLE OF THESIS	:	**Peroxisome Dynamics in the Yeast *Saccharomyces cerevisiae***
DEGREE	:	**Doctor of Philosophy**
YEAR THIS DEGREE GRANTED	:	**2005**

Permission is hereby granted to the University of Alberta Library to reproduce single copies of this thesis and to lend or sell such copies for private, scholarly or scientific research purposes only.

The author reserves all other publication and other rights in association with the copyright in the thesis, and except as herein before provided, neither the thesis nor any substantial portion thereof may be printed or otherwise reproduced in any material form whatever without the author's prior written permission.

Franco J. Vizeacoumar
#212, 10840, 81st Avenue,
Edmonton, Alberta,
Canada, T6E1Y4

DATE

"I can do everything through Him who gives me strength"

Philippians 4:13

TO MY DEAREST

APPA, AMMA, FREDDY and JESS

for their unwavering support and encouragement

Abstract

This thesis describes the identification and characterization of five novel *PEX* genes, namely *PEX28, PEX29, PEX30, PEX31* and *PEX32.*

The peroxins *PEX28* and *PEX29* were identified because of their high sequence similarity to Pex24p of the yeast *Y. lipolytica*. Peroxisomes of cells deleted for either or both of the *PEX28* and *PEX29* genes are increased in number, exhibit extensive clustering, are smaller in area, often exhibit membrane thickening between adjacent peroxisomes and have a decreased buoyant density compared to peroxisomes isolated from wild-type cells. Our data suggest that Pex28p and Pex29p, together with Pex11p, Pex25p and Vps1p, regulate peroxisome number, size and distribution in *S. cerevisiae*.

The peroxins *PEX30, PEX31* and *PEX32* were identified because of their high sequence similarity to Pex23p of the yeast *Y. lipolytica*. Cells deleted for *PEX30* exhibit increased numbers of peroxisomes, while cells deleted for *PEX31* and *PEX32* exhibit enlarged peroxisomes. Pex30p, Pex31p and Pex32p interact within themselves and with Pex28p and Pex29p. *PEX28* and *PEX29* function upstream of *PEX30, PEX31* and *PEX32* in the regulation of peroxisome size and number.

Additionally, we have addressed the role of Pex19p in the assembly of the PMPs, Pex30p and Pex32p. Systematic truncations from the carboxyl terminus, together with in-frame deletions of specific regions, have identified the mPTSs essential for the targeting of Pex30p and Pex32p to peroxisomes. Both Pex30p and Pex32p interact with Pex19p in regions that do not overlap with their experimentally identified mPTSs. However, Pex19p is required for localizing Pex30p and Pex32p to peroxisomes, because mutations that

disrupt the interaction of Pex30p and Pex32p with Pex19p lead to their mislocalization to a compartment other than peroxisomes.

Pex19p also interacts with the dynamin-like protein Vps1p. Mutation of one of the putative Pex19p-binding regions does not affect vacuolar assembly but leads to cells with reduced numbers of enlarged peroxisomes, the phenotype of cells lacking Vps1p. Our data suggest that the interaction of Pex30p, Pex32p and Vps1p with Pex19p is required for their roles in peroxisome biogenesis and are consistent with a role for Pex19p in stabilizing membrane proteins in peroxisomes.

Acknowledgments

First and foremost I would like to sincerely thank my supervisor, Rick Rachubinski, for giving me one of the greatest opportunities of my life. I have benefited tremendously from this opportunity and the completion of this thesis is a testament to the quality of research and leadership in his laboratory.

I would next like to thank the members of my supervisory committee, Rick Wozniak and Zhixiang Wang for their time, insights and critical comments during my program. Thanks to John Aitchison, Gary Eitzen, Richard Lehner and Andrew Simmonds for useful discussions.

I would also like to thank for the great international laboratory that Rick has assembled, over the years, the Rach team both past and present members: Juan Carlos for taking time to teach me the basic principles of Molecular Biology and Biochemistry when I joined the lab, Wanda Vreden for being a great friend and working together with me in my last two projects, Chris Tam for being a good colleague, Vladimir Titorenko and Oleh Petriv for being a great inspiration to work late nights listening to Easy Rock 104.9, Mellisa Dobson for her professional advice, Andrei and Monica Fagarasanu for making the work place filled with fun, Jean Francoise and David Bouard for making me a good teacher, Martine Approuial for all the funny jokes, Yuping Luo for the dumplings, Gareth Lambkin, Cleofe Hurtado and Roger Bascom for not scarring me away when I was new and finally to David Lancaster, Barbara Knoblach and Jenny Chang, for being new good friends.

If everything is organized and always readily available, it is because of Rick Porier. Thank you Rick, for being the same since the day one I met you and also for being

my very good friend, Elena Savidov for always willing to help with any last minute requests and for never forgetting my birthdays, Honey Chan for always willing to cut my EM sections, Dwayne Weber and Hanna Kroliczak for making the lab go smoothly and Robert Venkatraman for all his advice. Fond memories of him will always linger in our hearts.

Above all, my sincere and greatest appreciation to my brother Frederick for being my greatest strength in times of difficulties and struggles - without him, I am nothing. Freddy, I am greatly indebted to you for my whole life. My dad and mom, whose love and continuing support of my decision to pursue graduate studies, even when it took me all across the world, was an unbelievable act of selflessness. Many thanks and love to my wife Jesslet for her unwavering support and continued love since the time I knew her. They, most of all, are the reason for what I am.

Technical Acknowledgements

Many people have contributed in many ways to help me in the completion of this thesis. There are, however, certain individuals who contributed directly to this thesis through collaborative work and who are recognized below.

Invaluable assistance was provided by Dr. Juan Carlos Guzman Torres especially in constructing number of double deletion mutants and Wanda Vreden for constructing all the truncated mutants, in-frame deletions, two-hybrid analysis of the truncated mutants. Their contribution is duly recognized and mentioned under the respective illustrations. Thanks to Frederick Vizeacoumar for the PSMA software, Rick Porier for the help with Confocal microscopy and Honey Chan for assistance with electron microscopy and in preparation of ultra-thin sections.

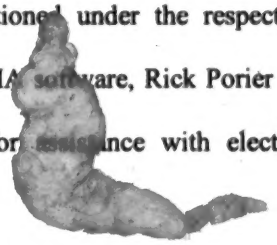

Special thanks to Elena Savidov for all the reagents and buffers, Hanna Kroliczak for instantaneous providing us with enzymes and media and Dwayne Weber for thriftly managing the laboratory requirements.

Finally I would like to thank the Alberta Heritage Foundation for Medical Research, the Faculty of Medicine and Dentistry and the Department of Cell Biology for their financial support.

TABLE OF CONTENTS

CHAPTER 1 INTRODUCTION 1

1.1 Principles of organelle biogenesis 2
1.2 Peroxisomes 3
1.2.1 Functions of Peroxisomes 4
1.2.2 Peroxisomes in Human health 5
1.3 Assembly and proliferation of peroxisomes 7
1.3.1 Endoplasmic reticulum as the template for origin 9
1.3.2 Import of matrix proteins into peroxisomes 12
1.3.3 Import of membrane proteins into peroxisomes 15
1.3.4 Regulation of peroxisomal abundance – fission and segregation 18
1.4 Experimental approaches to study peroxisome biogenesis 20
1.4.1 Yeast as a model system 20
1.4.2 Classical genetic screening 21
1.4.3 Live cell imaging 22
1.4.4 Systems biology approaches 22
1.5 Focus of this thesis 24

CHAPTER 2 EXPERIMENTAL PROCEDURES 25

2.1 Materials 26
2.1.1 List of reagents and chemicals 26
2.1.2 List of enzymes 27
2.1.3 Multicomponent systems 28
2.1.4 Plasmids 28
2.1.5 Molecular size markers 28
2.1.6 Antibodies 29
2.1.6.1 Primary antibodies *29*
2.1.6.2 Secondary antibodies *29*
2.1.7 Software used in this study 30
2.1.8 Oligonucleotides 30
2.1.9 Standard buffers and solutions 35
2.2 Microorganisms and culture conditions 36
2.2.1 Yeast strains and culture conditions 36
2.2.2 Bacterial strains and culture conditions 36
2.3 Introduction of DNA into microorganisms 42
2.3.1 Chemical transformation of *E. coli* (Heat shock) 42
2.3.2 Electroporation of *E. coli* 42
2.3.3 Chemical transformation of *S. cerevisiae* 43
2.3.4 Electroporation of *S. cerevisiae* 44
2.4 Isolation of nucleic acids 44
2.4.1 Plasmid DNA isolation from *E. coli* 44
2.4.2 Genomic DNA isolation from *S. cerevisiae* 45
2.5 Standard DNA manipulation 46
2.5.1 Amplification of DNA by the polymerase chain reaction 46
2.5.2 Restriction endonuclease digestion 46
2.5.3 Dephosphorylation and phosphorylation of 5'ends 47

2.5.4 Separation of DNA fragments and PCR products 47
2.5.5 Purification of DNA fragments from agarose gels 48
2.5.6 Purification of DNA from solution 48
2.5.7 Ligation of DNA fragments 48
2.5.8 Molecular cloning and sub-cloning by ligation 49
2.5.9 DNA sequencing 49
2.6 Analysis of Proteins 50
2.6.1 Determination of protein concentration 50
2.6.2 Electrophoretic separation of proteins 50
2.6.3 Precipitation of proteins 51
2.6.4 Detection of proteins 51
2.6.4.1 Staining with Coomassie blue staining 51
2.6.4.2 Staining with Ponceau S 52
2.6.4.3 Immunoblot analysis 52
2.7 Cell Disruption and Subcellular fractionation 53
2.7.1 Preparation of whole cell lysates 53
2.7.1.1 Glass bead lysate method 53
2.7.1.2 Magic method 54
2.7.2 Subcellular fractionation 54
2.7.3 Isolation of organelles by isopycnic centrifugation 56
2.7.4 Membrane extraction 56
2.8 Microscopy 57
2.8.1 Immunofluorescence microscopy 57
2.8.2 Staining of yeast Nucleus with Hoechst dye 58
2.8.3 Staining of yeast vacuole with FM4-64 dye 59
2.8.4 Staining of yeast mitochondria with MitoTracker Red 59
2.8.5 Electron microscopy 60
2.8.5.1 Processing of whole cells 60
2.8.5.2 Processing of purified organelles 61
2.8.6 Morphometric analysis of peroxisomes 62
2.9 Construction of plasmids 63
2.9.1 Construction of plasmids for epitope tagging 63
2.9.2 Construction of pNLS-PEX19 for nuclear targeting of Pex19p 63
2.9.3 Construction of plasmids for over expression 64
2.10 Construction of yeast-gene deletion 64
2.10.1 Mating, sporulation and tetrad dissection 65
2.10.2 Construction of double deletion mutants 66
2.10.3 Construction of triple deletion mutant 66
2.11 Epitope tagging 67
2.12 Construction of in-frame deletion mutants 67
2.12.1 Construction of *FD30* and *FD32* mutants 67
2.12.2 Construction of *S30* and *S32* mutants 68
2.12.3 Construction of *FDV1* and *FDV2* mutants 71
2.13 Oligonucleotide directed mutagenesis 72
2.14 CP-Y filter assay 73
2.15 Two-hybrid Analysis 73
2.15.1 Construction of Chimeric genes 73
2.15.2 Two-hybrid analysis 74
2.16 Computer aided analysis 74

CHAPTER 3 *PEX28* AND *PEX29* ENCODE PEROXISOMAL INTEGRAL MEMBRANE PROTEINS INVOLVED IN THE REGULATION OF PEROXISOME NUMBER, SIZE, AND DISTRIBUTION 76

3.1 Overview 77
3.2 Yhr150p and Ydr479p share extensive similarity with YlPex24p 77
3.3 Synthesis of Yhr150p and Ydr479p are not induced 78
3.4 Yhr150p and Ydr479p are integral membrane proteins 80
3.5 Abnormal peroxisomes are found in both single and double mutants of yhr150w and ydr479c 86
3.6 Overexpression of *PEX11*, *PEX25* and *VPS1* 95
3.7 Discussion 107
3.7.1 Database mining as a tool to identify novel *PEX* genes 107
3.7.2 A role for the novel genes in peroxisome biogenesis 108
3.7.3 Regulation of peroxisome division 109
3.7.4 Mechanism of peroxisome division 110

CHAPTER 4 *PEX30*, *PEX31*, AND *PEX32* ENCODE A FAMILY OF PEROXISOMAL INTEGRAL MEMBRANE PROTEINS REGULATING PEROXISOME SIZE AND NUMBER 113

4.1 Overview 114
4.2 Ylr324p, Ygr004p and Ybr168p share extensive sequence similarity with YlPex23p 114
4.3 Synthesis of Ylr324p andYbr168p are inducible 115
4.4 Ylr324p, Ybr168p and Ygr004p are integral membrane proteins 120
4.5 Ylr324p, Ygr004p and Ybr168p act to control the number and size of peroxisomes 125
4.6 Overexpression studies of *YGR004w*, *YLR324w* and *YBR168w* 131
4.7 Interacting partners of Ylr324p, Ygr004p and Ybr168p 133
4.8 *PEX28* and *PEX29* function upstream of *YLR324w*, *YGR004w* and *YBR168w* 137
4.9 Discussion 140
4.9.1 Growth and division of peroxisomes 140
4.9.2 Molecular components in division 141
4.9.3 A role for the novel genes in peroxisome biogenesis 142
4.9.4 Interaction of genes involved in the same process 144

CHAPTER 5 THE PEX19P-BINDING REGIONS OF THE PEROXINS PEX30P AND PEX32P ARE REQUIRED FOR THEIR PEROXISOMAL LOCALIZATION BUT ARE SEPARATE FROM THEIR PEROXISOMAL TARGETING SIGNALS 147

5.1 Overview 148
5.2 Identification of the region containing the targeting information in Pex30p and Pex32p 149
5.3 The region containing the 20 amino acid recidues constitute the mPTS 153
5.4 Mapping of Pex19p binding region on Pex30p and Pex32p 154
5.5 Pex19p controls the cellular distribution of Pex30p and Pex32p 157
5.6 Pex19p is essential to target PMPs to the peroxisomal compartment 161
5.7 Mapping the functional domains of Pex30p and Pex32p 166
5.8 Discussion 169
5.8.1 Role of Pex19p in membrane biogenesis 169
5.8.2 Pex30p and Pex32p are ideal candidates to study PMP targeting 169
5.8.3 m-PTS signals of Pex30p and Pex32p 170
5.8.4 Interaction of Pex19p with the PMPs 172
5.8.5 The role of Pex19p in PMP targeting 174

5.8.6 Functional domains of Pex30p and Pex32p 175
5.8.7 Factors governing targeting of PMPs 176

CHAPTER 6 THE DYNAMIN LIKE PROTEIN VPS1P ASSOCIATES WITH PEROXISOMES IN A PEX19P-DEPENDENT MANNER 178

6.1 Overview 179
6.2 Pex19p interacts with Vps1p 180
6.3 Disrupting Pex19p interaction causes *VPS1* deletion mutant phenotype 183
6.4 Vacuolar protein sorting function is normal in *FDV1* mutant 183
6.5 Effect of point mutation in Vps1p 187
6.6 Pex19p does not control the subcellular distribution of Vps1p 190
6.7 Vps1p is not recruited to the peroxisomes in a Pex19p dependent manner 190
6.8 Vps1p associates with the membrane fraction in a Pex19p-dependent manner 191
6.9 Discussion 194
6.9.1 Organelle division 194
6.9.2 Pex19p and Vps1p 195
6.9.3 Distribution of Vps1p-GFP chimera 196
6.9.4 Vps1p and membrane fission 197

CHAPTER 7 PERSPECTIVES 200

7.1 Synopsis: 201
7.2 Fusion or fission mutants? 201
7.3 Transcriptional regulation of *PEX* genes 204
7.4 Regulated division versus constitutive division 204
7.5 The enigma of peroxisomal subforms 205
7.6 Are there multiple m-PTS signals on the same PMP? 206
7.7 Can Pex19p function as a cytosolic PMP chaperone? 208
7.8 Which protein recruits Vps1p to the peroxisome? 209
7.9 How does Vps1p regulate fission? 209
7.10 Is there a dynamin independent mechanism of peroxisome fission? 210
7.11 Conclusion 211

CHAPTER 8 REFERENCES 212

LIST OF TABLES

Table 1-1	Peroxins and their functions	7
Table 2-1	Oligonucleotides used in this study	30
Table 2-2	Media components	37
Table 2-3	Antibiotics used in this study	37
Table 2-4	Strains used in this study	38
Table 3-1	Average area and numerical density of peroxisomes in wild-type and deletion strains of *PEX28* and *PEX29*	94
Table 3-2	Summary of phenotypes observed in overexpressing the genes *PEX11, PEX25, VPS1, PEX28* and *PEX29* in various deletion backgrounds	100
Table 4-1	Putative OREs in the promoter regions of the *YLR324w*, *YGR004w* and *YBR168w* genes	119
Table 4-2	Average area and numerical density of peroxisomes in cells of wild-type and mutants of PEX30 family of proteins	130
Table 5-1	A general consensus for m-PTS signal present in most PMPs.	155
Table 5-2	Putative Pex19p binding sites in Pex30p and Pex32p.	159
Table 6-1	Putative Pex19p binding regions in Vps1p	181

LIST OF FIGURES

Figure 2-1	Schematic representation of genomic integration for epitope tagging.	69
Figure 2-2	Over lapping PCR strategy.	70
Figure 3-1	Sequence alignment of *Yarrowia lipolytica* Pex24p with the proteins Yhr150p and Ydr479p encoded by the *Saccharomyces cerevisiae* genome.	79
Figure 3-2	Yhr150p-prA and Ydr479p-prA remain at constant levels during incubation of *S. cerevisiae* in oleic acid-containing medium.	81
Figure 3-3	Yhr150p-prA and Ydr479p-prA are peroxisomal proteins by microscopy.	82
Figure 3-4 A and B	Yhr150p-prA and Ydr479p-prA are primarily peroxisomal proteins.	84
Figure 3-4 C	Yhr150p-prA and Ydr479p-prA are not mitochondrial proteins by microscopy.	85
Figure 3-4 D	Yhr150p-prA and Ydr479p-prA are integral peroxisomal membrane proteins.	87
Figure 3-4 E	Growth of strains deleted for *YHR150w* and *YDR479c* on YPBO medium.	89
Figure 3-4 F	Distribution of matrix proteins in the mutants.	90
Figure 3-5	Abnormal peroxisome morphology in cells deleted for either or both of the *YHR150w* and *YDR479c* genes.	91
Figure 3-5 E	Morphometric analysis of peroxisomes.	92
Figure 3-5 F and G.	Analysis of the clustering of the peroxisomes.	93
Figure 3-6 A	Peroxisomes isolated from *yhr150Δ /ydr479Δ* cells are less dense than isolated wild-type peroxisomes and retain a clustered phenotype.	96
Figure 3-6 B	Peroxisomes isolated from *yhr150Δ /ydr479Δ* cells retain a clustered phenotype.	97
Figure 3-7	Peroxisome morphology in cells of gene overexpression strains by immunofluorescence microscopy.	98
Figure 3-8.	Peroxisome morphology in cells overexpressing *YHR150w*	101

Figure 3-9.	Peroxisome morphology in cells overexpressing *YDR479c*	102
Figure 3-10.	Peroxisome morphology in cells overexpressing *PEX11*	103
Figure 3-11.	Peroxisome morphology in cells overexpressing *PEX25*	104
Figure 3-12.	Peroxisome morphology in cells of overexpressing *VPS1*	105
Figure 3-13.	Peroxisome morphology in deletion mutants	106
Figure 4-1.	Sequence alignment of *Yarrowia lipolytica* Pex23p with the proteins Ylr324p, Ygr004p and Ybr168p encoded by the *S. cerevisiae* genome.	116
Figure 4-2.	The levels of Ylr324p-prA and Ybr168-prA, but not of Ygr004p-prA, are increased during incubation of *S. cerevisiae* in oleic acid-containing medium.	118
Figure 4-3 A	Ylr324p-prA, Ygr004p-prA and Ybr168p-prA are peroxisomal proteins by microscopy	121
Figure 4-3 B and C.	Ylr324p-prA, Ygr004p-prA and Ybr168p-prA are peroxisomal proteins by sub cellular fractionation	122
Figure 4-3. D	Ylr324p-prA, Ygr004p-prA and Ybr168p-prA are integral membrane Proteins	124
Figure 4-3. E	Growth of different strains deleted for either of or all the three genes, *YLR324w*, *YGR004w* and *YBR168w* on YPBO medium.	126
Figure 4-4.	Cells deleted for one or more of the *YLR324w*, *YGR004w* and *YBR168w* genes exhibit altered peroxisome morphology.	127
Figure 4-5.	Cells harboring deletions in one or more of the *YLR324w*, *YGR004w* and *YBR168w* genes exhibit peroxisomes that are altered in number and/or size.	128
Figure 4-5. I	Morphometric analysis of peroxisomes of oleic acid-incubated wild-type	129
Figure 4- 5. J	Abnormal morphology of peroxisomes in a double deletion mutant, *DK2* showing clustering of peroxisomes with membrane thickening	132
Figure 4-6.	Peroxisome morphology in cells overexpressing *YLR324w*	134
Figure 4-7.	Peroxisome morphology in cells overexpressing *YGr004w*	135
Figure 4-8.	Peroxisome morphology in cells overexpressing *YBR168w*	136
Figure 4-9.	Yeast two-hybrid analysis of the interaction partners of Ylr324p, Ygr004p and Ybr168p	138

Figure 4-10. Peroxisome morphology in *S. cerevisiae* cells deleted for a *YlPEX23* homolog and a *YlPEX24* homolog 139

Figure 5-1 A-D. Sub cellular fractionation of full length and truncation mutants of Pex30p and Pex32p. 151

Figure 5- 2 A-D. Confocal analysis of full length and truncation mutants of Pex30p and Pex32p 152

Figure 5-3 A and B. Identification of Pex19p-binding site in Pex30p and Pex32p. 158

Figure 5-3 C. Schematic view of Pex30p and Pex32p showing that the Pex19p binding site and the m-PTS signal are separable. 160

Figure 5-4 A and B. Sub cellular distribution of Pex30p and Pex32p in a strain expressing a form of Pex19p that gets targeted to the nucleus. 162

Figure 5-4 C. Cells expressing Pex30p-GFP+ and Pex32p-GFP+ 163

Figure 5-4 D and E Sub cellular fractionation of cells expressing protein A chimeras of Pex30p and Pex32p. 165

Figure 5-5. Peroxisome morphology in cells either deleted for *PEX30* or truncated mutants of *PEX30* exhibit peroxisomes that are altered in number and/or size. 167

Figure 5-6. Peroxisome morphology in cells either deleted for *PEX32* or truncated mutants of *PEX30* exhibit peroxisomes that are altered in number and/or size. 168

Figure 6-1. Interaction of Vps1p with Pex19p in a yeast two-hybrid assay. 182

Figure 6-2. Analysis of in-frame deletions of Vps1p by immunofluorescence microscopy (*FDV1* and *FDV2* respectively). 184

Figure 6-3 A and B. Analysis of Vacuolar morphology and protein sorting function. 186

Figure 6-4 A and B. The effect of mutating the Pex19p-binding site in vivo. 188

Figure 6-5. Peroxisome morphology in wild-type cells and Vps1p mutants. 189

Figure 6-6 A and B. Effect of Pex19p on Vps1p. 192

Figure 6-7. Sub cellular fractionation of full length, in-frame deletion mutant and the point mutant. 193

Figure 7-1. A model for protein targeting and the dynamic events that occur during the assembly of peroxisomes. 202

LIST OF SYMBOLS AND ABBREVIATIONS

20KgP	pellet obtained from centrifugation at 20,000 × *g*
20KgS	supernatant obtained from centrifugation at 20,000 × *g*
250KgP	pellet obtained from centrifugation at 250,000 × *g*
250KgS	supernatant obtained from centrifugation at 250,000 × *g*
AAA	ATPase associated with various cellular activities
AOX	acyl-CoA oxidase
ATP	adenosine triphosphate
bp	base pair
BSA	bovine serum albumin
Ca	*Candida albicans*
Cb	*Candida boidinii*
CFP	cyan fluorescent protein
CHO	chinese hamster ovary
CoA	coenzyme A
COP	coat protein
CPY	Carboxy peptidase Y
Da	Dalton
DMF	N,N-Dimethylformamide
dNTP	deoxyribonucleoside triphosphate
DsRed	*Discosoma sp.* red fluorescent protein
DTT	Dithiothreitol
ECL	enhanced chemiluminescence
EDTA	ethylene diaminetetraacetic acid
ER	endoplasmic reticulum
g	gravitational force
G6PDH	glucose-6-phosphate dehydrogenase
GFP	green fluorescent protein
Hp	*Hansenula polymorpha*
HRP	horseradish peroxidase
Hsp	heat shock protein
IgG	immunoglobulin G
IPTG	isopropyl β-D-thiogalactoside
m	Milli
M	Molar
mA	milli Ampere
Min	minute(s)
Mol	mole(s)
mPTS	Membrane protein peroxisomal targeting signal
mRFP	monomeric red fluorescent protein
mRNA	Messenger ribonucleic acid
n	Nano
NTP	Nucleoside 5'-triphosphate
OD	optical density
OD_x	optical density measure at the wavelength of x nanometers
ORF	open reading frame
p	Pico
pA	protein A
PAGE	polyacrylamide gel electrophoresis

PBD	peroxisome biogenesis disorder
PBS	phosphate-buffered saline
PCR	polymerase chain reaction
PEX#	wild-type gene encoding Pex#p
pex#	mutant *PEX#* gene
PMD	peroxisomal metabolic disorder
PMP	peroxisomal membrane protein
PNS	post-nuclear supernatant
Pp	*Pichia pastoris*
PPAR	peroxisome proliferators activated receptor
PTS	peroxisome targeting signal
RNA	Ribonucleic acid
RNase	Ribonuclease
rpm	Revolutions per minute
Sc	*Saccharomyces cerevisiae*
SDS	sodium dodecyl sulphate
TBE	tris-buffered saline plus Tween 20
TCA	Trichloroacetic acid
TE	10 mM Tris-HCl (pH 7.5), 1mM EDTA
THI	3-ketoacyl-CoA thiolase
TPR	tetratricopetide repeat
Tris	Tris(hydroxymethyl)aminoethane
U	unit of enzyme activity
X-gal	5-bromo-4-chloro-3-indolyl-β-D-galactopyranoside
YFP	yellow fluorescent protein
Yl	*Yarrowia lipolytica*
µ	Micro

CHAPTER ONE

INTRODUCTION

1.1 Principles of organelle biogenesis

Eukaryotes have evolutionarily organized various cellular processes into functionally distinct, membrane enclosed compartments called organelles. The ability to keep numerous chemical processes separate from one another in distinct organelles has permitted increased metabolic complexity and the concomitant diversification of cellular functions in eukaryotes. Hence, understanding the functionality of these organelles has increasingly become more complex, especially, as these structures are often derived from each other, share many of the same components with one another, communicate with the rest of the cell and behave dynamically. Organelle biogenesis requires at least three conceptually distinct processes: the formation of lipid bilayer, the insertion of membrane proteins into this lipid bilayer and the import of soluble proteins across the membrane into the matrix.

Most cellular proteins encoded by nuclear genes are transported to their destined organelles by certain *cis*-acting sequences that are recognized by cytosolic chaperones/receptors. On the surface of the organelles protein translocation machinery moves the protein across the membrane or inserts it into the membrane. The intricate details that occur at the surface of mitochondria (Hartl *et al.*, 1989; Schatz and Dobberstein, 1996; Schwartz and Neupert 1994; Rapaport 2003; Koehler 2004), endoplasmic reticulum (ER) (Blobel and Dobberstein, 1975; Blobel, 1980; Sabatini *et al.*, 1982; Lyman and Schekman, 1995; Haigh and Johnson, 2002; Romisch *et al.*, 2003) and the chloroplast (Robinson and Klösgen, 1994) are now well-understood. The corresponding events that occur at the peroxisomal membrane are just beginning to be

elucidated (Hettema and Tabak, 2000; Veenhuis *et al.*, 2002; Eckert and Erdmann 2003; Schliebs and Kunau, 2004). Additionally, for efficient segregation, cells must have a mechanism to ensure the growth and partitioning of these functionally intact organelles. This mechanism will help the cell to regulate the number, size, composition and distribution of organelles to meet varying cellular demands.

This chapter will focus on the molecular mechanisms involved in these processes during the biogenesis of peroxisomes.

1.2 Peroxisomes

Peroxisomes are ubiquitous organelles found in most eukaryotes. Peroxisomes, together with the glyoxysomes of plants and glycosomes of trypanosomes, make up the "microbody" family of organelles. They play diverse roles in the cell, compartmentalizing many activities related to lipid metabolism and functioning in the decomposition of toxic hydrogen peroxide. It was Rhodin in 1954, who first identified these microbodies in ultra-structural studies in mouse kidney cells. Later de Duve and colleagues coined the term "peroxisome" as they found both H_2O_2-forming oxidase and degrading catalase during their studies on rat liver (de Duve and Baudhuin, 1966). Since then, related organelles were described in plants (glyoxysomes) and in trypanosomes (glycosomes) (Breidenbach and Beevers, 1967; Opperdoes and Borst, 1977). Morphologically, peroxisomes are spherical in shape ranging from 0.1μm to 1μm in diameter, bound by a lipid bilayer membrane and are of high equilibrium density in Nycodenz (~1.23 g/cm^3) at maturation. In the filamentous fungi *Neurospora crassa,* specialized peroxisomes that contain a hexagonal crystalloid core have been described

(Jedd and Chua 2000). Unlike mitochondria, peroxisomes do not contain DNA (Kamiryo *et al.*, 1982) and all peroxisomal proteins are encoded in the nucleus.

1.2.1 Functions of Peroxisomes

Peroxisomes perform diverse metabolic roles including certain specialized roles in different organisms (reviewed in Titorenko and Rachubinski, 2001; Eckert and Erdmann, 2003). Two widely distributed and well-conserved functions are fatty acid β-oxidation and H_2O_2-based respiration. These processes appear to be ubiquitous, occurring in the peroxisomes of animals (Lazarow and de Duve, 1976), plants (Beevers *et al.*, 1969) and yeasts (Tanaka *et al.*, 1982). Additionally, in humans, peroxisomes are involved in the synthesis of ether lipids (plasmalogens) that are abundant in nervous tissue such as myelin (Hajra *et al.*, 1979; Hajra and Bishop, 1982), cholesterol and bile acid synthesis (Keller *et al.*, 1985, 1986; Krisans, 1996), and in the degradation of long chain fatty acids and phytanic acid (Mannaerts and Van Veldhoven, 1996; Olivier *et al.*, 2000). In fungi, these organelles are involved in the biosynthesis of penicillin. In higher plants, glyoxysomes house enzymes of the glyoxylate cycle, photorespiration and ureide biosynthesis (Van den Bosch *et al.*, 1992). In some yeast species, peroxisomes are involved in methanol and/or amine oxidation and assimilation (Veenhuis *et al.*, 1983). Also recent developments have shown that peroxisomes function as an intracellular signaling compartment and as an organizing platform that orchestrates certain developmental decisions from inside the cell (Titorenko and Rachubinski, 2004). Remarkably, the peroxisomal sorting of HIV Nef1 is mandatory for the life cycle of the

HIV virus and is essential for the development and manifestation of AIDS (Cohen et al., 2000).

1.2.2 Peroxisomes in Human health

Goldfisher in 1973, established the link between the absence of peroxisomes (although 'peroxisomal ghosts' were reported in later studies) and Zellweger syndrome. Later various groups reported other peroxisomal abnormalities such as increased amount of very long chained fatty acids and deficiency of plasmalogen in Zellweger patients (Brown *et al.*, 1980; Heyman *et al.*, 1983). These findings triggered intense research in the field of peroxisome biology. Rapid progress has largely depended on extensive clinical, metabolic, cellular and molecular studies in different model organisms and in patients with inborn errors of these processes. Genetic disorders of peroxisome biogenesis and function are broadly classified into Peroxisomal Biogenesis Disorders (PBDs) and Peroxisomal Metabolic Disorders (PMDs). PBDs are a genetically heterogeneous group of autosomal recessive human disorders in which peroxisomes fail to assemble properly and do not import critical matrix proteins (Lazarow and Moser, 1994; Brosius and Gärtner, 2002). PBDs comprise 12 complementation groups and are characterized by deficiency of multiple peroxisomal functions. At present, all genes responsible for each of these complementation groups have been identified. Clinically, PBDs are classified into two broad spectra namely, Zellweger spectrum (ZS) accounting for about 80% of the PBD patients and Rhizomelic chondrodysplasia punctata (RCDP).

Zellweger spectrum includes three overlapping phenotypes comprising Zellweger syndrome, neonatal adrenoleukodystrophy, and infantile Refsum disease of which

Zellweger syndrome is the most severe. They are characterized by severe neurological and hepatic dysfunction, mental retardation, craniofacial abnormalities, and hypotonia. Patients have very high levels of phytanic acid and very-long chain fatty acids in the blood and cannot synthesize plasmalogens, a very important class of phospholipids in nervous tissue (Schutgens *et al.*, 1986). Survival beyond infancy for these patients is extremely rare. Peroxisomes in the cells of this group of patients are unable to import proteins targeted by either PTS1 or PTS2 (Peroxisomal Targeting Signals), and thus most of their peroxisomal metabolic functions are impaired.

Rhizomelic chondrodysplasia punctata is characterized by severe growth defects, rhyzomelia, cataracts, proximal limb shortening and ichthyosis (Lazarow and Moser, 1995). These patients have normal blood levels of very-long chain fatty acids but have increased levels of phytanic acid and also lack plasmalogens. Unlike ZS patients, peroxisomes in the cells of RCDP patients are deficient in the import of PTS2 proteins only and have normal PTS1 import (Braverman *et al.*, 1997; Motley *et al.*, 1997; Purdue *et al.*, 1997).

Peroxisomes in cells of ZS patients were originally thought to be absent (Goldfischer *et al.*, 1973), but later studies revealed the existence of peroxisomal structures in cell lines from several patients (Santos *et al.*, 1988). In fact, studies showed that while matrix proteins containing PTS1 or PTS2 were mislocalized to the cytosol in these cell lines, peroxisomal membrane proteins (PMP) were correctly targeted. This indicates that the machinery involved in the matrix protein import is different from that of peroxisomal membrane proteins (Slawecki *et al.*, 1995; Hettema *et al.*, 2000).

PMDs do not involve a general mislocalization of peroxisomal matrix proteins. Rather, the milder symptoms associated with this class of disorder are the result of mutations in single genes which affect the function or targeting of individual peroxisomal enzymes. Examples of PMDs are X-linked adrenoleukodystrophy, acatalasaemia (catalase deficiency) and adult Refsum disease.

1.3 Assembly and proliferation of peroxisomes

Assembly and proliferation of peroxisomes are controlled by a set of proteins called *peroxins* and the genes that encode them are called *PEX* genes. During the commencement of this work, only 24 *PEX* genes were known. An update of peroxins and their characteristic functions are listed in the Table 1-1. Peroxisome biogenesis was once believed to occur similar to that of endosymbiotic mitochondria and chloroplasts. However, identification of a number of core components has greatly changed this view stressing the significance of diverse mechanisms of transport of proteins into the organelles. They differ from other organelles in that, first, unlike mitochondria, peroxisomes do not contain DNA and peroxisomal proteins are encoded by the nucleus. Second, peroxisomes can arise newly in cells that apparently lack peroxisomal remnants. Third, protein unfolding is not a prerequisite for import of matrix proteins, suggesting a novel mechanism for the translocation of oligomers across the peroxisomal membrane. Currently, understanding the mechanism of membrane biogenesis, matrix protein import and the division and segregation of mature peroxisomes from the mother cells to the daughter cells are areas of intense research.

Table 1-1 Peroxins and their characteristic features

Peroxin	Localization and function	Interaction	PBD group
Pex1p	Cytosolic and/or peripherally associated with peroxisomal membrane. Member of the AAA-ATPase family. Required for fusion of early peroxisomal precursors.	Interacts with Pex6p	1
Pex2p	Integral to peroxisomal membrane. Member of the RING-finger complex. Required for peroxisomal matrix protein import.	Interacts with Pex19p	10
Pex3p	Integral to peroxisomal membrane. Required for assembly of peroxisomal membrane.	Interacts with Pex19p.	12
Pex4p	Ubiquitin conjugating enzyme. Peripherally associated with outer face of peroxisomal membrane. Required for peroxisomal matrix protein import.	Interacts with Pex22p.	
Pex5p	Cytosolic and peroxisome-associated. PTS1 receptor. Contains TPR motifs at its carboxyl terminus.	Interacts with Pex7p, Pex8p, Pex12p, Pex13p, and Pex14p.	2
Pex6p	Cytosolic and peripherally associated with peroxisomal precursors. Member of the AAA-ATPase family. Required for fusion of early peroxisomal precursors.	Interacts with Pex1p.	4
Pex7p	Cytosolic and peroxisome-associated. PTS2 receptor. Member of WD-40 family.	Interacts with Pex5p, Pex18p, Pex20p, Pex21p Pex13p, and Pex14p.	11
Pex8p	Peroxisomal matrix and peripherally associated with inner face of peroxisomal membrane. Required for peroxisomal matrix protein import.	Interacts with Pex5p and Pex20p	
Pex9p	Integral to peroxisomal membrane. Required for peroxisomal matrix protein import.		
Pex10p	Integral to peroxisomal membrane. Member of the RING-finger complex. Required for peroxisomal matrix protein import.	Interacts with itself, Pex4p, Pex12p and Pex22p.	7
Pex11p	Peripherally associated with peroxisomal membrane. Required for peroxisome proliferation.	Interacts with itself and Pex19p.	
Pex12p	Integral to peroxisomal membrane. Member of the RING-finger complex. Required for peroxisomal matrix protein import.	Interacts with Pex5p, Pex10p, Pex13p and Pex14p.	3
Pex13p	Integral to peroxisomal membrane. Contains SH3 domain. Part of receptor docking complex. Required for peroxisomal matrix protein import.	Interacts with Pex5p, Pex7p and Pex14p.	13
Pex14p	Peripherally associated with peroxisomal membrane. Part of receptor docking complex. Required for peroxisomal matrix protein import.	Interacts with Pex5p, Pex7p, Pex13p and Pex17p	
Pex15p	Integral to peroxisomal membrane. Required for peroxisomal matrix protein import.		
Pex16p	Integral to peroxisomal membrane. Required for peroxisome proliferation and/or assembly of peroxisome membrane.		9
Pex17p	Peripherally associated with outer face of	Interacts with Pex14p.	

	peroxisomal membrane. Part of receptor docking complex. Required for peroxisomal matrix protein import.		
Pex18p	Cytosolic and peroxisome-associated. Involved in PTS2 pathway. Functionally redundant with Pex21p. Has similarity to *Y. lipolytica* Pex20p.	Interacts with Pex7p.	
Pex19p	Cytosolic and peroxisome-associated and farnesylated. Required for stability and import of numerous peroxisomal membrane proteins and/or assembly of peroxisomal membrane.	C-terminus interacts with Pex3p and the N-terminus with many PMPs	14
Pex20p	Cytosolic and peroxisome-associated. Required for thiolase oligomerization and import.	Interacts with Pex8p.	
Pex21p	Cytosolic and peroxisome-associated. Involved in PTS2 pathway. Functionally redundant with Pex18p. Has similarity to *Y. lipolytica* Pex20p.	Interacts with Pex7p.	
Pex22p	Integral to peroxisomal membrane. Required for peroxisomal matrix protein import.	Interacts with Pex4p.	
Pex23p	Integral to peroxisomal membrane. Required for peroxisomal matrix protein import. Has similarity to *S. cerevisiae* Pex30p, Pex31p and Pex32p.		
Pex24p	Integral to peroxisomal membrane. Required for peroxisomal matrix and membrane protein import.		
Pex25p	Peripherally associated with peroxisomal membrane. Required for peroxisome proliferation.	Interacts with itself and Pex27p.	
Pex26p	Integral to peroxisomal membrane.	Interacts with Pex1p and Pex6p.	8
Pex27p	Peripherally associated with peroxisomal membrane. Required for peroxisome proliferation.	Interacts with itself and Pex25p.	
Pex28p	Integral to peroxisomal membrane. Required for peroxisome separation and declustering.	Interacts with Pex32p and Pex19p	
Pex29p	Integral to peroxisomal membrane. Required for peroxisome separation and declustering.	Interacts with Pex30p and Pex19p	
Pex30p	Integral to peroxisomal membrane. Functions as a negative regulator of peroxisome number.	Interacts with itself, Rho1p, Pex29p, Pex31p, Pex32p and Pex19p.	
Pex31p	Integral to peroxisomal membrane. Functions as a negative regulator of peroxisome size.	Interacts with itself and Pex30p.	
Pex32p	Integral to peroxisomal membrane. Functions as a negative regulator of peroxisome size.	Interacts with itself and Pex30p, Pex28p and Pex19p.	

1.3.1 Endoplasmic reticulum as the template for origin

Early studies suggested that peroxisomes are formed by budding off from the endoplasmic reticulum, primarily because of studies suggesting that peroxisome membranes were spatially associated with the ER *in vivo* (Novikoff and Shin, 1964). This concept was then abandoned leading to the generally accepted growth and division model

of Lazarow and Fujiki (1985), which states that new peroxisomes arise exclusively by budding and fission of pre-existing peroxisomes. Evidence in support of this model came from the demonstration that the peroxisomal proteins were synthesized in the cytosol and then post-translationally imported into the peroxisome (reviewed in Lazarow and Fujiki, 1985). Also, studies showed that peroxisomal matrix proteins lacking PTSs were mislocalized to the cytosol and not the ER (Gould *et al.*, 1989; Elgersma *et al.*, 1996).

However, intense research has dramatically increased our knowledge in the biogenesis of peroxisomes resulting in the acceptance of the original hypothesis that peroxisomes indeed arise from the ER. Some of the major evidence for the ER origin of peroxisomes are listed here. In rat liver, the predominantly peroxisome-associated integral membrane protein PMP50 is preferentially synthesized on ER-bound ribosomes (Bodnar and Rachubinski, 1991). In *H. polymorpha*, the N -terminal portion of the peroxisomal membrane protein (PMP) Pex3p directs a fused reporter protein to the ER when overexpressed (Baraends *et al.*, 1996). Also, observations like overproduction of *H. polymorpha* PMPs Pex3p and Pex14p, *S. cerevisiae* PMP Pex15p and human PMP Pex3p leading to a profound proliferation of ER membranes, strongly suggests in a link between ER and peroxisomes (Elgersma *et al.*, 1997; Kammerer *et al.*, 1998; Komori *et al.*, 1997).

The C-terminal portion of *S. cerevisiae* Pex15p, produced at a normal level, directs a fused reporter protein to the ER, and when overproduced, accumulates in the ER and is O-mannosylated in the ER lumen (Elgersma *et al.*, 1997). Unfortunately, in most of these experiments the trafficking of the protein from the ER to the peroxisome was not tested and the protein was found in the ER only when overproduced. Some proteins like Pex3p, Pex8p and Pex14p of *H. polymorpha* and the peroxisomal ascorbate peroxidase

(pAPX) of cottonseed accumulate in the ER in brefeldin A (BFA)-treated cells and can be chased from the ER to peroxisomes after removal of BFA (Salomons *et al.*, 1997; Mullen *et al.*, 1999). Recruitment of ADP-ribosylation factor and COPI in vitro by rat liver peroxisomes requires the PMP Pex11p (Passreiter *et al.*, 1998). *S. cerevisiae* Pex15p and cottonseed pAPX post-translationally insert *in vitro*, in an ATP-and cytosolic Hsp70 chaperone-dependent manner, only into ER membranes but not into peroxisomal or any other purified organelle membrane (Mullen *et al.*, 1999). In fact, pAPX was largely detected in the sub domains of rough ER in the cells of wild type Arabidopsis (Lisenbee *et al.*, 2003).

In the yeast *Y. lipolytica*, Titorenko and co-workers have demonstrated that mutations in certain secretory genes, as well as in two *PEX* genes (*PEX1* and *PEX6*), can result in the accumulation of the PMPs Pex2p and Pex16p in the ER (Titorenko *et al.*, 1997). Specifically, mutations in sec238A and srp54, were found to result in the accumulation of coated vesicles containing, Pex2p, Pex16p, and the COPII components Sec13p and Sec23p (Titorenko and Rachubinski, 1998). Although Ben Distel and co-workers have shown that COP-I and COP-II vesicles are not necessary for targeting proteins to peroxisomes (Voorn-Brouwer *et al.*, 2001), the same group has eventually shown by three-dimensional image reconstruction of peroxisomes, that ER serves as a major source from which peroxisomal membrane is derived (Geuze *et al.*, 2003). Recently, it has been shown that Pex10p of *Arabidopsis* is localized within the sub domains of ER from where it participates in peroxisome formation (Flynn *et al.*, 2005). Taken together, these observations strongly suggest that the ER serves as a template in

peroxisome biogenesis. Yet, interestingly enough, a requirement for a known ER-protein import and export pathways, is still left to be established.

1.3.2 Import of matrix proteins into peroxisomes

Peroxisomal matrix proteins have been found to be targeted to peroxisomes by peroxisome targeting signals (PTS). PTS1 is a conserved tripeptide located at the extreme C-terminal end of a protein (Gould *et al.*, 1987, 1989). It consists of the sequence Ser-Lys-Leu or conserved variants of these residues. Most peroxisomal matrix proteins contain a PTS1 (Gould *et al.*, 1989; Aitchison *et al.*, 1991; Swinkels *et al.*, 1992; Motley *et al.*, 1995; Elgersma *et al.*, 1996). Mutants defective only in the import of PTS1 proteins led to the identification of the PTS1 receptor, Pex5p, in *P. pastoris* (McCollum *et al.*, 1993; Terlecky *et al.*, 1995). Subsequently, Pex5p was identified in several other organisms (van der Leij *et al.*, 1993; Szilard *et al.*, 1995; van der Klei *et al.*, 1995), including humans (Dodt *et al.*, 1995). All Pex5p orthologs share a region comprised of six to seven tetratricopeptide repeats (TPRs) within the C-terminal half of the protein, which binds the cargo proteins (Brocard *et al.*, 1994; Dodt *et al.*, 1995; Fransen *et al.*, 1995; Otera *et al.*, 2002). The TPR domains form two clusters hinged by TPR 4 and the PTS1 signal binds to the groove between the TPR clusters (Gatto *et al.*, 2000). Pex5p functions as a mobile receptor, shuttling between the cytosol and the peroxisomes (Dammai and Subramani, 2001). These authors demonstrated proteolytic cleavage of a Pex5p fusion protein exclusively within the peroxisomes and detected the cleaved Pex5p in the cytosol.

A second PTS, PTS2, was also identified and is a conserved N-terminal nonapeptide (Arg/Lys) (Leu/Val/Ile) Xaa_5 (His/Gln) (Leu/Ala). Although, many mammalian proteins were shown to contain this signal, *Saccharomyces* seem to have only one protein, 3-ketoacyl-CoA thiolase, which is sorted through this signal (Swinkels *et al.*, 1991; Glover *et al.*, 1994b). In the nematode *C. elegans*, the PTS2 import pathway is completely absent (Motley *et al.*, 2000; Petriv *et al.*, 2004). Mutants defective solely in the import of PTS2 proteins led to the identification of the PTS2 receptor, Pex7p, in several organisms (Marzioch *et al.*, 1994; Rehling *et al.*, 1996; Elgersma *et al.*, 1998), including humans (Braverman *et al.*, 1997). Human Pex7p deficiency causes rhizomelic chondrodysplasia punctata (Braverman *et al.*, 1997; Motley *et al.*, 1997; Purdue *et al.*, 1997). Pex7p contains six WD repeats, which bind the cargo.

Redundant proteins Pex18p and Pex21p, which are predominantly cytosolic, interact with Pex7p while it binds the cargo, facilitating the PTS2 pathway (Purdue *et al.*, 1998). In the yeast *Yarrowia lipolytica*, Pex20p seems to fulfill the task of Pex7p as well as Pex18p and Pex21p; since this organism lacks Pex7p (Complementation studies of Einwachter *et al.*, 2001). Like Pex5p, Pex7p is also proposed to function as a mobile receptor (reviewed in Purdue and Lazarow, 2001). Apart from binding their ligands, Pex5p and Pex7p, bind to the components of the docking complex, Pex13p and Pex14p (Elgersma *et al.*, 1996; Albertini *et al.*, 1997; Girzalsky *et al.*, 1999; Brocard *et al.*, 1997; Will *et al.*, 1999). The interaction of Pex5p with Pex14p is much stronger when Pex5p is loaded with cargo. In contrast, the interaction with Pex13p is stronger when Pex5p is not loaded with cargo (Urquhart *et al.*, 2000). Similarly, thiolase, a PTS2 protein, interacts with Pex14p, via Pex7p, and not with Pex13p (Stein *et al.*, 2002). These data suggest that

Pex14p acts as the initial docking site for the cargo loaded receptors, which is subsequently transported to other components of the import machinery. This is supported by observations that Pex5p is cytosolic in mammalian CHO *pex14*Δ cells, but membrane associated in *pex13*Δ cells, and that Pex5p accumulates on peroxisomal membrane when Pex14p (but not Pex13p) is overexpressed (Otera *et al.*, 2000). However, Pex13p has been reported to be required for the targeting of Pex14p, thus suggesting both Pex13p and Pex14p form the initial docking complex. Recently, Schell-Steven *et al.*, (2005) have shown that the association of Pex13p with the docking complex is essential for matrix protein import and this association is stabilized by Pex5p.

Pex5p was also found to interact with Pex2p, Pex10p and Pex12p (Chang *et al.*, 1999a; Reguenga *et al.*, 2001). The level of Pex5p on the membrane seems to be unaffected by the effect of deleting or overexpressing these peroxins (Chang *et al.*, 1999a; Okumoto *et al.*, 2000). However, a mutation in Pex12p causes an accumulation of Pex5p in the lumen of the peroxisomes (Dodt and Gould 1996). Thus, these three RING finger peroxins are suggested to play a role in translocation of peroxins.

A few peroxins such as Pex1p, Pex4p, Pex6p and Pex22p have been suggested to act after matrix protein translocation, as the steady state level of Pex5p was affected in these mutants (Collins *et al.*, 2000). Based on this, it was suggested that these peroxins are involved in later events of import, probably in the recycling of the receptor. But this idea certainly deserves deeper investigation because in *Yarrowia lipolytica,* Pex1p and Pex6p are required for the fusion of small peroxisomal vesicles (Titorenko and Rachubinski, 2000; Titorenko and Rachubinski, 2001).

Another remarkable feature of peroxisomal protein import is that folded and assembled multimeric proteins can enter the organelle (Walton *et al.*, 1992, 1995; Glover *et al.*, 1994a; McNew and Goodman, 1994; Flynn *et al.*, 1998). The oligomerization of some of these multimeric proteins is facilitated by specific chaperone molecules, as in the case of the soluble peroxisomal matrix protein thiolase and its chaperone Pex20p (Titorenko *et al.*, 1998) or is self-assisted, as in the case of the heteropentameric fatty acyl-CoA oxidase (AOX) complex of the yeast *Yarrowia lipolytica* (Titorenko *et al.*, 2002). For Aox, the association of each subunit with FAD occurs in the cytosol, prior to transportation into the peroxisomes. However, monomers of *H. polymorpha* alcohol oxidase are transported into the peroxisomes and FAD is added inside peroxisomes (Evers *et al.*, 1994, 1996; Waterham *et al.*, 1996; Stewart *et al.*, 2001). This requires specific chaperones in the lumen of the peroxisomes. It is interesting to note that, although few chaperones have been identified to be involved in peroxisome biogenesis (Preisig-Muller *et al.*, 1994; Pause *et al.*, 1997; Hettema *et al.*, 1998), only hsp70 has been localized to peroxisomes (Walton *et al.*, 1994; Corpas and Trelease, 1997; Diefenbach and Kindl, 2000).

1.3.3 Import of membrane proteins into peroxisomes

The sorting of peroxisomal membrane proteins is much less understood and appears to be independent of matrix protein import. Evidence for this came from the identification of peroxisomal ghosts, spherical membranous structures containing peroxisomal membrane proteins (Hettema *et al.*, 2000). The same study has shown that Pex3p and Pex19p are the only two peroxins that are required for membrane biogenesis

in *S. cerevisiae*. Similar results were obtained in human fibroblasts cell lines silenced for *PEX3* or *PEX19* (Matsuzono *et al.*, 1999; Shimozawa *et al.*, 2000). From these results, Pex3p and Pex19p were thought to define essential components involved in the early biogenesis of the membrane. Pex3p is an integral membrane protein with its C-terminus exposed to the cytosol. It interacts with Pex19p, a farnesylated peroxin both *in vivo* and *in vitro* (Sacksteder *et al.*, 2000; Snyder *et al.*, 1999; Gotte *et al.*, 1998).

Pex19p is mostly cytosolic with a smaller fraction of it found to be associated with the peroxisomes. It interacts with a number of peroxisomal integral membrane proteins (PMPs) (Snyder *et al.*, 1999; 2000). Shibata *et al.*, (2004) has recently shown that mammalian Pex19p interacts with Pex3p through its flexible N-terminal half while its C-terminal region is responsible for its interaction with other PMPs. The cytosolic fraction of Pex19p has been suggested to act as a shuttling receptor for peroxisomal membrane proteins, while its peroxisome-associated form could function as an assembly factor, assisting the assembly of multimeric complexes following their binding to the peroxisome membrane (reviewed in Subramani, 1998; Hettema *et al.*, 1999; Terlecky and Fransen, 2000; Subramani *et al.*, 2000; Purdue and Lazarow, 2001; Titorenko and Rachubinski, 2001; Schleibs and Kunau, 2004). However, other protein sorting mechanisms may also exist. Several peroxins undergo N- or O- linked glycosylation, suggesting that these proteins are sorted to peroxisomes via ER. This is especially true in the yeast *Yarrowia lipolytica* where, Pex2p and Pex16p are N-Glycosylated (Titorenko and Rachubinski 1998).

Recent evidence from Gould's lab suggested that Pex19p could be bifunctional acting both as a cytosolic PMP chaperone and as a PMP import receptor (Jones *et al.*,

2004). Also, the same group has shown that Pex3p acts as a docking factor for Pex19p (Fang *et al.*, 2004). When considering all the above mentioned roles of Pex19p, a number of concerns are raised. First, Pex19p's function as PMP receptor is questionable as a number of studies have shown independently that the Pex19p binding region of PMPs does not overlap with their m-PTS signal (Fransen *et al.*, 2001, 2004; Snyder *et al.*, 2000; Biermanns and Gartner 2001). Second, no convincing data has so far been obtained determining if Pex19p recognize nascent PMPs. Snyder *et al.*, (2000) showed in *Pichia pastoris* that blocking protein synthesis followed by cross linking, the amount of PMP immunoprecipitated by Pex19p remained unchanged compared to the untreated cells and have concluded that Pex19p interacts with preexisting and not with newly synthesized pool of PMPs. Also, by subcellular fractionation of the cross linked cells, they found that the steady state of interaction occurs at the peroxisome and not in the cytosol. Thirdly, Pex19p is an extremely hydrophilic protein and it is intriguing as to how it could shield the TMDs (Trans Membrane Domains) to act as a chaperone. This role also requires that Pex19p must bind at multiple regions of the PMPs. Fourth, in *Candida boidinii,* Pex19p binding to PMP47 is oleic acid induced and that in non-inducing conditions, another non-redundant mPTS targets PMP47 to peroxisomes (Wang *et al.*, 2004). Fifth, in *Yarrowia lipolytica*, Pex19p is not involved in the membrane biogenesis as Pex19p null mutants appear to contain peroxisome-like structures (Lambkin and Rachubinski 2001). Sixth, overproduction of Pex3p in a *PEX19* deletion strain results in the formation of peroxisomal protein-containing vesicles (Otzen *et al.*, 2004). Thus, understanding the exact functional role of Pex19p in membrane biogenesis certainly need extensive investigation.

1.3.4 Regulation of peroxisomal abundance – fission and segregation

Organelle division is a dynamic process that takes place once the organelle is inherited. Division is orchestrated by multi-component protein complexes that assemble and drive the constriction and fission of the organellar membranes (Osteryoung, 2001; Shaw and Nunnari, 2002). Peroxisomes are highly plastic and their size, number and shape vary dynamically based on the organism and environmental ques (Chang *et al.*, 1999b; Gould *et al.*, 2001; Purdue and Lazarow, 2001). Certain naturally occurring lipids and xenobiotics have been shown to increase peroxisome number and induce expression of genes encoding peroxisome matrix and membrane proteins (Reddy *et al.*, 1986; Reddy and Hashimoto, 2001; Zomer *et al.*, 2000). Evidence for metabolic control of peroxisome division has also been presented (Poll-The *et al.*, 1988; Sacksteder and Gould, 2000; Smith *et al.*, 2000) and might be mediated by signals derived from the ß-oxidation of fatty acids (Chang *et al.*, 1999b; van Roermund *et al.*, 2000).

An increase in peroxisome number is usually achieved by maturation and division of preexisting peroxisomes (South and Gould, 1999; Gould *et al.*, 2001). It has been suggested that peroxisomes can undergo constitutive division in the absence of a stimulator or a regulated division under induced conditions (Marshall *et al.*, 1996). But weather the components required for these different types of division are one and the same or different is not clear.

Members of the Pex11p family of peroxins, including Pex25p (Smith *et al.*, 2002) and Pex27p (Tam *et al.*, 2003; Rottensteiner *et al.*, 2003a) of *S. cerevisiae*, have been shown to affect peroxisome division in different organisms (Erdmann and Blobel, 1995; Marshall *et al.*, 1995; Sakai *et al.*, 1995; Li and Gould, 2002; Li *et al.*, 2002). In the yeast

Y. lipolytica, the membrane-bound pool of Aox interacts with Pex16p, a membrane-associated protein that negatively regulates the division of early intermediates in the assembly pathway. This interaction inhibits the negative action of Pex16p, thereby allowing mature peroxisomes to divide (Guo *et al.*, 2003; Titorenko and Rachubinski, 2004).

Another family of proteins that were thought to be involved in organelle fission are the dynamins. Dynamin and dynamin related proteins are highly conserved family of large GTPases involved in a variety of cellular processes such as endocytosis, intracellular protein trafficking and organelle partitioning (Hinshaw, 2000; Danino and Hinshaw, 2001). The yeast genome contains three genes coding for dynamin related proteins. Studies in mitochondria have demonstrated the involvement of one of the members, Dnm1p in mitochondrial fission. Dnm1p structures assemble at the outer membrane and at a rate-limiting step in the divisional pathway, mediate the division of the mitochondrial membranes (Osteryoung and Nunnari, 2003).

Recently, Hoepfner *et al.* (2002) has convincingly demonstrated that Vps1p is involved in peroxisome fission and that peroxisomes are transported via actin cables to the bud in a Myo2p-dependent process. Vps1p is more related to DLP1, a human homologue of Vps1p, than to conventional dynamins. In mammalian cells, it has been shown that peroxisome elongation and constriction can occur independently of DLP1, while the fission of peroxisomes requires it (Koch *et al.*, 2003; 2004). Pex11p has been suggested to indirectly recruit DLP1 to the peroxisomes, although the authors were unable to detect any physical interaction between these two proteins (Li and Gould 2003). Vps1p has also been suggested to regulate actin cytoskeleton structure through its

interaction with Sla1p (Yu and Cai, 2004). Sla1p is known to play an important role in the regulation of actin cytoskeleton through its interaction with several proteins capable of promoting actin assembly, such as Pan1p, Las17p, and Abp1p (Tang *et al.*, 1997; Howard *et al.*, 2002; Warren *et al.*, 2002; Gourlay *et al.*, 2003). Interestingly, *vps1Δrho1Δ* double mutants showed accumulation of actin patches on peroxisomes, which suggests that the majority of actin is reorganized/disassembled before organelle fission (Marelli *et al.*, 2004). How may Vps1p and the Pex11p family of proteins regulate the fission of peroxisomes is still unclear. Thus, as it appears molecular mechanism of peroxisome division and segregation with high fidelity, especially as it progresses through cell cycle is poorly understood.

1.4 Experimental approaches to study peroxisome biogenesis

The molecular mechanism of peroxisome assembly has been essentially conserved from yeasts to humans. Studies combining classical cell biological analyses and standardized biochemical analyses with global biology approaches such as transcriptome profiling, organellar proteomics, database mining and genomic comparative analyses, to determine novel genes, were applied in various model organisms.

1.4.1 Yeast as a model system

Easy and cost effective cultivation has made yeast an ideally suited model system for studying the mechanisms of various cellular dynamics. In the yeast cells, peroxisomes

are the only sites of fatty acid β-oxidation (Tanaka *et al.*, 1982) and induction of peroxisome proliferation occurs when the cells are grown on certain "peroxisome-requiring" carbon sources such as oleate (Veenhuis *et al.*, 1987; Kunau *et al.*, 1988) or methanol (Fukui *et al.*, 1975). Peroxisomes proliferation in yeast cells can either be accelerated by carbon sources such as oleic acid or repressed by growing on carbon sources such as glucose, which do not require the metabolizing functions of peroxisomes for conversion to a usable energy source. This remarkable quality is exploited to construct mutants, thereby facilitating the cloning of genes required for peroxisome assembly. Also, the presence of large and numerous peroxisomes facilitate their isolation for biochemical studies and morphological analysis. Many different yeast species are currently being used as model systems for peroxisome biogenesis. For our studies, we use *Saccharomyces cerevisiae* as numerous molecular tools are available to manipulate the genome.

1.4.2 Classical genetic screening

Early approaches in studying peroxisome biogenesis used yeast genetic screens to identify mutants of peroxisome assembly. Yeast cells are mutagenized in order to make *pex* mutants defective in peroxisome biogenesis that are isolated through either positive or negative selection procedures. These mutants are then rescued by transformation with a genomic library in order to complement the mutant phenotype. The complementing gene is isolated and its gene product characterized (Elgersma and Tabak, 1996). Fujiki and colleagues developed an alternative method to identify mammalian genes that depends on functional complementation of PBD-CHO cells (Peroxisome defective

Chinese Hamster Ovary) with human cDNA expression libraries. These methods have been powerful, as 32 individual *PEX* genes have been isolated to date from CHO cells (Tsukamoto *et al.*, 1990; Shimozawa *et al.*, 1992; Suzuki *et al.*, 2001) and a variety of yeast species, including *S. cerevisiae* (Erdmann *et al.*, 1989; Vizeacoumar *et al.*, 2004), *P. pastoris* (Gould *et al.*, 1992), *H. polymorpha* (Cregg *et al.*, 1990) and *Y. lipolytica* (Nuttley *et al.*, 1993).

1.4.3 Live cell imaging

One of the rapidly developing techniques to screen mutants and identify novel genes is by live cell imaging-4D microscopy. Fluorophores like GFP (Green Fluorescent Protein) and its variants, cyan fluorescent protein (CFP), yellow fluorescent protein (YFP) and *Discosoma* sp. red fluorescent protein (DsRed) are used as reporters to identify various cellular compartments (Ward *et al.*, 1998). An improved photo-stable GFP+ is also now available (Scholz *et al.*, 2000). A library of yeast strains genomically tagged with GFP has been extensively used to identify localization of over 70% of proteins (Huh *et al.*, 2003). This study has facilitated to identify a novel protein, Ymr204p, as a component involved in the inheritance of peroxisomes. Currently, further characterization of this protein is in progress in our laboratory

1.4.4 Systems biology approaches

Bioinformatics and systems biology tools have revolutionized and have greatly replaced the traditional approach of single gene analysis. Homology probing has exploited the evolutionary conservation of genes from yeast to mammals to identify

mammalian genes and genes in other organisms. *PEX28, PEX29, PEX30, PEX31* and *PEX32* were identified this way in *S. cerevisiae*. Proteomics approaches were used to identify components of the yeast protein translocation apparatus (Erdmann and Blobel, 1996). Microarray screening was used to identify oleic acid-induced yeast genes and this way, *PEX25* and its homolog *PEX27* were identified (Smith *et al*, 2002; Tam *et al*., 2004). And more recently, ICAT (isotope-coded affinity tag) coupled with mass spectrometry has revealed that the small GTPase, Rho1p to be enriched in the peroxisomal fraction. Further analysis has revealed that Rho1p is involved in peroxisome movement along actin (Marelli *et al*., 2005). Genome wide phenomics has facilitated to identify Ymr204p as a novel protein that localizes to peroxisomes. Further characterization of this protein is under progress in our laboratory. Genome wide interaction data has facilitated the identification of Ymr163p, as another component of peroxisome biogenesis that interacts with Pex19p.

1.5 Focus of this thesis

The identification of genes involved in peroxisome assembly and elucidation of the roles of the proteins they encode would provide greater understanding of the molecular bases of lethal disorders like Zellweger syndrome. Completion of the *S. cerevisiae* genome sequencing project proved invaluable in that it provides the opportunity to identify these components through sequence similarity between proteins of unknown function encoded by the *S. cerevisiae* and proteins already shown to be required for peroxisome biogenesis in other organisms. Rachubinski's laboratory has extensively used the model organism *Y. lipolytica* to identify such novel components necessary for peroxisome biogenesis. Thus taking advantage of this, I report the identification and characterization of five genes in *S. cerevisiae*, of previously unknown function and localization, now renamed *PEX28, PEX29, PEX30, PEX31*and *PEX32.* Additionally, I report on how their protein products are targeted to the peroxisomal membrane defining a role for Pex19p in this process.

CHAPTER TWO

EXPERIMENTAL PROCEDURES

2.1 Materials

2.1.1 List of reagents and chemicals

Product	Supplier
Acetone	Fisher
Acrylamide	Roche
Agar	Difco
Agarose, electrophoresis grade	Invitrogen
Agarose, Seakem GTG	FMC Bioproducts
Albumin, bovine serum (BSA) fraction V	Roche
Ammonium persulphate	BDH
Ampicillin	Sigma
Antipain dihydrochloride	Roche
Aprotinin	Roche
Benzamidine hydrochloride	Sigma
BioRad protein assay dye reagent	BioRad
Brij-35 (polyoxyethylene 23-lauryl ether)	Sigma
Chloroform	Fisher
Chymostatin	Sigma
Complete Protease inhibitor cocktail	Roche
Complete Supplement mixture (CSM)	BIO101
Coomassie Brilliant Blue (R-250)	ICN
DDSA	Marivac
D-glucose	BDH
Dithiothreitol (DTT)	Roche
Ethylene dinitro tetra acetic acid (EDTA)	Sigma
FM4-64 dye	Molecular probes
Formaldehyde, 37% (v/v)	ICN
Formamide	Fisher
Geneticin	Invitrogen
Glass Beads	Sigma
Glutaraldehyde,25%	EMS
Glycerol	BDH
Hoechst 33342 dye	Sigma
IPTG (isopropyl β-D-thiogalactopyranoside	Vector Biosystems
Isoamyl alcohol	Fisher
L-amino acids	Sigma
Leupeptin	Roche
Lithium acetate	Sigma
Magnesium sulphate	Sigma
Mitotracker CMXRos	Molecular probes
2- mercaptoethanol	BDH
2-(N-morpholino) ethane sulfonic acid (MES)	Sigma
N,N'-methylenebisacrylamide	Sigma
NAT (Nourseothricin)	Invitrogen
Nitrocellulose (Hybond-C and Transblot)	Pharmacia / BioRad

Nycodenz	BioLynx
Oleic acid	Fisher
Osmium tetroxide	EMS
p- nitrophenyl phosphate	Sigma
Pefabloc SC	Roche
Pepstatin A	Sigma
Peptone	Difco
Phenol, buffer saturated	Invitrogen
PMSF (phenylmethylsulphonylfluoride)	Roche
Poly *L*-lysine	Sigma
Ponceau S	Sigma
Potassium permanganate	Fisher
Pottasium phosphate, dibasic	EM Science
Pottasium phosphate, monobasic	EM Science
Protein A-Sepharose	Sigma
Salmon testes DNA, sodium salt	Sigma
Skimmed milk powder	Carnation
Sodium Cacodylate	Fisher
Sodium dodecyl sulfate (SDS)	Sigma
Sodium periodate	Sigma
Sorbitol	BDH
Sucrose	BDH
TAAB 812 resin	Marivac
TEMED (*N,N,N',N'*-tetramethylethylenediamine)	EM Science
Trichloroacetic acid (TCA)	BDH
Tris (Tris(hydroxymethyl)aminomethane)	Roche
Triton X-100	Sigma
Tryptone	Difco
Tween 20 (polyoxyethylene monolaurate)	Sigma
Tween 40 (polyoxyethylene sorbitan palmitate)	Sigma
Uranyl acetate	J.B. EM
Urea	ICN
X-gal (5-bromo-4-chloro-3-indolyl-B-D-galactoside)	Sigma
Yeast extract	Difco
Yeast nitrogen base without amino acids	Difco

2.1.2 List of enzymes

Enzyme	Supplier
Calf intestinal phosphatase (CIP)	NEB
DNA ligase, T4	NEB
DNA polymerase, Platinum *Pfx*	Invitrogen
DNA polymerase, T4	NEB
Restriction endonucleases	NEB / Roche / Promega
Ribonuclease A (RNase A)	Roche

Taq DNA polymerase	Roche
Zymolyase 100T	ICN

2.1.3 Multicomponent systems

Kit	Supplier
BigDye Terminator Cycle Sequencing Ready Reaction Kit	PE Applied Biosystems
DNA UltraFast Cleavage and Deprotection Kit	Beckman
ECL Western Blotting Detection Reagents	Amersham Pharmacia
Matchmaker Two-Hybrid system	Clontech
pGEM-T vector system	Promega
QIAprep Spin Miniprep Kit	QIAGEN
QIAquick Gel Extraction Kit	QIAGEN
QIAquick PCR purification Kit	QIAGEN
Random Hexanucleotide Primer Labeling Kit	Roche
Ready-To-Go-PCR Beads	Amersham
Reblot Western Blot Recycling Kit	Chemicon
Site directed mutagenesis Kit	Stratagene
West Pico-Super signal	Pierce

2.1.4 Plasmids

Plasmid	Reference
pBXA	Rout *et al.*, 2000
pDsRed-SKL	Smith *et al.*, 2002
pGEM-T	Promega
pHis5-GFP+	Dr.Rick Wozniak
pNLS-19	This study
pRS313, 314, 315	Sikorski *et al.*, 1989
Yep13	Broach *et al.*, 1979

2.1.5 Molecular size markers

Product	Supplier
1 kb DNA ladder	NEB
Prestained broad range protein Marker	NEB

2.1.6 Antibodies

2.1.6.1 Primary antibodies

Antibody	Type	Code	Dilution*	Reference
Carboxyl-terminal SKL	Rabbit	Steve#16	1:3000	Aitchison *et al.*, 1992
Rabbit antisera against mouse IgG	Rabbit	Anti-prA	1:3000	ICN
S. cerevisiae G6PDH	Rabbit	G6PDH	1:20,000	Sigma-Aldrich
S. cerevisiae MFP	Rabbit	Romeo E366#3	1:3000	This study
S. cerevisiae Pox1p	Rabbit	E261	1:5000	This study
S. cerevisiae Sdh2p	Rabbit	Sdh2	1:5000	Dibov *et al.*, 1998
S. cerevisiae CP-Y	Rabbit	CPY	1:5000	Dr.Gary Eitzen
S. cerevisiae Vps1p	Rabbit	Vps1p	1:5000	Dr.Gary Eitzen
Y. lipolytica thiolase	guinea pig	Notch-3*	1:10,000	Eitzen *et al.*, 1996

*Dilutions are for use in western blotting. Ten-fold higher concentrations are used for immunofluorescense.

2.1.6.2 Secondary antibodies

Antibody	Dilution	Supplier
Donkey anti-guinea pig-FITC conjugated	1:250	Jackson
Donkey anti-guinea pig-TRITC conjugated	1:250	Jackson
Donkey anti-rabbit-FITC conjugated	1:250	Jackson
Donkey anti-rabbit-TRITC conjugated	1:250	Jackson
Donkey anti-rabbit- HRPconjugated	1:30,000	Amersham Bioscience
Goat anti-guinea pig-HRP conjugated	1:30,000	Sigma

Secondary antibodies were either conjugated to horseradish peroxidase (HRP) for immunoblotting or to a fluorescent dye molecule (FITC (fluorescein) or TRITC (rhodamine)) for indirect immunofluorescence

2.1.7 Software used in this study

Software used	Reference
Image tools for windows, 2.0	UTHSC, Texas
Clone 3	Tulsa.org
Redasoft Visual cloning	United Bioinformatica Inc
EM analysis 3.1	Soft Imaging system
PSMA	Frederick Vizeacoumar
LSM Image browser, 3.2	Carl Zeiss
DNAstar	DNA STAR Inc.,

2.1.8 Oligonucleotides

Oligonucleotides were either synthesized on an Oligo 1000M DNA synthesizer (Beckman) or ordered from SIGMA. Oligonucleotides used in this study are described in the following table.

Table2-1 Oligonucleotides used in this study

Name	Sequence	Application
AA1293	CCAATGTTCAAGAGGAGGAGACTGATACATCGTGTTA TTAAGAATGCAACACCAGTAGCAGGTGAAGCTCAAAA ACTTAAT	*PEX28-pA* construction
AA1294	CTGTATTATTTATACTTCAAAAGCGCATTTTTGTATTTT ACCTAGTAATATTGATACATAGCTGACGGTATCGATAA G	*PEX28-pA* construction
AA1295	GACGCGGATGCATCTTATCCGTCAATCGAAGAGCTAA CAGACACTCTCAATTCAATCATAGGTGAAGCTCAAAA ACTTAAT	*PEX29-pA* construction
AA1296	CTCACTTACAAACCTTTTATCGAAAAGAAATCAAGAG AAAAAAATGGAAAAGAAGAAAAGGCTGACGGTATCG ATAAGCTT	*PEX29-pA* construction
AA1344	GTATAGTTAATAAAAAAAATTGGATTACTATTCATTGA AGAAGAGAGTTCTATACGTTCTGCTGACGGTATCGATA AGCTT	*PEX30-pA* construction
AA1343	GATACTGAAGAGAAAGAGCAATCAAATCCAACCATTG GTCGCGATAGCAAGAAGGCCGTAGGTGAAGCTCAAAA ACTTAAT	*PEX30-pA* construction
AA1342	TACAGTTCTTTGGAAAGTTTTACCAGGTCAAGAAAATG GAAACGACGCCTCTTCCATTTGGGTGAAGCTCAAAAA CTTAAT	*PEX32-pA* construction

AA1341	ATTATGAAATAACATACACAAAGTGCACATGATCTTAT AAAGTTTTACTTGTCCTATGTTGCTGACGGTATCGATA AGCTT	*PEX32-pA* construction
AA1340	AACTTGCCATAACCGCGCAGATACTTTAAAGCACAAG ATTGAATTTGTGCTCCATGCAGCGCTGACGGTATCGAT AAGCTT	*PEX31-pA* construction
AA1339	CCTTCCTCGGACAGTAGCAAATTAATACAAATATCTGA TGTTTCAATGTCTCCTTCTCTAGGTGAAGCTCAAAAAC TTAAT	*PEX31-pA* construction
AA1332	AGAATTGTTTTTATCCTTAGCTTTCCAAAAAGCTTGGT ATATATAACAAGATTTAGGGACGGTATCGATAAGCTT	*TOM20-pA* construction
AA1331	GGAGTTGTTGGAAGCAAGGCCGAATCTGATGCGGTTG CTGAAGCTAACGATATCGATGACGGTGAAGCTCAAAA ACTTAAT	*TOM20-pA* construction
0089SG	ATTCCTGCAGAGTTATGCTACTGGTGTTGCATT	pGAD424-PEX28, pGBT9-PEX28
0090SG	ATTCCTGCAGAGATGAGTGAGACCAGCTCAAGT	pGAD424-PEX28, pGBT9-PEX28
0091SG	ATTCCTGCAGAGATGGACTCGGTGACAAATTTT	pGAD424-PEX29, pGBT9-PEX29
0092SG	ATTCCTGCAGAGTTATATAGTTGAATTGAGAGT	pGAD424-PEX29, pGBT9-PEX29
0093SG	ATTCCTGCAGAGATGAGTGGTAACACAACTAAC	pGAD424-PEX30, pGBT9-PEX30
0094SG	ATTCCTGCAGAGTCATACGGCCTTCTTGCTATC	pGAD424-PEX30, pGBT9-PEX30
0095SG	ATTCCTGCAGAGATGAGCGAAATAAATAATGAA	pGAD424-PEX31, pGBT9-PEX31
0096SG	ATTCCTGCAGAGTTATAGAGAAGGAGACATTGA	pGAD424-PEX31, pGBT9-PEX31
0097SG	ATTCCTGCAGAGATGGACACAAATTCTAAAACC	pGAD424-PEX32, pGBT9-PEX32
0098SG	ATTCCTGCAGAGTTACAAATGGAAGAGGCGTCG	pGAD424-PEX32, pGBT9-PEX32
0111SG	ATTCCTGCAGAGATGGATGAGCATTTAATTTCT	pGAD424-VPS1, pGBT9-VPS1
0112SG	ATTCCTGCAGAGCTAAACAGAGGAGACGATTTG	pGAD424-VPS1, pGBT9-VPS1
0605SG	ATTCCTGCAGAGATGCCAAACATACAACACGAA	pGAD424-PEX19,

		pGBT9-PEX19
0606SG	ATTCCTGCAGAGTTATTGTTGTTTGCACCGTC	pGAD424-PEX19, pGBT9-PEX19
0628SG	ATTCCTGCAGAGTTATATCAATGAAACAATATAATAC	pGBT9-PEX32(1-124)
0629SG	ATTCCTGCAGAGTTACCAAACATTCAGCTCGTT	pGBT9-PEX32(1-159)
0630SG	ATTCCTGCAGAGTTAAAACAACCTCTTGCCAG	pGBT9-PEX32(1-179)
0631SG	ATTCCTGCAGAGTTATCTTGCTACTTTAGACC	pGBT9-PEX30(1-229)
0632SG	ATTCCTGCAGAGTTAACCAAGGTCTAAACCCG	pGBT9-PEX30(1-250)
0811SG	GTGGCAATACTACAAAAGTGCCGCGAGCTGCTTTGGAAAAG	pGBT9-PEX30(I32P)
0812SG	CTTTTCCAAAGCAGCTCGCGGCACTTTTGTAGTATTGCCAC	pGBT9-PEX30(I32P)
0813SG	GGACAGGAAAGAATATTTGGAGCAGTGTTCCGATGCTGTGTCTC	pGBT9-PEX30(L104P)
0814SG	GAGACACAGCATCGGAACACTGCTCCAAATATTCTTTCCTGTCC	pGBT9-PEX30(L104P)
0815SG	GGATGAAATTGTCGTGCTACCGGAGTCTGTGTTGGATAAACTGG	pGBT9-PEX32(L142P)
0816SG	CCAGTTTATCCAACACAGACTCCGGTAGCACGACAATTTCATCC	pGBT9-PEX32(L142P)
0817SG	CCTACGAATGAGTTTCCGGTCGATATCATCAAAGCTGAACAAAC	pGBT9-VPS1(V516P)
0818SG	GTTTGTTCAGCTTTGATGATATCGACCGGAAACTCATTCGTAGG	pGBT9-VPS1(V516P)
0146SG	ATTGCATGCTCTTCATCAAGCCCTGGAGATACTAACAGC	YEp-PEX29
0147SG	ATTGCATGCTGTATCCAGGTTAATTGCTTGAATTGTGAAAAG	YEp-PEX29
0148SG	ATTGCATGCACGGTGGAAACAGGTCCAGTAATACCA	YEp-VPS1
0149SG	ATTGCATGCGCAGAATCAATCAATACAATGAATAGTACC	YEp-VPS1
MG0212	ATTGGATCCACCGCTCATGTTCAGTACCAGCTC	YEp-PEX30
MG0213	ATTGGATCCAGGAATGATCGGAGTGTTATCATA	YEp-PEX30
MG0214	ATTGGATCCAGAATACATCCAGAGAAACGCAGA	YEp-PEX31
MG0215	ATTGGATCCTATCTGTACATATGTATTTAGATG	YEp-PEX31
MG0216	ATTGGATCCGTAGACTTAACGAAAATTGTTGTG	YEp-PEX32
0217QC	ATTGGATCCATTGGCTGAGCAAAGAAGGGCACG	YEp-PEX32
0105SG	ATTGGATCCTCGATATGGATAAAGACAAGGCCTG	YEp-PEX28
0106SG	ATTGGATCCTACTGTGTATTGTCGTTTACTT	YEp-PEX28

0075SG	ATTGGATCCAGCTCACTAACGACATTGGCCAGT	YEp-PEX11
0076SG	ATTGGATCCTAACTATTCCTTCCTAATCCTCT	YEp-PEX11
0804SG	ATTGGATCCGGACCCATCAGCTTTCTT	YEp-PEX19
0805SG	ATTGGATCCCTATTGAAGAGAGGTGAA	YEp-PEX19
0369SG	ACATTAGAAGATATTGCTCTCTTAATGAACAGAGTATC CTTGAAGTCAGATATTTTGCTCGGTGAAGCTCAAAAAC TTAAT	Pex30(1-170aa) construction
0370SG	CAGAAGCAAGTGAAAAAGTTGGCATCAACAGAAAAC AGTAATGGCGTATTATCCGATTCCGGTGAAGCTCAAA AACTTAAT	Pex30(1-282aa) construction
0371SG	GGTGCCATTCAAGTGCCCAATTCAAAGGCAAGAACTT CCGCAGATCCCTCCCCTGACGAGGGTGAAGCTCAAAA ACTTAAT	Pex30(1-374aa) construction
0375SG	GCTTCGTTAAGAGACACGGAACCTCCTACATTGGAGA AATTGTCGTGCTACTAGAGTCTGGTGAAGCTCAAAAA CTTAAT	Pex32(1-144aa) construction
0376SG	TTATTCGGTACAATTTTTCAAATTATTATCATGAGATA CATATCACCGGGAACTTATACTGGTGAAGCTCAAAAA CTTAAT	Pex32(1-203aa) construction
0377SG	CATATTCTACAGCTTCTACTTAATGAGCAAAAAGATAA CTTTGGTAATGAAGACCTTAAAGGTGAAGCTCAAAAA CTTAAT	Pex32(1-307aa) construction
0493SG	GTGCTACTAGAGTCTGTGTTGGATAAACTGGAAGTACT GAGAAACGAGCTGAATGTTTGGGGTGAAGCTCAAAAA CTTAAT	Pex32(1-159aa) construction
0494SG	AAATTAAAGCTTTCATTTGATGGCGTCAATAAGGAGTG TTCTGGCAAGAGGTGTTTGGTGAAGCTCAAAAACTTA AT	Pex32(1-179aa) construction
0507SG	GTTGCAATTTAGGATTCGAGCTGTCTAGTTGATCCTCC GGAGTGTAAAAACTGATTTTCAATGAGGCTTTTATGGA AGTTTAAG	*S30* construction
0508SG	GAAAAGTTCTTCTCCTTTGCTAGCCATACCAAGGTCTA AACCCGTGAC	*S30* construction
0509SG	TTCTACGTCACGGGTTTAGACCTTGGTATGGCTAGCAA AGGAGAAGAA	*S30* construction
0557SG	TTCTTTCATTGATCTTAATTTAGTTCAGTGGACATCATT TTGCTAATTTCAAGGAAAGAAATGAAAAAATTAAAGC TTTCATTTGAT	*S32* construction
0558SG	GAAAAGTTCTTCTCCTTTGCTAGCCATAAACAACCTCT TGCCAGAACAC	*S32* construction
0559SG	AAGGAGTGTTCTGGCAAGAGGTTGTTTATGGCTAGCA AAGGAGAAGAA	*S32* construction
0590SG	CCCTGGTCCTTATTTATTCCTCTTGCTACTTTAGACCAT G	*FD30* construction

0591SG	GGAATAAATAAGGACCAGGG	*FD30* construction
0592SG	CCGAATAAGAATAATCTGCACCAAACATTCAGCTCGTTTC	*FD32* construction
0593SG	TGCAGATTATTCTTATTCGG	*FD32* construction
0819SG	ATTGAATTCATGCCAAACATACAACAC	19-NLS-GFP construct
0820SG	ATTGAATTCTTGTTGTTTGCAACCGTC	19-NLS-GFP construct
0821SG	ATTGAGCTCTTGTTGTTTGCAACCGTC	PEX19-NLS construction
0826SG	ATTGAGCTCTTATTGTTGTTTGCAACCGTC	PEX19-NLS construction
0912SG	ATGAGTGGTAACACAACT	*P30-L104P-prA* and *P30-L104P-GFP+* construction
0913SG	TACGGCCTTCTTGCTATC	*P30-L104P-prA* and *P30-L104P-GFP+* construction
0914SG	ATGGACACAAATTCTAAA	*P32-L142P-prA* and *P32-L142P-GFP+* construction
0915SG	CAAATGGAAGAGGCGTCG	*P32-L142P-prA* and *P32-L142P-GFP+* construction
0669SG	CAAACTTACATCAATACAGCC	*VPS1(Δ509-523aa)* Construction
0670SG	AGGTATCCTGCTCTAAGAGAAGCGATTTCTAATCAGTTCATTCAGTTCTTAAAGGATGCTCAAACTTACATCAATACAGCC	*VPS1(Δ509-523aa)* Construction
0671SG	CTAACGCCGCCATCCAGTCTAAACAGGGAGACGATTT	*VPS1(Δ509-523aa)* and *VPS1(Δ633-647aa)* Construction
0672SG	AAATCGTCTCCTCTGTTTAGACTGGATGGCGGCGT	*VPS1(Δ509-523aa)* and *VPS1(Δ633-647aa)* Construction
0673SG	TTGATTGTGAAAAGTAAAACTG	*VPS1(Δ633-647aa)* Construction
0674SG	AGGGAAACAATGGAAACAGAAGTAATCAAGTTGTTGATTAGTAGTTATTTCTCTATTGTCTTGATTGTGAAAAGTAAAACT	*VPS1(Δ633-647aa)* Construction

2.1.9 Standard buffers and solutions

Solution	Composition	Reference
Breakage buffer	2% (v/v) Triton X-100, 1% SDS, 100 mM NaCl, 10 mM Tris-HCl, pH 8.0, 1 mM EDTA, pH 8.0	Ausubel *et al.*, 1989
Buffer H	0.6 M sorbitol, 5 mM MES, pH 6.0 and 1 mM EDTA	Smith *et al.*, 2002
Coomassie Blue stain solution	0.25% R-250 dye, 45% (v/v) methanol, 10% (v/v) acetic acid	Maniatis *et al.*, 1982
Disruption buffer	20 mM Tris-HCl, pH 7.5, 0.1 mM EDTA, pH 7.5, 100 mM KCl, 10% (w/v) glycerol	Eitzen, 1997
Magic A	1M unbuffered Tris and 13% SDS	This study
Magic B	30% (w/v) Glycerol, 0.25% Bromophenol blue, 200mM DTT	This study
Mounting media	0.4% *N*-propyl gallate, 74.8% (w/v) glycerol in 1 × PBS, pH 7.4	Maniatis *et al.*, 1982
Perforation buffer	10 mM DTT, 100 mM Tris-HCl, pH 9.4	Smith *et al.*, 2002
Ponceau stain	0.1% Ponceau S, 1% TCA	Szilard, 2000
Solution B	100 mM KH_2PO_4, 100 mM K_2HPO_4, 1.2 M sorbitol	Pringle *et al.*, 1991
TE	10 mM Tris-HCl, pH 7.0-8.0 (as needed), 1 mM EDTA	Maniatis *et al.*, 1982
Transformation buffer	10% of 1M Lithium acetate, 200mM DTT (freshly added) in TE buffer	This study
Zymolyase buffer	50 mM potassium phosphate, pH 7.5, 1.2 M sorbitol, 1mM EDTA	Smith *et al.*, 2002
1 × PBS	137mM NaCl, 2.7 mM KCl, 8 mM Na_2HPO_4, 1.5 mM K_2HPO_4, pH 7.3	Pringle *et al.*, 1991
1 × protease inhibitor (PIN) cocktail	1 µg/ml each of antipain, aprotinin, leupeptin, pepstatin, 0.5 mM benzamidine hydrochloride, 5 mM NaF, 1 mM PMSF or 0.5 mg Pefabloc SC	Smith, 2000
1 × TBST	20 mM Tris-HCl,150 mM NaCl, 0.05% (w/v) Tween 20	Huynh *et al.*, 1988

1 × Transfer buffer	20 mM Tris-HCl, 150 mM glycine, 20% (v/v) methanol	Towbin *et al.*, 1979; Burnette, 1981
2× sample buffer	20% (v/v) glycerol, 167 mM Tris-HCl ,pH 6.8, 2% SDS, 0.005% bromophenol blue	Ausubel *et al.*, 1989
5 × SDS-PAGE running buffer	0.25 M Tris-HCl, pH 8.8, 2 M glycine, 0.5% SDS	Ausubel *et al.*, 1989
6 × DNA loading dye	0.25% bromophenol blue, 0.25% xylene cyanol, 30% (v/v) glycerol	Maniatis *et al.*, 1982
10 × TBE	0.89 M Tris-borate, 0.89 M boric acid, 0.02 M EDTA	Maniatis *et al.*, 1982

2.2 Microorganisms and culture conditions

2.2.1 Yeast strains and culture conditions

The yeast strains and media components used in this study are listed in Table 2-4 and Table 2-2, respectively. All strains were cultured at 30°C as 10 ml cultures in glass tubes in a rotating wheel. For subcellular fractionation and similar experiments requiring large quantity of cells, cells were grown in flasks in a rotary shaker at 180 rpm. For all experiments, an overnight culture was subcultured so that cells grew to an OD_{600} of 0.75.

2.2.2 Bacterial strains and culture conditions

E. coli strains and culture media used in this study are described in Tables 2-2 and 2-1, respectively. Bacteria were grown at 37°C unless stated otherwise. Cultures of 5 ml or less were grown in culture tubes in a rotary shaker at ~180 rpm. Cultures greater than 5 ml were grown in flasks in a rotary shaker at 250 rpm. Culture volumes were approximately 20% of flask volumes.

Table 2-2 Media components

Medium	Composition	Reference
LB	1% tryptone, 0.5% yeast extract, 1% NaCl	Maniatis *et al.*, 1982
SOB	2% tryptone, 0.5% yeast extract, 10 mM NaCl, 2.5 mM KCl	Maniatis *et al.*, 1982
TYP	1.6% tryptone, 1.6% yeast extract, 0.5% NaCl, 0.25% K_2HPO_4	Promega Protocols and Applications Guide, 1989/1990
SCIM	0.67% YNB, 0.5% yeast extract, 0.5% peptone, 0.5% Tween (w/v) 40, 0.1% glucose, 0.15% (v/v) oleic acid, 1 × CSM	Erdmann *et al.*, 1989
Sporulation medium	1% potassium acetate, 0.1% yeast extract, 0.05% glucose	Rose *et al.*, 1988
CSM	0.67% YNB, 2% glucose, 1× CSM without histidine and/or leucine	Bio101
YEPA	1% yeast extract, 2% peptone, 2% sodium acetate	Brade, 1992
YEPD	1% yeast extract, 2% peptone, 2% glucose	Rose *et al.*, 1988
YNA	0.67% YNB, 2% sodium acetate	Brade, 1992
YND	0.67% YNB, 2% glucose	Rose *et al.*, 1988
YNO	0.67% YNB, 0.05% (w/v) Tween 40, 0.1% (v/v) oleic acid	Nuttley *et al.*, 1993
YPBO	0.3% yeast extract, 0.5% peptone, 0.5% K_2HPO_4, 0.5% KH_2PO_4, 0.2% (w/v) Tween 40 or 1% (v/v) Brij 35, 1% (v/v) oleic acid	Kamiryo *et al.*, 1982

Table 2- 3 Antibiotics used in this study

Antibiotic	Mechanism of Action	Working conc.
Ampicillin	Inhibits cell wall synthesis by inhibiting the formation of peptidoglycan cross-links	20-100 μg/ml
Kanamycin	Causes misreading of mRNA by binding to the 70S ribosome	10-50 μg/ml

Tetracycline	Prevents protein synthesis by preventing binding of aminoacyl tRNA to the ribosome A site	10-50 µg/ml
Geneticin	Interferes with the function of the 80S ribosome and blocks protein synthesis	50-1000 µg/ml
Nourseothricin	*Nat1* encodes a nourseothricin N-acetyl transferase. The mechanism of resistance is the monoacetylation of the ß-lysyl unit in clonNAT.	100-200 µg/ml

Table 2-4 Strains used in this study

Strain	Genotype	Derivation
DH5α	F$^-$, Φ80d*lacZ*ΔM15, Δ(*lacZYA-argF*), U169, *rec*A1, *end*A1, *hsd*R17(r_k^-, m_k^+), *pho*A, *sup*E44, λ$^-$, *thi*-1, *gyr*A96, *rel*A1	Invitrogen
BY4741	*MATa, his3Δ1, leu2Δ0, met15Δ0, ura3Δ0*	Giaever *et al.*, 2002
BY4742	*MATα, his3Δ1, leu2Δ0, lys2Δ0, ura3Δ0*	Giaever *et al.*, 2002
BY4743	*MATa/MATα, his3Δ1/his3Δ1, leu2Δ0/leu2Δ0, met15Δ0/+, +/lys2Δ0, ura3Δ0/ura3Δ0*	Giaever *et al.*, 2002
pex15Δ	*MATα, his3Δ1, leu2Δ0, lys2Δ0, ura3Δ0, pex15::KanMX4*	Giaever *et al.*, 2002
ydr479Δ	*MATα, his3Δ1, leu2Δ0, lys2Δ0, ura3Δ0, ydr479c::KanMX4*	Giaever *et al.*, 2002
yhr150Δ	*MATα, his3Δ1, leu2Δ0, lys2Δ0, ura3Δ0, yhr150w::KanMX4*	Giaever *et al.*, 2002
yhr150wΔ-HD	*MATa/MATα, his3Δ1/his3Δ1, leu2Δ0/leu2Δ0, met15Δ0/+, +/lys2Δ0, ura3Δ0/ura3Δ0, yhr150w::KanMX4/+*	Giaever *et al.*, 2002
ylr324Δ	*MATα, his3Δ1, leu2Δ0, lys2Δ0, ura3Δ0, ylr324w::KanMX4*	Giaever *et al.*, 2002
ygr004Δ	*MATα, his3Δ1, leu2Δ0, lys2Δ0, ura3Δ0, ygr004w::KanMX4*	Giaever *et al.*, 2002
ybr168Δ	*MATα, his3Δ1, leu2Δ0, lys2Δ0, ura3Δ0, ybr168w::KanMX4*	Giaever *et al.*, 2002
vps1Δ	*MATα, his3Δ1, leu2Δ0, lys2Δ0, ura3Δ0, vps1::KanMX4*	Giaever *et al.*, 2002
SFY526	*MATα, ura3-52, his3-200, ade2-101, lys2-801 Trp1-901, leu2-3, 112,gal4-542, gal80-538, LYS::GAL1$_{UAS}$ –*	Harper *et al.*,1993

	GAL1$_{TATA}$*-lacZ,MEL1*	
DF5a	*MATa, ura3-52, his3-200, trp1-1, leu2-3,112, lys2-801*	Finley *et al.*, 1987
DF5a	*MATa, ura3-52, his3-200, trp1-1, leu2-3,112, lys2-801*	Finley *et al.*, 1987
YDR479c-prA	*MATa, his3Δ1, leu2Δ0, lys2Δ0, ura3Δ0 ydr479c::YDR479c-protA (HIS5)*	This study
YHR150w-prA	*MATa, his3Δ1, leu2Δ0, lys2Δ0, ura3Δ0, yhr150w::YHR150w-protA (HIS5)*	This study
PEX3-prA	*MATa, his3Δ1, leu2Δ0, lys2Δ0, ura3Δ0, pex3::PEX3-protA (HIS5)*	This study
PEX17-prA	*MATa, his3Δ1, leu2Δ0, lys2Δ0, ura3Δ0, pex17::PEX17-protA (HIS5)*	This study
POT1-prA	*MATa, his3Δ1, leu2Δ0, lys2Δ0, ura3Δ0, pot1::POT1-protA (HIS5)*	This study
TOM20-prA	*MATa, his3Δ1, leu2Δ0, lys2Δ0, ura3Δ0, tom20::TOM20-protA*	This study
yhr150wΔ-A	*MATa, his3Δ1, leu2Δ1, met15Δ0, ura3Δ0, yhr150w::KanMX4*	This study
yhr150Δ/ydr479Δ	*MATa, his3Δ1, leu2Δ0, ura3Δ0, yhr150w::KanMX4, ydr479c::KanMX4*	This study
YLR324w-prA	*MATa, his3Δ1, leu2Δ0, lys2Δ0, ura3Δ0, Ylr324w::YLR324w-protA (HIS5)*	This study
YGR004w-prA	*MATa, his3Δ1, leu2Δ0, lys2Δ0, ura3Δ0, Ygr004w::YGR004w-protA (HIS5)*	This study
YBR168w-prA	*MATa, his3Δ1, leu2Δ0, lys2Δ0, ura3Δ0, Ybr168w::YBR168w-protA (HIS5)*	This study
DK1	*MATa, his3Δ1, leu2Δ0, ura3Δ0, ylr324w::KanMX4, ygr004w::KanMX4*	This study
DK2	*MATa, his3Δ1, leu2Δ0, ura3Δ0, ylr324w::KanMX4, ybr168w::KanMX4*	This study
DK3	*MATa, his3Δ1, leu2Δ0, ura3Δ0, ygr004w::KanMX4, ybr168w::KanMX4*	This study
CD1	*MATa, his3Δ1, leu2Δ0, ura3Δ0, pex28::KanMX4, ylr324w::KanMX4*	This study
CD3	*MATa, his3Δ1, leu2Δ0, ura3Δ0, pex28::KanMX4, ybr168w::KanMX4*	This study

CD4	*MATa, his3Δ1, leu2Δ0, ura3Δ0, pex29::KanMX4, ylr324w::KanMX4*	This study
CD5	*MATa, his3Δ1, leu2Δ0, ura3Δ0, pex29::KanMX4, ygr004w::KanMX4*	This study
CD6	*MATa, his3Δ1, leu2Δ0, ura3Δ0, pex29::KanMX4, ybr168w::KanMX4*	This study
TKO	*MATa, his3Δ1, leu2Δ0, ura3Δ0, ylr324w::KanMX4, ygr004w::KanMX4 ybr168w::NAT*	This study
ybr168Δ-NAT	*MATa, his3Δ1, leu2Δ0, lys2Δ0, ura3Δ0, ybr168w::NAT*	This study
PEX30-GFP+	*MATa his3Δ1, leu2Δ0, lys2Δ0, ura3Δ0, pex30::PEX30-GFP+ (His5)*	This study
PEX32-GFP+	*MATa his3Δ1, leu2Δ0, lys2Δ0, ura3Δ0, pex32::PEX32-GFP+ (His5)*	This study
PEX30(1-170aa)-prA	*MATa his3Δ1, leu2Δ0, lys2Δ0, ura3Δ0, pex30::PEX30(1-170aa)-protA (His5)*	This study
PEX30(1-230aa)-prA	*MATa his3Δ1, leu2Δ0, lys2Δ0, ura3Δ0, pex30::PEX30(1-230aa)-protA (His5)*	This study
PEX30(1-250aa)-prA	*MATa his3Δ1, leu2Δ0, lys2Δ0, ura3Δ0, pex30::PEX30(1-250aa)-protA (His5)*	This study
PEX30(1-282aa)-prA	*MATa his3Δ1, leu2Δ0, lys2Δ0, ura3Δ0, pex30::PEX30(1-282aa)-protA (His5)*	This study
PEX32(1-159aa)-prA	*MATa his3Δ1, leu2Δ0, lys2Δ0, ura3Δ0, pex32::PEX32(1-159aa)-protA (His5)*	This study
PEX32(1-179aa)-prA	*MATa his3Δ1, leu2Δ0, lys2Δ0, ura3Δ0, pex32::PEX32(1-179aa)-protA (His5)*	This study
PEX32(1-203aa)-prA	*MATa his3Δ1, leu2Δ0, lys2Δ0, ura3Δ0, pex32::PEX32(1-203aa)-protA (His5)*	This study
PEX32(1-307aa)-prA	*MATa his3Δ1, leu2Δ0, lys2Δ0, ura3Δ0, pex32::PEX32(1-307aa)-protA (His5)*	This study
PEX30(1-170aa)-GFP+	*MATa his3Δ1, leu2Δ0, lys2Δ0, ura3Δ0, pex30::PEX30(1-170aa)1-GFP+ (His5)*	This study
PEX30(1-230aa)-GFP+	*MATa his3Δ1, leu2Δ0, lys2Δ0, ura3Δ0, pex30::PEX30(1-230aa)-GFP+ (His5)*	This study
PEX30(1-250aa)-GFP+	*MATa his3Δ1, leu2Δ0, lys2Δ0, ura3Δ0, pex30::PEX30(1-250aa)-GFP+ (His5)*	This study
PEX30(1-282aa)-GFP+	*MATa his3Δ1, leu2Δ0, lys2Δ0, ura3Δ0, pex30::PEX30(1-282aa)-GFP+ (His5)*	This study
PEX32(1-159aa)-GFP+	*MATa his3Δ1, leu2Δ0, lys2Δ0, ura3Δ0, pex32::PEX32(1-159aa)-GFP+ (His5)*	This study

PEX32(1-179aa)-GFP+	*MATa his3Δ1, leu2Δ0, lys2Δ0, ura3Δ0, pex32::PEX32(1-179aa)-GFP+ (His5)*	This study
PEX32(1-203aa)-GFP+	*MATa his3Δ1, leu2Δ0, lys2Δ0, ura3Δ0, pex32::PEX32(1-203aa)-GFP+ (His5)*	This study
FD30	*MATa his3Δ1, leu2Δ0, lys2Δ0, ura3Δ0, pex30:: PEX30(Δ229-250aa)-GFP+ (His5*	This study
FD32	*MATa his3Δ1, leu2Δ0, lys2Δ0, ura3Δ0, pex32::PEX32(Δ159-179aa)-GFP+ (His5)*	This study
S30	*MATa his3Δ1, leu2Δ0, lys2Δ0, ura3Δ0, pex30:: PEX30(229-250aa)-GFP+ (His5)*	This study
S32	*MATa his3Δ1, leu2Δ0, lys2Δ0, ura3Δ0, pex32:: PEX32(159-179aa)-GFP+ (His5)*	This study
PEX30-prA-pex19Δ	*MATa his3Δ1, leu2Δ0, lys2Δ0, ura3Δ0, pex30::PEX30-protA (His5), pex19::KanMX4*	This study
PEX32-prA- pex19Δ	*MATa his3Δ1, leu2Δ0, lys2Δ0, ura3Δ0, pex32::PEX32-protA (His5), pex19::KanMX4*	This study
PEX30-GFP+pex19Δ	*MATa his3Δ1, leu2Δ0, lys2Δ0, ura3Δ0, pex30::PEX30-GFP+(His5), pex19::KanMX4*	This study
PEX32-GFP+pex19Δ	*MATa his3Δ1, leu2Δ0, lys2Δ0, ura3Δ0, pex32::PEX32-GFP+ (His5), pex19::KanMX4*	This study
P30-L104P-prA	*MATa his3Δ1, leu2Δ0, lys2Δ0, ura3Δ0, pex30::PEX30-L104P-protA (His5)*	This study
P32-L142P-prA	*MATa his3Δ1, leu2Δ0, lys2Δ0, ura3Δ0, pex32::PEX32-L142P-protA (His5)*	This study
P30-L104P-GFP+	*MATa his3Δ1, leu2Δ0, lys2Δ0, ura3Δ0, pex30::PEX30-L104-GFP+ (His5)*	This study
P32-L142P-GFP+	*MATa his3Δ1, leu2Δ0, lys2Δ0, ura3Δ0, pex32::PEX32-L142P-GFP+ (His5)*	This study
VPS1-GFP+	*MATa his3Δ1, leu2Δ0, lys2Δ0, ura3Δ0, vps1::VPS1-GFP+ (NAT)*	This study
VPS1(Δ509-523aa)	*MATa his3Δ1, leu2Δ0, lys2Δ0, ura3Δ0, vps1:: VPS1(Δ509-523aa) (His5)*	This study
VPS1(Δ633-647aa)	*MATa his3Δ1, leu2Δ0, lys2Δ0, ura3Δ0, vps1:: VPS1(Δ633-647aa) (His5)*	This study
VPS1-GFP+pex19Δ	*MATa his3Δ1, leu2Δ0, lys2Δ0, ura3Δ0, vps1::VPS1-GFP+ (NAT), pex19::KanMX4*	This study
VPS1-V512P-GFP+	*MATa his3Δ1, leu2Δ0, lys2Δ0, ura3Δ0, vps1::VPS1-V512P-GFP+ (NAT)*	This study

2.3 Introduction of DNA into microorganisms

DNA was introduced into microorganisms via chemical transformation or eletroporation, and transformants were selected by antibiotic resistance or other genetic markers. Electroporation was performed in microelectroporation chambers (width ~0.15 cm) using a Cell-Porator connected to a Voltage Booster (BRL).

2.3.1 Chemical transformation of *E. coli* (Heat shock)

Plasmid DNA was introduced into transformation-competent DH5α cells (subcloning efficiency) as described in a protocol from Invitrogen. Generally, 1 to 2 μL of a ligation reaction or 0.25 μg of plasmid DNA was added to 25 μL of cells. The mixture was incubated on ice for 30 min, subjected to heat shock at 37°C for 20 sec and then returned to ice for 2 min. 1 ml of LB was added, and the cells were incubated in a rotary shaker at 37°C for 45 min. Cells were spread onto LB agar plates containing ampicillin or another antibiotic for selection. When necessary, 75 μL of 2% X-gal in DMF and 50 μL of 100 mM IPTG were spread onto plates prior to the plating of cells to select for blue/white colonies carrying recombinant plasmids. Plates were incubated at 37°C for ~16 h for colony formation.

2.3.2 Electroporation of *E. coli*

High-efficiency electroporation-competent *E. coli* cells were prepared according to Maniatis *et al.* (1982). Freshly grown *E. coli* were used to inoculate 50ml of S.O.B. medium (Table 2-1) and were grown overnight at 37°C. Cultures were then diluted into

500 ml S.O.B. and grown for 2 to 3 h at 37°C until the OD_{600} was approximately 0.8. Cells were harvested by centrifugation and washed twice with 500 ml of sterile, ice-cold 10% (v/v) glycerol. The pellet was then resuspended in 10% (v/v) glycerol to a final volume of 2 ml, and 20 µl aliquots were subjected to electroporation using a Voltage Booster (Whatman Biometra) at 395 V (amplified to ~2.4 kV) at a capacitance of 2 µF and a resistance of 4 kΩ. Cells were then diluted to 1 ml with LB medium, grown for 1 h at 37°C and plated onto LB-agar plates containing ampicillin.

2.3.3 Chemical transformation of *S. cerevisiae*

This method is largely used to transform plasmid DNA into yeast cells (Gietz and Woods, 2002). Essentially, 25 µl of cells was scraped from a freshly grown plate with a sterile toothpick and resuspended in 1 ml of water. Cells were washed twice by centrifugation, resuspended in 1 ml of 100 mM lithium acetate, and incubated at 30°C for 10 min. Cells were again harvested by centrifugation, and the following components were added on top of the cell pellet in the following order: 240 µl of 50% (w/v) PEG, 36 µl of 1 mM lithium acetate, 50 µl of 2 mg sheared, denatured salmon sperm DNA/ml, 1 µl of plasmid DNA and 20 µl of water. Alternatively, a master mix can also be made without the plasmid, if different DNA molecules were to be transformed. The mixture was vortexed vigorously for 1 min and incubated at 42°C for 20 min. Cells were harvested by centrifugation, resuspended gently in 200 µl of water and plated onto CSM (Complete Synthetic Medium) for selection. Plates were incubated at 30°C for 3 days for colony formation.

2.3.4 Electroporation of *S. cerevisiae*

Yeast cells were made electrocompetent following the method of Ausubel *et al.* (1996). Cells were grown overnight in 10 ml of YEPD. 5 ml of culture was added to 50 ml of YEPD, and cells were grown to an OD_{600} of ~0.75. Cells were harvested by centrifugation, resuspended in Transformation buffer (pH 7.5) (Table 2-4) containing 10 mM lithium acetate and 20 mM DTT and incubated for 1h. Cells were harvested by centrifugation and washed successively with 50 ml each of ice-cold water, ice-cold 1M sorbitol. Cells were resuspended in a minimal volume of ice-cold sorbitol buffer. 20 µL of cells was added to 1 µL of plasmid DNA, and the cells were suspended between the bosses of an ice-cold electroporation chamber (Whatman Biometra). Cells were subjected to 250V (amplified to ~1.6 kV) at a capacitance of 2 µF and a resistance of 4 kΩ. Cells were immediately added to 100 µL of ice-cold 1 M sorbitol and plated onto CSM agar plates (Table 2-6). Plates were incubated at 30°C for 2 to 3 days for colony formation.

2.4 Isolation of nucleic acids

Chromosomal DNA from yeast cells and plasmid DNA from *E. coli* cells were isolated as follows:

2.4.1 Plasmid DNA isolation from *E. coli*

Plasmid DNA was isolated from small-scale bacterial cultures according to the alkaline lysis mini-prep procedure (Ausubel *et al.*, 1996) or by using the QIAprep Spin Miniprep Kit according to the manufacturer's instructions. Single colonies were inoculated into 2 ml of LB containing ampicillin and grown over night. Plasmid DNA

was isolated from 1.5 ml of culture by the alkaline lysis method (Maniatis *et al.*, 1982) or by using a QIAprepMiniprep Kit (Qiagen). This method employs essentially the same principles as the alkaline lysis method, except that after precipitation of proteins with potassium acetate solution, plasmid DNA is absorbed onto a silica-gel membrane in a high-salt environment. Chaotropic salts are passed over the column to remove contaminating proteins. Residual salts are removed, and plasmid DNA is eluted in 50 µL of 10 mM Tris-HCl (pH 7.5).

2.4.2 Genomic DNA isolation from *S. cerevisiae*

Total genomic DNA was isolated from yeast strains using the glass bead disruption technique (Ausubel *et al.*, 1989) in breakage buffer. Cells were grown overnight in 10 ml cultures of YEPD, washed three times with water and then resuspended in breakage buffer. Glass beads were added, tubes were vortexed three times for 1 min each, and then cell debris was removed by centrifugation for 5 min at maximum speed in a microfuge. Nucleic acids were separated from proteins with two phenol/chloroform/isoamyl alcohol (25:24:1) extractions and one chloroform/isoamyl alcohol (24:1) extraction. Total nucleic acids were precipitated by the addition of 2.5 volumes of absolute ethanol, pelleted by centrifugation in a microfuge for 4 min at maximum speed, and subsequently washed twice with 70% ethanol to remove contaminating salts. The nucleic acid pellet was then resuspended in approximately 50 µl of TE/RNase A (10 mM Tris-HCl, pH 8.0, 1 mM EDTA, 20 µg RNase A/ml) and incubated at 37°C to allow for RNA digestion and pellet dissolution. If plasmid DNA is to be recovered, subsequent electroporation into *E. coli* is performed and recovered.

2.5 Standard DNA manipulation

Unless otherwise stated, reactions were in 1.5 ml microcentriuge tubes, and microcentrifugation was done in an Eppendorf microcentrifuge at 16,000 x *g*.

2.5.1 Amplification of DNA by the polymerase chain reaction

PCR was used to amplify specific DNA fragments, to introduce restriction endonuclease sites within a DNA molecule or to facilitate the construction of hybrid DNA molecules. Integration of DNA fragments into the genome or deletion of specific sequences from the genome were also verified by PCR. PCR conditions (including primer design, cycling conditions and reaction components) were according to standard procedure (Innis and Gelfand, 1990; Saiki, 1990). Reactions were performed in 0.6 ml microcentrifuge tubes and typically contained 1.25 U of Platinum *Pfx* DNA polymerase, or *Taq* polymerase, 0.1µg of template DNA, 20 to 100 pmol of each primer, 1 mM Mg_2SO_4, 25 mM each of dATP, dCTP, dGTP and dTTP in 50µL of reaction buffer. Alternatively, Ready-To-GO PCR beads were used according to the specifications of the manufacturer (Amersham Biosciences). Reactions were cycled in a Robocycler 40 (Stratagene) with a Hot Top attachment.

2.5.2 Restriction endonuclease digestion

DNA was digested according to the restriction enzyme maufacturer's instructions. For diagnostic and preparative digests, 0.5 to 1µg and 2 to 3µg of DNA, respectively,

were digested respectively for 1 to 1.5 h at 37°C by 1 U of enzyme under optimal buffer concentration. Double digests were done according to the instructions supplied by NEB.

2.5.3 Dephosphorylation and phosphorylation of 5'ends

Prior to ligation, the 5' ends of linearized plasmid DNA molecules were usually dephoshorylated to prevent intramolecular ligations. Essentially, after plasmid digestion, reactions were mixed with 5 U of CIP and incubated for 30 min at 37°C. Also prior to ligation, the 5' termini of DNA molecules amplified by PCR were phosphorylated. Reactions were mixed with 10 U of T4 polynucleotide kinase and ATP and PNK buffer (to 10 mM and 1 × respectively) and incubated at 37°C for 1 h. Desphosphorylation and phosphorylation reactions were terminated by agarose gel electrophoresis of the DNA fragments.

2.5.4 Separation of DNA fragments and PCR products

DNA fragments produced in the course of molecular cloning and polymerase chain reaction (PCR) products were first separated by electrophoresis using 1% agarose in 1 × TBE buffer containing 5 μg ethidium bromide/ml. Gels were run at 8-10 v/cm of gel. Prior to loading, samples were mixed with 6 x Gel Dye. Fragments 100 bp in length or smaller were separated on 3% agarose gels consisting of 0.5% SeaKem Genetic Technology Grade (GTG) agarose and 2.5% NuSieve GTG agarose. Large DNA fragments were separated on 0.7 to 1.5% agarose gels. The bands of interest were

visualized by ultraviolet illumination (Photodyne, Model 3-3006) and excised from the gel. The QIAquick gel extraction kit was used to recover the DNA.

2.5.5 Purification of DNA fragments from agarose gels

DNA fragments were isolated from agarose gels using a QIAquick Gel Extraction Kit (Qiagen) according to the manufacturer's instructions. The gel fragment containing the DNA of interest is dissolved, the DNA is adsorbed to a silica-gel surface, contaminants are removed by washing and the DNA is eluted in 30 µL of 10 mM Tris-HCl (pH 8.5).

2.5.6 Purification of DNA from solution

Salts and enzyme contaminants present with the DNA in solutions, obtained after digestion can be removed by using the QIAquick PCR Purification Kit as described by the manufacturer (Qiagen). The principle of this method is similar to that of the QIAquick Gel Extraction Kit, except that no dissolution of agarose gel was involved. DNA was usually eluted in 30 to 50 µl of 10 mM Tris-HCl (pH 8.5).

2.5.7 Ligation of DNA fragments

DNA fragments treated with restriction endonucleases and purified were ligated using 1 µl of T4 DNA ligase in the buffer supplied by the manufacturer (NEB). The reaction was typically in a volume of 10 µl, with the molar ratio of vector to insert being between 1:3 and 1:10, and incubated overnight at 4°C. Alternatively, 1 µl of Quick T4

DNA ligase (NEB) in 1 × Quick Ligation Buffer was used in a reaction volume of 20 µl. The reaction was incubated at room temperature for 10 min.

2.5.8 Molecular cloning and subcloning by ligation

PCR products are conveniently cloned by using pGEMT vector system. The 3'-T overhang present at the ends greatly improve the efficiency of ligation of a PCR product into the plasmid by preventing the recircularization of the vector. The multiple cloning site is flanked by specific recognition sites for restriction enzymes and a single or double digestion may be used to release the insert from the vector. All molecular cloning was performed according to manufacturer's instructions (Promega).

2.5.9 DNA sequencing

Sequencing was performed with an ABI Prism 310 Genetic analyzer, an automated DNA sequencer, using BigDye Terminator Cycle Sequencing v1.1/3.1 Ready Reaction Kit as described by the manufacturer (Applied Biosystems). The system uses the method of Sanger (Sanger *et al,* 1977). It involves random incorporation of fluorescent dideoxy terminators during the elongation of DNA sequences with a modified version of *Taq* DNA polymerase. The reaction master mix contains 3 µL of Terminator Ready Reaction Mix, 1 µL of plasmid DNA, 3.2 pmol of primer and 2.5 µL of the supplied 5 × buffer in a total volume of 20 µl. The reaction was subjected to cycle sequencing using the Robocycler 40 with a Hot Top attachment (Stratagene) with the following conditions: 1 cycle at 96°C for 2 min; 25 cycles at 96°C for 46 sec, 50°C for 51 sec and 60°C for 4 min 10 sec; 1 cycle at 6°C to hold until ready to purify. Reaction

products were precipitated with 80 µl of 75% isopropanol for 20 min at room temperature, subjected to microcentrifugation at 16,000 × *g* for 20 min, washed twice with 250 µl of 75% isopropanol, dried in a rotary vacuum dessicator (Labconco, Centrivap concentrator) and resuspended in 15 µl of Template Suppression Reagent. Following a brief vortexing, the reaction mixture was then heated at 95°C for 2 min and immediately cooled on ice. This is loaded onto the ABI 310 Genetic analyzer, which separates by capillary electrophoresis, and the emitted fluorescence was detected and recorded to obtain the sequence.

2.6 Analysis of Proteins

2.6.1 Determination of protein concentration

Total protein was measured according to Bradford (1976) using a protein assay kit (BioRad) and bovine serum albumin as the standard. A standard curve was made by adding 1 ml of Bio-Rad Protein Assay Dye to 100 µl aliquots of water containing a series of different concentrations of BSA. Samples were incubated for 5 min at room temperature and briefly vortexed, and absorbance was measured at 595 nm using a Beckman DU640 spectrophotometer. Absorbance values were plotted against the BSA concentrations to generate a standard curve. Absorbance of a protein sample was measured in the same way as for BSA standards, and the protein concentration was estimated by comparing the absorbance value with the standard curve.

2.6.2 Electrophoretic separation of proteins

Protein samples were resolved according to the method of Laemmli (1970). Samples were denatured by boiling 5 min in SDS-PAGE sample buffer and then separated by discontinuous SDS-PAGE on a 10% gel. Samples were run at 50 to 200 V in 50 mM Tris-HCl, pH 8.8, 0.4 M glycine, 0.1% SDS until the dye front reached the bottom of the gel. Otherwise, proteins were electrophoretically transferred to nitrocellulose with either a BioRad western transblotter apparatus overnight at 100 mA in 20 mM Tris-HCl, pH 7.5, 150 mM glycine, 20% (v/v) methanol or by semi-dry electrophoretic transfer (Tyler Research Instruments, Edmonton, AB) for 1.5 h at 0.75 mA/cm^2 of transfer area, as described (Kyshe-Anderson, 1984).

2.6.3 Precipitation of proteins

Proteins were precipitated from solution by adding TCA to a final concentration of 10% and incubation on ice for 30 min to overnight. Precipitates were collected by microcentrifugation at 16,000 × *g* for 30 min at 4°C. The pellet was washed twice with 1 ml of ice-cold acetone, dried in a rotary vacuum dessicator and dissolved in 2 × sample buffer

2.6.4 Detection of proteins

Proteins extracted from the cells and separated on gels were detected and quantitated by the following ways.

2.6.4.1 Staining with Coomassie blue staining

Proteins in polyacrylamide gels were visualized by staining with 0.1% Coomassie Brilliant Blue R-250, 10% (v/v) acetic acid, 35% (v/v) methanol for 1 h with gentle agitation. Unbound dye was removed by multiple washes in 10% (v/v) acetic acid, 35% (v/v) methanol. Gels were dried for 1 h at 80°C on a Bio-Rad Model 583 gel drier. Proteins were directly visualized by staining in 0.1% Coomassie Brilliant Blue (R-250), 10% (v/v) acetic acid, 35% (v/v) methanol.

2.6.4.2 Staining with Ponceau S

Ponceau S (sodium salt) is used to prepare a stain for rapid reversible detection of protein bands on nitrocellulose membranes (Western blotting). Common stain formulations include 0.1% (w/v) Ponceau S in 5% acetic acid or 2% (w/v) Ponceau S in 30% TCA and 30% sulfosalicylic acid. Ponceau S stain is easily reversed with water washes, facilitating subsequent immunological detection.

2.6.4.3 Immunoblot analysis

Nitrocellulose was hydrated in water for 5 min and then equilibrated in Western transfer buffer. Proteins separated by SDS-PAGE were transferred to nitrocellulose in Western transfer buffer, using either a wet or semi-dry apparatus. For wet blotting, the transfer was carried out at 100 mA for approximately 16 h at room temperature or at 400 mA for approximately 4 h using a cooling coil, in a blotting tank (Bio-Rad Trans-Blot or Hoefér TE Series Transphor electrophoresis unit). For semi-dry blotting, the transfer was carried out at 0.8 mA per cm^2 of gel in an ET-20 electrophoretic transfer system (Tyler

Research Instruments, Edmonton, Alberta). Unoccupied protein binding sites on the nitrocellulose were blocked by incubating the blot in TBST-milk (1% skim milk powder in TBST) for 30 min with gentle agitation. Primary antiserum was diluted in TBST-milk at their respective concentrations. The blots were incubated with the primary antiserum for 60 min at room temperature. Excess primary antibody was removed by three 10 min washes in TBST. The appropriate secondary antibody conjugated to HRP was diluted in TBST-milk at a concentration of 1:30,000 and incubated with the blots for 60 min. Excess secondary antibody was removed by three 10 min washes in TBST. The blot was covered with ECL detection solution (a 1:1 mixture of the two ECL detection reagents) for 1 min, placed in a transparent plastic folder and exposed to Kodak XK-1 X-ray film. For quantitation of signals, densitometry was performed with a Bio-Rad GS800 calibrated densitometer.

2.7 Cell Disruption and Subcellular fractionation

Subcellular fractionation is an approach universally used with all cell types and tissues for the isolation of organelles. This method has been widely used to identify the different protein compositions of isolated cellular compartments.

2.7.1 Preparation of whole cell lysates

Total cell lysates were prepared by different methods such as the glass bead lysis method or the alkaline lysis method.

2.7.1.1 Glass bead lysis method

Total cellular protein was isolated by glass bead disruption of cells. Cells grown in YEPD or YPBO were washed twice with water and pelleted by centrifugation at 2,500 x *g* and resuspended in ice-cold Disruption buffer containing protease inhibitors and 1 mM DTT (Needleman and Tzagoloff, 1975). Glass beads are added to the meniscus of cell suspension and vortexed for 5 min at 4°C. The suspensions were subjected to centrifugation in a microfuge for 5 min to pellet unbroken cells, cell debris and glass beads. Supernatants were removed and stored at -20°C or loaded onto the gels after mixing with the gel loading dye and boiling for 10 min.

2.7.1.2 Magic method

Alternatively, alkaline and reducing agents are used to prepare yeast cell lysates. Cells were harvested by centrifugation at 2,000 × *g* for 5 min, transferred to a microcentrifuge tube, and resuspended in 240 µl of 1.85 M NaOH and 7.4% β-mercaptoethanol. The cell suspension was incubated on ice for 5 min and mixed with an equal volume of pre-cooled 50% TCA by vortexing. The mixture was further incubated on ice for 5 min and subjected to microcentrifugation at 16,000 × *g* for 10 min at 4°C. The pellet was washed once with water, resuspended first in 100 µl of Magic A (1 M unbuffered Tris-HCl and 13% SDS) and then in an equal volume of Magic B (30% (v/v) glycerol, 200 mM DTT and 0.25% bromophenol blue). The mixture was boiled for 10 min and then subjected to microcentrifugation at 16,000 × *g* for 30 seconds to pellet unbroken cells and cell debris. Supernatants were removed and stored at -20°C or loaded onto the gels.

2.7.2 Subcellular fractionation

Subcellular fractionation and peroxisome isolation were done essentially as described (Bonifacino *et al.*, 2000; Vizeacoumar *et al.*, 2003). Cells were grown in YEPD for 12 h, shifted to oleic acid-containing medium and induced for 9 h. Cells were harvested by centrifugation at 800 × *g* in a Beckman JA10 rotor at room temperature and washed twice with water. Cells were resuspended in perforation buffer, at a concentration of 10 ml per gram of wet cells, and incubated at 30°C for 30 min at 70 rpm to loosen the outer mannoprotein layer. Cells were collected by centrifugation at 2,500 × *g* in a pre-cooled Beckman JS13.1 rotor for 8 min at 4°C and washed once with Zymolyase buffer without Zymolyase. Cells were then resuspended in Zymolyase buffer containing 0.125 mg of Zymolyase 100T/ml at a concentration of 8 ml per gram of wet cells and incubated at 30°C for 45 min to 1 h at 70 rpm to obtain spheroplasts. The rest of the treatment is done at 4°C or on ice bucket. Spheroplasts were harvested by centrifugation at 2,200 × *g* in a Beckman JS13.1 rotor for 8 min at 4°C and washed once with washing buffer (1.2 M sorbitol, 5 mM MES, pH 6.0, 1 mM EDTA). They were then resuspended in buffer H containing 1 × complete protease inhibitor cocktail (Roche) at a concentration of 3 ml per gram of wet cells. Resuspended spheroplasts were transferred to a homogenization mortar and disrupted by 10-15 strokes of a Teflon pestle driven at 1,000 rpm by a stirrer motor (Model 4376-00, Cole-Parmer). Disruption is monitored in a microscope for the release of organelles. Cell debris, unbroken cells and nuclei were pelleted by centrifugation at 1,000 × *g* in a Beckman JS13.1 rotor for 8 min at 4°C. The resultant supernatant is the postnuclear supernatant (PNS). The PNS was subjected to four to five additional centrifugations at 1,000 × *g* in a Beckman JS13.1 rotor for 8 min at 4°C. The PNS was

fractionated by centrifugation at 20,000 × *g* in a Beckman JS13.1 rotor for 30 min at 4°C into pellet (20KgP) and supernatant (20KgS) fractions. The 20KgP fraction is enriched in organelles. Aliquots of PNS, 20KgS and 20KgP were stored at -20°Cfor later analysis. Proteins in equal portions of each fraction were separated by SDS-PAGE and analyzed by immunoblotting.

2.7.3 Isolation of organelles by isopycnic centrifugation

The 20KgP fraction was resuspended in buffer H containing 11% Nycodenz and 2× PINS (Protease Inhibitors), and a volume containing 5 mg of protein was overlaid onto either a 30-ml discontinuous gradient consisting of 17%, 25%, 35% and 50% (w/v) Nycodenz (6.6 ml of 17%, 16.5 ml of 25%, 4.5 ml of 35% and 3 ml of 50% (w/v) Nycodenz in buffer H) or a 30-ml continuous gradient of 25% to 50% (w/v) Nycodenz, both in buffer H containing PINS. Organelles were separated by centrifugation at 100,000 × *g* for 90 min in a VTi50 rotor (Beckman). Fractions of 2 ml were collected from the bottom of the tube by puncturing the optiseal tube using an 18 gauge needle. 18 fractions of 2 ml each were collected from the bottom of the gradient. The 20KgS fraction was subfractionated by ultracentrifugation at 200,000 × *g* in a Beckman TLA120.2 rotor for 1 h at 4°C into a pellet (200KgP) fraction enriched for high-speed pelletable organelles and a supernatant (200KgS) fraction enriched for cytosol. Aliquots of fractions were mixed with 6× dye, boiled for 10 min and loaded onto gels.

2.7.4 Membrane extraction

Peroxisomal membrane fractions were prepared by extraction of purified peroxisomes isolated from Nycodenz gradients, as described (Fujiki *et al.*, 1982; Nuttley *et al.*, 1990). Essentially, organelles in the 20KgP fraction (50 µg of protein) were lysed by quick freezing and thawing (3 times) followed by incubation in 10 volumes of Ti8 buffer (10 mM Tris-HCl, pH 8.0) containing 3 × PINS on ice for 1 h and separated into pellet (Ti8P) and supernatant (Ti8S) fractions by centrifugation at 245,000 × *g* for 1 h at 4°C in a TLA120.2 rotor (Beckman). The Ti8P fraction was resuspended in Ti8 buffer to a final protein concentration of 0.5 mg/ml, and a portion of the resuspended fraction was extracted with 0.1 M Na_2CO_3, pH 11.3, for 1 h on ice and then separated into supernatant (CO_3S) and pellet (CO_3P) fractions by centrifugation at 245,000 × *g* in a TLA120.2 rotor at 4°C for 1 h. Proteins in the Ti8S, Ti8P, CO_3S and CO_3P fractions were precipitated by addition of 50% TCA, and the precipitates were washed with acetone. Proteins in equal portions of each fraction were separated by SDS-PAGE and analyzed by immunoblotting. Alternatively, the purified peroxisomal fractions were also subjected to treatment with Ti8 or alkaline carbonate buffer.

2.8 Microscopy

2.8.1 Immunofluorescence microscopy

Imunofluorescence of yeast cells was performed as described (Pringle *et al.*, 1991; Smith, 2000). This technique was performed either to localize protein A chimeras or endogenous proteins. Strains encoding protein A chimeras were transformed with the

plasmid pDsRed-PTS1, grown in SM medium for 12 h and then incubated in YPBO medium for 8 h. Following induction, cells were fixed in 3.7% (v/v) formaldehyde for 30 min at room temperature in an orbital shaker. Cells were then pelleted by centrifugation at 2,000 × *g* for 5 min, washed with 2 ml of solution B, and resuspended with the same solution B at a concentration of 1 ml per 100 µl of wet cells. 1 ml of cell suspension was mixed with 1mg of Zymolyase 100 T/ml and 28 mM β-mercaptoethanol and incubated for 1 h at 30ºC with gentle rotation. Spheroplasts were spotted onto slides precoated with poly *L*-lysine and allowed to dry at room temperature. Spheroplasts were permeabilized by immersion of the slides for 6 min in -20ºC methanol and for 30 sec in -20ºC acetone, and allowed to air dry. For the rest of the treatment, slides were put in a dark humid box at room temperature. Spheroplasts were covered with 50 µl of blocking solution (1% milk in TBST) for 1 h. Slides were incubated with primary antibody diluted in blocking solution for 1 h, washed 10 to 20 times with 1 × TBST, and then incubated with secondary antibody conjugated to fluorescein or rhodamine diluted in blocking solution for 1 h. Cells were washed again 10 to 20 times with 1 × TBST and covered with 1 drop of mounting medium. Coverslips were placed on top of slides, and the edges were sealed with nail polish. Protein A chimeras were detected using rabbit antiserum to mouse IgG (ICN, Aurora, OH) and fluorescein isothiocyanate (FITC)-conjugated goat anti-rabbit IgG. Primary antibodies listed in Table 2.1.6 were used to detect endogenous proteins. Images were captured on a LSM510 META (Zeiss) laser scanning microscope or an Olympus BX50 microscope with a digital camera (Spot Diagnostic Instruments, Sterling Heights, MI).

2.8.2 Staining of the yeast nucleus with Hoechst dye

Cell nuclei of live yeast cells can be visualized using Hoechst 33342 dye. Common stain formulations include 1 mM dye (56 mg) in 1 % (v/v) ethanol (Stock). Cells expressing GFP chimeras were grown in YEPD, induced with YPBO for 8 h and were treated with 10 nM Hoechst dye (Sigma) per µl of cells at 30°C for 5 to 15 min in a rotary shaker at 150 rpm. Cells were washed once, and images were obtained using an Olympus BX50 microscope.

2.8.3 Staining of the yeast vacuole with FM4-64 dye

Cells were grown overnight and subcultured to reach an OD_{600} of 0.5. To about 100 µl of cells, 1 µl of 8 mM FM4-64 dye was added, and cells were incubated for 30 min at 30°C. Cells were washed and reincubated in fresh YPD medium for 1.5 h. These cells were washed with water twice before examination. Images were captured on an Olympus BX50 microscope equipped with a digital fluorescence camera.

2.8.4 Staining of yeast mitochondria with MitoTracker Red

Mitochondria of live yeast cells were stained with MitoTracker Red CMXRos according to the manufacturer's instructions (Molecular Probes). Cells grown in 10 ml of YPBO (Table 2-9) were harvested, washed once with water and resuspended in 10 ml of pre-warmed YPBO. The cell suspension was mixed with 2 µl of 1 mM MitoTracker Red CMXRos and incubated at 30°C for 10 to 15 min in a rotary shaker at 150 rpm. 1.5 ml of

culture was pelleted, washed twice with water, and viewed on an Olympus BX50 microscope equipped with a digital fluorescence camera.

2.8.5 Electron microscopy

Whole cells and subcellular fractions were processed for EM as described (Eitzen *et al.*, 1997; Eitzen, 1997; Goodman *et al.*, 1990). All microcentrifugations were performed at 16,000 × *g* for 1 min, and all incubations were done in 1.5 ml microcentrifuge tubes at room temperature with agitation in an orbital shaker, unless indicated otherwise.

2.8.5.1 Processing of whole cells

Cells were harvested and washed twice with water. Approximately 100 µl of cell pellet was fixed in 1 ml of 3% freshly prepared $KMnO_4$ for 20 min, washed twice with water, and incubated in 1 ml of 1% sodium periodate for 10 min. Cells were pelleted, washed once with water, and incubated with 1 ml of 1% NH_4Cl for 15 min. Cells were again pelleted, washed once with water, and subjected to serial dehydration in 60%, 80%, 95%, and 100% ethanol and in propylene oxide. Incubation in the graded alcohol was for 5 min and in propylene oxide for 3 min. Incubation in propylene oxide was repeated three times. Cells were collected and incubated in 1 ml of a 1:1 mixture of propylene oxide and resin (a mixture of TAAB 812 resin, specially distilled DDSA, methyl nadic anhydride and 2,4,6,-tri-(dimethylaminomethyl) phenol in proportions suggested by the manufacturer (Marivac)) for 1 h. Cells were next pelleted and resuspended in 1 ml of

resin. Incubation in resin was carried out for 1 h with agitation and 3 h in a fume hood with caps opened. Finally, cells were pelleted by microcentrifugation for 8 min, and small portions of cells were transferred to embedding capsules (EMS) containing resin. Embedding capsules were placed in an oven at 60°C to allow the resin to polymerize. Ultra-thin sections were cut (performed by Honey Chan, Department of Cell Biology, University of Alberta) using an Ultra-Cut E Microtome (Reichert-Jung) and viewed on a Phillips 410 electron microscope. Images were captured with a digital camera (Soft Imaging System). For time point experiments, cells were prefixed in 1 ml of 3% glutaldehyde prepared in 0.1 M cacodylate buffer, pH 7.2, for 15 min at 4°C with agitation. In this way, cells could be stored at 4°C until needed and processed for electron microscopy as described above.

2.8.5.2 Processing of purified organelles

To the 2 ml fractions of purified organelles in Nycodenz, 25% glutaraldehyde was added to a final concentration of 0.5%, and organelles were fixed for 15 min at 4°C with agitation. These fixed organelles were pelleted using the Type 70Ti rotor (Beckman), and the pellet was covered with 2.5% glutaraldehyde in 0.1M cacodylate buffer. This is left for further fixation overnight at 4°C with very gentle agitation. Care must be taken that the pellet does not get dispersed in the fixative. Once fixed, the pellet is washed three times with 0.1M cacodylate, followed by incubating with 10% osmium tetroxide for 5 min. The pellet turns brown and can be washed with water and dehydrated with a series of alcohol and propylene oxide, as is done for processing whole cells. Embedding was

done as described for whole cells. Ultrathin sections were cut and mounted onto carbon-coated nickel grids. For better contrast, samples were also poststained with 2% uranyl acetate.

2.8.6 Morphometric analysis of peroxisomes

For each strain analyzed, electron micrographs of 50 randomly selected cells at ×17,000 magnification were developed (captured on film and printed) and scanned, and the areas of individual cells and of individual peroxisomes were determined by counting the number of individual pixels in a particular cell or peroxisome with Image Tool for Windows, Version 2.00 (University of Texas Health Sciences Center, San Antonio, TX). Alternatively, for each strain analyzed, electron microscopic images of 50 randomly selected cells at ×17,000 magnification were captured with a digital camera (Soft Imaging System), and the areas of individual cells and of individual peroxisomes were determined by the program analySIS 3.1 (Soft Imaging System). To determine the average area of a peroxisome, the total peroxisome area was calculated and divided by the total number of peroxisomes counted. To quantify peroxisome number, the numerical density of peroxisomes (number of peroxisomes per μm^3 of cell volume) was calculated by the method of Weibel and Bolender (1973) for spherical organelles as follows. First, the total number of peroxisome profiles was counted and reported as the number of peroxisomes per cell area assayed (N_A). Next, the peroxisome volume density (V_V) was calculated for each strain (total peroxisome area/total cell area assayed). Using the values

V_V and N_A, the numerical density of peroxisomes was determined (Weibel and Bolender, 1973).

2.9 Construction of plasmids

2.9.1 Construction of plasmids for epitope tagging

CFP- and YFP-containing plasmids were constructed in the same manner. Genes encoding fluorescent proteins with different auxotrophic markers that could functionally complement *S. cerevisiae* genes were used (Lys1 of *S. pombe*, Leu-1 of *S. pombe* and Ura-4 of *S. pombe*) to clone into the *Sac*II site of pGEMT (Promega) to generate the following plasmids: pCFP-ura, pYFP-ura, pCFP-leu, pYFP-leu, pCFP-lys and pYFP-lys. All the constructs carry a small section of protein A and Ura3. These cassettes were used to PCR from these plasmids with homologous region to the genes of interest and integrated into the genome by homologous recombination.

2.9.2 Construction of pNLS-PEX19 for nuclear targeting of Pex19p

The plasmid pMad1NLS-GFP constructed in pRS316 with an entire expression cassette under the control of the Pho4 promotor was a gift from Dr. Wozniak's laboratory. Two constructs under the Pho4 promoter containing the expression cassette Mad1-NLS and PEX19 (pNLS-PEX19) in-frame or just Mad1-NLS, GFP and *PEX19* (pNLS-GFP-PEX19) in-frame were constructed. The original construct was digested with *Eco*RI and *Not*I to release the GFP and *PEX19* was amplified with similar sites and cloned. For the second construct, the original plasmid was digested with *Sac*I and *Xba*I to open the plasmid, and *PEX19* was ligated downstream of GFP. In this way, although GFP

loses two amino acids along with the stop codon, the expression of GFP was found to be unaffected.

2.9.3 Construction of plasmids for overexpression

The plasmids pDsRed-PTS1 (Smith *et al.*, 2002) and pProtA/HIS5 (Rout *et al.*, 2000) have been described. Genes to be overexpressed were amplified by PCR and cloned into the *Bam*HI site of YEp13 (Broach *et al.*, 1979). For ovexpression, the *YHR150w* gene included 492 bp of upstream and 398 bp of downstream sequence, the *YDR479c* gene included 642 bp of upstream and 335 bp of downstream sequence, the *PEX11* gene included 599 bp of upstream and 329 bp of downstream sequence, the *PEX25* gene included 753 bp of upstream and 319 bp of downstream sequence, and the *VPS1* gene included 555 bp of upstream and 324 bp of downstream sequence. For overexpression, the *YLR324w* gene included 609 bp of upstream and 348 bp of downstream sequence, the *YGR004w* gene included 625 bp of upstream and 217 bp of downstream sequence, and the *YBR168w* gene included 592 bp of upstream and 381 bp of downstream sequence.

2.10 Construction of a yeast-gene deletion

Separation of the four ascospores from individual asci by micromanipulation is required for the construction of deletion strains with different auxotrophic markers. Although targeted integrative disruptions of specific genes were used (Longtine *et al.*, 1998), construction of double and triple mutants can be easily achieved by tetrad

dissection. Various gene deletion strains were generated by mating, sporulation and tetrad dissection as described by Sherman and Hicks (1991).

2.10.1 Mating, sporulation and tetrad dissection

To generate diploid strains, haploid strains of opposite mating types were streaked in single straight lines on separate YEPD agar plates and incubated overnight at 30°C. They were then replica plated in such a way that streaks of cells of opposite mating types were perpendicular to each other and incubated overnight. Diploids were selected by replica plating these overnight grown colonies onto YND agar supplemented with the auxotrophic requirements of the diploid strain. Diploid cells grow at the intersection of the streaks after overnight incubation. The diploid strain is selected and grown in 5 ml of YND medium supplemented with its auxotrophic requirements. Cells were harvested by centrifugation and washed twice with 10 ml of water. 10 µl of cell pellet was added to 3 ml of sporulation medium and incubated for 3 to 7 days. Formation of tetrads was examined by light microscopy. When approximately 10-15% of the cells formed tetrads, 1 ml of cells was transferred to a microcentrifuge tube and washed twice with water. The cell pellet was resuspended in 1 ml of water, and 10 µl of cells was taken from this for dissection. This 10 µl of cells was suspended in 1ml of water containing 3 to 5 µg of Zymolyase 20T and incubated at 30°C in a rotating wheel for 15 min. 20 µl of spheroplasted cells was spread in a single line on one side of a thin YEPD plate. Tetrads were dissected using a Zeiss Axioskop 40 microscope equipped with a Tetrad Manipulator System (Carl Zeiss). Isolated spores were incubated for 2 days at 30°C.

Based on the auxotrophic marker, the spores that have grown will be checked for the required gene deletion by PCR from the genomic DNA.

2.10.2 Construction of double deletion mutants

The homozygous deletion diploid strain *yhr150wΔ-HD* (Giaever *et al.*, 2002) was sporulated, and the tetrads were dissected to select for the haploid *MATa* strain. This strain was mated to the haploid *MATα* deletion strain *ydr479Δ* by replica plating to obtain a heterozygous diploid strain harboring deletions for both *YHR150w* and *YDR479c*. The diploid strain was sporulated, and tetrads from 10 heterozygous diploids were dissected by micromanipulation. All spores were grown in YPD medium, and DNA was extracted. Haploid strains carrying deletions in both the *YDR479c* and *YHR150w* genes were selected by PCR analysis. Strains harboring different double deletions of the *YLR324w*, *YGR004w*, *YBR168w*, *PEX28* and *PEX29* genes were constructed in the manner described above for a strain deleted for the *YHR150w* and *YDR479c* genes. In this way, ten strains containing the following double gene deletions were constructed: *yhr150Δ/ydr479Δ* (*DKO*), *ylr324Δ/ygr004Δ* (*DK1*), *ylr324Δ/ybr168Δ* (*DK2*), *ygr004Δ/ybr168Δ* (*DK3*), *pex28Δ/ylr324Δ* (*CD1*), *pex28Δ/ygr004Δ* (*CD2*), *pex28Δ/ybr168Δ* (*CD3*), *pex29Δ/ylr324Δ* (*CD4*), *pex29Δ/ygr004Δ* (*CD5*), and *pex29Δ/ybr168Δ* (*CD6*).

2.10.3 Construction of a triple deletion mutant

The gene conferring kanamycin resistance used to disrupt the *YBR168w* gene in the *MATa* strain of *ybr168Δ* was replaced with the gene encoding resistance to the drug

nourseothricin (Werner BioAgents, Jena, Germany) from the plasmid pHN15 (Krügel *et al.*, 1993). This nourseothricin-resistant *MATa* strain deleted for *YBR168w* was crossed with the *MATα* strain *DK1* (*YLR324Δ/YGR004Δ*), and the resultant diploid was sporulated. The strain *TKO* deleted for the *YBR168w, YLR324w and YGR004w* genes was selected on agar plates containing both kanamycin and nourseothricin, and deletion of the three genes in this strain was confirmed by PCR analysis.

2.11 Epitope tagging

Genes were genomically tagged with the sequence encoding *Staphylococcus aureus* protein A or with the sequence encoding GFP+ by homologous recombination using PCR-based integrative transformation into parental *BY4742* haploid cells (Aitchison *et al.*, 1995; Dilworth *et al.*, 2001). The functionality of fusion proteins was confirmed by the ability of transformed strains to grow and to proliferate peroxisomes like the wild-type strain *BY4742* in medium containing oleic acid as the sole carbon source. A schematic representation of the technique is shown in Figure 2-1. Strains constructed this way are listed in Table 2-4.

2.12 Construction of in-frame deletion mutants

2.12.1 Construction of *FD30* and *FD32* mutants

Yeast strains carrying in-frame deletions of the putative Pex19p binding regions in the gene of interest were constructed by overlapping PCR. This method uses a similar strategy as described in Longtine *et al.*, (1998). Briefly, the *FD30* strain was constructed

as follows. Two individual PCR fragments were initially generated. Using the genomic DNA extracted from Pex30(1-230)p as template, a forward primer upstream of the 20 amino acid of interest and a reverse primer 5'CCCTTGGTCCTTATTTATTCCTCTTGCTACTTTAGACCATG, which consists of nucleotide sequences before and after (overhang) the 20 amino acids, a first PCR fragment was generated. Thus this fragment does not have the 20 amino acids of interest. A second PCR fragment was generated using the genomic DNA extracted from Pex30p-GFP as template with a forward primer annealing immediately after the 20 amino acids of interest and a reverse primer downstream of the GFP-His5 integration (3'UTR). Thus this second PCR product has an overlapping region with the first PCR fragment. These two products were amplified together to generate a final fragment lacking the 20 amino acids of interest. This final fragment is cloned and sequenced to verify the construct and transformed into the wild type strain. The strain is once again checked by sequencing for correct in-frame deletion. Strain *FD32* was also generated in a similar manner. A schematic representation of the technique is shown in Figure 2-2.

2.12.2 Construction of *S30* and *S32* mutants

Strains carrying only the amino acid residues of interest tagged with GFP+ were constructed by overlap PCR. Here the genes of interest were cloned in plasmids and were used as template so that the integration cassette could be engineered under the control of the endogenous gene promoter (if genomic DNA were to be used, during the PCR, the homologous promoter region will anneal and the entire region will be amplified). Briefly,

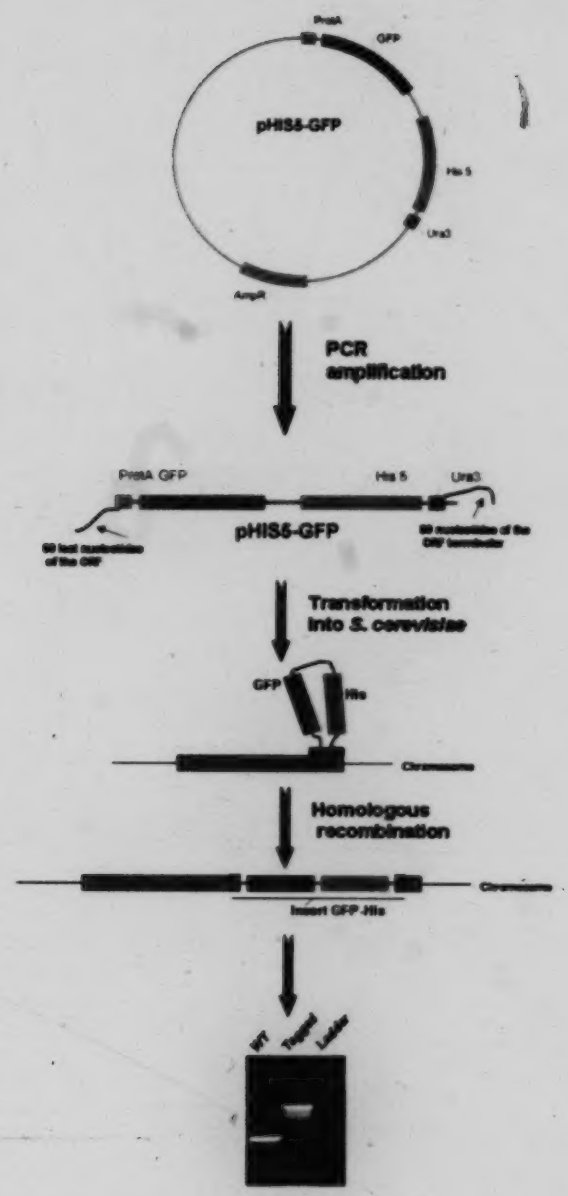

Figure 2-1. Schematic representation of genomic integration for epitope tagging genes of interest. The photograph shows the result of a strain checked for genomic integration.

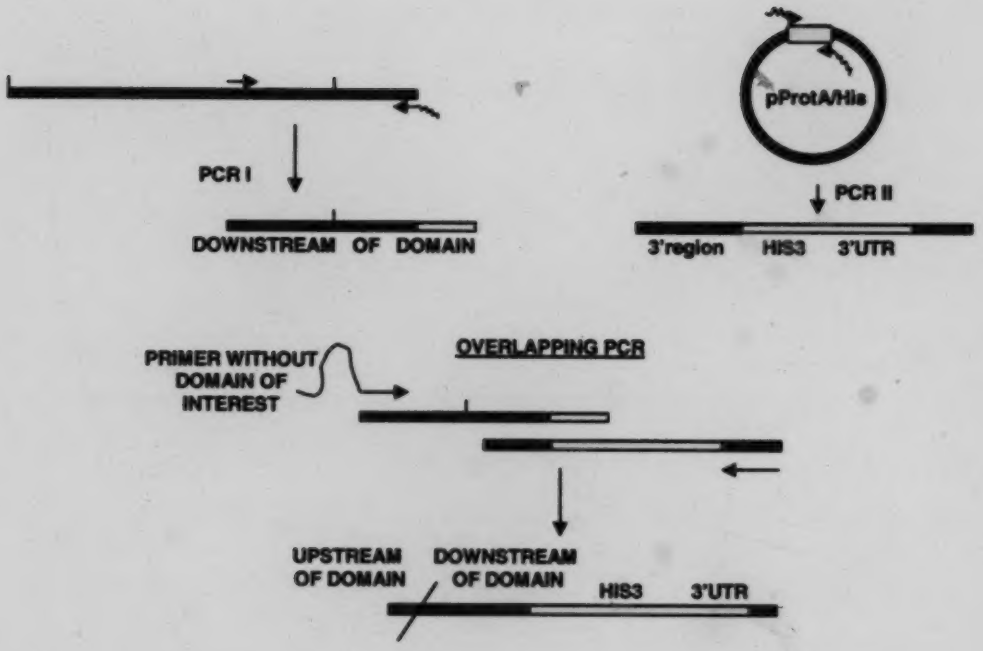

Figure 2-2. Over lapping PCR strategy. Two different PCRs will be done, one amplifying the gene of interest downstream the domain to be deleted and the second to amplify an auxotrophic marker containing sharing region with the 3'terminator region of the gene of interest. These two PCR products will be used as templates for an overlapping PCR with a forward primer without the domain of interest. The final fragment will be cloned in pGEMT easy vector (Promega) and sequenced. After verification, it will be integrated into the genome of the yeast strain and selected with the His marker.

S30 strain was constructed as follows. Two individual PCR fragments were initially generated. Using the plasmid with the gene of interest as template, forward primer 0507SG, GTTGCAATTTAGGATTCGAGCTGTCTAGTTGATCCTCCGGAGTGTA AAAACTGATTTTCAATGAGGCTTTTATGGAAGTTTAAG (which consists of 60bps of promoter region, ATG and 21bps of the beginning of the 20 amino acids of interest), and the reverse primer 0508SG, GAAAAGTTCTTCTCCT TTGCTA GCCATACCA AGGTCTAAACCCGTGAC (which consists of an overhanging GFP fragment and the last few bases of the 20 amino acid of interest), a PCR reaction was performed. A second PCR was performed using the pHis5-GFP+ plasmid as template, forward primer 0509SG, TTCTACGTCACGGGTTTAGACCTTGGTATGGCTAGCAAAGGAGAAGAA (which consists of an overhanging region of the last few bases of 20 amino acid of interest and the first 21 bases of GFP+) and a regular reverse primer normally used to make integration constructs. Thus this second PCR product has an overlapping region with the first PCR fragment. These two products were amplified together to generate a final fragment containing the 20 amino acids of interest. This final fragment is cloned and sequenced to verify the construct and transformed into the wild type strain. The strain is once again checked by sequencing for correct in-frame integration. Strains *S32* was also generated in a similar manner. A schematic representation of the technique is shown in Figure 2-2.

2.12.3 Construction of *FDV1* and *FDV2* mutants

Yeast strains carrying in-frame deletions of the putative Pex19p binding regions in the gene of interest were constructed by overlap PCR. Briefly, *FDV1* strain was

constructed as follows. Two individual PCR fragments were initially generated. Using the genomic DNA extracted from wild-type strain as template, a forward primer downstream of the amino acids of interest and a reverse primer which consists of nucleotide sequences of the last few bases of Vps1p with the stop codon, a first PCR fragment was generated. A second PCR fragment was generated using the plasmid pProtA/His5 as a template, with a forward primer containing the last few bases of Vps1 gene and a reverse primer downstream of the His5 integration. Thus this second PCR product has an overlapping region with the first PCR fragment. These two products were amplified together to generate a final fragment using a forward primer AGGTATCCTGCTCTAAGAGAAGCGATTTCTAATCAGTTCATTCAGTTCTTAAA GGATGCTCAAACTTACATCAATACAGCC lacking the amino acids of interest. This final fragment is cloned and sequenced to verify the construct and transformed into the wild type strain. The strain is once again checked by sequencing for correct in-frame deletion. Strain *FDV2* was generated in a similar manner. A schematic representation of the technique is shown in Figure 2-2.

2.13 Oligonucleotide directed mutagenesis

To construct yeast strains with desired point mutations in the gene of interest, standard PCR-based site-directed mutagenesis (Quick change XL Site directed mutagenesis kit, Stratagene, La Jolla, CA) on the plasmid pGBT9 with *PEX30* and *PEX32* cloned individually was used. Manufacturer's instructions were followed to make these constructs, briefly, 50 ng of the plasmid containing the gene and 125 ng of site-directed mutant primer were used in the mutagenesis reaction, followed by DpnI

digestion and transformed into E. coli strain. All constructs were sequenced through the coding regions of *PEX30* or *PEX32* or *VPS1*.

2.14 CP-Y filter assay

CP-Y is cotranslationally translocated into the ER, where it gets glycosylated. It is then transported to the Golgi where a sorting signal present in its propeptide form is recognized and then finally sorted to the vacuoles. Defect in this vacuolar sorting, leads to the secretion of CP-Y, through the secretory pathway, outside the cell (Marcusson *et al.*, 1994).The CPY secretion assay was performed according to the method of Roberts *et al.* (1991) with minor modifications. Briefly, cells were grown to an OD_{600} of 0.5 and spotted on YEPD plates with serial dilution and allowed to dry before filter overlay and incubation. Nitrocellulose sheet was spread on these plates spotted with diluted cells and left to grow for 24 h. The membrane is carefully lifted and rinsed to remove the cells stuck to it. Immunoblotting using the CP-Y antibody is done on the membrane and the secreted protein is detected by immunoblotting.

2.15 Two-hybrid Analysis

2.15.1 Construction of Chimeric genes

Physical interactions between Pex30p, Pex31p, Pex32p, Pex28p and Pex29p were detected using the Matchmaker Two-Hybrid System (Clontech). Chimeric genes were generated by amplifying the ORFs of the *PEX30, PEX31, PEX32, PEX28* and *PEX29* genes by PCR and ligating them in-frame and downstream of the DNA encoding the

transcription-activating domain (AD) and the DNA-binding domain (DB) of the GAL4 transcriptional activator in the plasmids pGAD424 and pGBT9, respectively. Cells of *S. cerevisiae* strain *SFY526* were transformed simultaneously with a pGAD424-derived plasmid and a pGBT9-derived plasmid.

2.15.2 Two-hybrid analysis

Transformants were grown on SM medium lacking tryptophan and leucine and tested for activation of the integrated *lacZ* construct using a β-galactosidase filter assay (Smith and Rachubinski, 2001). Plasmid pairs encoding AD and DB fusion proteins were transformed into *S. cerevisiae* strain *SFY526*. Transformants were grown in SM medium (Table 2-9). Possible interaction between AD and DB fusion proteins were detected by testing for activation of the integrated *lacZ* construct using β-galactosidase filter and liquid assays according to the instructions of Clontech, with modifications. For filter assays, cells were streaked directly onto filter paper placed on solid media and broken by 4 freeze-thaw cycles at -80°C. Z buffer was used to detect the β-galactosidase activity.

2.16 Computer aided analysis

Major contribution to this study was brought about by computer aided analysis. Protein sequences of *Yl*Pex23p and *Yl*Pex24p were compared to other sequences in the database using the BLAST algorithms (http://www.ncbi.nlm.nih.gov/BLAST/) (National Center for Biotechnology Information) and aligned using the ClustalW program

(http://www.edi.ac.uk/clustalw/) (EMBL-EBI). This led to the identification of Pex28p, Pex29p, Pex30p, Pex31p and Pex32p.

The promoter regions of *PEX30*, *PEX31* and *PEX32* contain sequences that resemble the canonical sequence $CCGN_3TNAN_{8-12}CGG$ of the oleic acid response element (ORE) (Rottensteiner *et al.*, 2002; 2003a), which acts to increase gene transcription in *S. cerevisiae* in the presence of oleic acid as a carbon source through the binding of the transcription factors Pip2p and Oaf1p (Rottensteiner *et al.*, 1996; Karpichev *et al.*, 1997). This was identified by computer analysis. Whether these sequences actually do function as OREs is yet to be determined.

To identify the putative Pex19p binding site using the consensus sequence developed by Rottensteiner *et al.*, 2004, we used Protein Sub-string Match Analysis (PSMA) software developed in C++ on Linux operating system. It uses pattern matching algorithm from pair wise alignment of multiple sequence alignment (MSA). This matches the consensus motifs which may include unknown or multiple combinations of different factors and extracts from any given sequence. Using this, we could identify any consensus sequence of interest present in any protein of interest.

Also, protein sequences were analyzed using the CBS Prediction Servers (http://www.cbs.dtu.dk/services/TMHMM/) (Center for Biological Sequence Analysis) for identification of transmembrane domains. Apart from this, Yeast Proteome Database (http://www.proteome.com/) (Incyte genomics) and the *Saccharomyces* Genome Database (http://www.yeastgenome.org/) (Stanford University) were extensively used for a number of purposes.

CHAPTER THREE

PEX28 AND *PEX29* ENCODE PEROXISOMAL INTEGRAL MEMBRANE PROTEINS INVOLVED IN THE REGULATION OF PEROXISOME NUMBER, SIZE, AND DISTRIBUTION

A portion of this chapter has previously been published as "*YHR150w* and *YDR479c* encode peroxisomal integral membrane proteins involved in the regulation of peroxisome number, size, and distribution in *Saccharomyces cerevisiae*" (Franco J. Vizeacoumar, Juan C. Torres-Guzman, Yuen Yi C. Tam, John D. Aitchison, and Richard A. Rachubinski. 2003. *J Cell Biol.* 2003 Apr 28; 161(2):321-32). Reprinted with permission.

3.1 Overview

The peroxin Pex24p of the yeast *Yarrowia lipolytica* exhibits high sequence similarity to two hypothetical proteins, Yhr150p and Ydr479p, encoded by the *Saccharomyces cerevisiae* genome. Like *Yl*Pex24p, both Yhr150p and Ydr479p have been shown to be integral to the peroxisomal membrane, but unlike *Yl*Pex24p, their levels of synthesis are not increased upon a shift of cells from glucose- to oleic acid-containing medium. Peroxisomes of cells deleted for either or both of the *YHR150w* and *YDR479c* genes are increased in number, exhibit extensive clustering, are smaller in area than peroxisomes of wild-type cells, and often exhibit membrane thickening between adjacent peroxisomes in a cluster. Peroxisomes isolated from cells deleted for both genes have a decreased buoyant density compared to peroxisomes isolated from wild-type cells and still exhibit clustering and peroxisomal membrane thickening. Overexpression of the genes *PEX25* or *VPS1*, but not the gene *PEX11*, restored the wild-type phenotype to cells deleted for one or both of the *YHR150w* and *YDR479c* genes. Together, our data suggest a role for Yhr150p and Ydr479p, together with Pex25p and Vps1p, in regulating peroxisome number, size and distribution in *S. cerevisiae*.

3.2 Yhr150p and Ydr479p share extensive similarity with YlPex24p

*Yl*Pex24p is an integral peroxisomal membrane protein that has been shown to be required for peroxisome assembly in the yeast *Y. lipolytica* (Tam and Rachubinski, 2002). A search of protein databases with the GENEINFO(R)BLAST Network Service of the National Center for Biotechnology Information revealed two proteins encoded by the

ORFs *YHR150w* and *YDR479c* of the *S. cerevisiae* genome that exhibit extensive sequence similarity to *Yl*Pex24p (Figure 3-1). The alignment and homology identification was done by Dr. Richard A. Rachubinski. *Yl*Pex24p and Yhr150p exhibit 21.1% amino acid identity and 44.4% amino acid similarity, *Yl*Pex24p and Ydr479p exhibit 20.8% amino acid sequence identity and 42.1% amino acid similarity, while Yhr150p and Ydr479p exhibit 20.4% amino acid identity and 41.3% amino acid similarity. Yhr150p is predicted to be a protein of molecular weight 66,145 Daltons and to have two transmembrane helices at amino acid residues 246-268 and 393-415 (http://www.cbs.dtu.dk/services/TMHMM-2.0/) (Krogh et al., 2001). Ydr479p is predicted to be a protein of molecular weight 63,533 Dalton and to have four transmembrane helices at amino acid residues 146-165, 172-194, 265-284 and 291-308. Some potential functional redundancy between Yhr150p and Ydr479p may have prevented them from being identified as being involved in peroxisome assembly in *S. cerevisiae* by procedures involving random mutagenesis and negative selection for growth of yeast on oleic acid-containing medium.

3.3 Synthesis of Yhr150p and Ydr479p are not induced

The synthesis of many peroxisomal proteins is induced by the incubation of yeast cells in oleic acid-containing medium. Genomically encoded protein A chimeras of Yhr150p and Ydr479p were monitored to analyze the expression of *YHR150w* and *YDR479c*, respectively, under the control of their endogenous gene promoters. Yeast strains synthesizing Yhr150p-prA, Ydr479p-prA, thiolase-prA and Pex17p-prA were

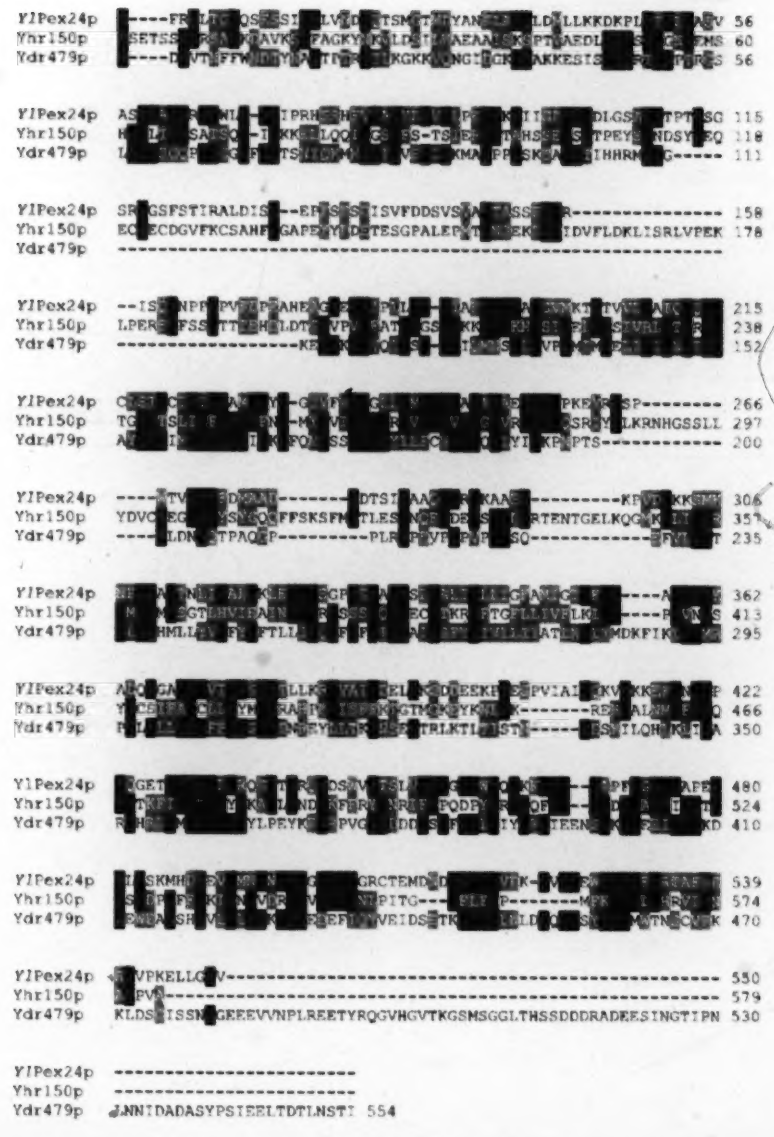

Figure 3-1. Sequence alignment of *Yarrowia lipolytica* Pex24p with the proteins Yhr150p and Ydr479p encoded by the *Saccharomyces cerevisiae* genome. Amino acid sequences were aligned with the use of the ClustalW program (EMBL-EBI, Cambridge, United Kingdom) (http://www.ebi.ac.uk/clustalw/). Identical residues (black) and similar residues (gray) in at least two of the proteins are shaded. Similarity rules: G = A = S; A = V; V = I = L = M; I = L = M = F = Y = W; K = R = H; D = E = Q = N; and S = T = Q = N. Dashes represent gaps. This figure was aligned Dr. Richard A. Rachubinski.

grown in glucose-containing YPD medium and then shifted to oleic acid-containing YPBO medium. Aliquots of cells were removed at various times after the shift to YPBO medium, and their lysates were subjected to SDS-PAGE and immunoblotting (Figure 3-2). Yhr150p-prA and Ydr479-prA, as well as Pex17p-prA (Huhse et al., 1998), were detected in glucose-containing YPD medium at the time of transfer, and their respective levels did not increase with time of incubation of cells in YPBO medium. In contrast, thiolase-prA was barely detectable in cells at the time of transfer to YPBO medium, and its levels were substantially increased with time of incubation in YPBO medium.

3.4 Yhr150p and Ydr479p are integral membrane proteins

A carboxyl-terminal PTS1 is sufficient to direct a reporter protein to peroxisomes (for a review, see Purdue and Lazarow, 2001). A fluorescent chimera between *Discosoma sp.* red fluorescent protein (DsRed) and the PTS1 Ser-Lys-Leu has been shown to target to peroxisomes of *S. cerevisiae* (Smith et al., 2002). Genomically encoded protein A chimeras of Yhr150p, Ydr479p, the peroxisomal peroxin Pex17p (Huhse et al., 1998) and the mitochondrial translocon protein Tom20p (Lithgow et al., 1994) were localized in oleic acid-induced cells by indirect immunofluorescence microscopy combined with direct fluorescence from DsRed-PTS1 to identify peroxisomes (Figure 3-3). Yhr150p-prA, Ydr479p-prA and Pex17p-prA colocalized with DsRed-PTS1 to small punctate structures characteristic of peroxisomes by confocal microcopy. As expected, Tom20p-prA did not colocalize with DsRed-PTS1, as the respective individual green and red signals for these proteins remained separate in confocal microscopy.

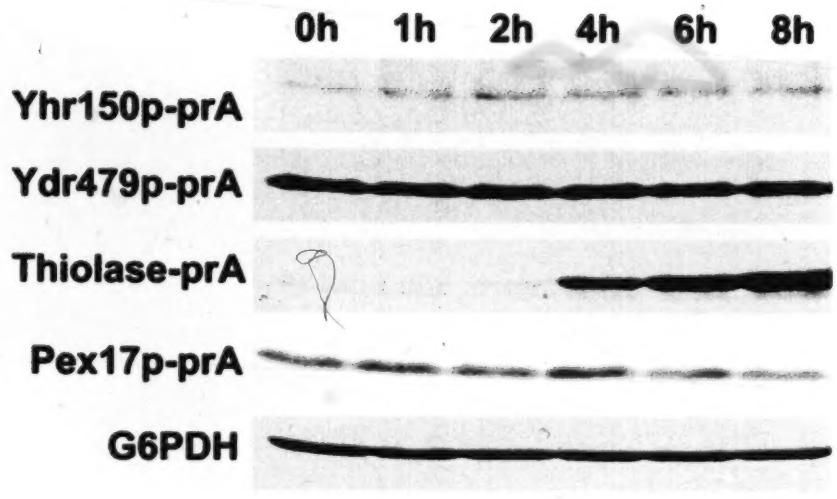

Figure 3-2. Yhr150p-prA and Ydr479p-prA remain at constant levels during incubation of *S. cerevisiae* in oleic acid-containing medium. Cells were grown for 16 h in glucose-containing YPD medium and then transferred to, and incubated in, oleic acid-containing YPBO medium. Aliquots of cells were removed from the YPBO medium at the times indicated, and total cell lysates were prepared. Equal amounts of protein from the total cell lysates were analyzed by SDS-PAGE and immunoblotting to visualize the protein A fusions. Antibodies directed against glucose-6-phosphatase (G6PDH) were used to confirm the loading of equal protein in each lane.

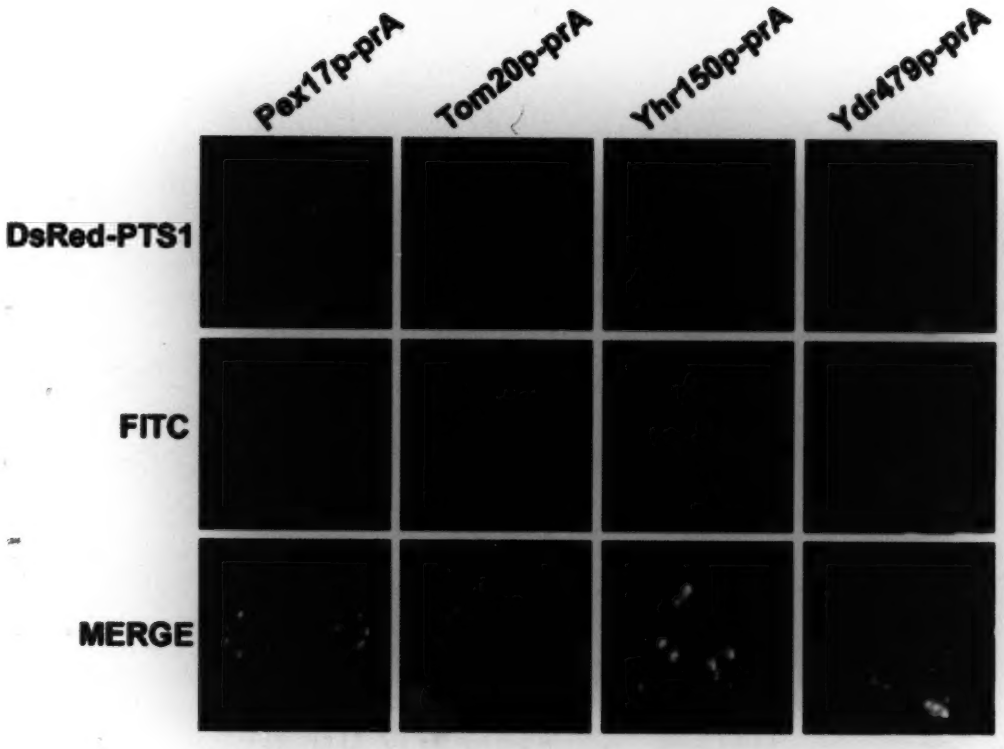

Figure 3-3. Yhr150p-prA and Ydr479p-prA are peroxisomal proteins by microscopy. The subcellular distributions of protein A chimeras were compared to that of DsRed-PTS1 in oleic acid-incubated cells by double labeling, indirect immunofluorescence microscopy. Yhr150p-prA and Ydr479p-prA colocalize with DsRed-PTS1 in punctate structures characteristic of peroxisomes. There is no colocalization of DsRed-PTS1 and the protein A chimera of the mitochondrial protein, Tom20p. Protein A chimeras were detected with rabbit antibodies to mouse IgG and FITC-conjugated goat anti-rabbit IgG secondary antibodies.

Subcellular fractionation and organelle extraction were used to establish if Yhr150p and Ydr479p are associated with peroxisomes and to determine their suborganellar locations. Cells expressing Yhr150p-prA, Ydr479p-prA and Pex17p-prA were incubated in oleic acid-containing medium and subjected to subcellular fractionation to yield postnuclear supernatant (PNS) fractions. The PNS fractions were subjected to further centrifugation to yield a supernatant fraction (20KgS) enriched for cytosol and a crude organellar pellet fraction (20KgP). Equal portions of the PNS, 20KgS and the 20KgP were analyzed by immunoblotting. Yhr150p-prA, Ydr479p-prA and Pex17p-prA all preferentially localized to the 20KgP fraction (Figure 3-4 A). Peroxisomes were isolated from the 20KgP fractions of each of the strains expressing Yhr150p-prA, Ydr479p-prA and Pex17p-prA. The gradients were fractionated, and equal portions of each fraction were analyzed by immunoblotting (Figure 3-4 B). Yhr150p-prA and Ydr479p-prA coenriched with the peroxisomal peroxin Pex17p-prA and not with the mitochondrial protein, Sdh2p. Therefore, both microscopic analysis and subcellular fractionation showed Yhr150p and Ydr479p to be peroxisomal proteins. Some amount of Ydr479p-prA was always present in the 20KgS fraction and in the lighter fractions during the gradient isolation of peroxisomes. Whether this represents a selective liberation of a soluble form of Ydr479p-prA during the isolation of peroxisomes remains undetermined. It is unlikely that Ydr479p-prA is found in a cellular compartment in addition to peroxisomes, as immunostaining for Ydr479p-prA yielded exclusively a punctate pattern corresponding to the punctate pattern of peroxisomes defined by DsRed-PTS1 (Figure 3-3). In addition, this punctate compartment does not correspond to mitochondria, as the fluorescence pattern generated with the mitochondria-specific dye MitoTracker did not

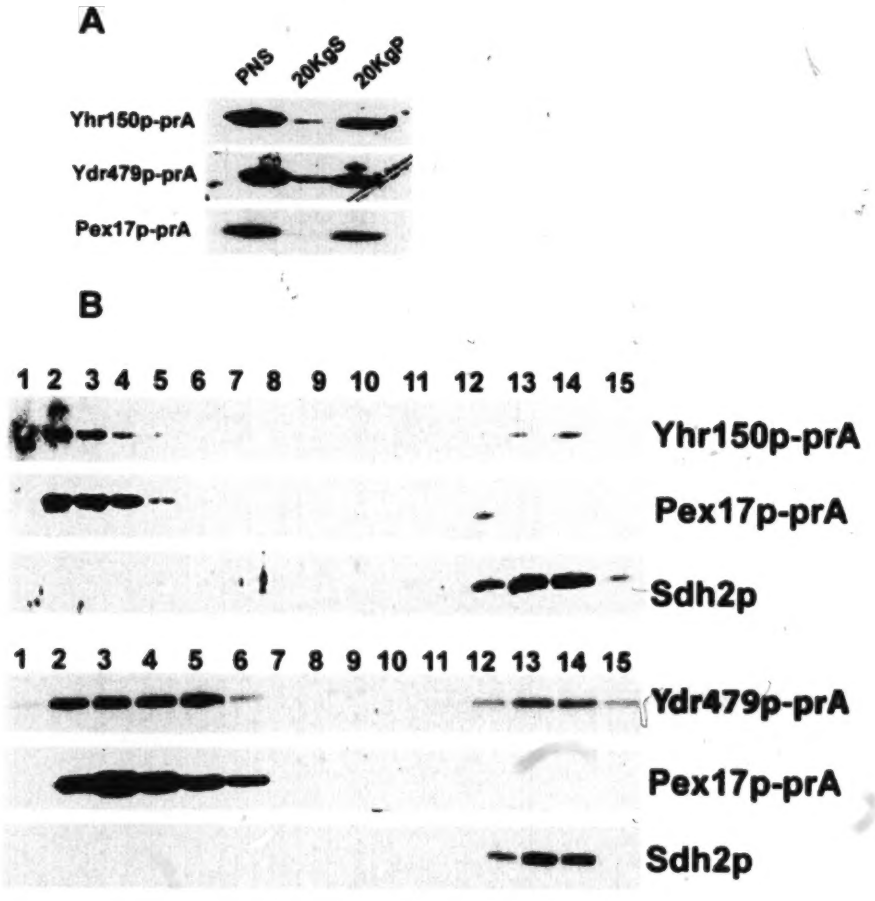

Figure 3-4 A and B. Yhr150p-prA and Ydr479p-prA are primarily peroxisomal proteins. (A) A PNS fraction was divided by centrifugation into a supernatant (20KgS) fraction enriched for cytosol and a pellet (20KgP) fraction enriched for peroxisomes and mitochondria. Equivalent portions of each fraction were analyzed. Immunoblotting detected the protein A chimeras shown, including that of the peroxisomal protein Pex17p. (B) Yhr150p-prA and Ydr479p-prA cofractionate with peroxisomes. Organelles in the 20KgP fraction were separated by isopycnic centrifugation on a discontinuous Nycodenz gradient. Fractions were collected from the bottom of the gradient, and equal portions of each fraction were analyzed by immunoblotting. Fractions enriched for peroxisomes and mitochondria were identified by immunodetection of the protein A chimera of Pex17p and Sdh2p, respectively.

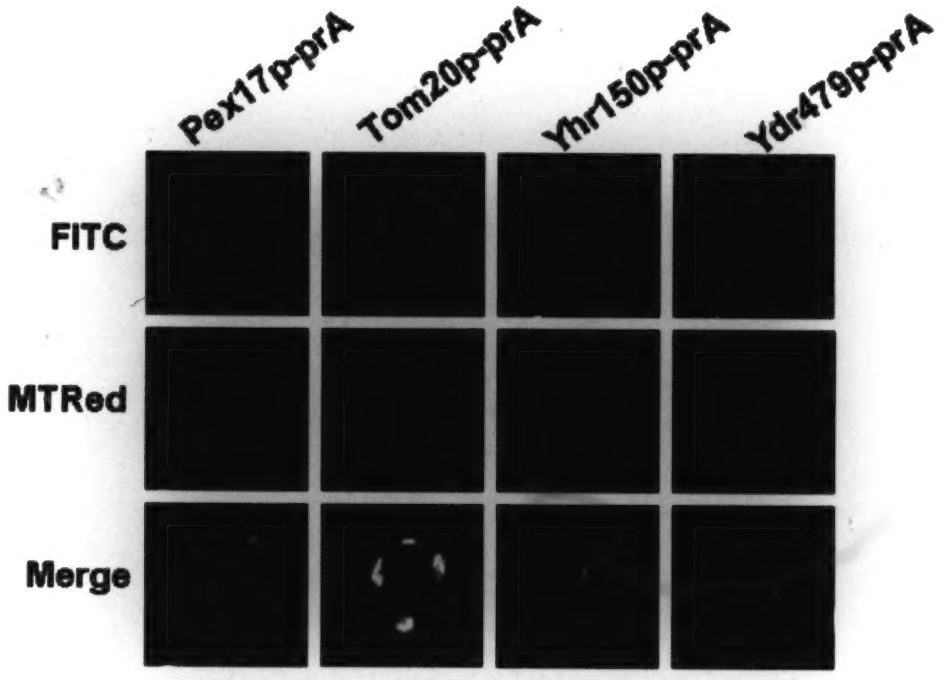

Figure 3-4 C. Yhr150p-prA and Ydr479p-prA are not mitochondrial proteins by microscopy. The subcellular distributions of protein A chimeras were compared to that of fixable dye Mitotracker in oleic acid-incubated cells by double labeling, indirect immunofluorescence microscopy. Tom20p-prA colocalize with Mitotracker in elongated tubular structures characteristic of mitochondria. Protein A chimeras were detected with rabbit antibodies to mouse IgG and FITC-conjugated goat anti-rabbit IgG secondary antibodies.

overlap with the punctate pattern generated by detection of Ydr479p-prA by immunofluorescence (Figure 3-4 C).Peroxisomes were hypotonically lysed by incubation in dilute alkali Tris buffer and subjected to centrifugation to yield a supernatant (Ti8S) enriched for matrix proteins and a pellet (Ti8P) enriched for membrane proteins (Figure 3-4 D). The chimeras of Yhr150p and Ydr479p localized primarily to the Ti8P fraction, as did the chimeras of the peripheral peroxisomal membrane protein Pex17p (Huhse et al., 1998) and the integral peroxisomal membrane protein Pex3p (Höhfeld et al., 1991). The soluble peroxisomal matrix protein thiolase was found almost exclusively in the Ti8S fraction. The reproducible presence of some Ydr479p in the Ti8S fraction may again be representative of a soluble form of this protein that is selectively liberated during the isolation of peroxisomes (see Figure 3- 4 A, B). The Ti8P fractions were then extracted with alkali sodium carbonate and subjected to centrifugation (Figure 3- 4 D). This treatment releases proteins associated with, but not integral to, membranes (Fujiki et al., 1982). Under these conditions, Yhr150p-prA and Ydr479p-prA fractionated with Pex3p-prA to the pellet fraction enriched for integral membrane proteins, while Pex17p-prA fractionated to the supernatant fraction enriched for soluble proteins, including peripheral membrane proteins. These data suggest that Yhr150p and Ydr479p are both primarily integral peroxisomal membrane proteins, as has been shown for *Yl*Pex24p (Tam and Rachubinski, 2002).

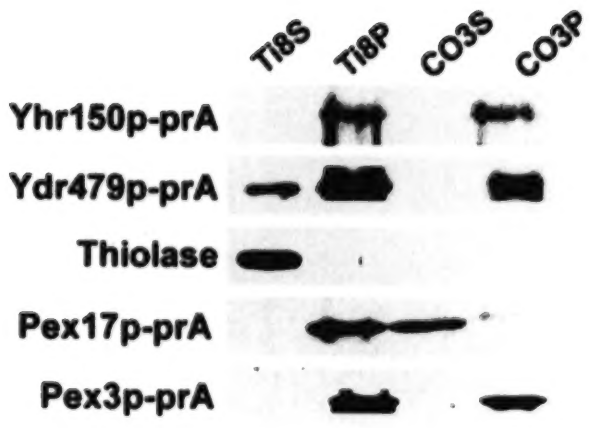

Figure 3-4 D. Yhr150p-prA and Ydr479p-prA are integral peroxisomal membrane proteins. Peroxisomes purified by isopycnic density gradient centrifugation were lysed by treatment with 10 mM Tris-HCl, pH 8.0, releasing matrix proteins to a supernatant fraction (Ti8S) after centrifugation. The membrane-containing pellet fraction (Ti8P) was treated with 0.1 M Na_2CO_3, pH 11.3, and then subjected to centrifugation to yield a supernatant fraction (CO3S) enriched for peripherally associated membrane proteins and a pellet fraction (CO3P) enriched for integral membrane proteins. Equal portions of the respective supernatant and pellet fractions were analyzed by immunoblotting. Immunodetection of thiolase, Pex17p-prA and Pex3p-prA marked the fractionation profiles of a matrix, peripheral membrane and integral membrane protein, respectively.

3.5 Abnormal peroxisomes are found in both single and double mutants of yhr150w and ydr479c

We next investigated the functionality of peroxisomes in the deletion mutants of these genes. Dr.Juan Carlos Guzman Torres constructed the double deletion mutant and checked for their growth defect. Both the single and double deletion mutants grew like the wild-type cells on oleic acid-containing medium (Figure 3-4 E). Import of matrix proteins in these mutants were unaffected (Figure 3-4 F). We next investigated the ultrastructure of cells incubated in oleic acid-containing YPBO medium by transmission EM. Wild-type cells (Figure 3- 5 A) consistently showed individual peroxisomes well separated from one another. In contrast, cells of the *yhr150Δ* (Figure 3-5 B), *ydr479Δ* (Figure 3-5 C) and, particularly, the *yhr150Δ/ydr479Δ* (Figure 3-5 D) strains contained peroxisomes that exhibited clustering. 28.0%, 19.2% and 20.4% of peroxisomes of cells of the *yhr150Δ/ydr479Δ*, *ydr479Δ* and *yhr150Δ* strains, respectively, showed clustering, in contrast to 4.0% of peroxisomes of wild-type cells - a cluster of peroxisomes was operationally defined as 3 or more adherant peroxisomes (Figure 3-5 F and G). The clustered peroxisomes often showed evidence of membrane thickening between adjacent peroxisomes in the cluster. Morphometric analysis showed that cells of the deletion strains contained a greater number of peroxisomes than did wild-type cells and that, on average, these peroxisomes were smaller in size than those of wild-type cells (Table 3-1). Cells of the deletion strains contained much greater numbers of peroxisomes with areas of 0.02 μm^2 or less than did wild-type cells (Figure 3-5 E). Nycodenz density gradient centrifugation analysis showed that peroxisomes purified from *yhr150Δ/ydr479Δ* cells

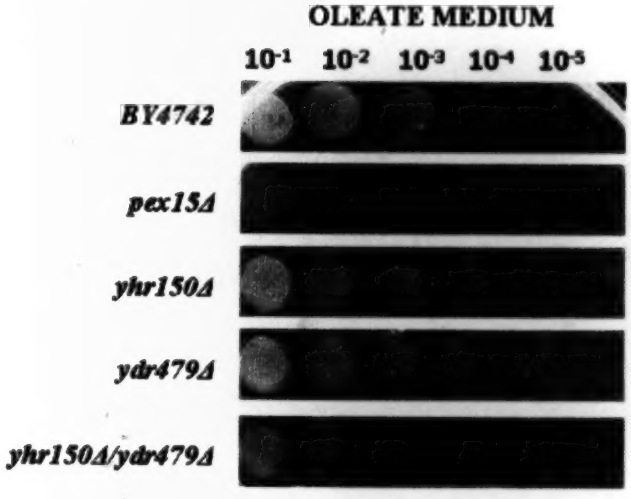

Figure 3-4 E. Growth of different strains on YPBO medium. All strains were spotted after serial dilution and grown over a period of 4 days at 30C. This figure was contributed by Dr.Juan carlos Guzman Torres.

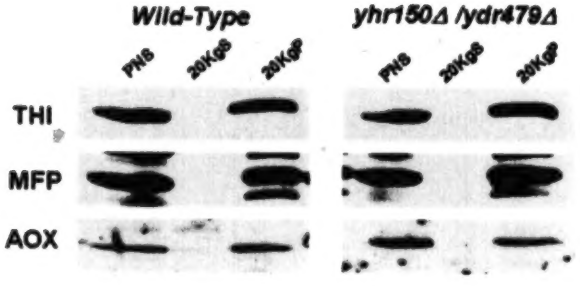

Figure 3-4 F. Distribution of matrix proteins in the mutants. Subcellular localization of matrix proteins were analysed by differential fractionation. A PNS fraction was divided by centrifugation into a supernatant (20KgS) fraction enriched for cytosol and a pellet (20KgP) fraction enriched for peroxisomes and mitochondria. Equivalent portions of each fraction were analyzed.

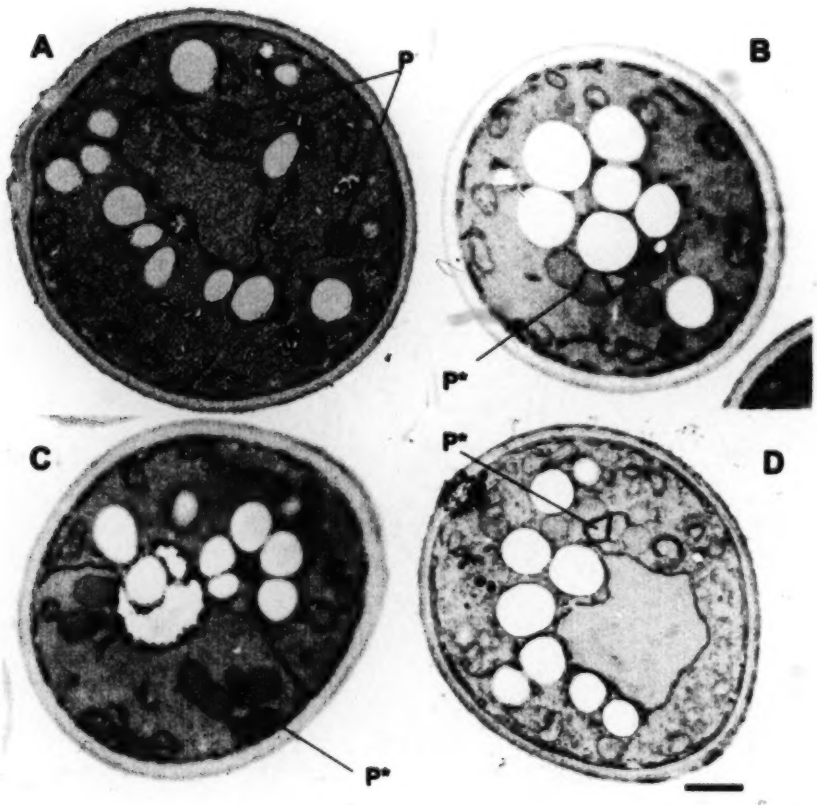

Figure 3-5. Peroxisomes are smaller, more abundant and exhibit clustering in cells deleted for either or both of the *YHR150w* and *YDR479c* genes. Ultrastructure of wild-type *BY4742* (A), *yhr150Δ* (B), *ydr479Δ* (C) and *yhr150Δ/ydr479Δ* (D) cells. Cells were grown in YPD medium overnight, transferred to YPBO medium and incubated in YPBO medium for 8 h. Cells were fixed and processed for EM. P, peroxisome. P*, peroxisome cluster. Bar, 0.5 μm. The double deletion mutant was constructed by Dr.Juan Carlos Torres Guzman.

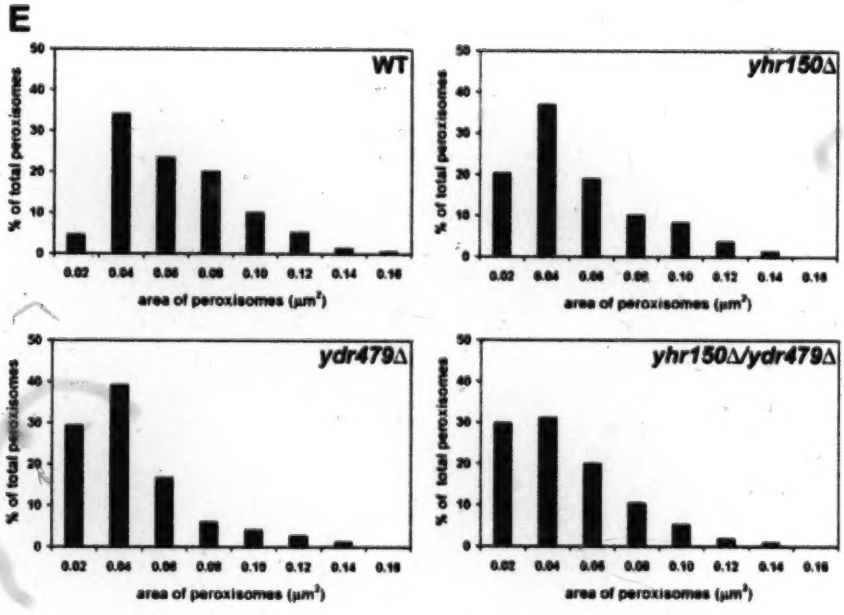

Figure 3-5 E. Morphometric analysis of peroxisomes. Oleic acid-incubated wild-type (*WT*) *BY4742* and deletion mutant cells were analyzed. For each strain analyzed, electron micrographs of 50 randomly selected cells at × 17,000 magnification were scanned, and the areas of individual peroxisomes were determined by counting the number of individual pixels in a peroxisome with Image Tools for Windows, Version 2.00. The peroxisomes were then separated into size categories. A histogram was generated for each strain depicting the percentage of total peroxisomes occupied by the peroxisomes of each category. The numbers along the *x*-axis are the maximum sizes of peroxisomes in each category (in μm^2).

F

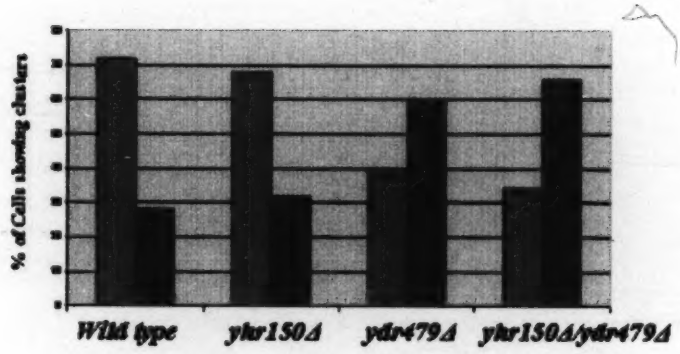

G

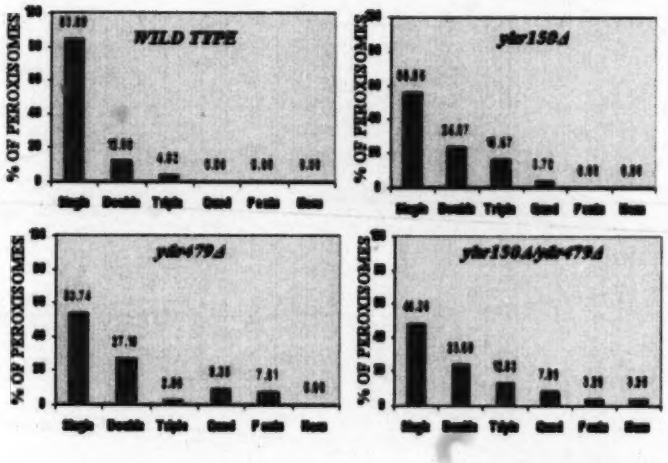

Figure 3-5 F and G. Analysis of the clustering of the peroxisomes. (F) The number of cells exhibiting clusters were counted and represented graphically. (G) The number of different peroxisomal clusters that were present in the wild type and various mutants quantitated were represented graphically.

Table 3-1. Average area and numerical density of peroxisomes in wild-type and deletion strains

Strain	Cell area assayed (μm^2)	Peroxisome count[a]	Numerical density of peroxisomes[b]	Average area of peroxisomes[c] (μm^2)
WT (BY4742)	404	0.37	1.71	0.055
yhr150Δ	424	0.51	2.59	0.048
ydr479Δ	382	0.56	3.20	0.039
yhr150Δ/ydr479Δ	381	0.80	4.38	0.040

[a]Number of peroxisomes counted per μm^2 of cell area on micrographs.
[b]Number of peroxisomes per μm^3 of cell volume (Weibel and Bolender, 1973).
[c]Average area on micrographs.

have a greatly reduced density (peak fraction 8, 1.19 g/cm^3) compared to peroxisomes from wild-type cells (peak fraction 1, 1.22 g/cm^3) (Figure 3-6 A). Peroxisomes isolated from cells deleted for *YHR150w* or *YDR479c* were also less dense than wild-type peroxisomes, although the differences in density were less than that observed between peroxisomes from *yhr150Δ/ydr479Δ* cells and wild-type peroxisomes (Figure 3-6 A). EM analysis showed that the peroxisomes purified from *yhr150Δ/ydr479Δ* cells still exhibited clustering and evidence of thickened peroxisomal membranes, while peroxisomes purified from wild-type cells were largely well separated from one another, with no evidence of membrane thickening (Figure 3-6 B).

3.6 Overexpression of *PEX11*, *PEX25* and *VPS1*

Since cells deleted for one or both of the *YHR150w* and *YDR479c* genes are compromised in their regulation of peroxisome number, size and distribution, we investigated the effects of overexpression of three genes previously shown to be involved in these processes in *S. cerevisiae*. Cells of strains mutant for the genes encoding the peroxisomal peroxins Pex11p (Erdmann and Blobel, 1995; Marshall et al., 1995, 1996), Pex25p (Smith et al., 2002) and the dynamin-like protein Vps1p (Hoepfner et al., 2001) have reduced numbers of enlarged peroxisomes compared to wild-type cells (Figure 3-13). Overexpression of *PEX25* (Figure 3-7 and Figure 3-11) or *VPS1* (Figure 3- 7 and Figure 3-12) in cells deleted for one or both of the *YHR150w* and *YDR479c* genes led to a partial restoration of the wild-type peroxisomal phenotype, with overexpressing cells containing increased numbers of separate, individual peroxisomes and reduced numbers of peroxisomal clusters. In contrast, overexpression of *PEX11* did not appear to have any

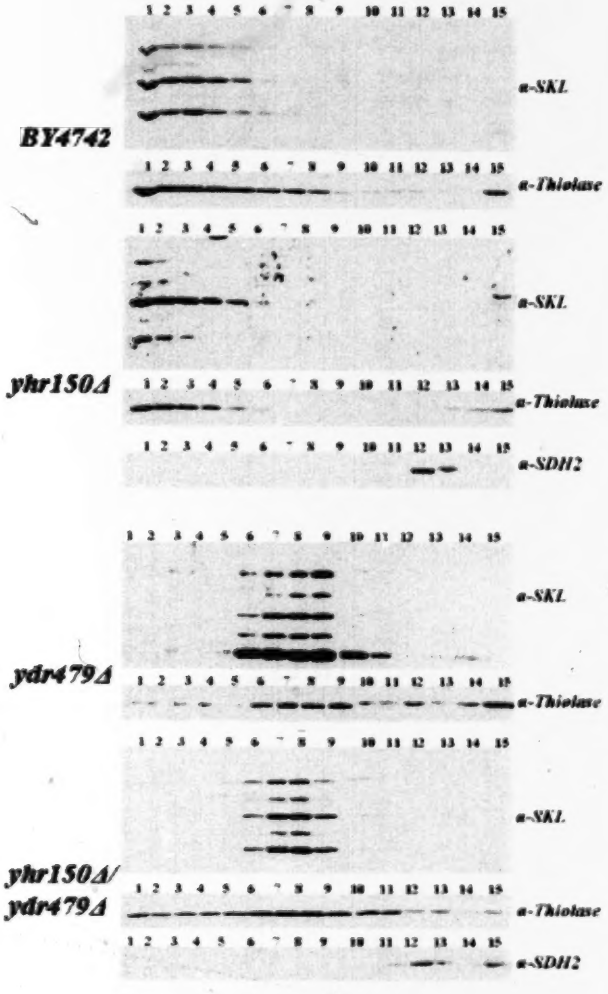

Figure 3-6. Peroxisomes isolated from *yhr150Δ /ydr479Δ* cells are less dense than isolated wild-type peroxisomes and retain a clustered phenotype. (A) The wild-type (*WT*) strain *BY4742* and the mutant strain *yhr150Δ/ydr479Δ* were grown overnight in YPD medium, transferred to oleic acid-containing YPBO medium and incubated in YPBO medium for 8 h. A PNS fraction was prepared from cells of each strain and divided by centrifugation into 20KgS and 20KgP fractions. Organelles in the 20KgP fraction were separated by isopycnic centrifugation on a continuous 30% to 45% Nycodenz gradient. Fractions were collected from the bottom of the gradient, and equal portions of each fraction were analyzed by immunoblotting with antibodies to the PTS1, Ser-Lys-Leu, to detect peroxisomes.

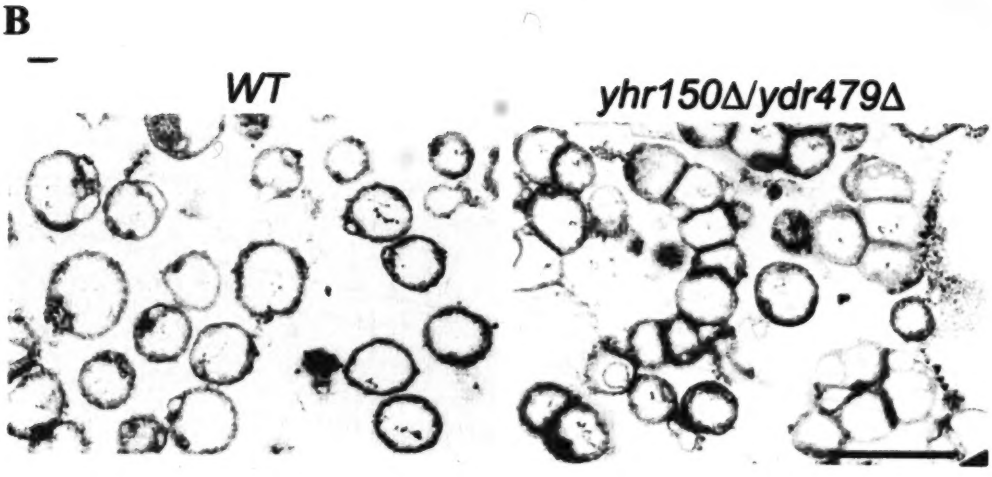

Figure 3-6 B. Electron micrographs of purified peroxisomes. Peak peroxisomal fractions from cells of the wild-type strain (*WT*) *BY4742* (Fraction 1) and the mutant strain *yhr150Δ/ydr479Δ* (Fraction 8). Bar, 0.5 µm.

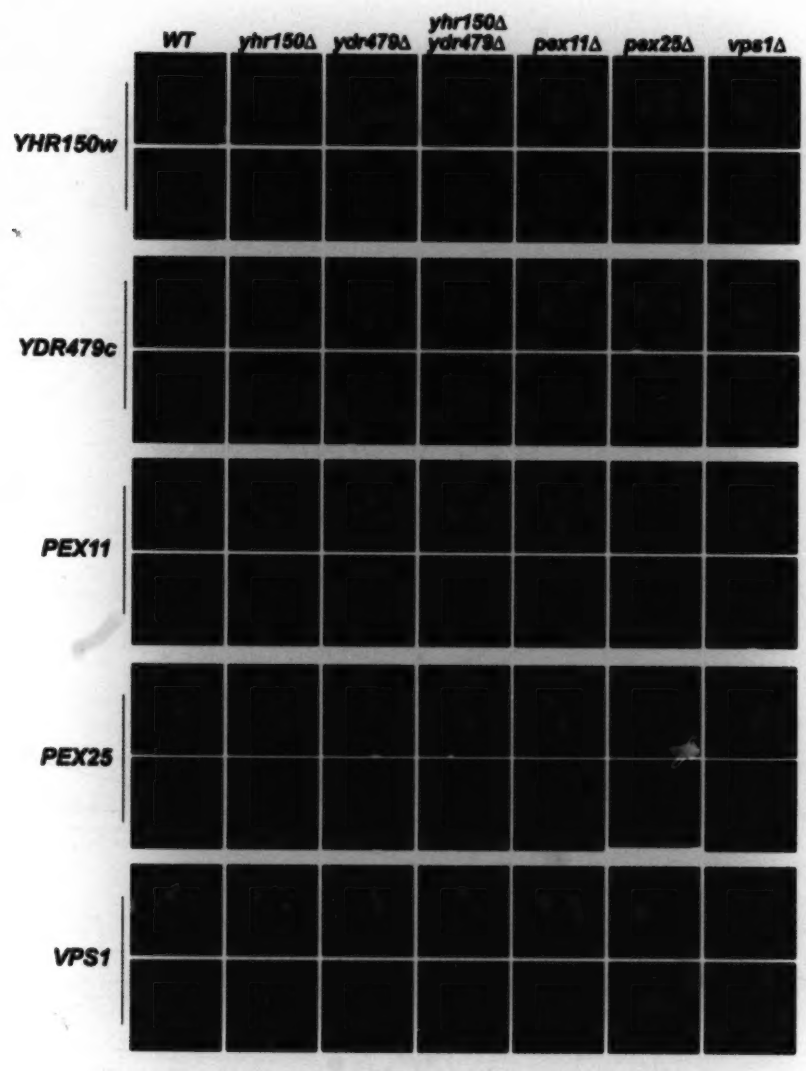

Figure 3-7. Peroxisome morphology in cells of gene overexpression strains. Cells were grown in SM medium overnight, transferred to YPBO medium and incubated in YPBO medium for 8 h. Peroxisomes were detected by double labeling, indirect immunofluorescence microscopy with antibodies to the PTS1 Ser-Lys-Leu (SKL) and FITC-conjugated goat anti-rabbit IgG secondary antibodies, and with guinea pig antibodies to the PTS2-containing protein thiolase and rhodamine-conjugated donkey anti-guinea pig IgG secondary antibodies. The genetic backgrounds of the different yeast strains are given at *Top*, and the genes that are overexpressed are denoted at *Left*.

effect on the abnormal peroxisome morphology observed in cells mutant for the *YHR150w* and *YDR479c* genes (Figure 3-7, Figure 3-10). It should be noted that overexpression of the *YHR150w* gene led to restoration of wild-type peroxisome morphology in ***yhr150Δ*** cells but not in ***ydr479Δ*** cells or in cells deleted for both the *YHR150w* and *YDR479c* genes (Figure 3-7, Figure 3-8). In contrast, overexpression of *YDR479c* led to restoration of wild-type peroxisome morphology not only in ***ydr479Δ*** cells, but also in ***yhr150Δ*** cells and cells deleted for both genes (Figure 3-7, Figure 3-9). Therefore, it appears that Yhr150p may be in large part redundant in its functions in regulating peroxisome dynamics vis-à-vis Ydr479p. Attempts at demonstrating physical interactions, either direct or indirect, between Yhr150p and Ydr479p or between these two proteins and Pex11p, Pex25p or Vps1p were unsuccessful.

As reported previously (Erdmann and Blobel, 1995; Marshall et al., 1995, 1996; Hoepfner et al., 2001; Smith et al., 2002), cells deleted individually for the *PEX11*, *PEX25* and *VPS1* genes contained reduced numbers of enlarged peroxisomes (Figure 3-7 and Figure 3-13). Overexpression of the *PEX11* gene in wild-type cells or in cells deleted for *PEX11*, *PEX25* or *VPS1* led to a proliferation of smaller peroxisomes (Figure 3-7 and Figure 3-10). However, overexpression of *PEX25* or *VPS1*, while resulting in normal peroxisome morphology in their respective mutant backgrounds, did not affect the peroxisome morphology in the opposite mutant background (Figure 3-7, Figure 3-11 and Figure 3-12). Overexpression of *PEX25*, but not *VPS1*, led to only a nominal increase in the number of normal peroxisomes in cells deleted for the *PEX11* gene (Figure 3-7 and Figure 3-11). Moreover, the ***pex11Δ*** cells retained their enlarged peroxisomal phenotype when either *YHR150w* or *YDR479c* was overexpressed (Figure 3-7, Figure 3-8 and Figure

Table 3-2. Summary of results of gene overexpression

	NORMAL PEROXISOMES	CLUSTERED PEROXISOMES	ENLARGED PEROXISOMES
***YHR150w* overexpression in**			
Wild-Type	++++*		
yhr150Δ	++++		
ydr479Δ	+++	+	
yhr150Δ/ydr479Δ	++	++	
pex11Δ	+		+++
pex25Δ	+		+++
vps1Δ			++++
***YDR479w* overexpression in**			
Wild-Type	++++		
yhr150Δ	++++		
ydr479Δ	++++		
yhr150Δ/ydr479Δ	++++		
pex11Δ	+		+++
pex25Δ	+		+++
vps1Δ			++++
***PEX11* overexpression in**			
Wild-Type	++	++	
yhr150Δ	+	+++	
ydr479Δ	+	+++	
yhr150Δ/ydr479Δ	+	+++	
pex11Δ	+	+++	
pex25Δ	++	+	+
vps1Δ	+	++	+
***PEX25* overexpression in**			
Wild-Type	++		++
yhr150Δ	++++		
ydr479Δ	++++		
yhr150Δ/ydr479Δ	+++	+	
pex11Δ	++		++
pex25Δ	++++		
vps1Δ			++++
***VPS1* overexpression in**			
Wild-Type	++++		
yhr150Δ	+++	+	
ydr479Δ	+++	+	
yhr150Δ/ydr479Δ	++	++	
pex11Δ	+		+++
pex25Δ	+		+++
vps1Δ	++++		
Controls			
Wild-Type	++++		
yhr150Δ	+	+++	
ydr479Δ	+	+++	
yhr150Δ/ydr479Δ	+	+++	
pex11Δ	+		+++
pex25Δ	+		+++
vps1Δ			++++

*The (+) symbol denotes the presence of a particular peroxisomal morphological phenotype. Increased numbers of (+) symbols denote increased prevalence of a particular peroxisomal morphological phenotype. The absence of a (+) symbol denotes the absence of particular peroxisomal morphological phenotype.

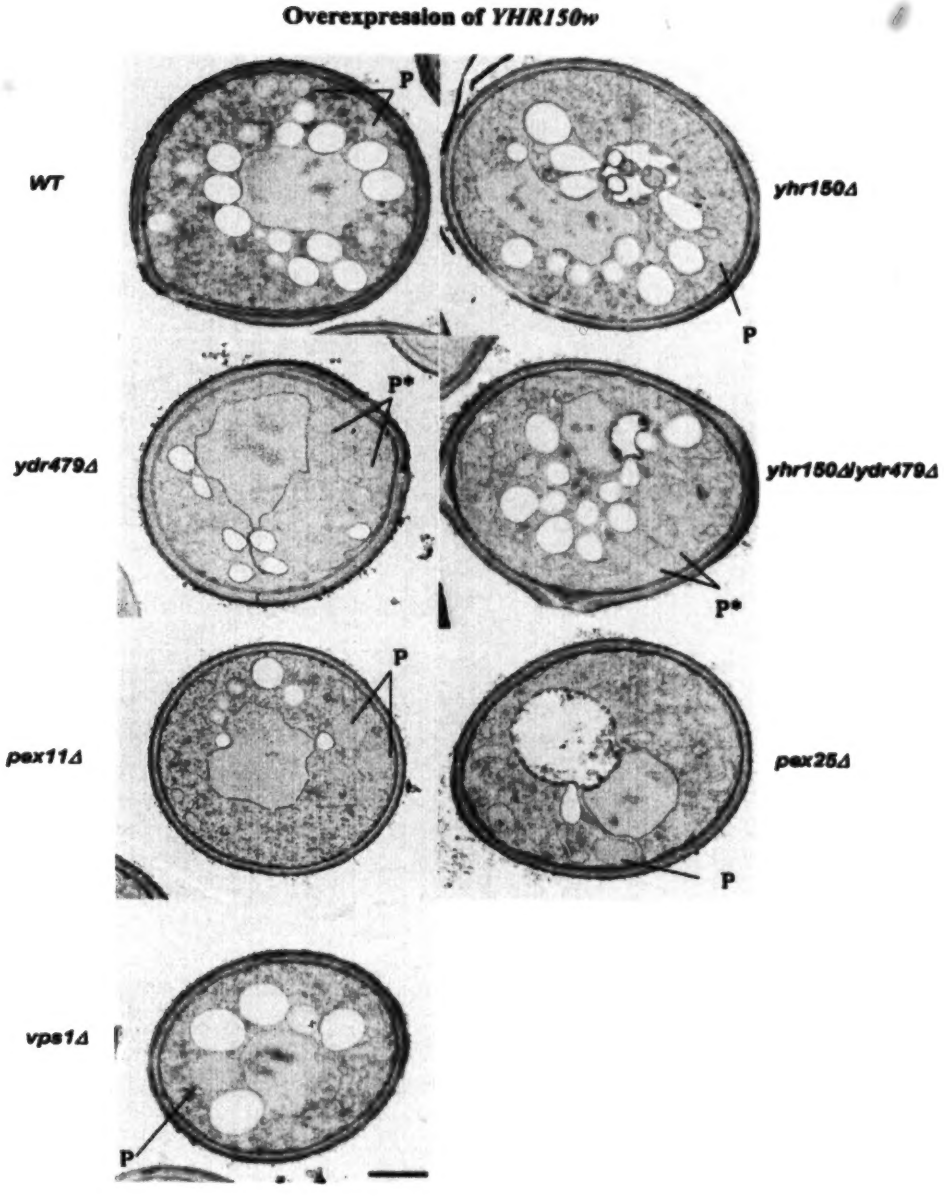

Figure 3-8. Peroxisome morphology in cells of gene overexpression strains

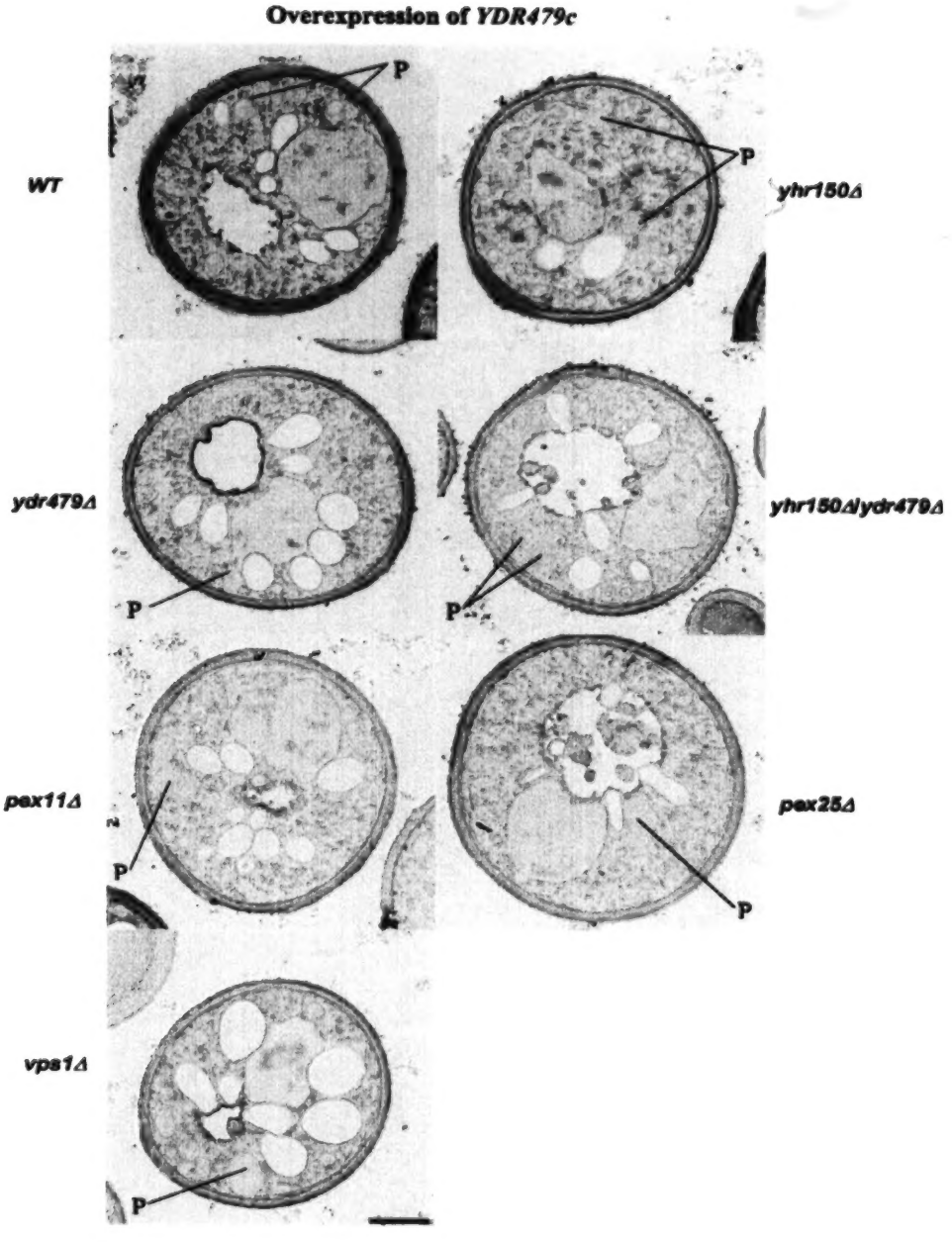

Figure 3-9. Peroxisome morphology in cells of gene overexpression strains

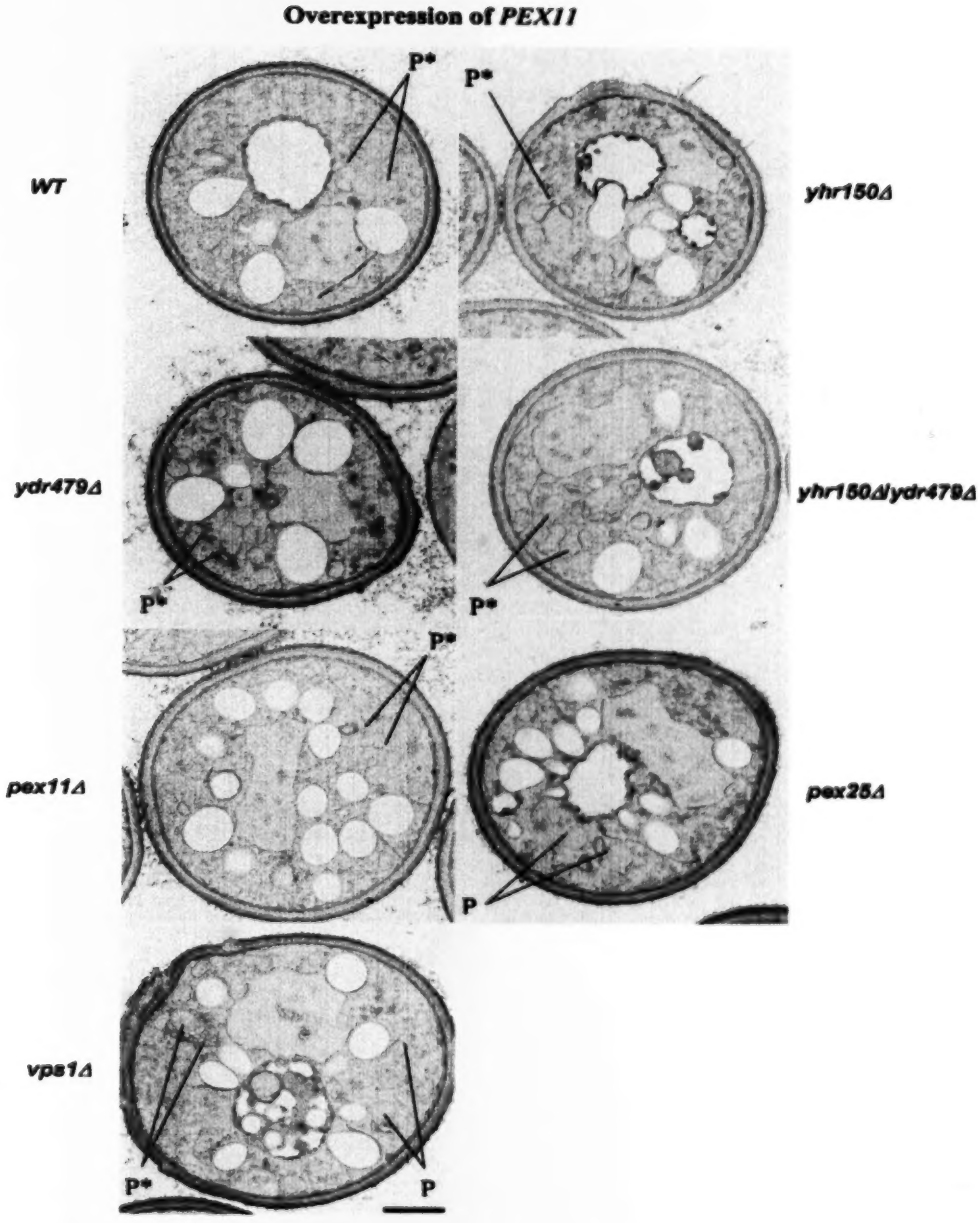

Figure 3-10. Peroxisome morphology in cells of gene overexpression strains

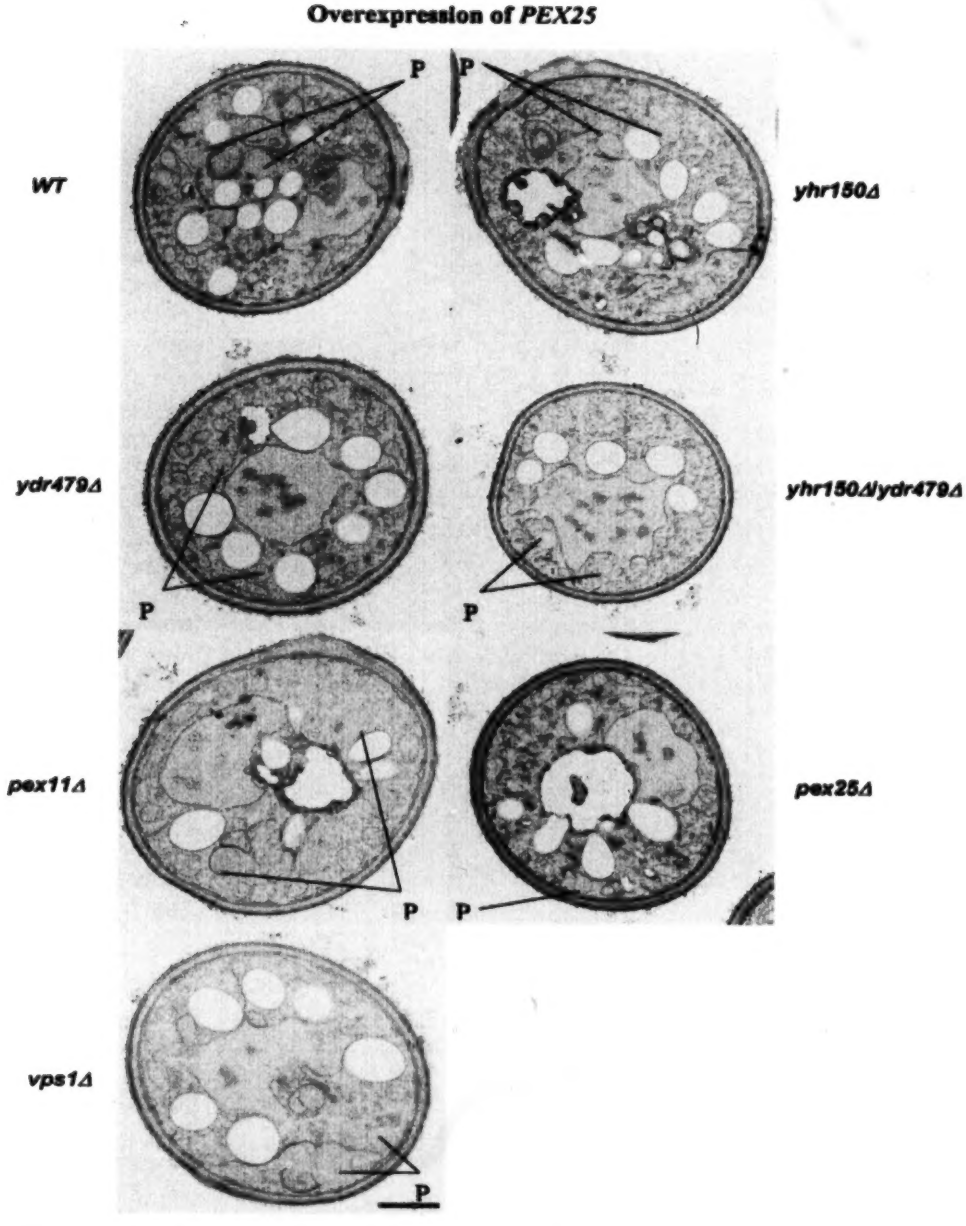

Figure 3-11. Peroxisome morphology in cells of gene overexpression strains

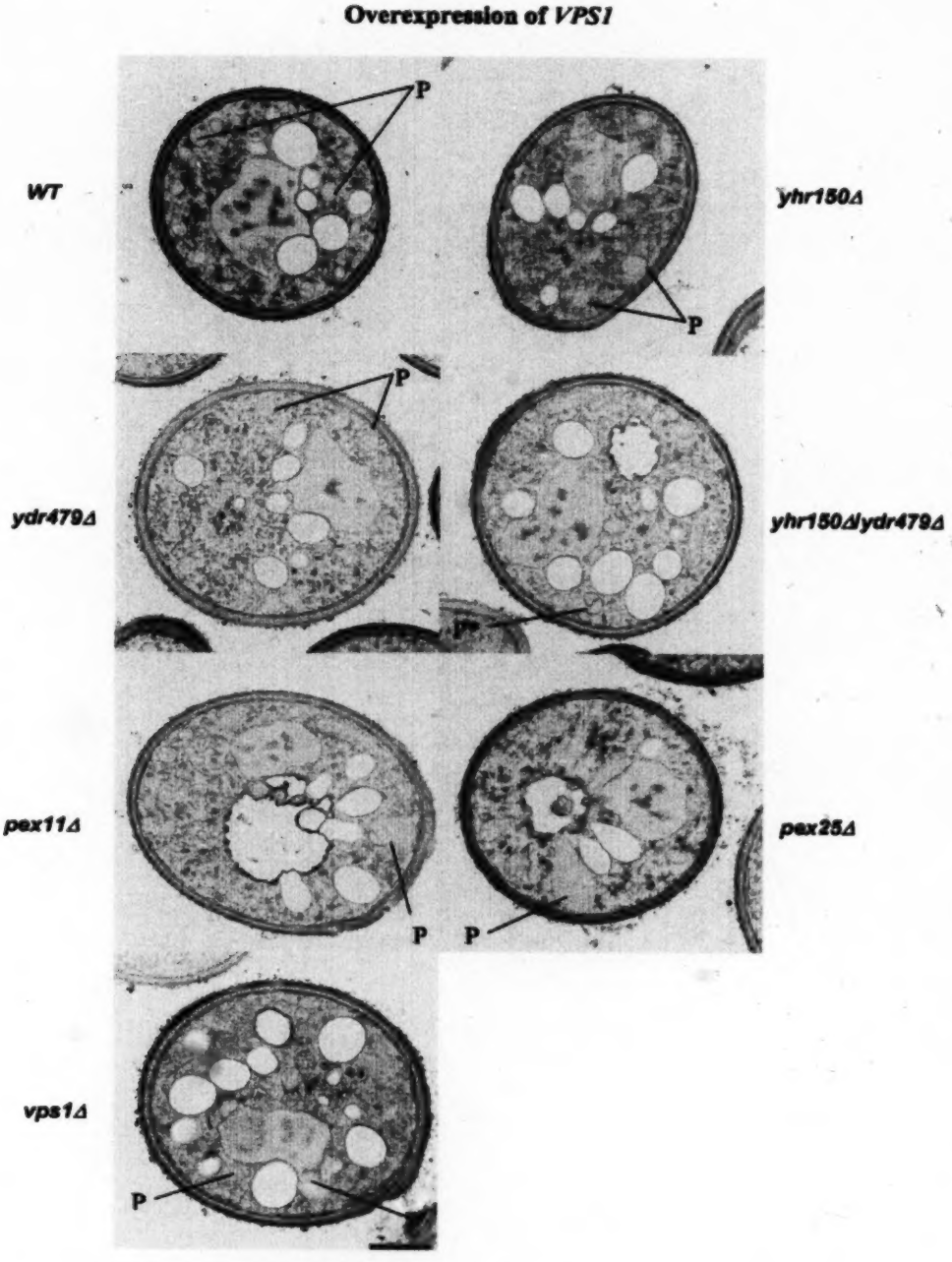

Figure 3-12. Peroxisome morphology in cells of gene overexpression strains

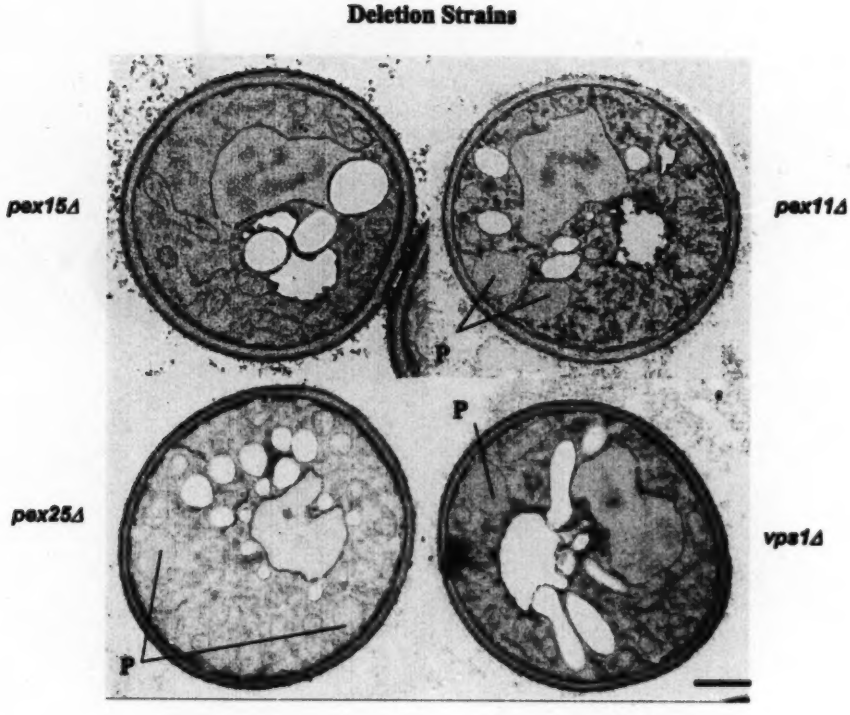

Figure 3-13. Peroxisome morphology in deletion mutants

3-9). Our results suggest that Pex11p plays a central role in regulating peroxisome division. The results of gene overexpression studies are summarized in Table 3-2.

3.7 Discussion

3.7.1 Database mining as a tool to identify novel *PEX* genes

Completion of the *S. cerevisiae* genome sequencing project proved invaluable for the identification of a novel *PEX* gene, *PEX25*, by transcriptome profiling of cells grown in oleic acid-containing medium versus cells grown in glucose-containing medium (Smith et al., 2002). The completed *S. cerevisiae* genome sequence is added value in that it provides the opportunity to identify novel proteins required for peroxisome biogenesis in *S. cerevisiae* through sequence similarity between proteins of unknown function encoded by the *S. cerevisiae* and proteins already shown to be required for peroxisome biogenesis in other organisms. The requirement of the peroxisomal integral membrane protein Pex24p for peroxisome assembly in the yeast *Y. lipolytica* was recently demonstrated (Tam and Rachubinski, 2002). *Yl*Pex24p was shown to share extensive sequence similarity to two proteins of unknown function and unknown localization encoded by the ORFs *YHR150w* and *YDR479c* of the *S. cerevisiae* genome. In this manuscript, genomically encoded protein A chimeras of Yhr150p and Ydr479p were shown by a combination of microscopic and subcellular fractionation analyses to be peroxisomal proteins. In their response to extraction by different salts, Yhr150p and Ydr479p act primarily as integral membrane proteins. However, a fraction of Ydr479p consistently acts as a soluble protein. The exact nature of this soluble form of Ydr479p

and its origin (Is it in equilibrium with the peroxisomal membrane form of Ydr479p?) remain under investigation.

3.7.2 A role for the novel genes in peroxisome biogenesis

The proteins encoded by the *YHR150w* and *YDR479c* genes are not required for peroxisome assembly, as cells harboring deletions for one or both of these genes still contain peroxisomes. These peroxisomes were functional, at least to some degree, as the cells containing one or both of the gene deletions were able to grow in oleic acid-containing medium with essentially the same kinetics as the wild-type strain (Figure 3-4 E). However, the peroxisomes in the deleted strain are not normal and show phenotypic characteristics distinct from those of wild-type peroxisomes. The peroxisomes of cells deleted for one or both of the *YHR150w* and *YDR479c* genes are more abundant and smaller, and show extensive clustering, as compared to wild-type peroxisomes. In addition, the membranes of the clustered peroxisomes of the gene deletion strains are often thickened in appearance. These characteristics of peroxisomes of the deletion strains are consistent with a role for *YHR150w* and *YDR479c* in the control of peroxisome size, number and distribution within cells. However, it does not appear that *YHR150w* and *YDR479c* are required for peroxisome inheritance per se, as all cells deleted for one or both of these genes still contained peroxisomes after numerous cell divisions. Also, if *YHR150w* or *YDR479c* had a direct role in the inheritance of peroxisomes, one might expect that a loss of peroxisomes from cells over time resulting from impaired segregation of peroxisomes into daughter cells would lead to decreased kinetics of growth in oleic acid-containing medium for the deletion strains vis-à-vis the wild-type strain, which, as reported above, was not observed. It is interesting to note that *Y.*

lipolytica cells deleted for the *PEX24* gene also show evidence of abnormal peroxisomal divisional control. These cells lack mature peroxisomes but do accumulate membrane structures that contain both peroxisomal matrix and membrane proteins (Tam and Rachubinski, 2002). However, these membrane structures are not functional peroxisomes in *Y. lipolytica*, as *pex24Δ* cells cannot grow on medium containing oleic acid as the sole carbon source. Therefore, although *Yl*Pex24p, like Yhr150p and Ydr479p, most likely has a role in the regulation of peroxisome division, *Yl*Pex24p probably does not function identically to Yhr150p or Ydr479p or is modulated in its actions differently than are Yhr150p and Ydr479p.

3.7.3 Regulation of peroxisome division

The size, number and distribution of peroxisomes are tightly controlled by the cell. Loss of the enzymatic activities of individual peroxisomal β-oxidation enzymes has been shown to result in pronounced changes in peroxisome size and/or number (Fan et al., 1998; Chang et al., 1999; Smith et al., 2000; van Roermund et al., 2000), due primarily to the increased levels of the remaining peroxisomal β-oxidation enzymes. The molecular mechanisms underlying this so called metabolic control of peroxisome abundance (Chang et al., 1999) remain essentially unknown.

In contrast, members of the Pex11 family of peroxins have been implicated as effectors of peroxisome division in multiple species (Erdmann and Blobel, 1995; Marshall et al., 1995, 1996; Sakai et al., 1995; Abe and Fujiki, 1998; Lorenz et al., 1998; Passreiter et al., 1998; Schrader et al., 1998; Li and Gould, 2002). The recently reported *PEX25* gene has also been implicated in the regulation of peroxisome size and number in

S. cerevisiae (Smith et al., 2002), as has the dynamin-like protein Vps1p (Hoepfner et al., 2001). Like other dynamin-related proteins, Vps1p was proposed to be involved in a membrane fission event required for the regulation of peroxisome size and abundance. The thickened membranes between some peroxisomes of a peroxisome cluster seen in cell deleted for the *YHR150w* and/or *YDR479c* genes are also suggestive of a role for Yhr150p and Ydr479p in controlling fission of the peroxisomal membrane.

3.7.4 Mechanism of peroxisome division

How might Yhr150p, Ydr479p, Pex11p, Pex25p and Vps1p act and interact to control the abundance, size and distribution of peroxisomes in the *S. cerevisiae* cell? We sought to get some insight into this question by determining the effects on peroxisome morphology of overexpressing the genes for these proteins in wild-type cells and cells deleted for the different genes.

Overexpression of the *PEX11* gene in the *pex11Δ* genetic background has been reported to result in large numbers of small peroxisomes (Marshall et al., 1995). In contrast, overexpression of the *PEX25*, *VPS1*, *YHR150w* and *YDR479c* in their respective gene deletion backgrounds does not result in the production of large numbers of small peroxisomes but instead restores the wild-type peroxisomal phenotype. Considering the proliferation of peroxisomes as a two step pathway, namely division of peroxisomes and separation of peroxisomes, overexpression of the *PEX11* gene either in wild-type cells or in cells of the various deletion strains leads to a significant proliferation of peroxisomes, which remain for the most part adherant to one another. Thus, Pex11p plays a central and positive regulatory role in the division step of peroxisome proliferation but has little or no

readily apparent role in the separation step of the process. The presence of reduced numbers of enlarged peroxisomes in *pex25Δ* cells (Smith et al., 2002; Figure 3-13) and *vps1Δ* cells (Hoepfner et al., 2001; Figure 3-13) suggests that Pex25p and Vps1p function in addition to Pex11p in the divisional step of peroxisome proliferation.

Upon completion of peroxisome division, peroxisomes must be separated from one another. Yhr150p and Ydr479p are two proteins required for this process, as their absence leads to an arrest or retardation of the peroxisome proliferation pathway, leading to the presence of clusters of peroxisomes with evidence of thickened membranes sometimes occurring between adjacent peroxisomes. Significant recovery of the wild-type peroxisomal phenotype by overexpression of *PEX25* or *VPS1* in cells deleted for one or both of the *YHR150w* or *YDR479c* genes implies that Pex25p and Vps1p have roles in the separation of peroxisomes in addition to their roles in peroxisome division discussed above. In contrast, overexpression of *PEX11* in cells deleted for one or both of the *YHR150w* or *YDR479c* genes did not result in the reappearance of wild-type peroxisomes, and peroxisomes remained clustered and sometimes exhibited membrane thickening between adjacent peroxisomes, as in the original strains deleted for *YHR150w* and/or *YDR479c*. Therefore, Pex11p appears to function primarily or only at the divisional step of peroxisome proliferation but not at the separation step.

Organelles are highly dynamic structures that undergo fission and fusion processes to allow cells to respond to intracellular and extracellular cues and to allow for their correct segregation at cell division. The maintenance of compartmental integrity in the eukaryotic cell therefore requires tight control mechanisms for these events. In the control of peroxisome number, size and distribution, our data suggest that Pex11p plays a

pre-eminent role in controlling peroxisome division, while Pex25p, Vps1p and the newly identified peroxisomal proteins Yhr150p and Ydr479p all play a prominent role in controlling the separation of peroxisomes from one another. The challenge for the future lies in understanding further the interplay amongst these proteins and the signaling events they respond to and initiate in order to control peroxisomal dynamics in the cell.

CHAPTER FOUR

PEX30, *PEX31*, AND *PEX32* ENCODE A FAMILY OF PEROXISOMAL INTEGRAL MEMBRANE PROTEINS REGULATING PEROXISOME SIZE AND NUMBER

A portion of this chapter has previously been published as "Pex30p, Pex31p, and Pex32p form a family of peroxisomal integral membrane proteins regulating peroxisome size and number in *Saccharomyces cerevisiae*" (Franco J. Vizeacoumar, Juan C. Torres-Guzman, David Bouard, John D. Aitchison, and Richard A. Rachubinski. 2003. *Mol Biol. Cell*. 2004 Feb; 15(2):665-77. Reprinted with permission

4.1 Overview

The peroxin Pex23p of the yeast *Yarrowia lipolytica* exhibits high sequence similarity to the hypothetical proteins Ylr324p, Ygr004p and Ybr168p encoded by the *Saccharomyces cerevisiae* genome. Ylr324p, Ygr004p and Ybr168p are integral to the peroxisomal membrane and act to control peroxisome number and size. Synthesis of Ylr324p and Ybr168p, but not of Ygr004p, is induced during incubation of cells in oleic acid-containing medium, the metabolism of which requires intact peroxisomes. Cells deleted for *YLR324w* exhibit increased numbers of peroxisomes, while cells deleted for *YGR004w* or *YBR168w* exhibit enlarged peroxisomes. Ylr324p and Ybr168p cannot functionally substitute for one another or for Ygr004p, while Ygr004p shows partial functional redundancy with Ylr324p and Ybr168p. Ylr324p, Ygr004p and Ybr168p interact within themselves and with Pex28p and Pex29p, which have been shown also to regulate peroxisome size and number. Systematic deletion of genes demonstrated that *PEX28* and *PEX29* function upstream of *YLR324w*, *YGR004w* and *YBR168w* in the regulation of peroxisome proliferation. Our data suggest a role for Ylr324p, Ygr004p and Ybr168p – now designated Pex30p, Pex31p and Pex32p, respectively – together with Pex28p and Pex29p in controlling peroxisome size and proliferation in *S. cerevisiae*.

4.2 Ylr324p, Ygr004p and Ybr168p share extensive sequence similarity with YlPex23p

*Yl*Pex23p is an integral peroxisomal membrane protein that has been shown to be required for peroxisome assembly in the yeast *Y. lipolytica* (Brown *et al.*, 2000). A search

of protein databases with the GENEINFO(R)BLAST Network Service of the National Center for Biotechnology Information revealed three proteins encoded by the ORFs *YLR324w, YGR004w* and *YBR168w* of the *S. cerevisiae* genome that exhibit extensive sequence similarity to *Yl*Pex23p (Figure 4-1). *Yl*Pex23p and Ylr324p exhibit 36.3% amino acid sequence identity and 20.9% amino acid similarity (at positions of non-identity), *Yl*Pex23p and Ygr004p exhibit 35.6% amino acid sequence identity and 19.3% amino acid similarity, *Yl*Pex23p and Ybr168p exhibit 17.6% amino acid identity and 24.4% amino acid similarity, while Ylr324p, Ygr004p and Ybr168p exhibit 9.3% amino acid identity and 20.7% amino acid similarity among themselves. Ylr324p is predicted to be a protein of molecular weight 59,461 and to have two transmembrane helices at amino acids 3-22 and 191-209 (http://www.cbs.dtu.dk/services/TMHMM-2.0/) (Krogh *et al.*, 2001). Ygr004p is predicted to be a protein of molecular weight 52,942 and to have four transmembrane helices at amino acids 93-111, 110-129, 178-195 and 226-244. Ybr168p is predicted to be a protein of molecular weight 48,578 and to have six transmembrane helices at amino acids 45-62, 69-86, 102-121, 178-197, 205-224 and 230-249. Partial functional redundancy among Ylr324p, Ygr004p and Ybr168p (discussed below) may have prevented them from being identified as being involved in peroxisome biogenesis in *S. cerevisiae* by procedures involving random mutagenesis and negative selection for growth of yeast on oleic acid-containing medium.

4.3 Synthesis of Ylr324p andYbr168p are inducible

The culturing of yeast cells in oleic acid-containing medium elicits a dual cellular response in that it promotes the proliferation of peroxisomes and induces the expression

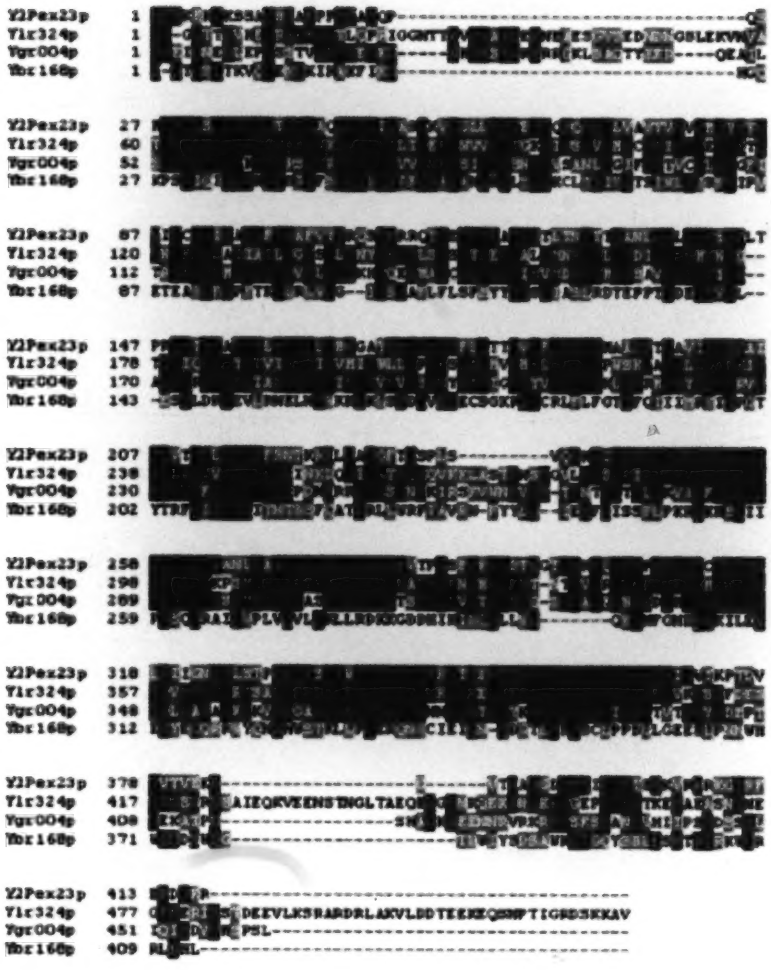

Figure 4-1. Sequence alignment of *Yarrowia lipolytica* Pex23p with the proteins Ylr324p, Ygr004p and Ybr168p encoded by the *Saccharomyces cerevisiae* genome. Amino acid sequences were aligned with the use of the ClustalW program (EMBL-European Bioinformatics Institute, http://www.ebi.ac.uk/clustalw/). Identical residues in at least three of the proteins are shaded black, while identical residues in two proteins are shaded blue. Similar residues are shaded gray. Similarity rules: G = A = S; A = V; V = I = L = M; I = L = M = F = Y = W; K = R = H; D = E = Q = N; and S = T = Q = N. This figure was aligned by Dr. Richard A. Rachubinski.

of many genes encoding peroxisomal proteins. Genomically encoded protein A chimeras of Ylr324p, Ygr004p and Ybr168p were monitored to analyze the expression of *YLR324w, YGR004w* and *YBR168w*, respectively, under the control of their endogenous gene promoters. Yeast strains synthesizing Ylr324p-prA, Ygr004p-prA and Ybr168p-prA were grown in glucose-containing YPD medium and then shifted to oleic acid-containing YPBO medium. Aliquots of cells were removed at various times after the shift to YPBO medium, and their lysates were analyzed by SDS-PAGE and immunoblotting (Figure 4-2). Ylr324p-prA, Ygr004p-prA and Ybr168p-prA were all detected in glucose-containing YPD medium at the time of transfer. The levels of Ylr324p-prA and Ybr168p-prA increased with time of incubation of cells in YPBO medium, but not as dramatically as the levels of Pot1p (peroxisomal thiolase). The levels of Ygr004p-prA did not show any apparent increase with time of incubation of cells in YPBO medium. It is noteworthy that the promoter regions of *YLR324w*, *YGR004w* and *YBR168w* contain sequences that resemble the canonical sequence $CCGN_3TNAN_{8\text{-}12}CGG$ of the oleic acid response element (ORE) (Table 4-1) (Rottensteiner *et al.*, 2002; 2003a), which acts to increase gene transcription in *S. cerevisiae* in the presence of oleic acid as a carbon source through the binding of the transcription factors Pip2p and Oaf1p (Rottensteiner *et al.*, 1996; Karpichev *et al.*, 1997). Whether these sequences actually do function as OREs remains to be determined.

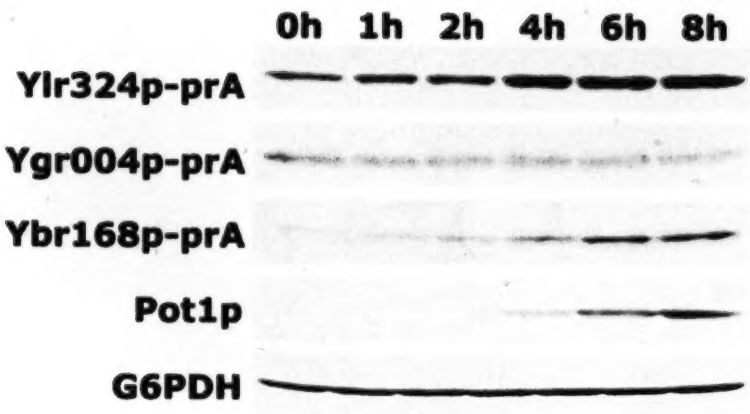

Figure 4-2. The levels of Ylr324p-prA and Ybr168-prA, but not of Ygr004p-prA, are increased during incubation of *S. cerevisiae* in oleic acid-containing medium. Cells were grown for 16 h in glucose-containing YPD medium and then transferred to, and incubated in, oleic acid-containing YPBO medium. Aliquots of cells were removed from the YPBO medium at the times indicated, and total cell lysates were prepared. Equal amounts of protein from the total cell lysates were analyzed by SDS-PAGE and immunoblotting to visualize the protein A fusions and Pot1p. Antibodies directed against glucose-6-phosphatase (G6PDH) were used to confirm the loading of equal protein in each lane.

Table 4-1. Putative OREs in the promoter regions of the *YLR324w*, *YGR004w* and *YBR168w* genes

Gene	ORE Canonical Sequence ($CCGN_3TNAN_{8-12}CGG$)
PEX7	$CAGN_{10}TNAN_3CCG$
PEX13	$CGGN_{12}TNAN_3CCG$
YLR324w	$CGGN_{12}TNAN_3CCG$
YGR004w	$CGGN_{13}TNAN_8CCG$
YBR168w	$CAGN_2TNAN_{13}CCG$

4.4 Ylr324p, Ybr168p and Ygr004p are integral membrane proteins

A carboxyl-terminal PTS1 is sufficient to direct a reporter protein to peroxisomes. A fluorescent chimera between *Discosoma sp.* red fluorescent protein (DsRed) and the PTS1 Ser-Lys-Leu has been shown to target to peroxisomes of *S. cerevisiae* (Wang *et al.*, 2001; Smith *et al.*, 2002). Genomically encoded protein A chimeras of Ylr324p, Ygr004p, Ybr168p and the peroxisomal matrix protein Pot1p were localized in oleic acid-induced cells by indirect immunofluorescence microscopy combined with direct fluorescence of DsRed-PTS1 to identify peroxisomes (Figure 4-3A). Ylr324p-prA, Ygr004p-prA, Ybr168p-prA and Pot1p colocalized with DsRed-PTS1 to small punctate structures characteristic of peroxisomes by confocal microcopy.

Subcellular fractionation and organelle extraction were used to establish if Ylr324p, Ygr004p and Ybr168p are associated with peroxisomes and to determine their suborganellar locations. Ylr324p-prA, Ygr004p-prA and Ybr168p-pA, like Pot1p, preferentially localized to the 20KgP fraction enriched for peroxisomes (Figure 4-3B). Peroxisomes were isolated from the 20KgP fractions of each of the strains expressing Ylr324p-prA, Ygr004p-prA or Ybr168p-prA. The gradients were fractionated, and equal portions of each fraction were analyzed by immunoblotting (Figure 4-3C). Ylr324p-prA, Ygr004p-prA and Ybr168p-prA coenriched with the peroxisomal matrix protein thiolase (Pot1p) and not with the mitochondrial protein, Sdh2p. Therefore, both microscopic analysis and subcellular fractionation showed Ylr324p, Ygr004p and Ybr168p to be peroxisomal proteins. Some amount of Ylr324p-prA was always present in the lighter fractions during the gradient isolation of peroxisomes, while Ygr004-prA consistently enriched in fraction 9 at a density lighter than that of peroxisomes. Whether there is a

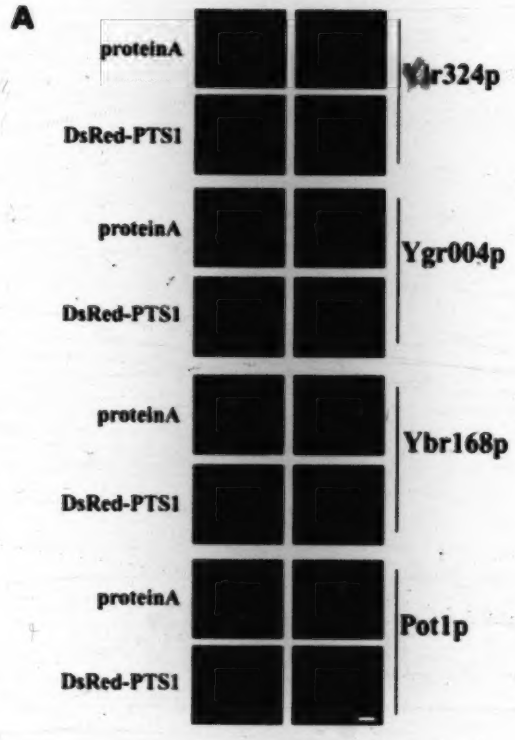

Figure 4-3 A. Ylr324p-prA, Ygr004p-prA and Ybr168p-prA are peroxisomal proteins by confocal microscopy. (A) The subcellular distributions of protein A chimeras were compared to that of DsRed-PTS1 in oleic acid-incubated cells by double labeling, indirect immunofluorescence microscopy. Ylr324p-prA, Ygr004p-prA and Ybr168-prA, along with the peroxisomal matrix protein Pot1p, colocalize with DsRed-PTS1 in punctate structures characteristic of peroxisomes. Protein A chimeras were detected with rabbit antibodies to mouse IgG and FITC-conjugated goat anti-rabbit IgG secondary antibodies.

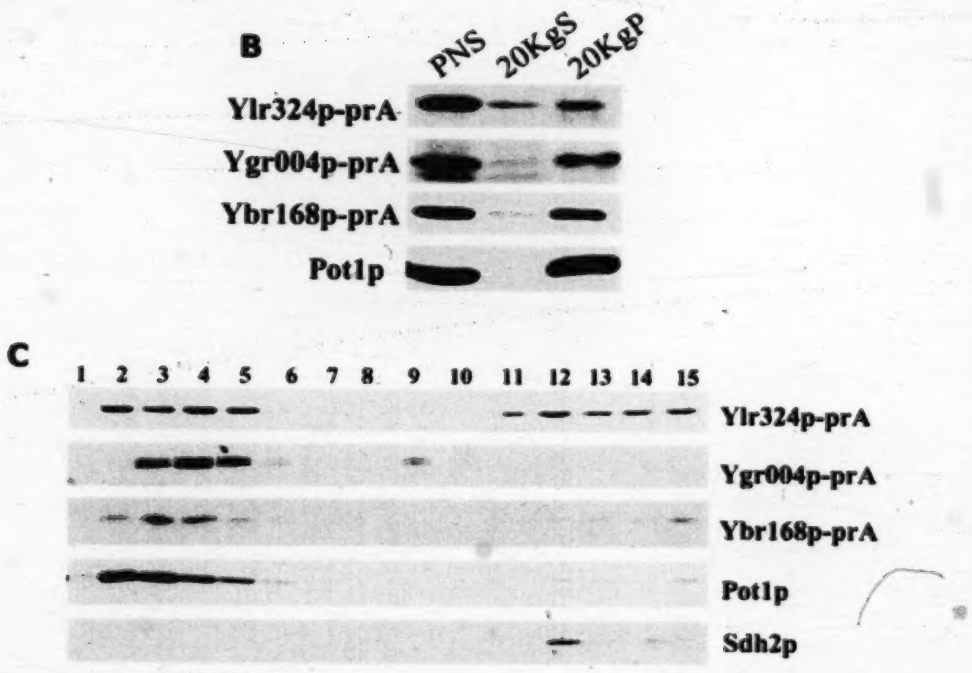

Figure 4-3 B and C. Ylr324p-prA, Ygr004p-prA and Ybr168p-prA are peroxisomal proteins by sub cellular fractionation. (B) A PNS fraction was divided by centrifugation into a supernatant (20KgS) fraction enriched for cytosol and a pellet (20KgP) fraction enriched for peroxisomes. Equivalent portions of each fraction were analyzed. Immunoblotting with rabbit anti-Pot1p antibodies detected both the protein A chimeras shown and Pot1p. (C) Ylr324p-prA, Ygr004p-prA and Ybr168-prA cofractionate with peroxisomes. Organelles in the 20KgP fraction were separated by isopycnic centrifugation on a discontinuous Nycodenz gradient. Fractions were collected from the bottom of the gradient, and equal portions of each fraction were analyzed by immunoblotting. Fractions enriched for peroxisomes and mitochondria were identified by immunodetection of Pot1p and Sdh2p, respectively.

selective liberation of a soluble form of Ylr324p-prA during the isolation of peroxisomes or there are vesicular elements containing either Ylr324p or Ygr004p remains to be determined. It is also noteworthy that Ygr004p-prA consistently migrated as two distinct molecular species in SDS-PAGE (see Figure 4-3C). The reason for this heterogeneity is unknown but could be due to some form of posttranslational modification, e.g. phosphorylation, of Ygr004p-prA.

Peroxisomes were hypotonically lysed by incubation in dilute alkali Tris buffer and subjected to centrifugation to yield a supernatant (Ti8S) enriched for matrix proteins and a pellet (Ti8P) enriched for membrane proteins (Figure 4-3D). The chimeras of Ylr324p, Ygr004p and Ybr168p localized primarily to the Ti8P fraction, as did the chimeras of the peripheral peroxisomal membrane protein Pex17p (Huhse *et al.*, 1998) and the integral peroxisomal membrane protein Pex3p (Höhfeld *et al.*, 1991). The soluble peroxisomal matrix protein Pot1p was found almost exclusively in the Ti8S fraction. The reproducible presence of some Ylr324p-prA in the Ti8S fraction may again be representative of a soluble form of this protein that is selectively liberated from peroxisomes during their isolation (see Figure 4-3, B and C). The Ti8P fractions were then extracted with alkali sodium carbonate and subjected to centrifugation (Figure 4-3D). This treatment releases proteins associated with, but not integral to, membranes (Fujiki *et al.*, 1982). Under these conditions, Ylr324p-prA, Ygr004p-prA and Ybr168p-pA fractionated with Pex3p-prA to the pellet fraction enriched for integral membrane proteins, while Pex17p-prA fractionated to the supernatant fraction enriched for soluble proteins, including peripheral membrane proteins. These data suggest that Ylr324p,

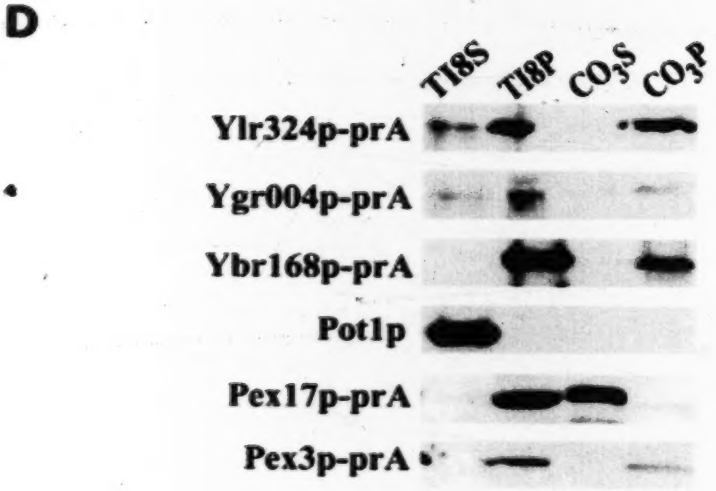

Figure 4-3 D. Ylr324p-prA, Ygr004p-prA and Ybr168p-prA are integral membrane proteins of peroxisomes. (D) Peroxisomes purified by isopycnic density gradient centrifugation were lysed by treatment with 10 mM Tris-HCl, pH 8.0, releasing matrix proteins to a supernatant fraction (Ti8S) after centrifugation. The membrane-containing pellet fraction (Ti8P) was treated with 0.1 M Na_2CO_3, pH 11.3, and then subjected to centrifugation to yield a supernatant fraction (CO_3S) enriched for peripherally associated membrane proteins and a pellet fraction (CO_3P) enriched for integral membrane proteins. Equal portions of the respective supernatant and pellet fractions were analyzed by immunoblotting. Immunodetection of Pot1p, Pex17p-prA and Pex3p-prA marked the fractionation profiles of a matrix, peripheral membrane and integral membrane protein, respectively.

Ygr004p and Ybr168p are primarily integral peroxisomal membrane proteins, as has been shown for *Yl*Pex23p (Brown *et al.*, 2000).

4.5 Ylr324p, Ygr004p and Ybr168p act to control the number and size of peroxisomes

Immunofluorescence analysis of oleic acid-incubated wild-type *BY4742* cells with antibodies to the carboxyl-terminal PTS1 tripeptide Ser-Lys-Leu (SKL) or to the PTS2-containing enzyme Pot1p showed a pattern of small punctate structures characteristic of peroxisomes (Figure 4-4). In contrast, the majority of cells of the *ylr324Δ* strain showed increased numbers of punctate structures, while cells of the *ygr004Δ* and *ybr168Δ* strains showed a reduced number of often enlarged punctate structures. There was no evidence of increased cytosolic immunofluorescence with either anti-SKL or anti-Pot1p antibodies in cells deleted for one or more of the *YLR324w*, *YGR004w* and *YBR168w* genes, suggesting that these genes do not encode proteins required for the import of matrix proteins into peroxisomes (Figure 4-4). Dr. Juan Carlos Guzman Torres constructed the double deletion mutant *DK1* and *DK2* and checked for their growth defect. Both the single and double deletion mutants grew like the wild-type cells on oleic acid-containing medium (Figure 4-3 E).

In electron micrographs, wild-type cells grown in oleic acid-containing medium contained characteristic peroxisomes of 0.3 μm to 0.5 μm in diameter that were well separated from one another (Figure 4-5, A and I). In contrast, cells of the *ylr324Δ* strain (Figure 4-5 B) showed increased numbers of peroxisomes (Table 4-2) that were similar in

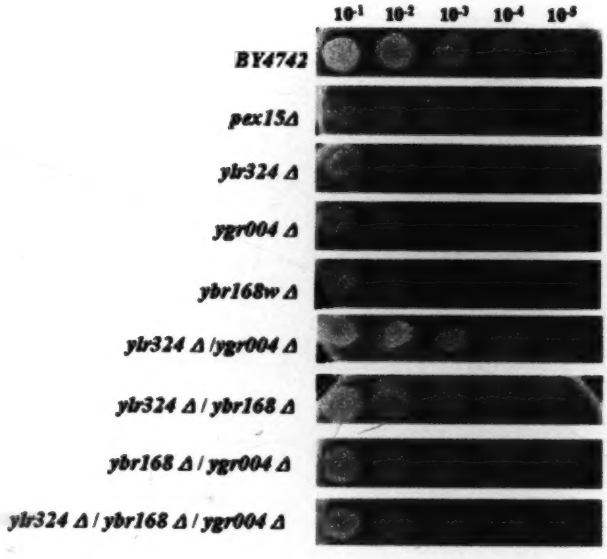

Figure 4-3 E. Growth of different strains on YPBO medium. All strains were spotted after serial dilution and grown over a period of 4 days at 30°C. *DK1* and *DK2* were constructed by Dr.Juan Carlos Guzman Torres.

Figure 4-4. Cells deleted for one or more of the *YLR324w*, *YGR004w* and *YBR168w* genes exhibit altered peroxisome morphology. Cells of the wild-type strain *BY4742* and of the *ylr324Δ*, *ygr004Δ*, *ybr168Δ*, *ylr324wΔ/ygr004wΔ* (*DK1*), *ylr324wΔ/ybr168wΔ* (*DK2*), *ygr004wΔ/ybr168wΔ* (*DK3*) and *ylr324wΔ/ygr004wΔ/ybr168wΔ* (*TKO*) deletion strains were grown in YPD medium for 16 h, transferred to YPBO medium, and incubated for 8 h in YPBO medium. Cells were observed by immunofluorescence microscopy with antibodies to the PTS1 tripeptide SKL (SKL) or to the PTS2-containing protein, Pot1p. Rabbit primary antibodies (SKL) were detected with FITC-conjugated secondary antibodies. Guinea pig primary antibodies (Pot1p) were detected with rhodamine-conjugated secondary antibodies. Bar, 1 μm.

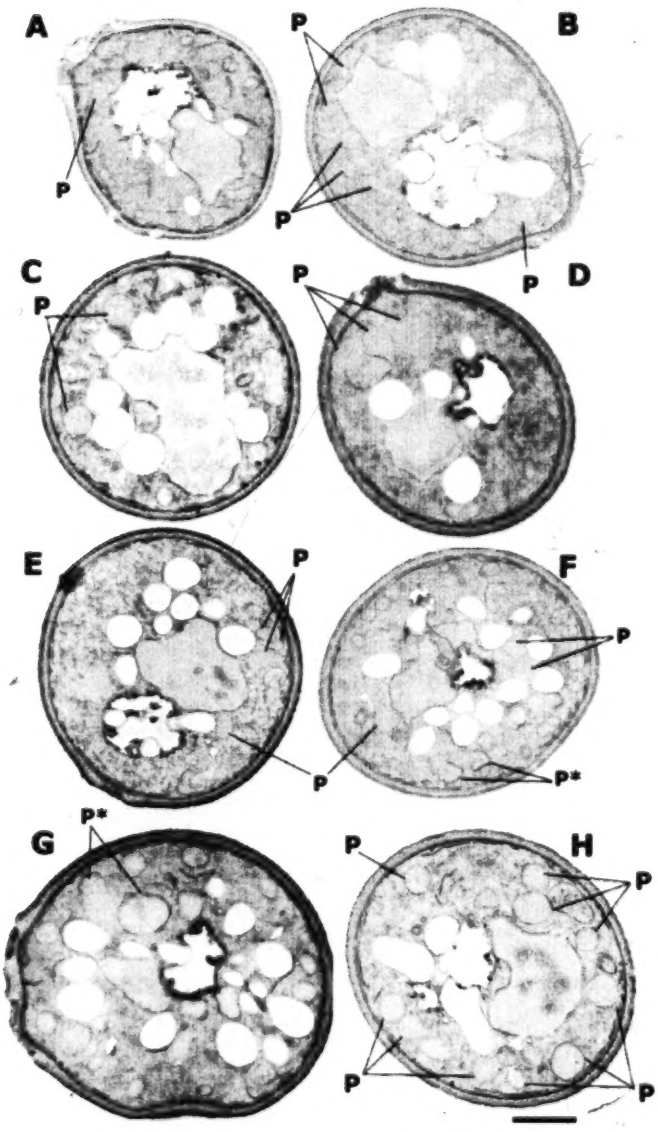

Figure 4-5. Cells harboring deletions in one or more of the *YLR324w, YGR004w* and *YBR168w* genes exhibit peroxisomes that are altered in number and/or size. Ultrastructure of wild-type *BY4742* (A), *ylr324Δ* (B), *ygr004Δ* (C) *ybr168Δ* (D) *ylr324Δ/ygr004Δ* (E), *ylr324Δ/ybr168Δ* (F), *ygr004Δ/ybr168Δ* (G) and *ylr324Δ/ygr004Δ/ybr168Δ* (H) cells. Cells were grown in YPD medium for 16 h, transferred to YPBO medium and incubated in YPBO medium for 8 h. Cells were fixed and processed for electron microscopy. P, peroxisome; P*, peroxisome cluster. Bar, 1.0 μm.

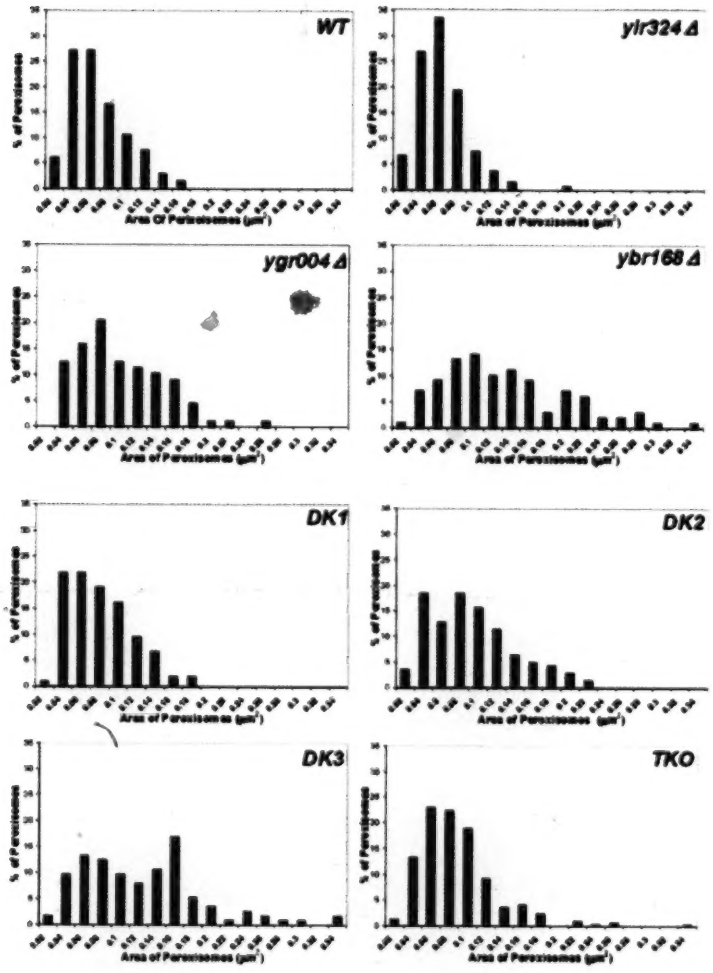

Figure 4-5 I. Morphometric analysis of peroxisomes of oleic acid-incubated wild-type (*WT*) *BY4742* and deletion mutant cells. Fifty randomly selected cells from each strain were analyzed by the program analySIS 3.1 (Soft Imaging System) to determine the areas of individual peroxisomes. Peroxisomes were then separated into size categories. A histogram was generated for each strain depicting the percentage of total peroxisomes occupied by the peroxisomes of each category. The numbers along the x-axis are the maximum sizes of peroxisomes in each category (in μm^2).

Table 4-2. Average area and numerical density of peroxisomes in cells of wild-type and mutant strains

Strain	Cell area assayed (μm^2)	Average area of peroxisomes[a] (μm^2)	Average number of peroxisomes per cell	Peroxisome count[b]	Numerical density of peroxisomes[c]
WT (BY4742)	402	0.06	1.32	0.16	0.73
Ylr324Δ	447	0.05	3.02	0.34	1.75
ygr004Δ	434	0.09	1.68	0.19	0.70
ybr168Δ	461	0.13	1.72	0.19	0.56
DK1	478	0.07	2.20	0.23	0.95
DK2	490	0.08	2.64	0.27	1.02
DK3	463	0.12	1.98	0.21	0.66
TKO	498	0.08	6.24	0.63	2.43

[a]Average area on micrographs.
[b]Number of peroxisomes counted per μm^2 of cell area on micrographs.
[c]Number of peroxisomes per μm^3 of cell volume (Weibel and Bolender, 1973).

size to peroxisomes of wild-type cells (Figure 4-5 I) (Table 4-2). Cells of the *ygr004Δ* (Figure 4-5 C) and *ybr168Δ* (Figure 4-5 D) strains exhibited similar numbers of peroxisomes to wild-type cells (Table 4-2), but these peroxisomes were noticeably larger than wild-type peroxisomes, particularly in the case of *ybr168Δ* cells (Figure 4-5 I) (Table 4-2). Cells of strain *DK1* (Figure 4-5 E) carrying deletions in the *YLR324w* and *YGR004w* genes exhibited a mixed phenotype of increased numbers of peroxisomes (Table 4-2) of normal to enlarged size (Figure 4-5 I) (Table 4-2). Cells of strain *DK2* (Figure 4-5 F) carrying deletions in the *YLR324w* and *YBR168w* genes showed increased numbers of peroxisomes (Table 4-2) of normal to enlarged size (Figure 4-5 I), some of which exhibited clustering (Figure 4-5 J), while cells of strain *DK3* (Figure 4-5 G) deleted for the *YGR004w* and *YBR168w* genes also contained greatly enlarged peroxisomes (Figure 4-5 I) (Table 4-2). Cells of the strain *TKO* carrying deletions in all three genes showed an approximately 5-fold increase in the average number of peroxisomes per cell, but the size distribution of peroxisomes was similar to that of wild-type cells (Figure 4-5 I). Our results suggest that Ylr324p acts primarily as a negative regulator of peroxisome number, while Ygr004p and particularly Ybr168p act as negative regulators of peroxisome size.

4.6 Overexpression studies of *YGR004w*, *YLR324w* and *YBR168w*

Because cells deleted for one or more of the *YLR324w*, *YGR004w* and *YBR168w* genes are compromised in their regulation of peroxisome size and number, we investigated the effects of overexpression of these genes on the overall peroxisome phenotype in cells harboring various combinations of deletions of these genes.

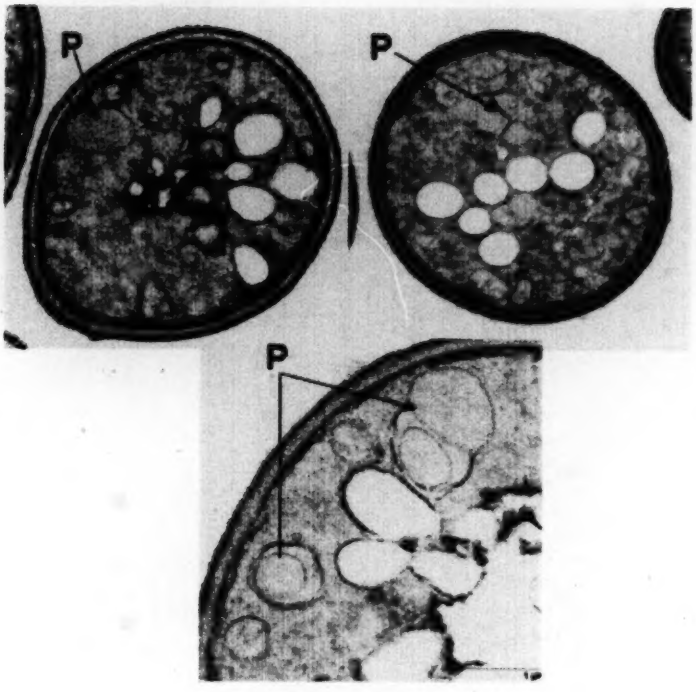

Figure 4- 5 J. Abnormal morphology of peroxisomes in a double deletion mutant, *DK2* showing clustering of peroxisomes with membrane thickening, suggesting that this could be a fission or a fusion mutant.

Overexpression of *YLR324w*, *YGR004w* and *YBR168w* (Figure 4-6) in their respective deletion backgrounds led to restoration of the wild-type peroxisomal phenotype. Overexpression of *YLR324w* in cells deleted for one or both of *YGR004w* and *YBR168w* did not lead to the complementation of the peroxisomal phenotype observed in cells deleted for either or both of *YGR004w* and *YBR168w* (Figure 4-6). Similarly, overexpression of *YBR168w* in cells deleted for one or both *YLR324w* and *YGR004w* did not lead to complementation of the peroxisomal phenotype seen in cells deleted for either or both of the *YLR324w* and *YGR004w* genes (Figure 4-8). In contrast, overexpression of the *YGR004w* gene in cells deleted for one or both of the *YLR324w* and *YBR168w* gene led essentially to the restoration of the wild-type peroxisomal phenotype, although evidence of peroxisomal clustering was still observed in cells deleted for both the *YLR324w* and *YBR168w* genes (Figure 4-7). Taken together, these data suggest that Ylr324p and Ybr168p cannot functionally substitute for one another or for Ygr004p, while Ygr004p shows partial, but not complete, functional redundancy with Ylr324p and Ybr168p.

4.7 Interacting partners of Ylr324p, Ygr004p and Ybr168p

A limited yeast two-hybrid screen was performed to identify physical interactions between Ylr324p, Ygr004p and Ybr168p and between these proteins and Pex11p, Pex25p, Pex28p, Pex29p and Vps1p, which have also been implicated in the control of peroxisome size and number (Erdmann and Blobel, 1995; Marshall *et al.*, 1995; Hoepfner *et al.*, 2001; Smith *et al.*, 2002; Vizeacoumar *et al.*, 2003). Others have used this methodology to detect interactions between peroxins (for examples, see Girzalsky *et al.*,

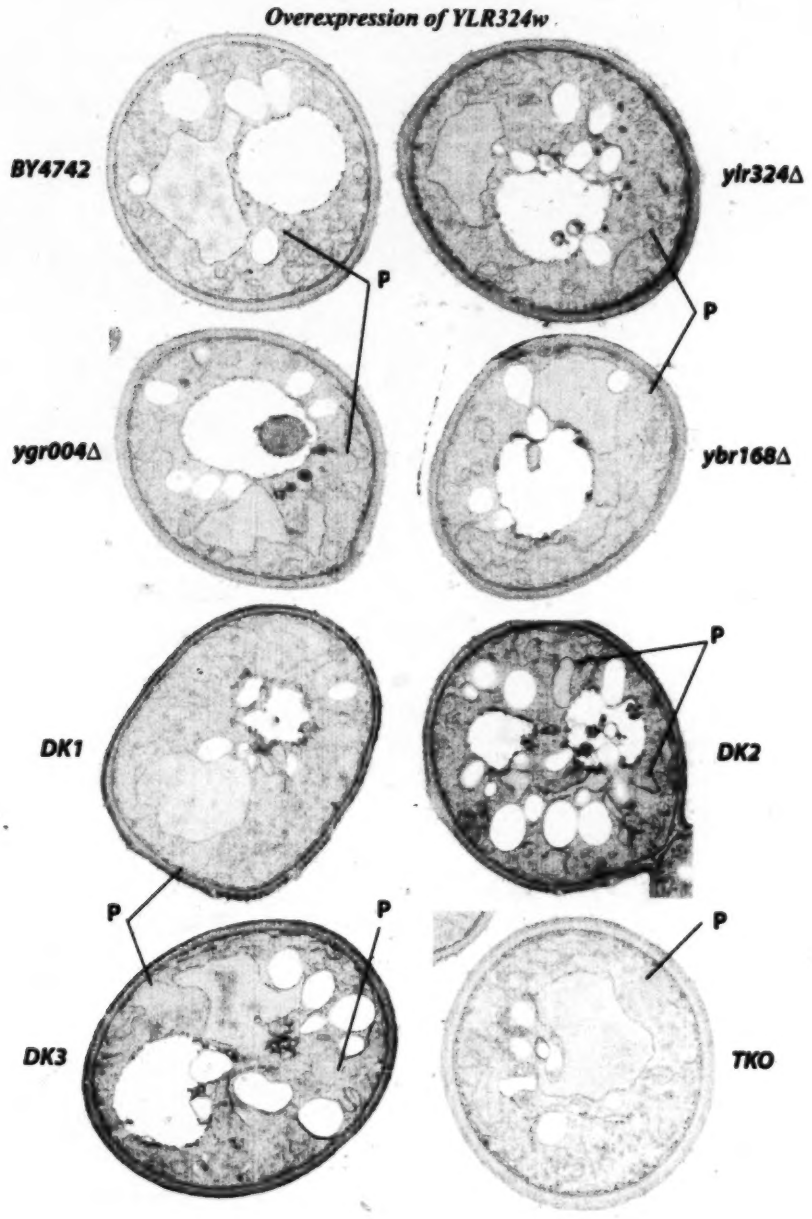

Figure 4-6. Peroxisome morphology in cells of gene overexpression strains

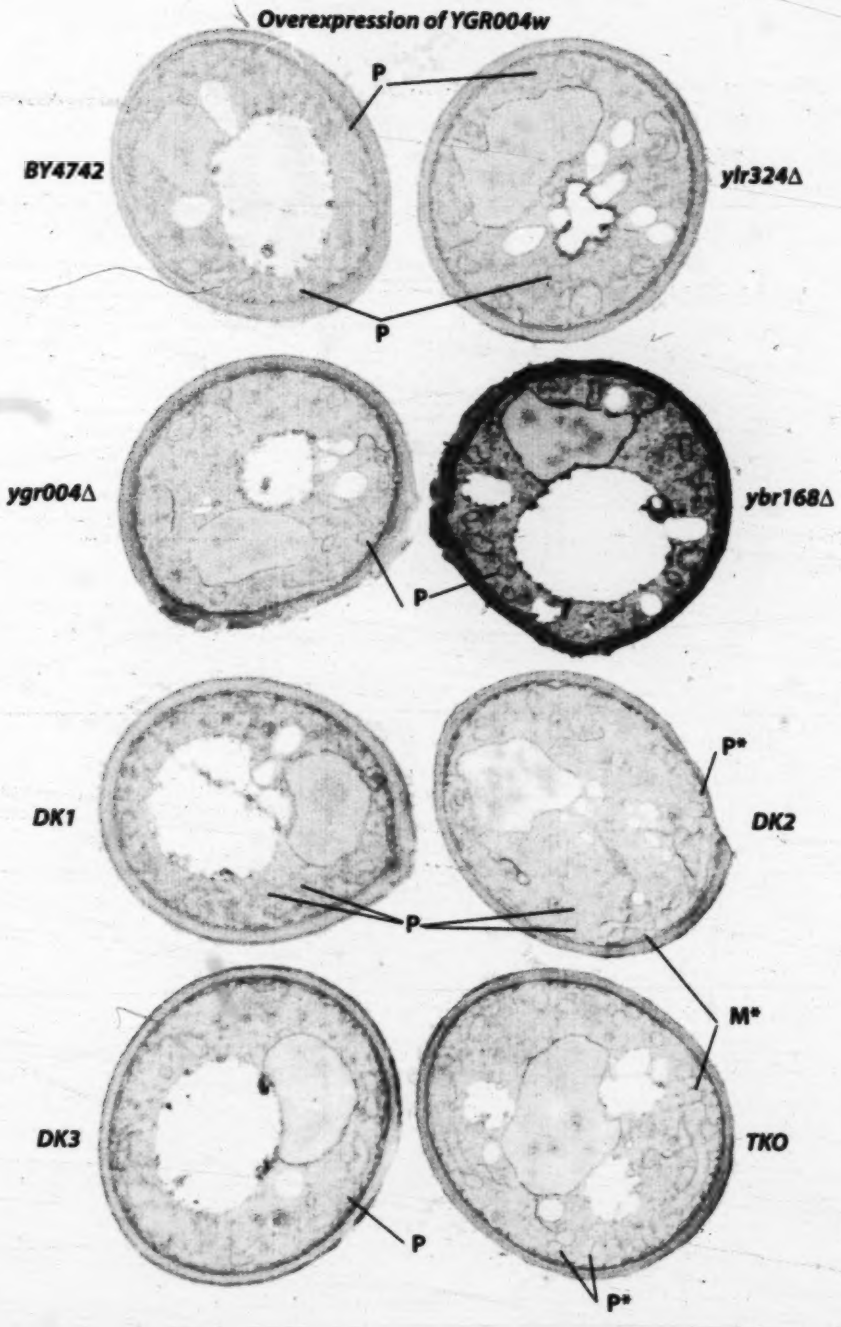

Figure 4-7. Peroxisome morphology in cells of gene overexpression strains

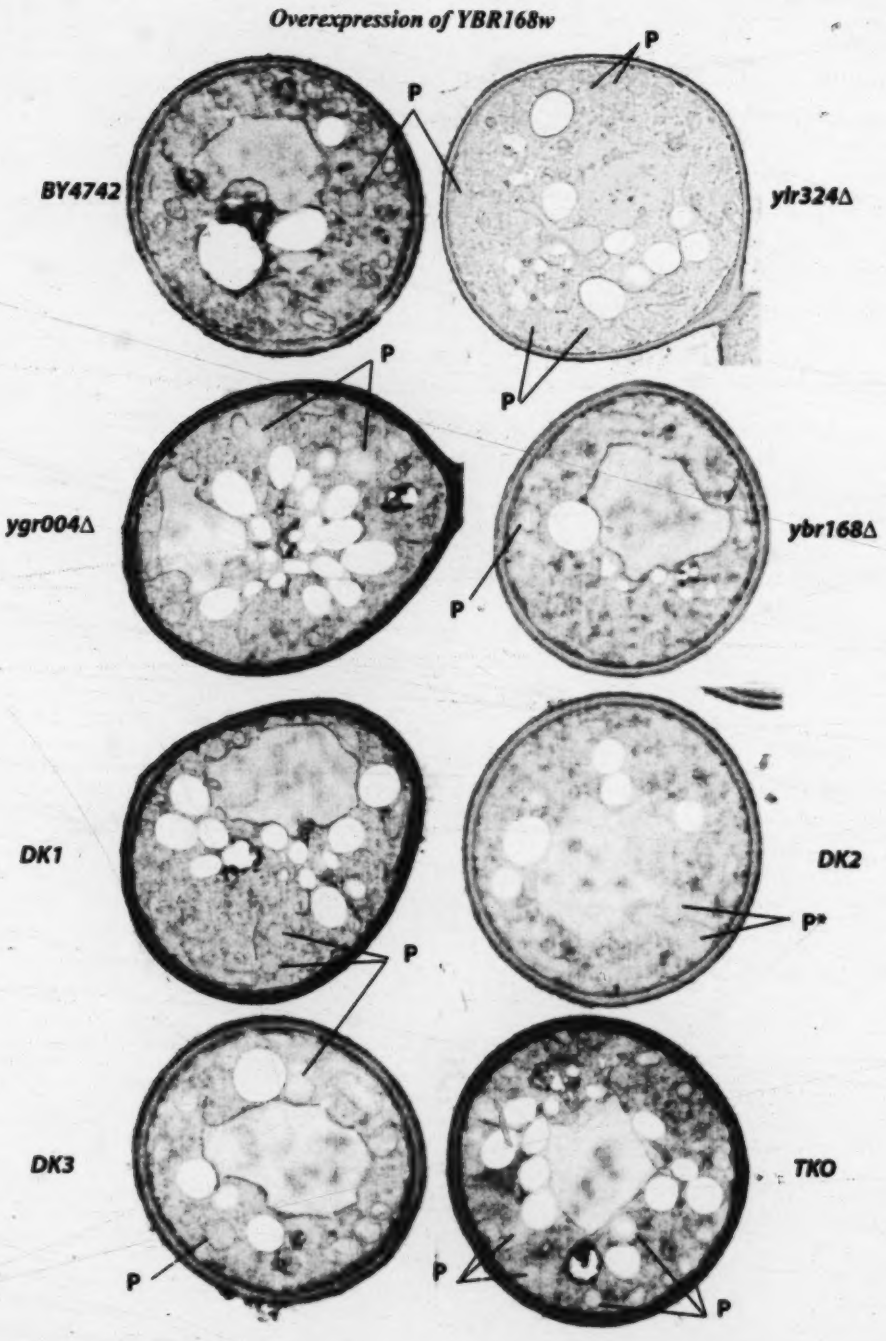

Figure 4-8. Peroxisome morphology in cells of gene overexpression strains

1999; Smith and Rachubinski, 2001; Sichting *et al.*, 2003). Chimeric genes were made by ligating the ORFs of *YLR324w*, *YGR004w*, *YBR168w*, *PEX11*, *PEX25*, *PEX28*, *PEX29* and *VPS1* in frame and downstream of sequences encoding one of the two functional domains (AD or DB) of the GAL4 transcriptional activator. All possible combinations of plasmid pairs encoding AD and DB fusion proteins were transformed into *S. cerevisiae* strain *SFY526*, and β-galactosidase filter detection assays were performed. Interactions were detected between Ylr324p and Ygr004p, Pex29p and itself (Figure 4-9). Ygr004p also interacted with itself, while weak interactions were detected between Ybr168p and Ylr324p and between Ybr168p and Pex28p (Figure 4-9). No interactions were detected between Ylr324p, Ygr004p or Ybr168p and any of Pex11p, Pex25p, Pex29p and Vps1p.

4.8 *PEX28* and *PEX29* function upstream of *YLR324w*, *YGR004w* and *YBR168w*

Since yeast two-hybrid analysis provided evidence of interaction between the *S. cerevisiae* homologs of *Yl*Pex23p and the *S. cerevisiae* homologs of *Yl*Pex24p and because cells of deletion mutants of the genes encoding these proteins are affected in the control of peroxisome size and number (data herein and Vizeacoumar *et al.*, 2003), we investigated the hierarchical organization of these genes. Strains containing systematic pairwise gene deletions of the *S. cerevisiae* homologs of *YlPEX23* and *YlPEX24* were made, namely *pex28Δ/ylr324Δ* (*CD1*), *pex28Δ/ygr004Δ* (*CD2*), *pex28Δ/ybr168Δ* (*CD3*),

Gal4-AD fused to	Gal4-DB fused to		Gal4-AD fused to	Gal4-DB fused to
Ylr324p	Ygr004p		Ylr324p	-
Ygr004p	Ylr324p		-	Ylr324p
Ylr324p	Ybr168p		Ygr004p	-
Ybr168p	Ylr324p		-	Ygr004p
Ylr324p	Pex29p		Ybr168p	-
Pex29p	Ylr324p		-	Ybr168p
Ybr168p	Pex28p		Pex28p	-
Pex28p	Ybr168p		-	Pex28p
Ylr324p	Ylr324p		Pex29p	-
Ygr004p	Ygr004p		-	Pex29p

Figure 4-9. Yeast two-hybrid analysis of the interaction partners of Ylr324p, Ygr004p and Ybr168p. A β-galactosidase filter detection assay is presented. *SFY526* cells synthesizing both Gal4-AD (left columns) and Gal4-DB (right columns) fusion proteins were tested for β-galactosidase activity. The color intensities of transformants for each strain is shown.

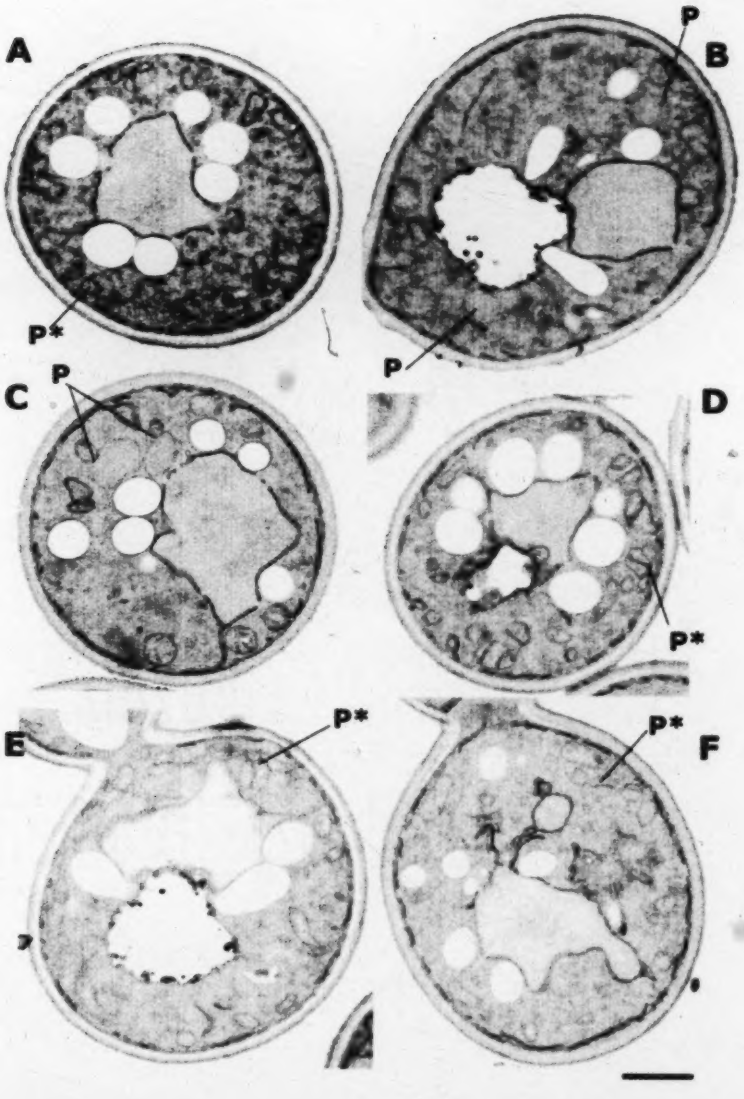

Figure 4-10. Peroxisome morphology in *S. cerevisiae* cells deleted for a *YlPEX23* homolog and a *YlPEX24* homolog. Ultrastructure of *pex28Δ/ylr324Δ* (A), *pex28Δ/ygr004Δ* (B), *pex28Δ/ybr168Δ* (C), *pex29Δ/ylr324Δ* (D), *pex29Δ/ygr004Δ* (E), and *pex29Δ/ybr168Δ* (F) cells. Cells were grown in YPD medium for 16 h, transferred to YPBO medium and incubated in YPBO medium for 8 h. Cells were fixed and processed for electron microscopy. P, peroxisome; P*, peroxisome cluster. Bar, 1 μm.

pex29Δ/ylr324Δ (*CD4*), *pex29Δ/ygr004Δ* (*CD5*) and *pex29Δ/ybr168Δ* (*CD6*). Electron microscopy analysis (Figure 4-10) showed that the majority of cells containing double deletions of a *YlPEX23* gene homolog and a *YlPEX24* gene homolog exhibited the clustered peroxisomal phenotype typical of *pex28Δ* and *pex29Δ* cells (Vizeacoumar *et al.*, 2003), although cells of the *CD2* and *CD3* strains (Figure 4-10 B and C, respectively) often exhibited enlarged peroxisomes that were well separated one from another. Together our data suggest that *YLR324w*, *YGR004w* and *YBR168w* function downstream of *PEX28* and *PEX29*.

4.9 Discussion

4.9.1 Growth and division of peroxisomes

Studies combining electron microscopy morphometry, pulse-chase analysis of peroxisomal protein trafficking *in vivo*, and the isolation and protein characterization of distinct peroxisomal subforms have shown that yeast peroxisomes do not grow and divide at the same time (Veenhuis and Goodman, 1990; Tan *et al.*, 1995; Titorenko *et al.*, 2000). There appears to be at least two different temporal patterns of peroxisome growth and division. In the yeast *Candida boidinii* (Veenhuis and Goodman, 1990), an initial event in peroxisome development is the extensive proliferation of immature peroxisomal vesicles containing only minor amounts of matrix proteins. This large increase in the number of immature peroxisomes by division precedes their growth through the import of membrane and matrix proteins and their conversion to mature organelles containing the complete set of peroxisomal proteins (Veenhuis and Goodman, 1990). The timing of

events of peroxisome growth and division is different in *Y. lipolytica*. In this organism, the growth of immature peroxisomal vesicles, which is accomplished by the import of matrix proteins, and their development into mature peroxisomes occur before completely assembled mature peroxisomes undergo division (Titorenko *et al.*, 2000). Similar temporal patterns of peroxisome growth and division have been observed for the yeast *Hansenula polymorpha* (Tan *et al.*, 1995). In human cells, both immature peroxisomal vesicles and mature peroxisomes are proposed to be able to divide (Gould and Valle, 2000). However, the division of immature peroxisomes prior to their growth and maturation by peroxisomal protein import can be seen only in some peroxin-deficient fibroblasts following reactivation or reexpression of an originally defective peroxin-encoding gene (Matsuzono *et al.*, 1999; South and Gould, 1999; Sacksteder and Gould, 2000). In normal human cells, in contrast, conversion of immature peroxisomal vesicles to mature peroxisomes by membrane and matrix protein import may occur before peroxisomes undergo division (Gould and Valle, 2000).

4.9.2 Molecular components in division

Members of the Pex11 family of peroxins, including Pex25p (Smith *et al.*, 2002) and Pex27p (Tam *et al.*, 2003; Rottensteiner *et al.*, 2003b) of *S. cerevisiae*, have been shown to effect peroxisome division in different organisms (Erdmann and Blobel, 1995; Marshall *et al.*, 1995; Sakai *et al.*, 1995; Li and Gould, 2002; Li *et al.*, 2002). The dynamin-like protein Vps1p has also been implicated in this process (Hoepfner *et al.*, 2001), and we recently showed that the peroxisomal integral membrane proteins Pex28p and Pex29p are also involved in controlling the number, size and separation of

peroxisomes in *S. cerevisiae* (Vizeacoumar *et al.*, 2003). Here, we have identified three novel peroxisomal proteins encoded by the ORFs *YLR324w*, *YGR004w* and *YBR168w* of *S. cerevisiae* and demonstrated that these proteins also act to control peroxisome size and number in this organism.

The identification of novel proteins required for peroxisome biogenesis in *S. cerevisiae* through their sequence similarity with known peroxins in other organisms enabled the identification of Pex28p and Pex29p (Vizeacoumar *et al.*, 2003). *Yl*Pex23p is a peroxisomal integral membrane protein required for peroxisome assembly in *Y. lipolytica* that shares extensive sequence similarity to three proteins of unknown function and unknown localization encoded by the ORFs *YLR324w*, *YGR004w* and *YBR168w* of the *S. cerevisiae* genome. Genomically encoded protein A chimeras of Ylr324p, Ygr004p and Ybr168p were shown by a combination of confocal microscopy and subcellular fractionation to be peroxisomal proteins. In their response to extraction by different chaotropic agents, Ylr324p, Ygr004p and Ybr168p act primarily as integral membrane proteins.

4.9.3 A role for the novel genes in peroxisome biogenesis

Ylr324p, Ygr004p and Ybr168p are not required for peroxisome assembly *per se*, as cells harboring deletions for one, two or all three of these genes still contain peroxisomes that are unaffected in their capacity to import PTS1- or PTS2-containing proteins. These peroxisomes are functional, at least to a degree, as the cells harboring deletions of these genes are able to grow in oleic acid-containing medium with essentially the same kinetics as wild-type cells (Figure 4-3 E). *YLR324w*, *YGR004w* and *YBR168w*

are also apparently not required for peroxisome inheritance, as all cells deleted for one or more of these genes still contained peroxisomes after numerous cell divisions. Also, if *YLR324w*, *YGR004w* and *YBR168w* had a direct role in the inheritance of peroxisomes, one might expect that a loss of peroxisomes from cells over time resulting from the impaired segregation of peroxisomes into daughter cells would lead to inhibited growth in oleic acid-containing medium for the deletion strains as compared to the wild-type strain, which was not observed.

Peroxisomes in cells deleted for the *YLR324w, YGR004w* and *YBR168w* genes are not normal and show distinctive phenotypic differences from wild-type peroxisomes. *ylr324Δ* cells showed increased numbers of peroxisomes versus wild-type cells, while *ygr004Δ* and *ybr168Δ* cells contained not only greater numbers of peroxisomes but also enlarged peroxisomes (Figure 4-5). Cells deleted for two of the *YLR324w*, *YGR004w* and *YBR168w* genes contained increased numbers of generally enlarged peroxisomes. Cells of the strain deleted for all three genes contained increased numbers of smaller to normally sized peroxisomes. Morphometric analyses and quantification revealed a 5-fold increase in the numbers of peroxisomes on average per cell for the triple deletion strain than for the wild-type strain. Although an occasional enlarged peroxisome was evident in cells deleted for all three genes, the peroxisomal phenotype of these cells strongly resembled that of cells deleted for only the *YLR324w* gene. The characteristics of peroxisomes of cells of the deletion strains are consistent with a role for *YLR324w, YGR004w* and *YBR168w* in the control of peroxisome size and number within *S. cerevisiae* cells. Our results suggest that Ylr324p acts primarily acts as a negative regulator of peroxisome number, while Ygr004p and particularly Ybr168p act as negative

regulators of peroxisome size. Nevertheless, Ygr004p shares some redundancy of function with Ylr324p and Ybr168p, but not *vice versa*, as overexpression of *YGR004w* in cells deleted for one or both of the *YLR324w* and *YBR168w* genes results essentially in the reestablishment of the wild-type peroxisome phenotype, but in contrast to wild-type cells, there is some evidence of peroxisome clustering. The reason why peroxisomes cluster in these overexpressing cells is unknown.

It is interesting to note that *Y. lipolytica* cells deleted for the *PEX23* gene also show evidence of abnormal peroxisomal divisional control. These cells lack mature peroxisomes but do accumulate small vesicular structures that contain both peroxisomal matrix and membrane proteins (Brown *et al.*, 2000). However, these membrane structures do not function as peroxisomes, as *pex23Δ* cells cannot grow on medium containing oleic acid as the sole carbon source. Therefore, although *Yl*Pex23p, like Ylr324p, Ygr004p and Ybr168p, likely has a role in the regulation of peroxisome division, *Yl*Pex23p probably does not function identically to Ylr324p, Ygr004p or Ybr168p in this process.

4.9.4 Interaction of genes involved in the same process

Pex28p and Pex29p have been implicated in the control of peroxisome size and number (Vizeacoumar *et al.*, 2003). A limited yeast two-hybrid screen revealed physical interactions among Ylr324p, Ygr004p, Ybr168p, Pex28p and Pex29p. No interactions were detected between these five proteins and Pex11p, Pex25p and Vps1p, which also have been shown to play a role in the control of peroxisome size and division. Further experimentation is required to determine whether these interactions are direct or bridged by other proteins. It is interesting to note that Ylr324p was shown to interact with

Pex29p. Some amount of Ylr324p (Figure 4-3) and of Pex29p (Vizeacoumar *et al.*, 2003) was always present in the 20KgS fraction in differential fractionation and in the less dense fractions during the gradient isolation of peroxisomes. Whether some portion of these proteins forms a complex and is localized to some compartment other than peroxisomes remains to be determined.

How might Ylr324p, Ygr004p, Ybr168p, Pex28p and Pex29p act to control the abundance, size and distribution of peroxisomes in the *S. cerevisiae* cell? Cells systematically deleted for one of the *YLR324w*, *YGR004w* and *YBR168w* genes and one of the *PEX28* and *PEX29* genes exhibited clusters of peroxisomes typically observed in cells deleted for the *PEX28* or *PEX29* gene (Vizeacoumar *et al.*, 2003). Our data suggest that Pex28p and Pex29p act upstream of Ylr324p, Ygr004p and Ybr168p in controlling peroxisome abundance and size.

Organelles are highly dynamic structures that undergo fission and fusion to control their numbers and modify their morphology in response to intracellular and extracellular cues and to permit their correct segregation at cell division. As a consequence, the maintenance of compartmental integrity by the eukaryotic cell requires the tight coordination of mechanisms controlling these events. Many proteins, including those encoded by the genes *YLR324w*, *YGR004w* and *YBR168w* of *S. cerevisiae*, are involved in controlling peroxisome number and size in the cell. Because of their role in the control of peroxisome size and number, we propose that *YLR324w*, *YGR004w* and *YBR168w* be designated as *PEX30*, *PEX31* and *PEX32*, respectively, and their encoded peroxins as Pex30p, Pex31p and Pex32p. The challenge remains to understand how the increasing number of proteins shown to be involved in controlling peroxisome number

and size interplay amongst themselves and signal to the cell how to control its peroxisome dynamics.

CHAPTER FIVE

THE Pex19p-BINDING REGIONS OF THE PEROXINS Pex30p AND Pex32p ARE REQUIRED FOR THEIR PEROXISOMAL LOCALIZATION BUT ARE SEPARATE FROM THEIR PEROXISOMAL TARGETING SIGNALS

5.1 Overview

The assembly of proteins at the peroxisomal membrane is a multi step process requiring their recognition in the cytosol, their targeting to the peroxisomal membrane, their insertion into that membrane and their stabilization within the lipid bilayer. The farnesylated peroxin (protein required for peroxisome assembly) Pex19p has been suggested to be the receptor that recognizes and targets newly synthesized peroxisomal membrane proteins (PMP). However, other evidence has implicated Pex19p not as an import receptor for PMPs but as a chaperoning molecule required for the stabilization of PMPs at the peroxisomal membrane. Differentiation between these two purported roles for Pex19p could be achieved by determining whether a PMP's targeting signal (mPTS) and region of Pex19p binding are one and the same or different. We have addressed the role of Pex19p in the assembly of two PMPs, Pex30p and Pex32p, of the yeast *Saccharomyces cerevisiae*. Pex30p and Pex32p are dispensable for normal peroxisome function, as cells lacking one or both of these proteins can still grow on oleic acid-containing medium, the metabolism of which requires functional peroxisomes. Systematic truncations from the carboxyl terminus, together with in-frame deletions of specific regions, have identified the mPTSs essential for the targeting of Pex30p and Pex32p to peroxisomes. Both Pex30p and Pex32p interact with Pex19p in regions that do not overlap with their experimentally identified mPTSs. However, Pex19p is required for localizing Pex30p and Pex32p to peroxisomes, because mutations that disrupt the interaction of Pex30p and Pex32p with Pex19p lead to their mislocalization to a compartment other than peroxisomes. Mutants of Pex30p and Pex32p that localize to peroxisomes but exhibit the phenotypes of cells lacking these proteins demonstrate that

the peroxisomal targeting and functionality of these two proteins are separable. Together, our data show that the interaction of Pex30p and Pex32p with Pex19p is required for their roles in peroxisome biogenesis and are consistent with a role for Pex19p in stabilizing or maintaining membrane proteins in peroxisomes

5.2 Identification of the region containing the targeting information in Pex30p and Pex32p

Pex30p and Pex32p are two newly identified peroxisomal integral membrane proteins (Vizeacoumar *et al.*, 2004). To delineate the mPTS of these two proteins, strains carrying deletions of varying lengths from the C-terminus regions were constructed. All these constructs were either fusion chimeras of protein A for biochemical analysis or GFP+ tagged for confocal microscopy. All constructs were made by Wanda N. Vreden. Several truncated mutants were constructed but only selective constructs will be discussed for simplicity. Subcellular fractionation was used to establish if the truncated mutants of Pex30p and Pex32p are associated with peroxisomes. In the case of Pex30p, the truncated protein Pex30(1-250)p, like the full length protein, preferentially localized to the 20KgP fraction enriched for peroxisomes. Further truncations of this protein preferentially accumulated in the 20KgS fraction (Figure 5-1 A) suggesting that the targeting information is present within the amino acid residues 230 to 250. In the case of Pex32p, the truncated protein Pex32(1-179)p, like the full length protein, preferentially localized to the 20KgP fraction enriched for peroxisomes. Further truncations of this protein preferentially accumulated in the 20KgS fraction (Figure 5- 1B) suggesting that

the targeting information for Pex32p is present within the amino acid residues 159 to 179. Peroxisomes were isolated from the 20KgP fractions of each of the strains expressing the truncated mutant proteins by isopycnic density gradient centrifugation. The gradients were fractionated, and equal portions of each fraction were analyzed by immunoblotting (Figure 5- 1C and 1D). All the truncated mutant proteins that enriched in the 20KgP fraction, co enriched with the peroxisomal matrix protein thiolase (Pot1p). As a slight shift in the peaking of the purified peroxisomal fraction was observed, the localization of the truncated proteins was determined by tagging them with GFP+ and performing a confocal microscopy analysis.

A fluorescent chimera of *Discosoma sp.* red fluorescent protein (DsRed) and the PTS1 Ser-Lys-Leu have been shown to target to peroxisomes of *S. cerevisiae* (Wang *et al.*, 2001; Smith *et al.*, 2002). Genomically encoded GFP+ chimeras of truncated proteins of Pex30p and Pex32p were localized in oleic acid-induced cells by fluorescence microscopy with DsRed-PTS1 to identify peroxisomes (Figure 5- 2A and 2B). Pex30(1-282)p, Pex30(1-250)p Pex32(1-203)p and Pex32(1-179)p, like their respective full lengths, colocalized with DsRed-PTS1 to small punctate structures characteristic of peroxisomes by confocal microcopy. Therefore, both microscopic analysis and sub-cellular fractionation showed that the truncated chimeric proteins are targeted to the peroxisomal compartment and that the targeting information lies in a span of 20 amino acid residues present in these proteins.

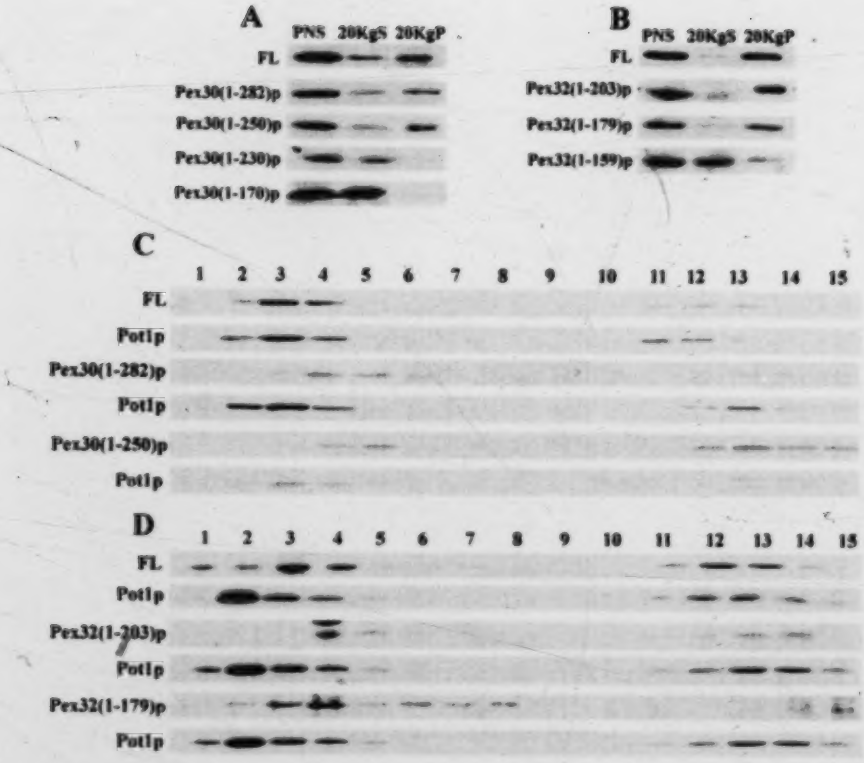

Figure 5-1 A-D. Subcellular fractionation of full length and truncated mutants. (A and B) Full length and truncated mutants of Pex30p and Pex32p are targeted to the organellar compartment. A PNS fraction was divided by centrifugation into a supernatant (20KgS) fraction enriched for cytosol and a pellet (20KgP) fraction enriched for peroxisomes. Equivalent portions of each fraction were analyzed. Immunoblotting with rabbit anti-Pot1p antibodies detected the protein A chimeras shown. (C and D) Organelles in the 20KgP fraction were separated by isopycnic centrifugation on a discontinuous Nycodenz gradient. Fractions were collected from the bottom of the gradient, and equal portions of each fraction were analyzed by immunoblotting. Fractions enriched for peroxisomes were identified by immunodetection of Pot1p. Strains expressing truncated protein were constructed by Wanda N. Vreden.

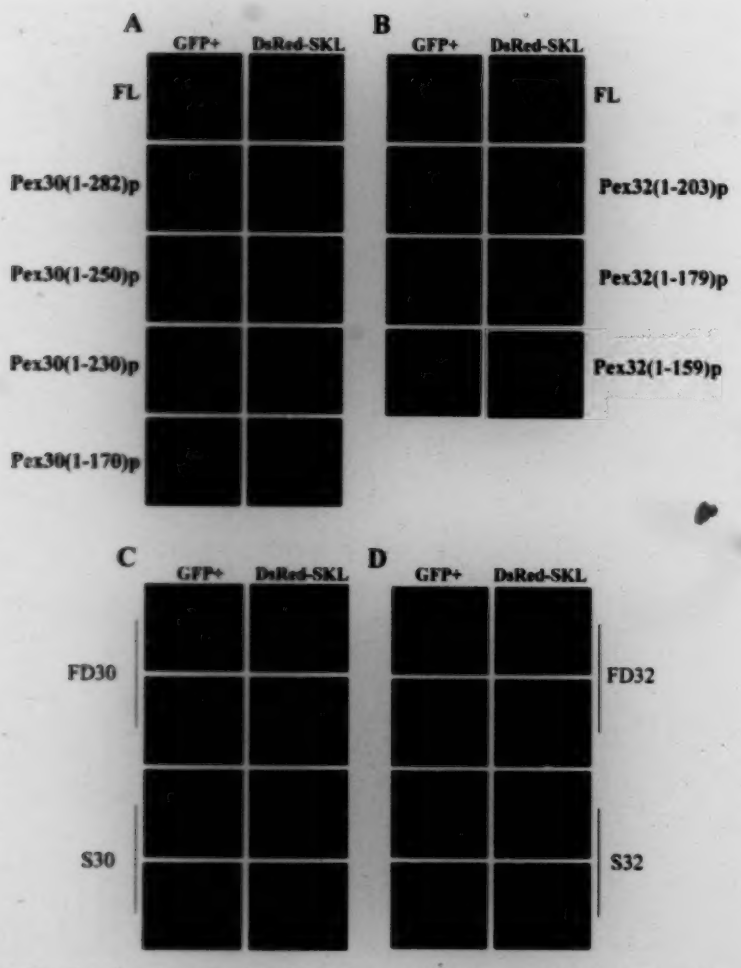

Figure 5- 2 A-D. Confocal analysis of full length and truncated mutants. (A and B) Full length and truncated mutants of Pex30p and Pex32p are targeted to the peroxisomal compartment. The sub cellular distributions of GFP+ chimeras were compared to that of DsRed-PTS1 in oleic acid-incubated cells by double labeling. Full length Pex30p and Pex32p colocalize with DsRed-PTS1 in punctate structures characteristic of peroxisomes. (C and D) In-frame deletion of Pex30p and Pex32p (*FD30* and *FD32* respectively), shows mislocalization of these proteins largely to the cytosol. Only the 20 amino acid of interest(Pex30p and Pex32p constructs are denoted by *S30* and *S32* respectively) fused to GFP+ showed shows diffused pattern. Strains expressing truncated protein were constructed by Wanda N. Vreden.

5.3 The region containing the 20 amino acid residues constitute mPTS

We next analyzed if the span of 20 amino acid residues is essential to target Pex30p and Pex32p to the peroxisomal compartment. For this, strains carrying in-frame deletions of the 20 amino acid residues of interest were constructed by overlap PCR for Pex30p (*FD30*) and Pex32p (*FD32*). The method of constructions of these strains is described in section 2.12.1. These constructs are under the control of the endogenous gene promoters. These constructs were made by Wanda N. Vreden. In the case of *FD30*, majority of the cells showed punctate pattern which colocalized with the peroxisomal marker, while a minor percentage of the cells exhibited a diffused pattern suggesting that the efficiency of targeting was greatly reduced. On the contrary, *FD32* cells, exhibited a diffused pattern with occasional punctate structures. This suggests that the region containing the 20 amino acid residues is essential for efficient targeting to the peroxisomal compartment.

To see if the 20 amino acid residues alone is sufficient for targeting, strains *S30* and *S32* were constructed. *S30* or *S32* carries only the 20 amino acid residues containing the targeting information fused to GFP+, with an ATG in the beginning of the segment while still remaining under the control of the endogenous gene promoter. These constructs were made by Wanda N. Vreden. Both *S30* and *S32* showed a diffused pattern with occasional punctate structures (Figure 5- 2 C and D). This suggests that the stretch of 20 amino acid residues alone is not sufficient for targeting of these peroxins. This was not surprising because these constructs lacked a transmembrane domain (TMD) that is essential for anchorage into the membrane. It has been shown that the TMD does not contain any

targeting information and that at least one TMD is essential for anchorage of the protein into the peroxisomal membrane (Mullen and Trelease 2000; Rottensteiner *et al.*, 2004). Remarkably, the amino acid residues within the 20 amino acid regions of Pex30p and Pex32p were strikingly similar to the sorting sequences identified in many other PMPs. The similarity is shown in the table 5-1. Using the similarity, we developed a general consensus sequence, R/K, (X_{0-3}), R/K, (X_{0-3}), R/K, X, I/L, for the sorting of membrane proteins. Thus from these results and by analytical reasoning, we address these sequences as mPTS in the rest of the document. It will be interesting to identify if Pex30p and Pex32p has multiple targeting sequences as reported in *Cb*PMP47 (Wang *et al.*, 2001). Further analysis by truncating these proteins from the N-terminal will reveal the answer to this question. However, we have discussed the significance of this in the later part of the text.

5.4 Mapping of Pex19p-binding region on Pex30p and Pex32p

From our analysis, we speculate that there could be multiple factors involved in the targeting of these proteins to the peroxisomal compartment. Pex19p has been shown to interact with a number of integral membrane proteins. We investigated if Pex19p interacts with Pex30p or Pex32p by yeast two hybrid analysis. Others have used this methodology to detect interactions between peroxins (for examples, see Girzalsky *et al.*, 1999; Sichting *et al.*, 2003; Vizeacoumar *et al.*, 2004). Chimeric genes were made by ligating the ORFs of *PEX30*, *PEX32* and *PEX19* in frame and downstream of sequences encoding one of the two functional domains (AD or DB) of the *GAL4* transcriptional activator. All possible combinations of plasmid pairs encoding AD and DB fusion

Table 5-1. A general consensus for mPTS signal present in most PMPs.

R/K, (X_{0-3}), R/K, (X_{0-1}), R/K, X, I/L		
*Sc*PEX3	RH--RG--KVL	13 - 19
*Sc*PEX15	K---KY--KSL	350 - 355
AtAPX	RK--RM--K	C-terminal
CbPMP47	KI--KK--RKI	232 - 238
*Hs*PEX16	R---KELRKKL	66 - 73
*Sc*Pex32	K---KL--K-L	160 - 164
*Sc*Pex30	RLLWKF--K-I	229 - 236
ScPex13	KFL-K---KIL	205 - 211
ScPex11	KVL-RLLQY-L	27 - 35
Hs ALDP	RLL-WLL-RLL	71 - 79

proteins were transformed into *S. cerevisiae* strains *HF7C* or *SFY526*, and tested for growth on selective plates lacking leucine, tryptophan and histidine or for the β-galactosidase filter detection assay. β-galactosidase filter detection assay yielded very weak or no interaction even in the known interactions such as Pex11p and Pex19p (Rottensteiner *et al.*, 2004). Hence we used the *His* reporter gene as selection marker. We found that Pex19p interacts with both Pex30p and Pex32p (Figure 5- 3A). None of the Gal4p fusion proteins alone were able to self activate the transcription of *His* reporter gene. However, since Pex19p self activates as a fusion with BD, we were not able to reverse the positions of the prey and bait vectors. It will be interesting to verify the binding properties of bacterially expressed recombinant proteins of Pex30p and Pex32p with Pex19p.

While our work was still in progress, Erdmann's group published (Rottensteiner *et al.*, 2004) an interesting consensus Pex19p binding region present in most integral membrane proteins of peroxisomes. By using a computer aided sequence analysis search, (Protein Sub-string Match Analysis (PSMA); OS, C++, in Unix platform), we searched for the presence of the consensus sequence and identified multiple putative Pex19p binding regions in Pex30p and Pex32p (listed in Table 5-2). It was interesting that the mPTS signals identified experimentally overlapped with one of the putative Pex19p binding region of Pex30p. In the case of Pex32p, we found that none of the putative Pex19p binding region overlapped with the experimentally determined mPTS signal. Based on this, we constructed truncated mutants to map the Pex19p binding regions on Pex30p and Pex32p. To further delineate the exact site of Pex19p interaction and to see if there are multiple interacting regions, we systematically constructed point mutants to

disrupt the interaction of Pex30p/Pex32p with Pex19p. Rottensteiner *et al.*, 2004, have shown that in *S. cerevisiae*, Pex11p and Pex13p interact with Pex19p at only one site by substituting proline within the core Pex19p binding region. This core Pex19p binding region, is suggested to form a small α-helix. Hence we made similar substitutions with proline in the listed (Table 5-2) putative Pex19p binding site. In the case of Pex30p, we found that the entire interaction was abolished when a proline substitution was made in the position L104 (Figure 5- 3B). Similarly, in the case of Pex32p, we found that a single substitution of L142P, abolished Pex19p interaction (Figure 5-3B). These point mutants L104P and L142P were still functional as they were able to interact with Pex28p and Pex29p respectively (Vizeacoumar *et al.*, 2004). Thus like Pex11p and Pex13p, Pex30p and Pex32p, interacts with Pex19p at only one site and this region does not overlap with the experimentally identified mPTS signal (Figure 5- 3C).

5.5 Pex19p controls the cellular distribution of Pex30p and Pex32p

Our result, thus far suggests that the mPTS signal and the Pex19p binding region are non-overlapping. This was interesting because, if Pex19p should act as a receptor for integral membrane proteins, then one would expect that the mPTS signal and the receptor binding region on the cargo must be one and the same. Since our data does not suggest that Pex19p functions as an import receptor, we next investigated if Pex19p has any role in controlling the distribution of these proteins to the peroxisomal compartment. To analyse this, we examined the distribution of Pex30p/Pex32p tagged with GFP+ in a strain expressing Mad1NLS-PEX19 (refer section 2.9.2), a form of Pex19p that is

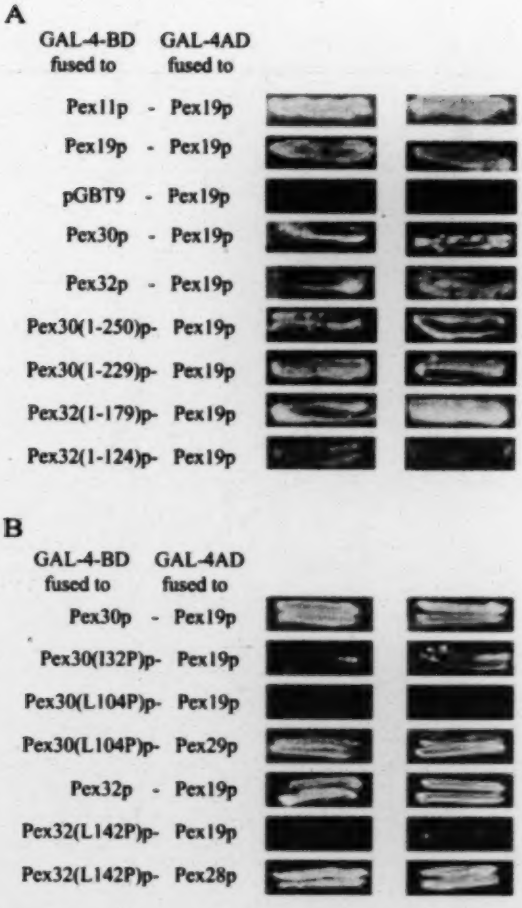

Figure 5-3 A and B. Identification of Pex19p-binding site in Pex30p and Pex32p. (A) Interaction of full length and truncated mutants with Pex19p in a yeast two-hybrid assay. Full-length and various truncations thereof were fused to the *GAL4* binding domain (Gal4p-BD) in vector pGBT9. The resulting plasmids were cotransformed into HF7C with a pGAD424-derived plasmid expressing a *PEX19-GAL4* activation domain (Gal4p-AD) fusion. As controls, empty pGBT9 or pGAD424 plasmids were used for transformation. Two independent sets of transformants were tested for growth on histidine, leucine and tryptophan dropout plates. Pex19p interactions were not tested in the opposite orientation because of auto activity of the Pex19p-Gal4p-BD fusion protein. (B) The effect of mutating the Pex19p-binding site in vivo. A yeast two-hybrid assay was used to study the interaction of Pex19p with full-length Pex30p and Pex32p, both mutated at position L104 and L142 respectively. Functionality of the mutated full-length-Gal4 BD fusions was tested for their known interaction with Pex29p and Pex28p respectively. Figure 5-3 A was contributed by Wanda N.Vreden.

Table 5-2. Putative Pex19p binding sites in Pex30p and Pex32p.

		[XXX][CFIL][YW][XX][ACFILQVWY][CILV][XX][ACFILVWY][LLQRV][XXX]
Pex30p	24-39	GGNTTKVIRAALEKN
	97-112	KNIWSSVLMLCLFIT
	232-247	KFKIVRLLVFYVTGL
Pex32p	93-108	FLPFTKILRLWLGII
	135-150	LDEIVVLLESVLDKL
	186-201	GTIFQIIIMRYISPG
	267-282	TVPLVEVLPKLLRDK

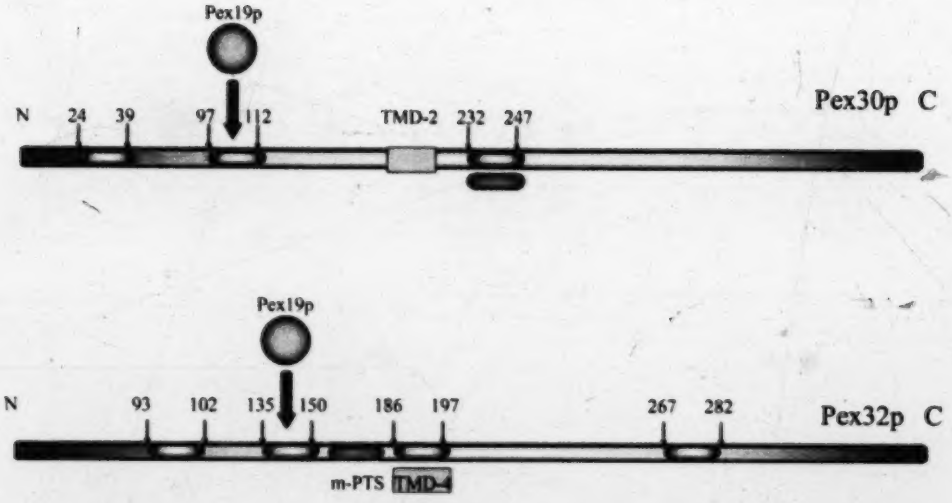

Figure 5-3 C. Schematic view of Pex30p and Pex32p showing that the Pex19p binding site and the mPTS signal are separable. A proposed TMD adjacent to the mPTS is also shown. Numbers indicate amino acid positions. Highlights in blue represent the Putative Pex19p binding site. Highlights in green represent mPTS signal. Yellow box represent the transmembrane domain (TMD) adjacent to the mPTS signal. The position of the amino acid residues are indicated.

efficiently targeted to the nucleus. Similar approaches were adapted in other studies (Jones *et al.*, 2001 and 2004). This is done in *pex19Δ* strain background. Briefly, cells expressing GFP+ chimeras of Pex30p or Pex32p in a *pex19Δ* strain were transformed with Mad1NLS-PEX19 plasmid. These cells were grown in minimal medium and induced for 8h with oleic acid-containing medium. Cells were washed and processed for fluorescence microscopy. Both Pex30p-GFP+ and Pex32p-GFP+ localized to punctate structures in a strain deleted for *PEX19* (Figure 5-4C). This suggests that these proteins are targeted to some other compartment as *pex19Δ* strain harbors no peroxisomes (Figure 5- 4C). While in the case of Mad1NLS-PEX19 expressing cells, Pex30p-GFP+ chimera and Pex32p-GFP+chimera localized to slightly elongate structures in the periphery of the nucleus (Figure 5-4 A and B). As a control, an NLS-GFP-PEX19 construct was used. This always showed a nuclear localization of Pex19p chimera. Thus the distribution of Pex30p and Pex32p seems to be under the control of Pex19p suggesting that Pex19p is indeed essential for targeting these proteins. This experiment also suggests that this interaction occurs in the cytosol possibly with the nascent polypeptides.

5.6 Pex19p is essential to target PMPs to the peroxisomal compartment

If Pex19p controls the subcellular distribution of these PMPs, then the disruption of the Pex19p binding site should lead to the original phenotype observed in the *pex19Δ* strain. Hence we constructed GFP+ chimeric proteins carrying the point mutation that abolishes the interaction with Pex19p. The mutant construct still remains under the control of the endogenous gene promoter. This strain was transformed with the

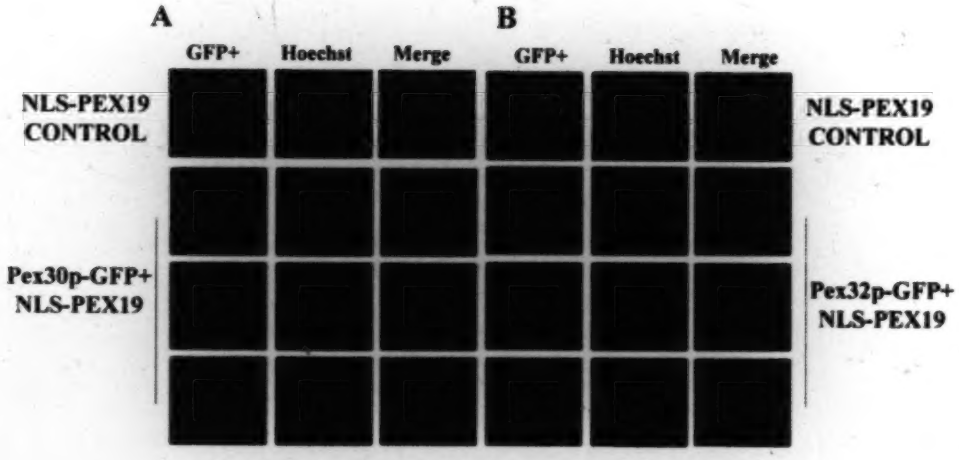

Figure 5-4 A and B. Sub cellular distribution of Pex30p and Pex32p in a strain expressing a form of Pex19p that gets targeted to the nucleus. (A and B) Cells expressing Pex30p-GFP+ and Pex32p-GFP+ in a *PEX19* deletion background were transformed with Mad1NLS-PEX19, were grown in SM medium (Ura-), induced in YNO medium for 8 h, stained with 10 nM per microlitres of cells with Hoescht 33342 (Sigma) for 2 min and images were obtained using Olympus BX50 microscope.

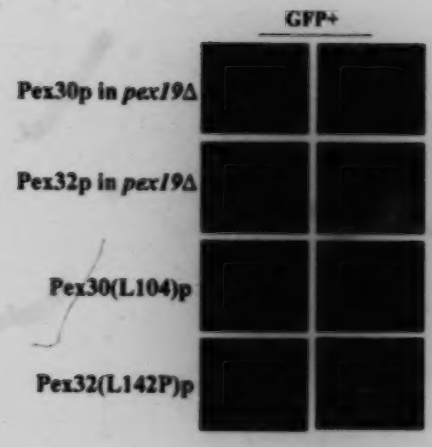

Figure 5-4 C. Cells expressing Pex30p-GFP+ and Pex32p-GFP+ in a *PEX19* deletion background or cells carrying a point mutation, disrupting Pex19p interaction and transformed with Mad1NLS-PEX19, were analysed the same way as described above.

Mad1NLS-PEX19 construct, induced in oleic acid-containing medium for 8 h and observed in the microscope for the localization of Pex30p and Pex32p GFP+ chimeras. The point mutants localized to random punctate structures that do not associate with the nuclear compartment, suggesting that Pex19p indeed controls the distribution of Pex30p and Pex32p (Figure 5-4 C). We performed biochemical analysis using protein A chimeras carrying the point mutations to see the localization of these mutants. Genomically encoding protein A chimeras of Pex30p and Pex32p carrying the point mutation in wild type cells and in *pex19Δ* cells were fractionated and a purified organellar fraction (20KgP) and a cytosolic fraction (20KgS) was obtained. We found that both Pex30p and Pex32p, in a strain deleted for *PEX19*, were enriched in the 20KgP (Figure 5-4 D). This is not surprising as it has been shown in *Hs*Pex14p and Pex3p of CHO cells are targeted to mitochondria in a *pex19Δ* strain (Otzen *et al.*, 2004; Honsho *et al.*, 2002) suggesting that PMPs are mistargeted in the absence of the correct compartment. When the organellar fraction was subjected to isopycnic gradient centrifugation to isolate different compartments, Pex30(L104P) and Pex32(L142P) did not co-fractionate with the purified peroxisomal fractions. Instead, they peaked at fractions 5 and 6 at the density of 1.150 g/cm^3 (Figure 5- 4E). It is interesting to note that in the strain deleted for *PEX19* these two proteins fractionated at the density of 1.156g/cm^3. Note that Pot1p is completely mislocalized to the cytosolic fraction when *PEX19* is deleted as there are no morphologically identifiable peroxisomes in this strain (Figure 5-4 E). Thus, either when Pex19p interaction is disrupted or when *PEX19* is deleted, Pex30p and Pex32p seem to be mistargeted.

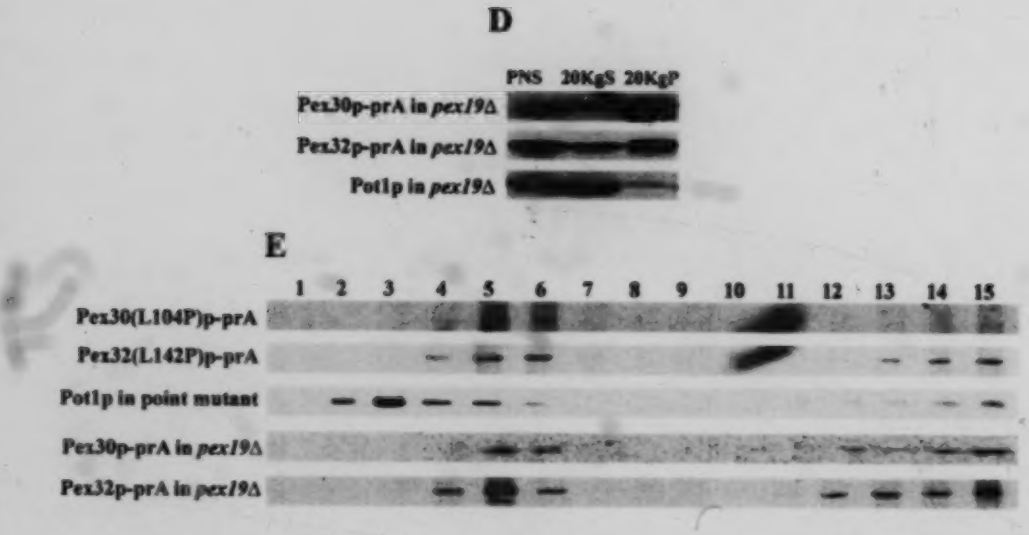

Figure 5-4 D and E. Sub cellular fractionation of cells expressing protein A chimeras of Pex30p and Pex32p. (D) Sub cellular fractionation of cells expressing protein A chimeras of Pex30p and Pex32p, in a *PEX19* deletion background were found to be enriched in the organellar compartment. (E) Organelles in the 20KgP fraction were separated by isopycnic centrifugation on a discontinuous Nycodenz gradient. Fractions were collected from the bottom of the gradient, and equal portions of each fraction were analyzed by immunoblotting. Fractions enriched for peroxisomes were identified by immunodetection of Pot1p. Note that these proteins are targeted to a less dense fraction (1.15g/cm3) either on the deletion of *PEX19* or upon making point mutations.

5.7 Mapping the functional domains of Pex30p and Pex32p

We next sought to identify the functional domains present in the PMPs, Pex30p and Pex32p. We processed all the strains expressing the truncated mutants for electron microscopy and analyzed the morphology of peroxisomes in all these strains. We found that in both the case of Pex30p and Pex32p, cells deleted for even the shortest sequence in the C-terminus, rendered the protein non functional even though the protein was still targeted to the peroxisomal compartment. Strains carrying Pex30(1-282)p and Pex30(1-250)p, although targeted these proteins to the peroxisomal compartments, they exhibited increased number of peroxisomes as observed in the full length deletion mutant (Figure 5-5). Similarly, Pex32(1-307)p, Pex32(1-203)p and Pex32(1-179)p although entered the peroxisomal membrane, exhibited enlarged peroxisomes as observed in *PEX32* deletion mutant (Figure 5- 6). Thus it seems that the C-terminus is essential for the functionality of these proteins. If Pex30p and Pex32p were to be targeted in a Pex19p dependent fashion, then the point mutants that do not interact with Pex19p must produce the deletion mutant phenotype. Indeed, this was the case as we found deletion mutant phenotype in these mutants (Figure 5-5 E and Figure 5-6 F). It is noteworthy to mention that in the *S. cerevisiae* genome Pex30p, Pex31p and Pex32p are the only three proteins that contain an unknown dysferlin domain. This domain is present towards the C-terminal region of these proteins. Truncation of this domain renders these proteins non functional. It has been suggested that these domains can bind caveolin in other organisms. However, yeast does not have any caveolin related proteins and it is of future interest to investigate the function of this domain in relation to peroxisomes. Pex24p of *Y. lipolytica* is yet another protein that contains this dysferlin domain.

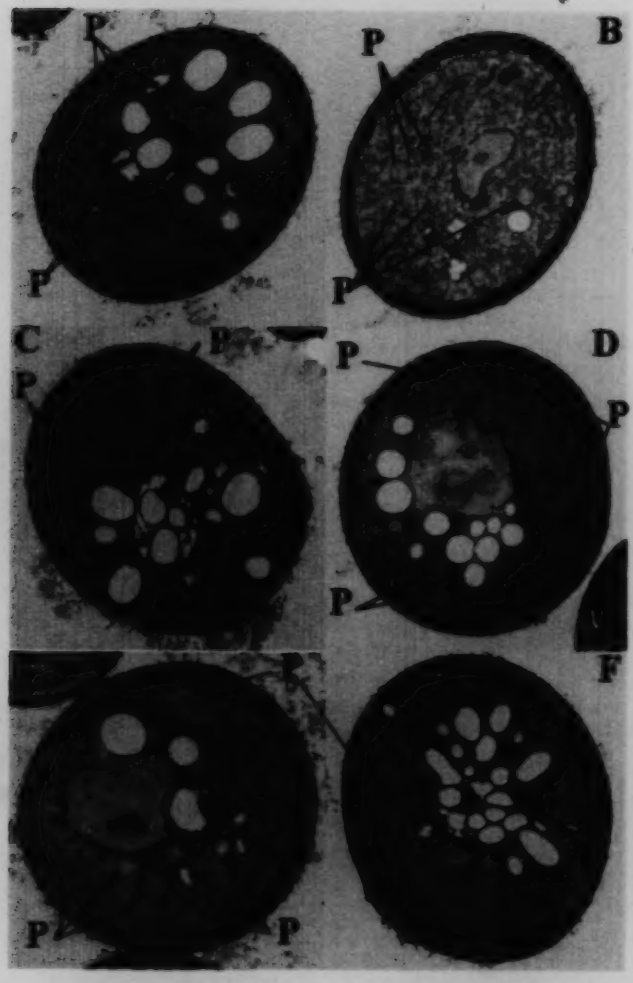

Figure 5-5. Peroxisome morphology in cells either deleted for *PEX30* or truncated mutants of *PEX30* exhibit peroxisomes that are altered in number and/or size. (A) *pex30Δ* (B) *PEX30(1-282aa)-prA* (C) *PEX30(1-250aa)-prA* (D) *PEX30(1-230aa)-prA* (E) *P30-L104P-prA* (F) *BY4742*. Cells were grown in YPD medium for 16 h, transferred to YPBO medium and incubated in YPBO medium for 8 h. Cells were fixed and processed for electron microscopy. P, peroxisome. Bar, 1 μm.

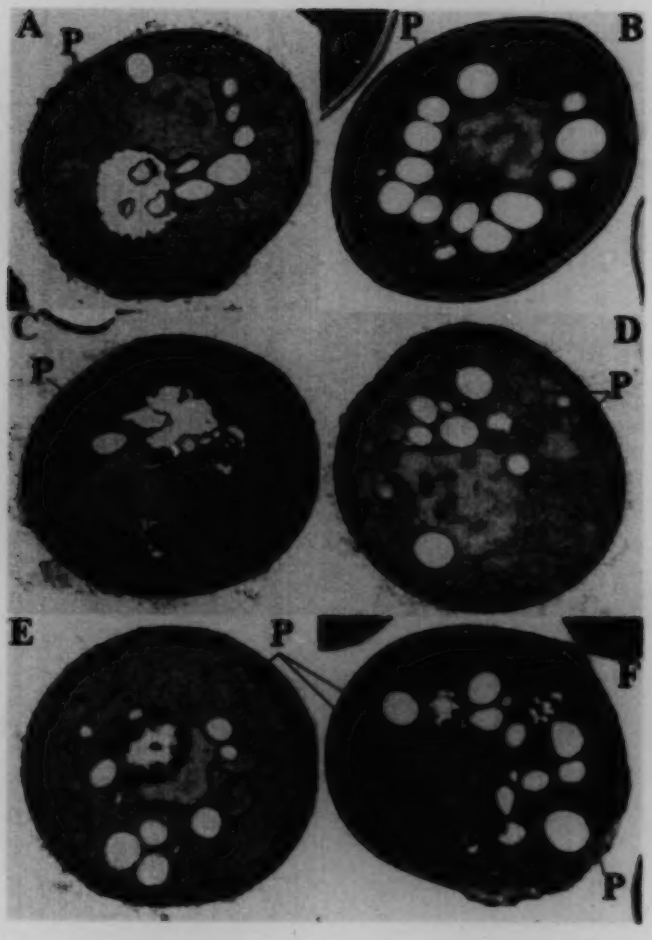

Figure 5-6. Peroxisome morphology in cells either deleted for *PEX32* or truncated mutants of *PEX30* exhibit peroxisomes that are altered in number and/or size. (A) *pex32Δ* (B) *PEX32(1-307aa)-prA* (C) *PEX32(1-203aa)-prA* (D) *PEX32(1-179aa)-prA* (E) *PEX32(1-159aa)-prA* (F) *P32-L142P-prA.* Cells were grown in YPD medium for 16 h, transferred to YPBO medium and incubated in YPBO medium for 8 h. Cells were fixed and processed for electron microscopy. P, peroxisome. Bar, 1 μm.

5.8 Discussion

5.8.1 Role of Pex19p in membrane biogenesis

The assembly of proteins at the peroxisomal membrane is a multi step process requiring their recognition in the cytosol, their targeting to the peroxisomal membrane, their insertion into that membrane and their stabilization within the lipid bilayer. While there is a general agreement that *PEX19* is required for peroxisomal membrane biogenesis, concerns have been raised regarding its specific role as an import receptor for newly synthesized PMPs (Subramani *et al.*, 1998, 2000; Schliebs and Kunau, 2004). One of the debated issues is whether the mPTS signal and the Pex19p binding region on the cargo are one and the same to validate Pex19p as a bona fide receptor (Snyder *et al.*, 2000; Fransen *et al.*, 2001, 2004; Biermanns and Gartner, 2001).

5.8.2 Pex30p and Pex32p are ideal candidates to study PMP targeting

Here the role of Pex19p in the targeting of the newly identified peroxins namely Pex30p and Pex32p of the yeast *S. cerevisiae* has been addressed. Most approaches using mutation of a peroxisomal integral membrane protein to probe for sequences that can act to target it to the peroxisomes lead to conditional lethal phenotype. This is due to the failure of cells to assemble peroxisomes and has been a major drawback to the study of membrane assembly. Accordingly, the newly identified PMPs, represent excellent experimental systems with which to define an mPTS, since they are dispensable for normal peroxisome function, as cells lacking one or both of these proteins can still grow on oleic acid-containing medium, the metabolism of which requires functional

peroxisomes. Various truncated forms of Pex30p and Pex32p to identify a minimal sequence that contained the targeting information were constructed. Subcellular fractionation was used to establish if the truncated mutants of Pex30p and Pex32p are associated with peroxisomes. Analysis of truncated form of Pex30p revealed that the targeting inf[illegible]ation is present within the amino acid residues 230 to 250. In the case of Pex32p, the targeting information is present within the amino acid residues 159 to 179. All the truncated mutant proteins that enriched in the 20KgP fraction, co-enriched with the peroxisomal matrix protein Pot1p (Figure 5- 1C). As we observed a slight shift in the peaking fraction, we determined the localization of the truncated proteins by tagging them with GFP+ and performing a confocal microscopy analysis.

Genomically encoded GFP+ chimeras of truncated proteins of Pex30p and Pex32p co-localized in oleic acid-induced cells by fluorescence microscopy with DsRed-PTS1. By this analysis, we confirm that the targeting information is present within a stretch of 20 amino acid residues as observed by subcellular fractionation. Therefore, both subcellular fractionation and microscopic analysis showed that the truncated chimeric proteins are targeted to the peroxisomal compartment and that the stretch of 20 amino acid residues is necessary for targeting.

5.8.3 mPTS signals of Pex30p and Pex32p

To verify if this stretch of 20 amino acid residues is essential, we constructed an in-frame deletion of these specific residues and determined its localization by confocal microscopy. In the absence of the 20 amino acid residues, Pex32p was not targeted to the peroxisomal compartment. Although, Pex30p still targeted, the efficiency of the targeting

was greatly reduced. This suggests that the stretch of 20 amino acid residues contain essential targeting information. To see if the information contained in this sequence is sufficient, we constructed two different strains containing only the 20 amino acid residues of interest fused to GFP+. We found that neither of the constructs was localized to the peroxisomal compartment. This suggests that this sequence alone is not sufficient for efficient targeting. This also indicates that there could be more factors playing a key role in the proper targeting of these novel peroxins. Interestingly, in mitochondria, for proteins that traverse the outer membrane once, it is now clear that the targeting signal is contained within the single TMD and its flanking region. To target proteins to mitochondria, this signal must contain a relatively short membrane spanning segment that has moderate hydrophobicity and is flanked by positively charged residues (Rapaport 2003). But in the case of peroxisomes, it has been shown that the TMD does not contain any targeting information. When a basic cluster of cottonseed ascorbate peroxidase (pAPX) containing the targeting information was fused to a synthetic membrane span, the reporter protein showed punctate pattern (Mullen and Trelease 2000). Hence we conclude that the region that contains this targeting information is the bona fide mPTS of these new peroxins. However, it has been shown that PMPs use multiple targeting signals (Dyer *et al.*, 1996; Jones *et al.*, 2001; Brosius *et al.*, 2002). Although it will be interesting to see if there are multiple mPTS signal present in these proteins by making N-terminal truncations, under the specific conditions used in these experiments, these mPTS signals seem to be functional. Especially, recent evidence from Goodman's laboratory suggest that multiple targeting modules on peroxisomal proteins are not redundant and that under different metabolic states, different mPTSs could function independently and efficiently

(Wang *et al.*, 2004). Interestingly, the amino acid residues within the mPTS regions of Pex30p and Pex32p were strikingly similar to each other and to the sorting sequences identified in many other PMPs. The similarity is shown in the table 5-1. This has led us to redefine and identify a unique signal sequence to target peroxisomal membrane proteins to the peroxisomal compartment. A general idea regarding the mPTS is that it is a hydrophilic stretch of amino acids with few basic residues. Of specific interest, this consensus mPTS signal happens to be an integral part of Pex19 binding site in Pex11p, Pex13p and even in HsALDP. Using the similarity, we developed a general consensus sequence, R/K, (X_{0-3}), R/K, (X_{0-3}), R/K, X, I/L, for the sorting of membrane proteins. The presence of this consensus pattern in the hydrophilic stretch of residues, could be beneficial in defining the membrane targeting signals of PMPs.

5.8.4 Interaction of Pex19p with the PMPs

The fact that Pex30p could still be targeted, although with poor efficiency, hinted us to search for other factors involved in targeting this protein to the peroxisomal compartment. In an attempt to understand the role of Pex19p, to target proteins effectively, as a first step, we performed yeast two-hybrid analysis. We found that both Pex30p and Pex32p interact with Pex19p. While our work was still in progress, Erdmann's group published some exciting finding by peptide scan analysis, a consensus sequence, for the identification of putative Pex19p binding sites on most PMPs (Rottensteiner *et al.*, 2004). Using this consensus sequence, we found that there are multiple putative Pex19p binding sites in these proteins (Listed in Table 5-2). It was interesting that the mPTS signals identified experimentally overlapped with one of the

putative Pex19p binding region of Pex30p. In the case of Pex32p, we found that the putative Pex19p binding region was at a closer proximity to the mPTS signal. We constructed truncated mutants to map the Pex19p binding regions on Pex30p and Pex32p. We also constructed some point mutants to delineate the exact site of Pex19p interaction and to see if there are multiple interaction sites. To do this, we systematically made point mutations in the sequences of putative Pex19p binding regions to disrupt the interaction of Pex30p/Pex32p with Pex19p. We made similar substitutions as described by Rottensteiner *et al.*, 2004, with proline in the putative Pex19p binding site. In the case of Pex30p, we found that the entire interaction was abolished when a proline substitution was made in the position L104. Similarly, in the case of Pex32p, we found that a single substitution of L142P, abolished Pex19p interaction. Thus like Pex11p and Pex13p, Pex30p and Pex32p, interacts with Pex19p at only one site in a region non-overlapping with the experimentally identified mPTS signal. Of particular interest is the interaction site on Pex32p with Pex19p. The interacting region and the mPTS signal are at a closer proximity separated by a distance of 9 amino acids. This is beneficial for an important reason. Reports have claimed that *PEX19* can function as an import receptor (Jones *et al.*, 2004). This is largely based on the analysis of several constructs made by Jones *et al.* These constructs contained a minimum of 60 to a maximum of 160 amino acid residues. Using these, it was shown that Pex19p interacts within this region and it is also sufficient to target proteins to the nuclear compartment in a Pex19p dependent manner (Jones *et al.*, 2004). What Jones *et al.*, has observed is probably a combinatorial action of two independent factors, the mPTS and its interaction with Pex19p. Furthermore, the argument that multiple mPTS could be found on the same protein is often used as an

argument to support the fact that Pex19p could probably interact in those other non redundant targeting modules. Here we provide evidence that Pex19p interacts at only one site, as in the case of Pex11p and Pex13p (Rottensteiner *et al.*, 2004) and this site is different from the mPTS signal. Interestingly, Pex19p binding regions of Pex11p and Pex13p were shown to be enough for targeting (Rottensteiner *et al.*, 2004). The possible explanation for this is that, these proteins seems to have the mPTS signal motif as an integral part of the Pex19p binding region (Table 5-1) It has been shown that multiple mPTS signals are non-redundant. PMP47 in *Candida boidini* has two discrete mPTS signals. One of them is responsible for targeting to the peroxisomes in an induced state and the other is responsible in a non induced state. PMP47 also interacts with Pex19p, but this association is only under inducible condition. Hence, without further molecular dissection, the data of Jones *et al.*, can only be interpreted as evidence favoring a role for *PEX19* as an import receptor.

5.8.5 The role of Pex19p in PMP targeting

We next investigated if Pex19p has any role as a receptor for targeting these proteins to the peroxisomal compartment. For this we examined the distribution of Pex30p/Pex32p genomically tagged with GFP+ in a strain expressing NLS-PEX19, a form of Pex19p that is efficiently targeted to the nucleus. Both Pex30p-GFP+ and Pex32p-GFP+ localized to a punctate structures in a strain deleted for *PEX19*. This suggests that these proteins are targeted to some other compartment as *pex19Δ* strain harbors no peroxisomes. Pex30p-GFP+ chimera and Pex32p-GFP+chimera in cells expressing Mad1-NLS-PEX19, localized to slightly elongate structures in periphery of

the nucleus. To further validate these findings, two different biochemical approaches were undertaken; first we monitored the localization of Pex30p and Pex32p chimeras in a strain where the interaction of these proteins with Pex19p was disrupted by point mutations. Second, we monitored these chimeric proteins in a *pex19Δ* strain. We found that in both cases, either when *PEX19* was deleted or when the interaction is disrupted Pex30p and Pex32p are targeted to a distinct compartment of lesser density than that of wild-type peroxisomes (1.15g/cm3). These results suggest that the distribution of Pex30p and Pex32p seem to be under the control of Pex19p. Since Pex30p and Pex32p are directed to the nuclear membrane, in a Pex19p dependent manner, one could conclude that Pex19p binds these proteins (nascent?) in the cytosol and directs them to the nuclear membrane. Alternatively, there could be other factors that could target these proteins to the membrane associated Pex19p for further assembly and insertion. It will be interesting to isolate such complexes from the cytosolic fraction and to see if Pex19p forms a part of this complex.

5.8.6 Functional domains of Pex30p and Pex32p

In addition, we have also mapped the region that is essential for the functionality of these two proteins. We found that in both the case of Pex30p and Pex32p, cells deleted for even the shortest sequence in the C-terminus, rendered the protein non functional even though the protein was still targeted to the peroxisomal compartment (Figure 5- 6A to G). Thus it seems that the C-terminus is essential for the functionality of these proteins. If Pex30p and Pex32p were to be targeted in a Pex19p dependent fashion, then the point mutants that do not interact with Pex19p should lead to the deletion mutant

phenotype. Indeed, this was the case as we found deletion mutant phenotype in these mutants (Figure 5- 5E and 6F). It is noteworthy to mention that in the yeast genome Pex30p, Pex31p and Pex32p are the only three proteins that contain an unknown dysferlin domain. This domain is present towards the C-terminus region of these proteins. Truncation of this domain renders the proteins non functional. It has been suggested that these domains can bind caveolin in other organisms. However, yeast does not have any caveolin related proteins and it is of future interest of our laboratory to investigate the function of this domain in relation to peroxisomes. Pex24p of *Y. lipolytica* is yet another protein that contains this dysferlin domain.

5.8.7 Factors governing targeting of PMPs

In summary, we find that Pex19p is essential for targeting these novel peroxins and there seems to be more factors that essentially contribute for proper targeting and insertion of PMPs into the peroxisomal compartment. Three factors can be envisioned: the interaction of the PMPs with Pex19p, the mPTS signal of the PMPs and a TMD, adjacent to the mPTS. As such, there is no credible evidence or argument that *PEX19* does not function as an assembly factor facilitating the insertion of membrane proteins or a cytosolic chaperone. Pex30p and Pex32p are not essential for early peroxisome membrane synthesis and hence the interaction of Pex30p and Pex32p cannot be attributed to a general role of Pex19 in peroxisome membrane synthesis. Therefore, Pex19p interactions may be connected with a transport function or to facilitate insertion of proteins into the peroxisomal membrane. From our data, we suggest that the mPTS could

be a separate entity or be an integral part of the Pex19p binding site. Also, in conjunction with an adjacent TMD, proper anchorage of the peroxin could be facilitated.

To obtain a more comprehensive picture of the biogenesis of membrane proteins, the following questions still need to be addressed. Are there any other cytosolic factors that contribute to the targeting of membrane proteins? Does the specific lipid composition of the membrane have any role in targeting? Finally, does the same mechanism apply to proteins irrespective of whether the signals are contained within the C- or N-terminal regions? Future research might reveal more exciting results on how the membrane is assembled.

CHAPTER SIX

THE DYNAMIN LIKE PROTEIN Vps1p ASSOCIATES WITH PEROXISOMES IN A Pex19p-DEPENDENT MANNER

6.1 Overview

Organelle division is a dynamic process regulated by multimeric protein machineries, the details of which are just beginning to be unveiled. The mechanisms underlying the accurate partitioning of yeast peroxisomes, mitochondria and vacuoles are distinct, yet share common elements. These organelles all move along actin filaments and require fusion and fission to maintain normal morphology. Dynamins are thought to play important roles in the fission of peroxisomes and mitochondria. The dynamin-related protein Vps1p is suggested to be involved in peroxisome fission, as cells lacking Vps1p contain a few enlarged peroxisomes. But if and how Vps1p associates with the peroxisomal membrane is unclear. Pex19p has been shown to function as an import receptor for peroxisomal membrane proteins (PMP) and/or as a chaperone acting to stabilize PMPs at the peroxisomal membrane. Pex19p recognizes two regions in Vps1p. Mutation of these Pex19p-binding regions does not affect vacuolar assembly, while mutation of only the first, more amino-terminal region leads to cells with reduced numbers of enlarged peroxisomes, the phenotype of cells lacking Vps1p. Vps1p does not associate with peroxisomes once its interaction with Pex19p is disrupted. However, overproduction of Pex19p does not alter the normal distribution of Vps1p within the cell. Together, our data suggest that Pex19p stabilizes the association of Vps1p with peroxisomes and that this interaction is required for peroxisome fission.

6.2 Pex19p interacts with Vps1p

Rottensteiner *et al.*, 2004, developed a consensus sequence of amino acid residues that seems to be recognized by Pex19p in most peroxisomal membrane proteins. We identified two such putative Pex19p binding sites in Vps1p using the Unix based Protein Sub-string match analysis software (Table 6-1). Vps1p belongs to the dynamin protein family and is essential for sorting proteins to the vacuolar compartment. Deletion mutant of Vps1p contains few enlarged peroxisomes (Hoepfner *et al.*, 2001). Since we found two putative Pex19p binding sites, we hypothesized that the association of Vps1p with the peroxisomes depends on Pex19p. Yeast two hybrid analysis was used to detect any interaction of these proteins. Others have used this methodology to detect interactions between peroxins (for examples, see Girzalsky *et al.*, 1999; Sichting *et al.*, 2003; Vizeacoumar *et al.*, 2004). Chimeric genes were made by ligating the ORF of *VPS1* in frame and downstream of sequences encoding one of the two functional domains (AD or DB) of the *GAL4* transcriptional activator. All possible combinations of plasmid pairs encoding AD and DB fusion proteins were transformed into *S. cerevisiae* strains *HF7C* or *SFY526*, and tested for growth on selective plates lacking leucine, tryptophan and histidine or for the β-galactosidase filter detection assay. β-galactosidase filter detection assay yielded a weak or no interaction even in the known interactions such as Pex11p and Pex19p (Rottensteiner *et al.*, 2004). Using *his* as the reporter gene, we found that Pex19p indeed interacts with Vps1p (Figure 6-1). None of the Gal4p fusion proteins alone were able to self activate the transcription of *his* reporter gene. However, since Pex19p self activates as a fusion with BD, we did not reverse the positions of the prey and bait vectors.

Table 6-1 Putative Pex19p binding regions in Vps1p

		(X)(X)[CFILTVW](X)(X)[ACFILQVWY][CILV](X)(X)[ACFILVWY][ILQRV](X)(X)
Vps1p	509-523	TIPTNEFVVDIIKAE
	633-647	KRTIADIIPKALMLK

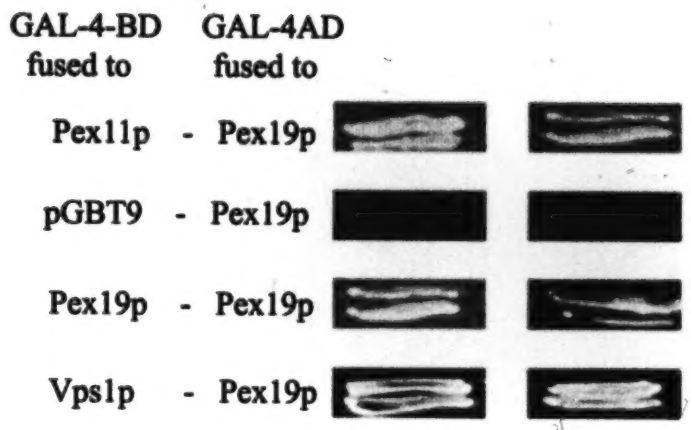

Figure 6-1. Interaction of Vps1p with Pex19p in a yeast two-hybrid assay. **Full-length genes** were fused to the *GAL4* binding domain (Gal4p-BD) in vector pGBT9. The resulting plasmids were cotransformed into HF7C with a pGAD424-derived plasmid expressing a *PEX19-GAL4* activation domain (Gal4p-AD) fusion. As controls, empty pGBT9 or pGAD424 plasmids were used for transformation. Two independent sets of transformants were tested for growth on histidine, leucine and tryptophan dropout plates. Pex19p interactions were not tested in the opposite orientation because of auto activity of the Pex19p-Gal4p-BD fusion protein.

6.3 Disrupting Pex19p interaction causes *VPS1* deletion mutant phenotype

We next wanted to see if the putative Pex19p binding regions, identified using the consensus Pex19p binding sequence, are essential for the association of Vps1p with Pex19p. For this, we constructed strains carrying in-frame deletions of these amino acids of interest by overlap PCR designated as *FDV1* for *Vps1(Δ509-523)* and *FDV2* for *Vps1(Δ633-647)*. These mutants are still under the control of the endogenous gene promoter. To analyse the morphology of peroxisomes, we performed an indirect immunofluorecence analysis using antibodies raised against thiolase and SKL-containing peroxisomal matrix proteins. *FDV1* mutant exhibited few enlarged peroxisomes as observed in a *vps1Δ* deletion mutant (Figure 6-2). The other mutant, *FDV2,* exhibited normal peroxisomes like the wild type strain (Figure 6-2). This suggests that the amino acid residues 501-523 in Vps1p are essential for its functional contribution towards peroxisomal compartment.

6.4 Vacuolar protein sorting function is normal in *FDV1* mutant

By making an in-frame deletion of the putative Pex19p binding site, one of the possibilities is that the entire protein Vps1p is rendered non functional. Alternatively, the amino acid residues between 501 and 523 could be essential for the abnormal peroxisome phenotype. This might help to dissect the domain that is essential for its function in the sorting of proteins to the vacuolar compartment to its peroxisomal role. Vacuolar

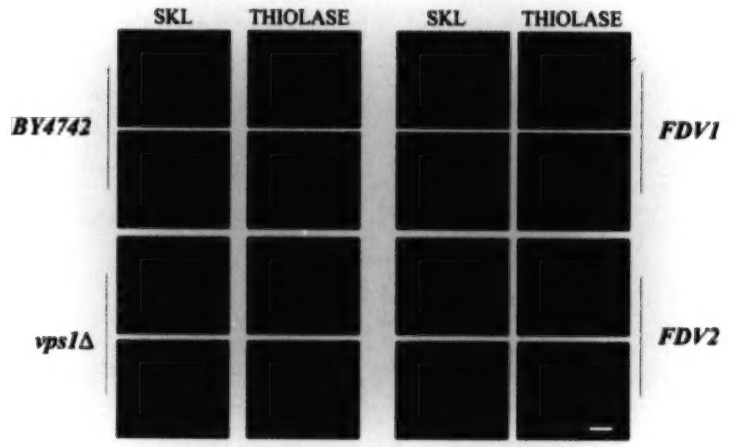

Figure 6-2. Analysis of in-frame deletions of Vps1p by immunofluorescence microscopy (*FDV1* and *FDV2* respectively). Mutant strains were grown in YPD medium for 16 h, transferred to YPBO medium, and incubated for 8 h in YPBO medium. Cells were observed by immunofluorescence microscopy with antibodies to the PTS1 tripeptide SKL (SKL) or to the PTS2-containing protein, Pot1p. Rabbit primary antibodies (SKL) were detected with FITC-conjugated secondary antibodies. Guinea pig primary antibodies (Pot1p) were detected with rhodamine-conjugated secondary antibodies. Bar, 1 μm.

homeostasis requires fusion, fission and actin-dependent transport of vacuolar membranes to the daughter cells. Mutations of proteins involved in these processes often results in aberrant vacuolar morphology (Seeley *et al.*, 2002). It has been known that at least 60% of the cells exhibit fragmented vacuolar morphology when *VPS1* is deleted (Seeley *et al.*, 2002; Peters *et al.*, 2004). Using the fluorescent vacuolar vital stain FM4-64 (Vida and Emr 1995), we analysed the morphology of vacuoles in the mutants that we have constructed. We found that both *FDV1* and *FDV2* exhibited normal vacuolar morphology, unlike the deletion mutant which showed higher percentage of fragmented vacuoles (Figure 6-3A). It has been suggested that the mixed phenotype observed in *vps1*Δ showing enlarged and fewer vacuoles (fission mutants) and many small fragmented vacuoles (fusion mutants), is due to its ability to mutually control membrane fission and fusion (Peters *et al.*, 2004). We also analysed the sorting of the soluble vacuolar hydrolase carboxypeptidase Y (CP-Y). CP-Y is cotranslationally translocated into the ER, where it is glycosylated. It is then transported to the Golgi where a sorting signal present in its propeptide form is recognized and then finally sorted to the vacuoles. Defects in this vacuolar sorting lead to the secretion of CP-Y through the secretory pathway, outside the cell (Marcusson *et al.*, 1994). We found that *FDV1* had a similar background as that of wild-type strain suggesting that vacuole protein sorting is unaffected in this strain (Figure 6-3B). However, the other in-frame deletion mutant *FDV2*, exhibited a slightly increased secretion of CP-Y, suggesting that it might be partly impaired in vacuolar protein sorting. As expected, *VPS1* deletion showed high secretion of CP-Y outside the cell (Figure 6-3 B).

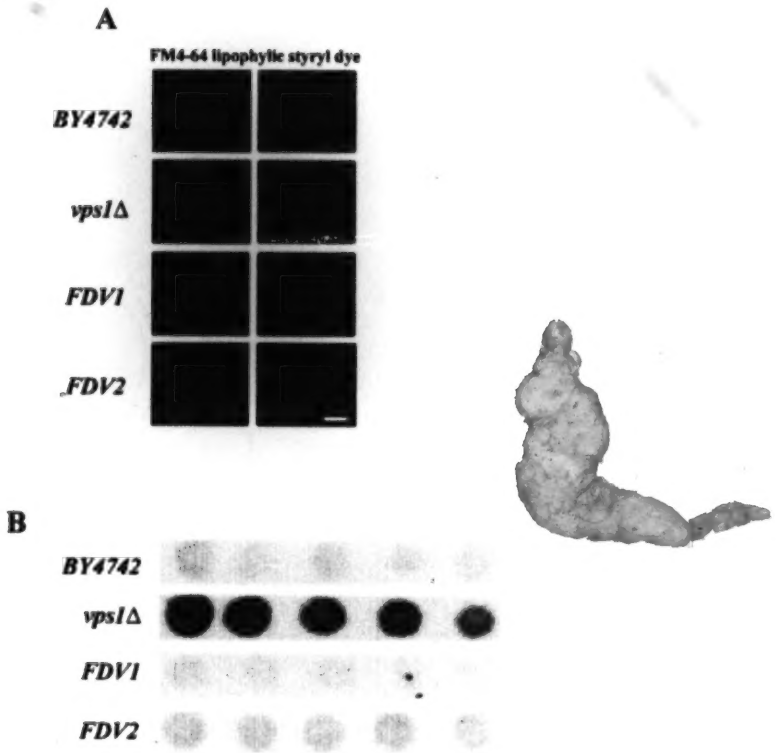

Figure 6-3 A and B. Analysis of vacuolar morphology and protein sorting function. (A) Cells were grown overnight and sub cultured to reach an OD of 0.5. To about 100 µl of cells, 1 µl of 8 mM FM4-64 dye was added and incubated for 30 minutes at 30 C. Cells were washed and re-incubated in fresh YPD medium for an hour and a half. Images were captured on an Olympus BX50 microscope (Olympus, Tokyo, Japan) equipped with a digital fluorescence camera (Spot Diagnostic Instruments, Sterling Heights, MI). (B) The CPY secretion assay was performed according to the method of Roberts *et al.* (1991) with minor modifications. Briefly, cells were grown to an OD of 0.5 and spotted on YEPD plates with serial dilution and allowed to dry before filter overlay and incubation. Nitrocellulose sheet was spread on these plates spotted with diluted cells and left to grow for 24 h. The membrane is carefully lifted and rinsed to remove the cells stuck to it. Immunoblotting using the CP-Y antibody is done on the membrane and the secreted protein is detected.

6.5 Effect of point mutation in Vps1p

Thus far, our results suggest that one of the putative Pex19p binding sequences in Vps1p is essential for its function in the fission of peroxisomes and we next wanted to investigate the exact site of interaction of between Pex19p and Vps1p. Hence we constructed point mutants to disrupt the interaction of Vps1p with Pex19p. Rottensteiner *et al.*, (2004), have shown that in *S. cerevisiae* Pex11p and Pex13p interact with Pex19p at only one site by substituting proline at any position within the core Pex19p binding region. Substitution of proline within the Pex19p binding region is likely to disrupt the α-helical conformation thought to enhance its association with Pex19p. Hence we made similar substitutions with proline in the putative Pex19p binding site at the residue 516 (*V516P*) instead of valine. We performed a two hybrid analysis to see if the interaction was disrupted. Although the interaction with Pex19p was disrupted (Figure 6-4A), the cells grew on drop- out plates over prolonged incubation. We then constructed a strain carrying this point mutation and monitored the morphology of peroxisomes by immunofluorescence and by electron microscopy. This way, the gene is still under the control of its endogenous gene promoter and does not lead to any aberrant expression. We found that the point mutant strain harbored a mixed phenotype of both enlarged peroxisomes and wild-type peroxisomes (Figure 6-4B and 6-5C). This suggests that either the point mutation substitution does not fully abolish its interaction with Pex19p or there could be other potential factors that could still associate Vps1p with the peroxisomes.

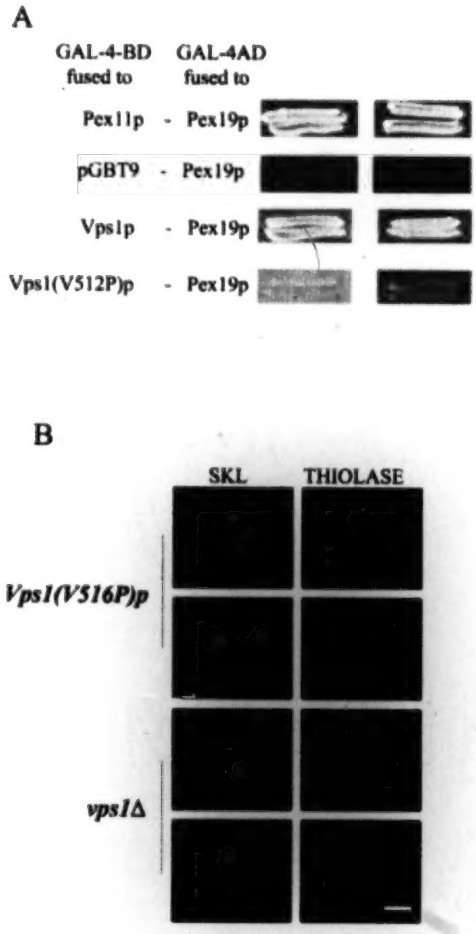

Figure 6-4 A and B. The effect of mutating the Pex19p-binding site in vivo. (A) A yeast two-hybrid assay was used to study the interaction of Pex19p with Vps1p, mutated at position V516. (B) Peroxisomal morphology of point mutant. Cells were observed by immunofluorescence microscopy with antibodies to the PTS1 tripeptide SKL (SKL) or to the PTS2-containing protein, Pot1p. Rabbit primary antibodies (SKL) were detected with FITC-conjugated secondary antibodies. Guinea pig primary antibodies (Pot1p) were detected with rhodamine-conjugated secondary antibodies

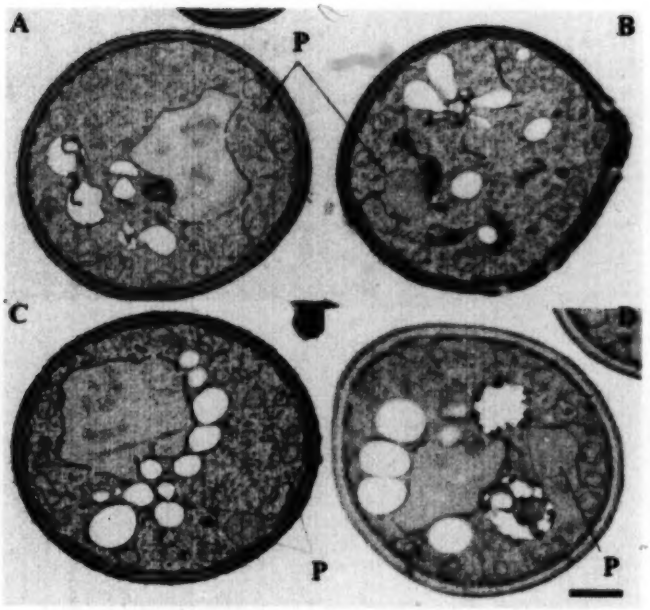

Figure 6-5. Peroxisome morphology in wild-type cells and Vps1p mutants. (A) *BY4742* (B) *FDV1* (C) *vps1Δ* (D) *vps(V516P)*. Cells were grown in YPD medium for 16 h, transferred to YPBO medium and incubated in YPBO medium for 8 h. Cells were fixed and processed for electron microscopy. P, peroxisome. Bar, 1 μm.

6.6 Pex19p does not control the subcellular distribution of Vps1p

We next attempted to find out if the distribution and association of Vps1p with peroxisomes was altered in a Pex19p-dependent fashion. To analyze this, we examined the distribution of Vps1p genomically tagged with GFP+ in a strain expressing Mad1NLS-PEX19, a form of Pex19p that is efficiently targeted to the nucleus. Similar approaches were adapted in other studies (Jones *et al.*, 2001 and 2004). This is done in *pex19*Δ strain background. Briefly, cells expressing GFP+ chimera of Vps1p in a *pex19*Δ, background were transformed with Mad1NLS-PEX19 plasmid. Cells were grown in minimal medium and induced for 8 h with oleic acid-containing medium. Induced cells were washed and processed for fluorescence microscopy. Vps1p-GFP+ localized to punctate structures with a diffused cytosolic background in both the strains, either deleted for *PEX19* or in the case of cells expressing Mad1NLS-PEX19, a pattern observed in wild type strains (Figure 6-6 B). As a control, an NLS-GFP-PEX19 construct was used. Thus the distribution of Vps1p seems to remain unaffected by Pex19p.

6.7 Vps1p is not recruited to the peroxisomes in a Pex19p dependent manner

Vps1p is predominantly a cytosolic protein and Vps1-GFP+ chimera often exhibit a diffused cytosolic stain with occasional punctate pattern. The nature of this punctate composite is unknown. Now that, we know Pex19p associates with Vps1p, we wanted to see if the localization pattern of Vps1p was altered in a strain overexpressing Pex19p. We hypothesized that overexpression of *PEX19*, could possibly lead to an increased,

detectable amount of Vps1p associating with the peroxisomes. We monitored the Vps1-GFP+ chimera by fluorescence microscopy using DsRed-PTS1 as the peroxisomal marker. A fluorescent chimera formed between *Discosoma sp.* red fluorescent protein (DsRed) and the PTS1 Ser-Lys-Leu have been shown to target to peroxisomes of *S. cerevisiae* (Wang *et al.*, 2001; Smith *et al.*, 2002). Briefly, cells expressing GFP+ chimera of Vps1p were transformed with the overexpression construct, *Yep13-PEX19* and the peroxisomal marker DsRed-PTS1 into a strain deleted for *PEX19*. Cells were grown in minimal medium and induced for 8 h with oleic acid-containing medium. Induced cells were washed and processed for fluorescence microscopy. Vps1p-GFP+ localized to punctate structures with diffused cytosolic staining. These punctuate structures did not colocalize with the peroxisomal marker and that the subcellular distribution of Vps1p-GFP+ chimera remained unaltered (Figure 6-6A). From these data we conclude that Pex19p does not recruit Vps1p to the peroxisomal compartment.

6.8 Vps1p associates with the membrane fraction in a Pex19p-dependent manner

Pex19p does not seem to recruit Vps1p to the peroxisomes. To understand the significance of this interaction, we monitored the endogenous level of Vps1p in a strain where the interaction with Pex19p was disrupted. Vps1p, being a cytosolic protein, was found to be preferentially enriched in the 20KgS fraction with a minimum amount in the 20KgP fraction (Figure 6-7). The control proteins G6PDH was found exclusively in the

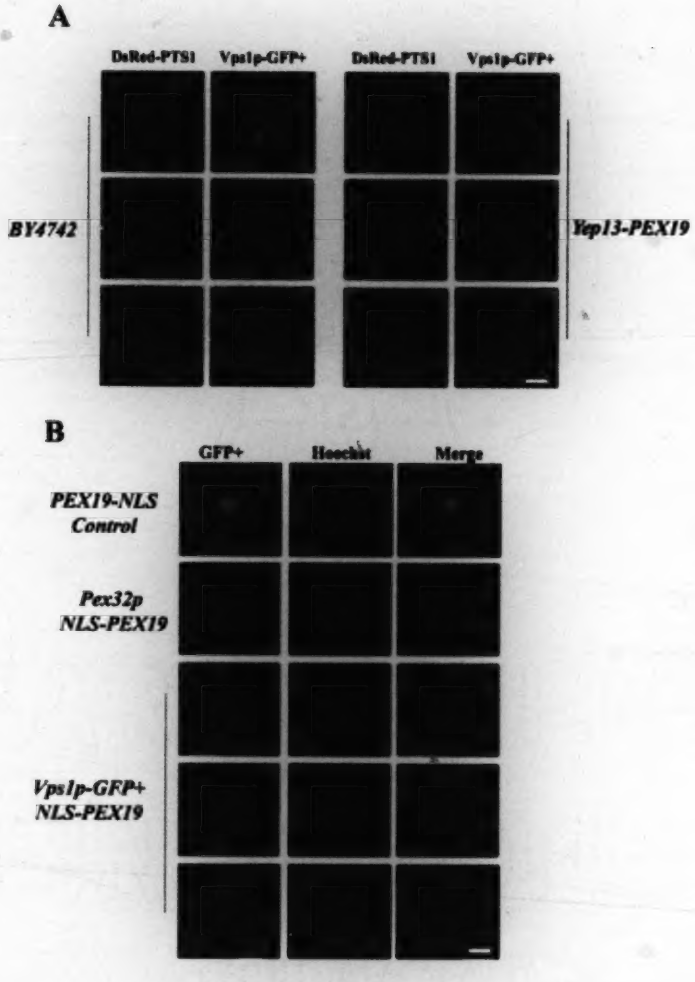

Figure 6-6 A and B. Effect of Pex19p on Vps1p. (A) The sub cellular distributions of GFP+ chimeras of Vps1p were compared to that of DsRed-PTS1 in oleic acid-incubated cells by double labeling, fluorescence microscopy, in a strain over expressing *PEX19*. GFP+ chimera of Vps1p does not colocalize with DsRed-PTS1. (B) Sub cellular distribution of GFP+ chimera of Vps1p in a strain expressing a form of Pex19p that gets targeted to the nucleus. Cells expressing Vps1p-GFP+ in a *PEX19* deletion background were transformed with *Mad1NLS-PEX19*, were grown in SM medium (Ura-), induced in YNO medium for 8 h, stained with 10 nM per microlitres of cells with Hoescht 33342 (Sigma) for 2 minutes and images were obtained using Olympus BX50 microscope.

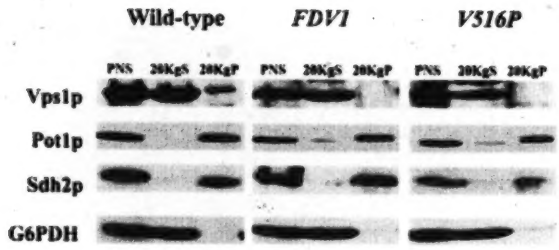

Figure 6-7. Subcellular fractionation of full length, in-frame deletion mutant and the point mutant. A fraction of full length Vps1p is targeted to the organellar compartment. A PNS fraction was divided by centrifugation into a supernatant (20KgS) fraction enriched for cytosol and a pellet (20KgP) fraction enriched for peroxisomes. Equivalent portions of each fraction were analyzed. Immunoblotting with rabbit anti-Vps1p, anti-Sdh2p, anti-G6PDH and guinea-pig anti-Pot1p were used.

cytosol and the mitochondrial protein Sdh2p and the peroxisomal protein Pot1p were found exclusively in the organellar pellet fraction. In the in-frame deletion mutant and the point mutant, no membrane associated Vps1p was detected (Figure 6-7). This suggests that once Vps1p is recruited to peroxisomes, its interaction with Pex19p perhaps could stabilize its association with peroxisomes.

6.9 Discussion

6.9.1 Organelle division

Organelles are highly dynamic structures that undergo fission and fusion to control their numbers and modify their morphology in response to intracellular and extracellular cues and to permit their correct segregation at cell division. As a consequence, the maintenance of compartmental integrity by the eukaryotic cell requires the tight coordination of mechanisms controlling these events. Although much progress has been made, many questions concerning the mechanisms of organelle fission still remain unanswered. Division is regulated by multimeric protein machinery, the details of which are just beginning to be unveiled. It seems that the mechanism of accurate partitioning of yeast peroxisomes, mitochondria and vacuoles are distinct, yet they share common elements. All these organelles move along actin filaments and they all require fusion and fission to maintain normal morphology. Dynamin like proteins have been suggested to play a role in organelle fission.

In mitochondria, fission seems to occur by a multi-step pathway, including the recruitment of the dynamin like protein Dnm1p (and any accessory proteins) to sites on

the sides of mitochondrial tubules, the constriction of mitochondrial tubules at these sites, and the coordinated division of the outer and inner mitochondrial membranes to generate new tubule ends. While Vps1p seems to regulate peroxisome fission. Vps1p is a major cytosolic protein belonging to the dynamin protein family and deletion mutant of Vps1p contains few enlarged peroxisomes (Hoepfner *et al.*, 2001). Vps1p has been shown to regulate the cytoskeleton through its interaction with Sla1p (Yu and Cai, 2004). Also a double deletion mutant of *vps1Δrho1Δ* has been found to accumulate actin patches on peroxisomal membrane. These evidences suggest that Vps1p perhaps regulates fission by controlling the actin dynamics. How may Vps1p regulate peroxisomal fission and how it is recruited to the peroxisomal membrane is unclear.

6.9.2 Pex19p and Vps1p

Since Pex19p was proposed to be an assembly factor, we hypothesized that Pex19p could recruit Vps1p to the peroxisomes and help in the membrane fission. We found two putative Pex19p binding sites, using the Pex19p binding consensus sequence (Rottensteiner *et al.*, 2004). By two hybrid analysis, we found that Pex19p indeed interacts with Vps1p (Figure 6-1).

If Pex19p is essential for the recruitment of Vps1p to the peroxisomes, mutations disrupting the Pex19p interaction region, should lead to the deletion mutant phenotype. Accordingly, in our immunofluorescence study, we found that *FDV1* mutant exhibit few enlarged peroxisomes as observed in a *vps1Δ* deletion mutant (Figure 6-2). To verify if the other functionalities of this protein is affected, we immediately analysed the vacuolar sorting function of Vps1p, as it plays a role in vacuolar protein sorting as well. We found

that both *FDV1* and *FDV2* exhibited normal vacuolar morphology, unlike the deletion mutant which showed higher percentage of fragmented vacuoles (Figure 6-3A). It has been suggested that this mixed phenotype observed in *vps1*Δ showing enlarged and fewer vacuoles (fission mutants) and many small fragmented vacuoles (fusion mutants) is due to mutual control of membrane fission and fusion by Vps1p (Peters *et al.*, 2004). We also analysed the sorting of the soluble vacuolar hydrolase carboxypeptidase Y (CP-Y), as mutants involved in this could lead to the sorting of this protein to the secretory pathway. We found that *FDV1* had the same background as that of wild-type strain suggesting that vacuole protein sorting is unaffected in this strain (Figure 6-3B). However, the other in-frame deletion mutant *FDV2* exhibited a relatively increased secretion of CP-Y suggesting that it might be partly impaired in vacuolar protein sorting. It is interesting to note that this mutation lies in the GED domain of Vps1p. This region has been proposed to form coiled coil structures and has been suggested to interact with Vam3p, an interaction that is essential for vacuolar fusion (Peters *et al.*, 2004).

6.9.3 Distribution of Vps1p-GFP chimera

Like, Pex11p and Pex13p, Vps1p interacts with Pex19p at only one site as substitution mutation within the core Pex19p binding region abolished the interaction to a considerable extent. In the strain carrying the point mutation, we found that the peroxisomes were of mixed phenotype of both wild-type peroxisomes and enlarged peroxisomes (Figure 6-4B and 5C). This suggests that either the point mutation substitution does not fully abolish its interaction with Pex19p or there could be other factors that could potentially associate Vps1p with the peroxisomes. To see if Pex19p

recruits Vps1p to peroxisomes, we examined the distribution of Vps1p-GFP+ chimera in a strain expressing *Mad1NLS-PEX19*, a form of Pex19p that is efficiently targeted to the nucleus. Vps1p-GFP+ localized to punctate structures with a diffused cytosolic staining. Thus the distribution of Vps1p seems to remain unaffected by Pex19p. We also conclude that Vps1p is not recruited to the peroxisomal compartment in a strain that overexpresses Pex19p. It will be interesting to see if this recruitment is cell cycle dependent.

Subcellular fractionation was done to analyze the association of Vps1p with the peroxisomes. In the in-frame deletion mutant and the point mutant, no membrane associated Vps1p was detected (Figure 6-7). This suggests that Pex19p is essential for the association of Vps1p with the peroxisomes, perhaps in the stabilization of its interaction with peroxisomes. Since Vps1p is not integral to the peroxisomal membrane, this result also suggests that Pex19p does not necessarily play a role in the insertion of the membrane proteins.

6.9.4 Vps1p and membrane fission

The observation that peroxisomes do manage to divide at cytokinesis in *vps1*Δ, suggest that there is also dynamin-independent peroxisome fission (Hoepfner *et al.*, 2001). In fact, this is re-inforced by our previous finding that more wild type peroxisomes were formed upon overexpression of *PEX11* in a *vps1*Δ mutant (Vizeacoumar *et al.*, 2003). Also, Pex11p has been suggested to indirectly recruit *DLP1* to the peroxisomes, although the authors were unable to detect any physical interaction between these two proteins (Li and Gould 2003). However, since we know Pex11p is recruited in a Pex19p

dependent fashion (Rottensteiner *et al.*, 2004), we speculate that Vps1p recruitment could perhaps be coordinated through both these proteins.

Members of the Pex11p family of peroxins, including Pex25p (Smith *et al.*, 2002) and Pex27p (Tam *et al.*, 2003; Rottensteiner *et al.*, 2003) of *S. cerevisiae*, have also been shown to affect peroxisome division in different organisms (Erdmann and Blobel, 1995; Marshall *et al.*, 1995; Sakai *et al.*, 1995; Li and Gould, 2002; Li *et al.*, 2002). We have also shown that the peroxins Pex28p and Pex29p are necessary for the separation of peroxisomes, an event that follows division (Vizeacoumar *et al.*, 2003). Also the newly identified Pex30p, Pex31p and Pex32p are involved in controlling the number, size and separation of peroxisomes in *S. cerevisiae* (Vizeacoumar *et al.*, 2004). Their exact roles in peroxisome fission are yet to be determined and that understanding how constriction and fission of these membranes are accomplished will require more detailed analyses of these divisional components.

Another important issue that is addressed by our study is the role of Pex19p in membrane protein sorting. It has been shown that Pex3p and Pex19p are the only two peroxins that are required for membrane biogenesis in *S. cerevisiae* and other mammalian cells (Hettema *et al.*, 2000; Matsuzono *et al.*, 1999; Shimozawa *et al.*, 2000). Pex19p is a major cytosolic protein with a smaller fraction of it found to be associated with the peroxisomes. It interacts with a number of peroxisomal integral membrane proteins (PMPs). The cytosolic fraction of Pex19p has been suggested to act as a shuttling receptor for peroxisomal membrane proteins, while its peroxisome-associated form could function as a chaperone, assisting the assembly of multimeric complexes following their binding to the peroxisome membrane (reviewed in Subramani, 1998; Hettema *et al.*,

1999; Terlecky and Fransen, 2000; Subramani *et al.*, 2000; Purdue and Lazarow, 2001; Titorenko and Rachubinski, 2001; Schleibs and Kunau, 2004). Recent evidence from Gould's lab has suggested that Pex19p could be bifunctional acting both as a cytosolic PMP chaperone and as a PMP import receptor (Jones *et al.*, 2004). In the light of many other evidences, whether Pex19p functions as an import receptor or an assembly factor, remains unclear (Fransen *et al.*, 2001, 2004; Snyder *et al.*, 2000; Biermanns and Gartner 2001; Wang *et al.*, 2004; Lambkin and Rachubinski 2001; Otzen *et al.*, 2004). Understanding the exact functional role of Pex19p needs more investigation and our results suggest that Pex19p interacts with the cytosolic Vps1p and that it functions as an assembly factor. Upon certain maturation signals, Vps1p is recruited to the peroxisomes and Pex19p stabilizes this association resulting in organelle fission. It still remains to be determined if the GTPase activity of Vps1p signals division.

The challenge remains to understand how the increasing number of proteins shown to be involved in controlling peroxisome number and size interplay amongst themselves and signal to the cell how to control its peroxisome dynamics.

CHAPTER SEVEN

PERSPECTIVES

7.1 Synopsis:

Peroxisome biogenetic pathway conceptually requires at least few distinct processes: the formation of lipid bilayer, the insertion of membrane proteins into this lipid bilayer, the import of soluble proteins across the membrane into the matrix and the division and segregation of the mature peroxisomes to the daughter cells. In this study, different experimental approaches were made to identify and characterize novel components involved in peroxisomal assembly, especially in the division and proliferation of peroxisomes. The peroxisomes of cells deleted for one or both of the *PEX28* and *PEX29* genes are more abundant and smaller, and show extensive clustering, as compared to wild-type peroxisomes. Cells deleted for two of the *PEX30*, *PEX31* and *PEX32* genes contained increased numbers of generally enlarged peroxisomes.

Additionally, we have analyzed the assembly of membrane proteins using Pex30p and Pex32p as experimental candidates. This has revealed that Pex19p acts as a targeting factor for PMPs. Our approach to understand the role of Pex19p in membrane biogenesis has revealed that the dynamin like protein Vps1p associates with peroxisomes in a Pex19p-dependent manner. The implications of these data in peroxisomal dynamics are discussed in the following section and represented in the model 7-1.

7.2 Fusion or fission mutants?

Upon completion of peroxisome division, peroxisomes must be separated from one another. Pex28p and Pex29p are two proteins required for this process, as their absence leads to an arrest or retardation of the peroxisome proliferation pathway, leading to the

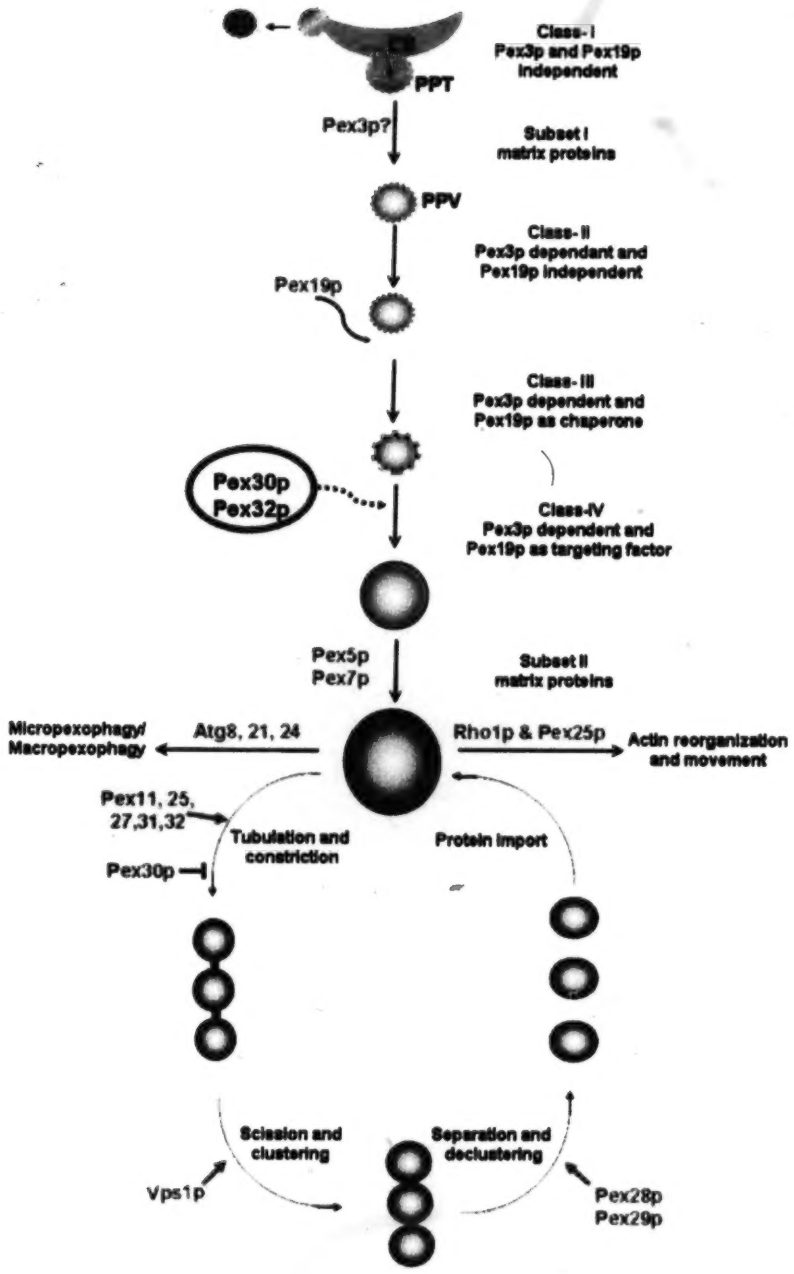

Figure 7-1. A composite model for protein targeting and the dynamic events that occur during the assembly of peroxisomes. PPV-Pre-Peroxisomal Vesicle, PPT-Pre Peroxisomal Template.

presence of clusters of peroxisomes with evidence of thickened membranes sometimes occurring between adjacent peroxisomes. The thickened membranes between some peroxisomes are also suggestive of a role for Pex28p and Pex29p in controlling fission of the peroxisomal membrane. One of the important aspects that needs to be scrutinized is that if they are peroxisomal fission or fusion mutants. So far, no study has identified components of peroxisomal fission or fusion mutants. One way to study this would be to mate a and α strains of the same mutant (for example *pex29*Δ) carrying different peroxisomal fluorophores (pGAL-Dsred-SKL and pGAL-GFP-SKL) and monitor the fusion events by time lapse imaging. If *PEX29*, is a fusion mutant, then we would observe clustering of red and green structures. If it is not affected in fusion, then we would observe yellow punctate structures.

Similar approaches can be made to study mutants of *PEX30, PEX31* and *PEX32*. Especially, the observation of increased number of peroxisomes in *pex30*Δ is suggestive of a fusion mutant phenotype. Fusion and fission events might require more than one component. Identification of more components will facilitate to resolve the chronological and spatial arrangement of protein complexes during these processes. A more straightforward approach will be based on immunoprecipitation studies. Tandem affinity purification can be used to isolate protein complexes; however, to understand the dynamics of interaction, cell biological approaches using fluorescent reporter proteins will be of immense use.

7.3 Transcriptional regulation of *PEX* genes

Pex30p-prA, Pex31p-prA and Pex32p-prA were all detected in glucose-containing YEPD medium at the time of transfer. The levels of Pex30p-prA and Pex32p-prA increased with time of incubation of cells in YPBO medium, but not as dramatically as the levels of Pot1p (peroxisomal thiolase). The levels of Pex31p-prA did not show any apparent increase with time of incubation of cells in YPBO medium. The promoter regions of *PEX30, PEX31* and *PEX32* contain sequences that resemble the canonical sequence $CCGN_3TNAN_{8\text{-}12}CGG$ of the oleic acid response element (ORE) (Rottensteiner *et al.*, 2002; 2003a), which acts to increase gene transcription in *S. cerevisiae* in the presence of oleic acid as a carbon source through the binding of the transcription factors Pip2p and Oaf1p (Rottensteiner *et al.*, 1996; Karpichev *et al.*, 1997). It will be interesting to verify if these sequences actually do function as OREs.

7.4 Regulated division versus constitutive division

Peroxisomes undergo either constitutive division to maintain the number of peroxisomes or a regulated division when there is an external stimuli. External stimuli can be oleic acid and methanol for yeasts or peroxisomal proliferators for mammalian cells. Pex11p has been suggested to play a role in both of these processes (Li and Gould, 2002). However, whether the machinery involved in these two processes is one and the same remains unclear. Pex30p is a constitutively produced protein and its levels are not altered by external stimuli, while Pex32p is induced upon shifting the cells to oleic acid containing medium. Two hybrid analysis has revealed that these two proteins interact

with each other. The significance of this interaction in constituting the same machinery of peroxisomal division during these different processes needs further studies. Also, since both these proteins are polytopic in nature, it will be necessary to determine the topology of these proteins to enhance our understanding of the complex formation. A similar situation can be observed in the Pex11 family of proteins. While the synthesis of Pex11p and Pex25p are induced, synthesis level of Pex27p is not induced. Pex27p and Pex25p interact within themselves and each other in a two hybrid analysis. Determining the spatial arrangements of these proteins and the nature of the complex that they form will elucidated the machinery involved in the two types of division.

7.5 The enigma of peroxisomal subforms

There had been significant evidence that, in a single cell, peroxisomes exist as a heterogeneous population of organelles that differ in their size, buoyant density, protein composition and protein import capacity. Titorenko and Rachubinski have convincingly demonstrated in the yeast *Y. lipolytica* that this heterogenous population of peroxisomes assembles in a systematic multi step pathway. On the basis of studies in *Y. lipolytica*, *P. pastoris* and human fibroblasts, different models, although with varying number of intermediates, provides a unified support for a multi step processes that involve the selective uptake of different matrix and membrane proteins into distinct intermediates along the peroxisomal biogenetic pathway. A major challenge for the future will be to define the applicability of the models presented in, to various model organisms such as *Saccharomyces cerevisiae*.

Significant amount of Pex30p and Pex29p were always present in the less dense fractions during the gradient isolation of peroxisomes. Of particular interest is that these two proteins interact with each other on a two hybrid analysis. Therefore it remains to be determined if some portion of these proteins form a complex and represent components *en route* to peroxisomes. Preliminary results in *S. cerevisiae* suggest existence of at least four different bonafide compartments containing different peroxisomal proteins (Figure 7-2). This is extremely exciting, as the mechanism of peroxisomal assembly has so far been an unsolved mystery. It still remains to be determined if these compartments assemble in a systematic pattern or if they randomly fuse to form a mature peroxisome. This has opened a new avenue for further future research challenging the old model of peroxisome biogenesis. In depth investigation requires studies on the molecular mechanisms regulating the formation, selective import competency, division and conversion of distinct intermediates along the peroxisome assembly pathway.

7.6 Are there multiple m-PTS signals on the same PMP?

Systematic truncation of the integral membrane proteins Pex30p and pex32p from the C-terminus region has led to the identification of a m-PTS signal for these proteins. However, a number of studies have demonstrated that multiple targeting signals are present on the same protein. Especially, recent evidence from Goodman's laboratory suggest that multiple targeting modules on peroxisomal proteins are not redundant and that under different metabolic states, different mPTSs could function independently and

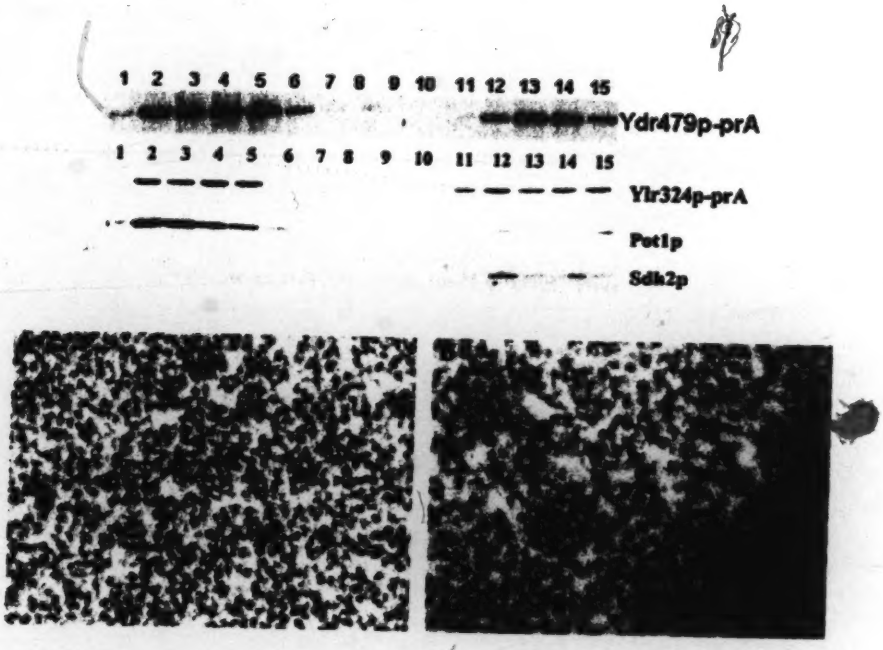

Figure 7-2. Subforms of peroxisomes? Lighter fractions where Pex30p and Pex29p constantly appeared were floated on a two step gradient, pelleted and processed for electron microscopy. (A) Fractions of Pex29p. (B) Fractions of Pex30p.

efficiently (Wang *et al.*, 2004). In *Candida boidinii* Pex19p binding to PMP47 is oleic acid induced and that in non-inducing conditions, another mPTS targets PMP47 to peroxisomes. Truncation of Pex30p and Pex32p from the N-terminus will help to identify such additional signals present in these proteins. Further investigation will be needed to verify if these signals are redundant and to determine the conditions under which they function.

7.7 Can Pex19p function as a cytosolic PMP chaperone?

Pex19p is a mostly cytosolic protein with a small fraction of it associated with the peroxisomes. The cytosolic fraction of Pex19p has been suggested to act as a shuttling receptor for peroxisomal membrane proteins, while its peroxisome-associated form could function as a chaperone, assisting the assembly of multimeric complexes following their binding to the peroxisome membrane (reviewed in Purdue and Lazarow, 2001; Titorenko and Rachubinski, 2001; Schleibs and Kunau, 2004). Recent evidence from Gould's lab has suggested that Pex19p could be bifunctional acting both as a cytosolic PMP chaperone and as a PMP import receptor (Jones *et al.*, 2004). Snyder *et al.*, (2000), have shown in *Pichia pastoris* that upon blocking protein synthesis followed by cross linking, the amount of PMP immunoprecipitated by Pex19p remained unchanged like the untreated cells and thus have concluded that Pex19p interacts with preexisting and not with newly synthesized pool of PMPs. For Pex19p to function as a cytosolic chaperone, it must bind nascent peroxisomal proteins. Hence, biochemical analysis can be done to isolate complexes from the cytosol that contains Pex19p as a component.

7.8 Which protein recruits Vps1p to the peroxisome?

The results of our experiments are suggestive of transient recruitment of Vps1p to the surface of the peroxisomes and this association is stabilized by Pex19p. The components involved in the recruitment of Vps1p to the peroxisomal surface are unknown. Hence, biochemical analyses need to be undertaken to identify the interacting partners of Vps1p. If these interacting partners have a role to recruit Vps1p, peroxisome morphology will be affected in the mutants of these genes. Alternatively, association of Vps1p-GFP chimeras or Vps1p-prA with the peroxisomal compartment can be monitored in the peroxisomal fission mutants or the interacting candidates.

Also, Pex11p has been suggested to indirectly recruit DLP1, a mammalian homolog of Vps1p, to the peroxisomes, although the authors were unable to detect any physical interaction between these two proteins (Li and Gould 2003). However, since we know Pex11p is recruited in a Pex19p dependent fashion (Rottensteiner *et al.*, 2004), we speculate that Vps1p recruitment could perhaps be coordinated through both these proteins. This is interesting because, deletion of *PEX11* has similar phenotype as the deletion of *VPS1*. Hence, tracking the Vps1p-GFP chimera in a *pex11*Δ mutant might reveal interesting data.

7.9 How does Vps1p regulate fission?

Vps1p is a dynamin like protein containing a tripartite GTP-binding domain towards its N-terminus and a GTPase effector domain towards its C-terminus. How may

Vps1p regulate peroxisomal fission is unclear. Experiments can be easily designed to understand the mechanism of this division. Essentially, expression of Vps1p-GFP chimera, under the *GAL* promoter using time lapse imaging can be monitored to visualize fission events in a strain with a peroxisomal reporter (DsRed-PTS1). This double labeling can show the formation of green ring like structures around the red (elongated?) peroxisomes. Similar observations were made in mitochondrial division.

Although Vps1p could be selectively recruited to the dividing peroxisomes, we believe that the GTPase activity of Vps1p could act as a signaling event in the fission of peroxisomes. This is supported by the fact that Vps1p has also been shown to regulate vacuole fusion (Christopher *et al.*, 2004) and Mgm1p (another dynamin like protein) has been shown to regulate mitochondrial fusion. Hence further investigation is needed to test this hypothesis.

7.10 Is there a dynamin independent mechanism of peroxisome fission?

The observation that peroxisomes manage to divide at cytokinesis in *vps1*Δ, suggest that there is also dynamin-independent peroxisome fission (Hoepfner *et al.*, 2001). In fact, this is re-inforced by our previous finding that more wild type peroxisomes were formed upon overexpression of PEX11 in a *vps1*Δ mutant (Vizeacoumar *et al.*, 2003). Vps1p has been shown to regulate the cytoskeleton through its interaction with Sla1p (Yu and Cai, 2004). Also a double deletion mutant of *vps1*Δ*rho1*Δ has been found to accumulate actin patches on peroxisomal membranes. These findings instigate us to see if there is a dynamin independent mechanism of peroxisome division.

7.11 Conclusion

The processes of protein import, membrane fission and fusion are important events that occur in all eukaryotes. Studies that focus on similar events in peroxisomes will definitely contribute to the understanding of fundamental processes that occur in membrane trafficking in the endocytic and secretory pathways. Prior to the work done in this thesis, only three components namely Pex11p, Pex25p and Pex27p were known to regulate peroxisome abundance. This thesis has broadened our understanding of peroxisome proliferation by identifying at least five more molecular players that co-ordinate this event. Work described here has opened new avenues of research, further understanding of which will produce exciting insights on organelle biogenesis.

CHAPTER EIGHT

REFERENCES

Abe, I., and Y. Fujiki. 1998. cDNA cloning and characterization of a constitutively expressed isoform of the human peroxin Pex11p. *Biochem. Biophys. Res. Commun.* 252:529-533.

Aitchison, J. D., W. W. Murray, and R. A. Rachubinski. 1991. The carboxyl-terminal tripeptide Ala-Lys-Ile is essential for targeting *Candida tropicalis* trifunctional enzyme to yeast peroxisomes. *J. Biol. Chem.* 266:23197-23203.

Aitchison, J. D., M. P. Rout, M. Marelli, G. Blobel, and R. W. Wozniak. 1995. Two novel related yeast nucleoporins Nup170p and Nup157p: complementation with the vertebrate homologue Nup155p and functional interactions with the yeast nuclear pore-membrane protein Pom152p. *J. Cell Biol.* 131:1133-1148.

Aitchison, J. D., R. K. Szilard, W. M. Nuttley, and R. A. Rachubinski. 1992. Antibodies directed against a yeast carboxyl-terminal peroxisomal targeting signalspecifically recognize peroxisomal proteins from various yeasts. *Yeast.* 8:721-734

Albertini, M., P. Rehling, R. Erdmann, W. Girzalsky, J. A. Kiel, M. Veenhuis, and W. H. Kunau. 1997. Pex14p, a peroxisomal membrane protein binding both receptors of the two PTS-dependent import pathways. *Cell.* 89:83-92.

Ausubel, F. J., R. Brent, R. E. Kingston, D. D. Moore, J. G. Seidman, J. A. Smith, and K. Struhl. 1996. Current Protocols in Molecular Biology. *Green Publishing Associates*, New York.

Beevers, H. 1969. Glyoxysomes of castor bean endosperm and their relation to gluconeogenesis. *Ann. N. Y. Acad. Sci.* 168:313-324.

Biermanns, M., and J. Gartner. 2001. Targeting elements in the amino-terminal part direct the human 70-kDa peroxisomal integral membrane protein (PMP70) to peroxisomes. *Biochem. Biophys. Res. Commun.* 285, 649-655.

Blobel, G. 1980. Intracellular protein topogenesis. *Proc. Natl. Acad. Sci. U. S. A.* 77:1496-1500.

Blobel, G., and B. Dobberstein. 1975. Transfer of proteins across membranes. II. Reconstitution of functional rough microsomes from heterologous components. *J. Cell Biol.* 67:852-862.

Bodnar, A. G., and R. A. Rachubinski. 1991. Characterization of the integral membrane polypeptides of rat liver peroxisomes isolated from untreated and clofibrate-treated rats. *Biochem. Cell Biol.* 69:499-508.

Brade, A. M. 1992. Peroxisome Assembly in *Yarrowia lipolytica*. *McMaster University, M.Sc. Thesis*.

Bradford, M. M. 1976. A rapid and sensitive method for the quantitation of microgram quantities of protein utilizing the principle of protein-dye binding. *Anal. Biochem.* 72:248-254.

Braverman, N., G. Steel, C. Obie, A. Moser, H. Moser, S. J. Gould, and D. Valle. 1997. Human PEX7 encodes the peroxisomal PTS2 receptor and is responsible for rhizomelic chondrodysplasia punctata. *Nat. Genet.* 15:369-376.

Breidenbach, R. W., and H. Beevers. 1967. Association of the glyoxylate cycle enzymes in a novel subcellular particle from castor bean endosperm. *Biochem. Biophys. Res. Commun.* 27:462-469.

Broach, J. R., J. N. Strathern, and J. B. Hicks. 1979. Transformation in yeast: development of a hybrid cloning vector and isolation of the *CAN1* gene. *Gene.* 8:121-133.

Brocard, C., F. Kragler, M. M. Simon, T. Schuster, and A. Hartig. 1994. The tetratricopeptide repeat-domain of the PAS10 protein of *Saccharomyces cerevisiae* is essential for binding the peroxisomal targeting signal-SKL. *Biochem. Biophys. Res. Commun.* 204:1016-1022.

Brocard, C., G. Lametschwandtner, R. Koudelka, and A. Hartig. 1997. Pex14p is a member of the protein linkage map of Pex5p. *EMBO J.* 16:5491-5500.

Brosius, U., and J. Gärtner. 2002. Cellular and molecular aspects of Zellweger syndrome and other peroxisome biogenesis disorders. *Cell. Mol. Life Sci.* 59:1058-1069.

Brown, T. W. 2000. A Study of Peroxisome Biogenesis in the Yeast *Yarrowia lipolytica*. *University of Alberta, M.Sc. Thesis*.

Brown, T. W., V. I. Titorenko, and R. A. Rachubinski. 2000. Mutants of the *Yarrowia lipolytica PEX23* gene encoding an integral peroxisomal membrane peroxin mislocalize matrix proteins and accumulate vesicles containing peroxisomal matrix and membrane proteins. *Mol. Biol. Cell.* 11:141-152.

Burnette, W. N. 1981. Western blotting: electrophoretic transfer of proteins from sodium dodecyl sulfate-polyacrylamide gels to unmodified nitrocellulose and radiographic detection with antibody and radioiodinated protein A. *Anal. Biochem.* 112:195-203.

Chang, C. C., S. South, D. Warren, J. Jones, A. B. Moser, H. W. Moser, and S. J. Gould. 1999a. Metabolic control of peroxisome abundance. *J. Cell Sci.* 112:1579-1590.

Chang, C. C., D. S. Warren, K. A. Sacksteder, and S. J. Gould. 1999b. PEX12 interacts with PEX5 and PEX10 and acts downstream of receptor docking in peroxisomal matrix protein import. *J. Cell Biol.* 147:761-774.

Collins, C.S., J.E. Kalish, J.C. Morrell, J. M. McCaffery, and S. J. Gould. 2000. The peroxisome biogenesis factors Pex4p, Pex22p, Pex1p, and Pex6p act in the terminal steps of peroxisomal matrix protein import. *Mol. Cell. Biol.* 20:7516-7526.

Corpas, F. J., and R. N. Trelease. 1997. The plant 73 kDa peroxisomal membrane protein (PMP73) is immunorelated to molecular chaperones. *Eur. J. Cell Biol.* 73:49-57.

Cregg, J. M., I. J. van der Klei, G. J. Sulter, M. Veenhuis, and W. Harder. 1990. Peroxisome-deficient mutants of *Hansenula polymorpha*. *Yeast.* 6: 87-97.

Dammai, V., and S. Subramani. 2001. The human peroxisomal targeting signal receptor, Pex5p, is translocated into the peroxisomal matrix and recycled to the cytosol. *Cell.* 105:187-196.

Danino, D., and J. E. Hinshaw. 2001. Dynamin family of mechanoenzymes. *Curr. Opin. Cell Biol.* 13.4: 454-60.

de Duve, C., and P. Baudhuin. 1966. Peroxisomes (microbodies and related particles). *Physiol. Rev.* 46: 323-357.

Dibrov, E., S. Fu, and B. D. Lemire. 1998. The *Saccharomyces cerevisiae TCM62* gene encodes a chaperone necessary for the assembly of the mitochondrial succinate dehydrogenase (complex II). *J. Biol. Chem.* 273:32042-32048.

Diefenbach, J., and H. Kindl. 2000. The membrane-bound DnaJ protein located at the cytosolic site of glyoxysomes specifically binds the cytosolic isoform 1 of Hsp70 but not other Hsp70 species. *Eur. J. Biochem.* 267:746-754.

Dilworth, D. J., A. Suprapto, J. C. Padovan, B. T. Chait, R. W. Wozniak, M. P. Rout, and J. D. Aitchison. 2001. Nup2p dynamically associates with the distal regions of the yeast nuclear pore complex. *J. Cell Biol.* 153:1465-1478.

Dodt, G., and S. J. Gould. 1996. Multiple PEX genes are required for proper subcellular distribution and stability of Pex5p, the PTS1 receptor: evidence that PTS1 protein import is mediated by a cycling receptor. *J. Cell Biol.* 135:1763-1774.

Dodt, G., N. Braverman, C. Wong, A. Moser, H. W. Moser, P. Watkins, D. Valle, and S. J. Gould. 1995. Mutations in the PTS1 receptor gene, PXR1, define complementation group 2 of the peroxisome biogenesis disorders. *Nat. Genet.* 9:115-125.

Dyer, J. M., J. A. McNew, and J. M. Goodman. 1996. The sorting sequence of the peroxisomal integral membrane protein PMP47 is contained within a short hydrophilic loop. *J. Cell Biol.* 133:269-280.

Eckert, J. H., and R. Erdmann. 2003. Peroxisome biogenesis. *Rev. Physiol. Biochem. Pharmacol.* 147:75-121.

Einwachter, H., S. Sowinski, W. H. Kunau, and W. Schliebs. 2001. *Yarrowia lipolytica* Pex20p, *Saccharomyces cerevisiae* Pex18p/Pex21p and mammalian Pex5pL fulfil a common function in the early steps of the peroxisomal PTS2 import pathway. *EMBO Rep.* 2:1035-1039.

Eitzen, G. A. 1997. An Analysis of Peroxisome Assembly Mutants of the Yeast *Yarrowia lipolytica*. *University of Alberta, Ph.D. Thesis.*

Eitzen, G. A., R. K. Szilard, and R. A. Rachubinski. 1997. Enlarged peroxisomes are present in oleic acid-grown *Yarrowia lipolytica* overexpressing the *PEX16* gene

encoding an intraperoxisomal peripheral membrane peroxin. *J. Cell Biol.* 137:1265-1278.

Eitzen, G. A., V. I. Titorenko, J. J. Smith, M. Veenhuis, R. K. Szilard, and R. A. Rachubinski. 1996. The *Yarrowia lipolytica* gene *PAY5* encodes a peroxisomal integral membrane protein homologous to the mammalian peroxisome assembly factor PAF-1. *J. Biol. Chem.* 271:20300-20306.

Elgersma, Y., and H. F. Tabak. 1996. Proteins involved in peroxisome biogenesis and functioning. *Biochim. Biophys. Acta.* 1286:269-283.

Elgersma, Y., A. Vos, M. van den Berg, C. W. van Roermund, P. van der Sluijs, B. Distel, and H. F. Tabak. 1996. Analysis of the carboxyl-terminal peroxisomal targeting signal 1 in a homologous context in *Saccharomyces cerevisiae*. *J. Biol. Chem.* 271:26375-26382.

Elgersma, Y., L. Kwast, M. van den Berg, W. B. Snyder, B. Distel, S. Subramani, and H. F. Tabak. 1997. Overexpression of Pex15p, a phosphorylated peroxisomal integral membrane protein required for peroxisome assembly in *S. cerevisiae*, causes proliferation of the endoplasmic reticulum membrane. *EMBO J.* 16:7326-7341.

Elgersma, Y., M. Elgersma-Hooisma, T. Wenzel, J. M. McCaffery, M. G. Farquhar, and S. Subramani. 1998. A mobile PTS2 receptor for peroxisomal protein import in *Pichia pastoris*. *J. Cell Biol.* 140:807-820.

Erdmann, R., and G. Blobel. 1995. Giant peroxisomes in oleic acid-induced *Saccharomyces cerevisiae* lacking the peroxisomal membrane protein Pmp27p. *J.Cell Biol.* 128:509-523.

Erdmann, R., and G. Blobel. 1996. Identification of Pex13p, a peroxisomal membrane receptor for the PTS1 recognition factor. *J. Cell Biol.* 135:111-121.

Erdmann, R., M. Veenhuis, D. Mertens, and W. H. Kunau. 1989. Isolation of peroxisome-deficient mutants of *Saccharomyces cerevisiae*. *Proc. Natl. Acad. Sci. U. S. A.* 86:5419-5423.

Fang, Y., J. C. Morrell, J. M. Jones, and S. J. Gould. 2004. PEX3 functions as a PEX19 docking factor in the import of class I peroxisomal membrane proteins. *J. Cell Biol.* 164:863-875.

Finley, D., E. Ozkaynak, and A. Varshavsky. 1987. The yeast polyubiquitin gene is essential for resistance to high temperatures, starvation, and other stresses. *Cell.* 48:1035-1046.

Flynn, C. R., R. T. Mullen, and R. N. Trelease. 1998. Mutational analyses of a type 2 peroxisomal targeting signal that is capable of directing oligomeric protein import into tobacco BY-2 glyoxysomes. *Plant J.* 16:709-720.

Fransen, M., C. Brees, E. Baumgart, J. C. Vanhooren, M. Baes, G. P. Mannaerts, and P. P. van Veldhoven. 1995. Identification and characterization of the putative human peroxisomal C-terminal targeting signal import receptor. *J. Biol. Chem.* 270:7731-7736.

Fransen, M., I. Vastiau, C. Brees, V. Brys, G. P. Mannaerts, and P. P. van Veldhoven. 2004. Potential role for Pex19p in assembly of PTS-receptor docking complexes. *J. Biol. Chem.* 279:12615-12624.

Fransen, M., T. Wylin, C. Brees, G. P. Mannaerts, and P. P. van Veldhoven. 2001. Human Pex19p binds peroxisomal integral membrane proteins at regions distinct from their sorting sequences. *Mol. Cell. Biol.* 21:4413-4424.

Fujiki, Y., A. L. Hubbard, S. Fowler, and P. B. Lazarow. 1982. Isolation of intracellular membranes by means of sodium carbonate treatment: application to endoplasmic reticulum. *J. Cell Biol.* 93:97-102.

Fukui, S., S. Kawamoto, S. Yasuhara, A. Tanaka, and M. Osumi. 1975. Microbody of methanol-grown yeasts. Localization of catalase and flavin-dependent alcohol oxidase in the isolated microbody. *Eur. J. Biochem.* 59:561-566.

Gatto, G. J., Jr., B. V. Geisbrecht, S. J. Gould, and J. M. Berg. 2000. Peroxisomal targeting signal-1 recognition by the TPR domains of human PEX5. *Nat. Struct. Biol.* 7:1091-1095.

Geuze, H. J., J. L. Murk, A. K. Stroobants, J. M. Griffith, M. J. Kleijmeer, A. J. Koster, A. J. Verkleij, B. Distel, and H. F. Tabak. 2003. Involvement of the endoplasmic reticulum in peroxisome formation. *Mol. Biol. Cell.* 14:2900-2907.

Giaever, G., A. M. Chu, L. Ni, C. Connelly, L. Riles, S. Véronneau, S. Dow, A. Lucau-Danila, K. Anderson, B. André, A. P. Arkin, A. Astromoff, M. El Bakkoury, R. Bangham, R. Benito, S. Brachat, S. Campanaro, M. Curtiss, K. Davis, A. Deutschbauer, K. D. Entian, P. Flaherty, F. Foury, D. J. Garfinkel, M. Gerstein, D. Gotte, U. Güldener, J. H. Hegemann, S. Hempel, Z. Herman, D. F. Jaramillo, D. E. Kelly, S. L. Kelly, P. Kötter, D. LaBonte, D. C. Lamb, N. Lan, H. Liang, H. Liao, L. Liu, C. Luo, M. Lussier, R. Mao, P. Menard, S. L. Ooi, J. L. Revuelta, C. J. Roberts, M. Rose, P. Ross-Macdonald, B. Scherens, G. Schimmack, B. Shafer, D. D. Shoemaker, S. Sookhai-Mahadeo, R. K. Storms, J. N. Strathern, G. Valle, M. Voet, G. Volckaert, C. Wang, T. R. Ward, J. Wilhelmy, E. A. Winzeler, Y. Yang, G. Yen, E. Youngman, K. Yu, H. Bussey, J. D. Boeke, M. Snyder, P. Philippsen, R. W. Davis, and M. Johnston. 2002. Functional profiling of the *Saccharomyces cerevisiae* genome. *Nature.* 418:387-391.

Gietz, R. D., and R. A.Woods. 2002. Transformation of yeast by lithium acetate/single-stranded carrier DNA/polyethylene glycol method. *Methods Enzymol.* 350:87-96.

Girzalsky, W., P. Rehling, K. Stein, J. Kipper, L. Blank, W. H. Kunau, and R. Erdmann. 1999. Involvement of Pex13p in Pex14p localization and peroxisomal targeting signal 2-dependent protein import into peroxisomes. *J. Cell Biol.* 144:1151-1162.

Glover, J. R., D. W. Andrews, and R. A. Rachubinski. 1994a. *Saccharomyces cerevisiae* peroxisomal thiolase is imported as a dimer. *Proc. Natl. Acad. Sci. U. S. A.* 91:10541-10545.

Glover, J. R., D. W. Andrews, S. Subramani, and R. A. Rachubinski. 1994b. Mutagenesis of the amino targeting signal of *Saccharomyces cerevisiae* 3-ketoacyl-CoA thiolase reveals conserved amino acids required for import into peroxisomes *in vivo*. *J. Biol. Chem.* 269:7558-7563.

Goldfischer, S., C. L. Moore, A. B. Johnson, A. J. Spiro, M. P. Valsamis, H. K. Wisniewski, R. H. Ritch, W. T. Norton, I. Rapin, and L. M. Gartner. 1973. Peroxisomal and mitochondrial defects in the cerebro-hepato-renal syndrome. *Science.* 182:62-64.

Goodman, J. M., S. B. Trapp, H. Hwang, and M. Veenhuis. 1990. Peroxisomes induced in *Candida boidinii* by methanol, oleic acid and *D*-alanine vary in metabolic function but share common integral membrane proteins. *J. Cell Sci.* 97:193-204.

Götte, K., W. Girzalsky, M. Linkert, E. Baumgart, S. Kammerer, W. H. Kunau, and R. Erdmann. 1998. Pex19p, a farnesylated protein essential for peroxisome biogenesis. *Mol. Cell. Biol.* 18:616-628.

Gould, S. J., D. McCollum, A. P. Spong, J. A. Heyman, and S. Subramani. 1992. Development of the yeast *Pichia pastoris* as a model organism for a genetic and molecular analysis of peroxisome assembly. *Yeast*. 8:613-628.

Gould, S. J., G. A. Keller, and S. Subramani. 1987. Identification of a peroxisomal targeting signal at the carboxy terminus of firefly luciferase. *J. Cell Biol.* 105:2923-2931.

Gould, S. J., G. A. Keller, M. Schneider, S. H. Howell, L. J. Garrard, J. M. Goodman, B. Distel, H. Tabak, and S. Subramani. 1990. Peroxisomal protein import is conserved between yeast, plants, insects and mammals. *EMBO J.* 9:85-90.

Gould, S. J., G. A. Keller, and S. Subramani. 1988. Identification of peroxisomal targeting signals located at the carboxy terminus of four peroxisomal proteins. *J. Cell Biol.* 107:897-905.

Gould, S. J., G. V. Raymond, and D. Valle. 2001. The peroxisome biogenesis disorders. *In* The Metabolic and Molecular Bases of Inherited Disease. C. R. Scriver, A. L. Beaudet, D. Valle, and W. S. Sly, editors. *McGraw-Hill*, New York, pp. 3181-3217.

Gould, S. J., and D. Valle. 2000. Peroxisome biogenesis disorders: genetics and cell biology. *Trends Genet.* 16:340-345.

Gourlay, C. W., H. Dewar, D. T. Warren, R. Costa, N. Satish, and K. R. Ayscough. 2003. An interaction between Sla1p and Sla2p plays a role in regulating actin dynamics and endocytosis in budding yeast. *J. Cell Sci.* 116:2551-2564.

Guo, T., Y. Y. Kit, J. M. Nicaud, M. T. Le Dall, S. K. Sears, H. Vali, H. Chan, R. A. Rachubinski, and V. I. Titorenko. 2003. Peroxisome division in the yeast

Yarrowia lipolytica is regulated by a signal from inside the peroxisome. *J. Cell Biol.* 162:1255-1266.

Haigh, N. G., and A. E. Johnson 2002. A new role for BiP: closing the aqueous translocon pore during protein integration into the ER membrane. *J. Cell Biol.* 156:261-270.

Hajra, A. K., and J. E. Bishop. 1982. Glycerolipid biosynthesis in peroxisomes via the acyl dihydroxyacetone phosphate pathway. *Ann. N. Y. Acad. Sci.* 386:170-182.

Hajra, A. K., C. L. Burke, and C. L. Jones. 1979. Subcellular localization of acyl coenzyme A: dihydroxyacetone phosphate acyltransferase in rat liver peroxisomes (microbodies). *J. Biol. Chem.* 254:10896-10900.

Hartl, F. U., N. Pfanner, D. W. Nicholson, and W. Neupert. 1989. Mitochondrial protein import. *Biochim. Biophys. Acta.* 988:1-45.

Hettema, E. H., and H. F. Tabak. 2000. Transport of fatty acids and metabolites across the peroxisomal membrane. *Biochim. Biophys. Acta.* 1486:18-27.

Hettema, E. H., B. Distel, and H. F. Tabak. 1999. Import of proteins into peroxisomes. *Biochim. Biophys. Acta.* 1451:17-34.

Hettema, E. H., C. C. Ruigrok, M. G. Koerkamp, M. van den Berg, H. F. Tabak, B. Distel, and I. Braakman. 1998. The cytosolic DnaJ-like protein Djp1p is involved specifically in peroxisomal protein import. *J. Cell Biol.* 142:421-434.

Hettema, E. H., W. Girzalsky, M. van den Berg, R. Erdmann, and B. Distel. 2000. *Saccharomyces cerevisiae* Pex3p and Pex19p are required for proper localization and stability of peroxisomal membrane proteins. *EMBO J.* 19:223-233.

Heyman, A., W. E. Wilkinson, B. J. Hurwitz, D. Schmechel, A. H. Sigmon, T. Weinberg, M. J. Helms, and M. Swift. 1983. Alzheimer's disease: genetic aspects and associated clinical disorders. *Ann. Neurol.* 14:507-515.

Hinshaw, J. E. 2000. Dynamin and its role in membrane fission. *Annu. Rev. Cell Dev. Biol.* 16: 483-519.

Hoepfner, D., M. van den Berg, P. Philippsen, H. F. Tabak, and E. H. Hettema. 2001. A role for Vps1p, actin, and the Myo2p motor in peroxisome abundance and inheritance in *Saccharomyces cerevisiae*. *J. Cell Biol.* 155:979-990.

Höhfeld, J., M. Veenhuis, and W. H. Kunau. 1991. PAS3, a *Saccharomyces cerevisiae* gene encoding a peroxisomal integral membrane protein essential for peroxisome biogenesis. *J. Cell Biol.* 114:1167-1178.

Honsho, M., T. Hiroshige, and Y. Fujiki. 2002. The membrane biogenesis peroxin Pex16p. Topogenesis and functional roles in peroxisomal membrane assembly. *J. Biol. Chem.* 277:44513-44524.

Howard, J. P., J. L. Hutton, J. M. Olson, and G. S. Payne. 2002. Sla1p serves as the targeting signal recognition factor for $NPFX_{(1,2)}D$-mediated endocytosis. *J. Cell Biol.* 157:315-326.

Huh, W. K., J. V. Falvo, L. C. Gerke, A. S. Carroll, R. W. Howson, J. S. Weissman, and E. K. O'Shea. 2003. Global analysis of protein localization in budding yeast. *Nature.* 425:686-691.

Huhse, B., P. Rehling, M. Albertini, L. Blank, K. Meller, and W. H. Kunau. 1998. Pex17p of *Saccharomyces cerevisiae* is a novel peroxin and component of the peroxisomal protein translocation machinery. *J. Cell Biol.* 140:49-60.

Huynh, T. V., R. A. Young, and R. W. Davis. 1985. DNA Cloning: A Practical Approach. *IRL Press*, Oxford.

Innis, M. A., and D. H. Gelfand. 1990. Optimization of PCRs. *In* PCR Protocols: A Guide to Methods and Applications. M. A. Innis, D. H. Gelfand, J. J. Sninsky, and T. J. White, editors. *Academic Press*, San Diego, pp. 3-12.

Jedd, G., and N. H. Chua. 2000. A new self-assembled peroxisomal vesicle required for efficient resealing of the plasma membrane. *Nat. Cell Biol.* 2:226-231.

Jones, J. M., J. C. Morrell, and S. J. Gould. Multiple distinct targeting signals in integral peroxisomal membrane proteins. *J. Cell Biol.* 153:1141-1150.

Jones, J. M., J. C. Morrell, and S. J. Gould. 2004. PEX19 is a predominantly cytosolic chaperone and import receptor for class 1 peroxisomal membrane proteins. *J. Cell Biol.* 164:57-67.

Kamiryo, T., M. Abe, K. Okazaki, S. Kato, and N. Shimamoto. 1982. Absence of DNA in peroxisomes of *Candida tropicalis*. *J. Bacteriol.* 152:269-274.

Kammerer, S., A. Holzinger, U. Welsch, and A. A. Roscher. 1998. Cloning and characterization of the gene encoding the human peroxisomal assembly protein Pex3p. *FEBS Lett.* 429:53-60.

Karpichev, I. V., Y. Luo, R. C. Marians, and G. M. Small. 1997. A complex containing two transcription factors regulates peroxisome proliferation and the coordinate induction of β-oxidation enzymes in *Saccharomyces cerevisiae*. *Mol. Cell. Biol.* 17:69-80.

Keller, G. A., M. C. Barton, D. J. Shapiro, and S. J. Singer. 1985. 3-Hydroxy-3-methylglutaryl-coenzyme A reductase is present in peroxisomes in normal rat liver cells. *Proc. Natl. Acad. Sci. U. S. A.* 82:770-774.

Koch, A., G. Schneider, G. H. Luers, and M. Schrader. 2004. Peroxisome elongation and constriction but not fission can occur independently of dynamin-like protein 1. *J. Cell Sci.* 117:3995-4006.

Koch, A., M. Thiemann, M. Grabenbauer, Y. Yoon, M. A. McNiven, and M. Schrader. 2003. Dynamin-like protein 1 is involved in peroxisomal fission. *J. Biol. Chem.* 278:8597-8605.

Koehler, C. M. 2004. New developments in mitochondrial assembly. *Annu. Rev. Cell Dev. Biol.* 20:309-335.

Kolodziej, P. A., and R. A. Young. 1991. Epitope tagging and protein surveillance. *Methods Enzymol.* 194:508-519.

Kragler, F., A. Langeder, J. Raupachova, M. Binder, and A. Hartig. 1993. Two independent peroxisomal targeting signals in catalase A of *Saccharomyces cerevisiae*. *J. Cell Biol.* 120:665-673.

Krisans, S. K. 1996. Cell compartmentalization of cholesterol biosynthesis. *Ann. N. Y. Acad. Sci.* 804:142-164.

Krogh, A., B. Larsson, G. von Heijne, and E. L. L. Sonnhammer. 2001. Predicting transmembrane protein topology with a hidden Markov model: application to complete genomes. *J. Mol. Biol.* 305:567-580.

Krügel, H., G. Fiedler, C. Smith, and S. Baumberg. 1993. Sequence and transcriptional analysis of nourseothricin acetyltransferase-encoding gene *nat1* from *Streptomyces noursei*. *Gene.* 127:127-131.

Kunau, W. H., S. Buhne, M. de la Garza, C. Kionka, M. Mateblowski, U. Schultz-Borchard, and R. Thieringer. 1988. Comparative enzymology of β-oxidation. *Biochem. Soc. Trans.* 16:418-420.

Kyshe-Andersen, J. 1984. Electroblotting of multiple gels: a simple apparatus without buffer tank for rapid transfer of proteins from polyacrylamide to nitrocellulose. *J. Biochem. Biophys. Meth.* 10:203-209.

Laemmli, U.K. 1970. Cleavage of structural proteins during the assembly of the head of bacteriophage T4. *Nature.* 227:680-685.

Lambkin, G. R., and R. A. Rachubinski. 2001. *Yarrowia lipolytica* cells mutant for the peroxisomal peroxin Pex19p contain structures resembling wild-type peroxisomes. *Mol. Biol. Cell.* 12:3353-3364.

Lazarow, P. B., and C. de Duve. 1976. A fatty acyl-CoA oxidizing system in rat liver peroxisomes; enhancement by clofibrate, a hypolipidemic drug. *Proc. Natl. Acad. Sci. U. S. A.* 73:2043-2046.

Lazarow, P. B., and H. W. Moser. 1994. Disorders of peroxisome biogenesis. *In* The Metabolic Basis of Inherited Disease. A. L. Beaudet, W. S. Sly, and A. D. Valle, editors. *McGraw-Hill,* New York, pp. 2287-2324.

Lazarow, P. B., and Y. Fujiki. 1985. Biogenesis of peroxisomes. *Annu. Rev. Cell Biol.* 1:489-530.

Li, X., and S. J. Gould. 2002. PEX11 promotes peroxisome division independently of peroxisome metabolism. *J. Cell Biol.* 156:643-651.

Li, X., and S. J. Gould. 2003. The dynamin-like GTPase DLP1 is essential for peroxisome division and is recruited to peroxisomes in part by PEX11. *J. Biol. Chem.* 278:17012-17020.

Li, X., E. Baumgart, G. X. Dong, J. C. Morrell, G. Jimenez-Sanchez, D. Valle, K. D. Smith, and S. J. Gould. 2002. PEX11α is required for peroxisome proliferation in response to phenylbutyrate but is dispensable for peroxisome proliferator-activated receptor α-mediated peroxisome proliferation. *Mol. Cell. Biol.* 22:8226-8240.

Lisenbee, C. S., M. Heinze, and R. N. Trelease. 2003. Peroxisomal ascorbate peroxidase resides within a subdomain of rough endoplasmic reticulum in wild-type *Arabidopsis* cells. *Plant Physiol.* 132:870-882.

Lithgow, T., T. Junne, C. Wachter, and G. Schatz. 1994. Yeast mitochondria lacking the two import receptors Mas20p and Mas70p can efficiently and specifically import precursor proteins. *J. Biol. Chem.* 269:15325-15330.

Longtine, M. S., A. McKenzie, III, D. J. Demarini, N. G. Shah, A. Wach, A. Brachat, P. Philippsen, and J. R. Pringle. 1998. Additional modules for versatile and economical PCR-based gene deletion and modification in *Saccharomyces cerevisiae*. *Yeast.* 14:953-961.

Lorenz, P., A. G. Maier, E. Baumgart, R. Erdmann, and C. Clayton. 1998. Elongation and clustering of glycosomes in *Trypanosoma brucei* overexpressing the glycosomal Pex11p. *EMBO J.* 17:3542-3555.

Lyman, S. K., and R. Schekman. 1995. Interaction between BiP and Sec63p is required for the completion of protein translocation into the ER of *Saccharomyces cerevisiae*. *J. Cell Biol.* 131:1163-1171.

Maniatis, T., E. F. Fritsch, and J. Sambrook. 1982. Molecular Cloning. A Laboratory Manual. *Cold Spring Harbor Laboratory*, Cold Spring Harbor.

Marcusson, E. G., B. F. Horazdovsky, J. L. Cereghino, E. Gharakhanian, and S. D. Emr. 1994. The sorting receptor for yeast vacuolar carboxypeptidase Y is encoded by the *VPS10* gene. *Cell.* 77:579-586.

Marelli, M., J. J. Smith, S. Jung, E. Yi, A. I. Nesvizhskii, R. H. Christmas, R. A. Saleem, Y. Y. Tam, A. Fagarasanu, D. R. Goodlett, R. Aebersold, R. A. Rachubinski, and J. D. Aitchison. 2004. Quantitative mass spectrometry reveals a role for the GTPase Rho1p in actin organization on the peroxisome membrane. *J. Cell Biol.* 167:1099-1112.

Marshall, P. A., J. M. Dyer, M. E. Quick, and J. M. Goodman. 1996. Redox-sensitive homodimerization of Pex11p: a proposed mechanism to regulate peroxisomal division. *J. Cell Biol.* 135:123-137.

Marshall, P. A., Y. I. Krimkevich, R. H. Lark, J. M. Dyer, M. Veenhuis, and J. M. Goodman. 1995. Pmp27 promotes peroxisomal proliferation. *J. Cell Biol.* 129:345-355.

Marzioch, M., R. Erdmann, M. Veenhuis, and W. H. Kunau. 1994. PAS7 encodes a novel yeast member of the WD-40 protein family essential for import of 3-oxoacyl-CoA thiolase, a PTS2-containing protein, into peroxisomes. *EMBO J.* 13:4908-4918.

Matsuzono, Y., N. Kinoshita, S. Tamura, N. Shimozawa, M. Hamasaki, K. Ghaedi, R. J. A. Wanders, Y. Suzuki, N. Kondo, and Y. Fujiki. 1999. Human *PEX19*: cDNA cloning by functional complementation, mutational analysis in a patient with Zellweger syndrome and potential role in peroxisomal membrane assembly. *Proc. Natl. Acad. Sci. U. S. A.* 96:2116-2121.

McCollum, D., E. Monosov, and S. Subramani. 1993. The *pas8* mutant of *Pichia pastoris* exhibits the peroxisomal protein import deficiencies of Zellweger syndrome cells--the PAS8 protein binds to the COOH-terminal tripeptide peroxisomal targeting signal, and is a member of the TPR protein family. *J. Cell Biol.* 121:761-774.

McNew, J. A., and J. M. Goodman. 1994. An oligomeric protein is imported into peroxisomes in vivo. *J. Cell Biol.* 127:1245-1257.

Motley, A., M. J. Lumb, P. B. Oatey, P. R. Jennings, P. A. De Zoysa, R. J. Wanders, H. F. Tabak, and C. J. Danpure. 1995. Mammalian alanine/glyoxylate aminotransferase 1 is imported into peroxisomes via the PTS1 translocation pathway. Increased degeneracy and context specificity of the mammalian PTS1

motif and implications for the peroxisome-to-mitochondrion mistargeting of AGT in primary hyperoxaluria type 1. *J. Cell Biol.* 131:95-109.

Motley, A. M., E. H. Hettema, E. M. Hogenhout, P. Brites, A. L. M. A. Ten Asbroek, F. A. Wijburg, F. Baas, H. S. Heijmans, H. F. Tabak, R. J. A. Wanders, and B. Distel. 1997. Rhizomelic chondrodysplasia punctata is a peroxisomal protein targeting disease caused by a non-functional PTS2 receptor. *Nat. Genet.* 15:377-380.

Mullen, R. T., and R. N. Trelease. 2000. The sorting signals for peroxisomal membrane-bound ascorbate peroxidase are within its C-terminal tail. *J. Biol. Chem.* 275:16337-16344.

Mullen, R. T., C. S. Lisenbee, J. A. Miernyk, and R. N. Trelease. 1999. Peroxisomal membrane ascorbate peroxidase is sorted to a membranous network that resembles a subdomain of the endoplasmic reticulum. *Plant Cell.* 11:2167-2185.

Needleman, R. B., and A. Tzagoloff. 1975. Breakage of yeast: a method for processing multiple samples. *Anal. Biochem.* 64:545-549.

Novikoff, A. B., and W. Shin. 1964. The endoplasmic reticulum in the Golgi zone and its relations to microbodies, Golgi apparatus and autophagic vacuoles in rat liver cells. *J. Microsc.* 3:187-206

Nuttley, W. M., A. G. Bodnar, D. Mangroo, and R. A. Rachubinski. 1990. Isolation and characterization of membranes from oleic acid-induced peroxisomes of *Candida tropicalis*. *J. Cell Sci.* 95:463-470.

Nuttley, W. M., A. M. Brade, C. Gaillardin, G. A. Eitzen, J. R. Glover, J. D. Aitchison, and R. A. Rachubinski. 1993. Rapid identification and characterization of peroxisomal assembly mutants in *Yarrowia lipolytica*. *Yeast.* 9:507-517.

Okumoto, K., I. Abe, and Y. Fujiki. 2000. Molecular anatomy of the peroxin Pex12p: ring finger domain is essential for Pex12p function and interacts with the peroxisome-targeting signal type 1-receptor Pex5p and a ring peroxin, Pex10p. *J. Biol. Chem.* 275:25700-25710.

Opperdoes, F. R., and P. Borst. 1977. Localization of nine glycolytic enzymes in a microbody-like organelle in *Trypanosoma brucei*: the glycosome. *FEBS Lett.* 80:360-364.

Osteryoung, K. W. 2001. Organelle fission in eukaryotes. *Curr. Opin. Microbiol.* 4:639-646.

Osteryoung, K. W., and J. Nunnari. 2003. The division of endosymbiotic organelles. *Science.* 302:1698-1704.

Otera, H., K. Setoguchi, M. Hamasaki, T. Kumashiro, N. Shimizu, and Y. Fujiki. 2002. Peroxisomal targeting signal receptor Pex5p interacts with cargoes and import machinery components in a spatiotemporally differentiated manner: conserved Pex5p WXXXF/Y motifs are critical for matrix protein import. *Mol. Cell. Biol.* 22:1639-1655.

Otera, H., T. Harano, M. Honsho, K. Ghaedi, S. Mukai, A. Tanaka, A. Kawai, N. Shimizu, and Y. Fujiki. 2000. The mammalian peroxin Pex5pL, the longer isoform of the mobile peroxisome targeting signal (PTS) type 1 transporter, translocates the Pex7p.PTS2 protein complex into peroxisomes via its initial docking site, Pex14p. *J. Biol. Chem.* 275:21703-21714.

Otzen, M., U. Perband, D. Wang, R. J. S. Baerends, W. H. Kunau, M. Veenhuis, and I. J. van der Klei. 2004. *Hansenula polymorpha* Pex19p is essential for the formation of functional peroxisomal membranes. *J. Biol. Chem.* 279:19181-19190.

Passreiter, M., M. Anton, D. Lay, R. Frank, C. Harter, F. T. Wieland, K. Gorgas, and W. W. Just. 1998. Peroxisome biogenesis: involvement of ARF and coatomer. *J. Cell Biol.* 141:373-383.

Pause, B., P. Diestelkotter, H. Heid, and W. W. Just. 1997. Cytosolic factors mediate protein insertion into the peroxisomal membrane. *FEBS Lett.* 414:95-98.

Peters, C., T. L. Baars, S. Buhler, and A. Mayer. 2004. Mutual control of membrane fission and fusion proteins. *Cell.* 119:667-678.

Petriv, O. I., and R. A. Rachubinski. 2004. Lack of peroxisomal catalase causes a progeric phenotype in *Caenorhabditis elegans*. *J. Biol. Chem.* 279: 9996-20001.

Poll-Thé, B.T., F. Roels, H. Ogier, J. Scotto, J. Vamecq, R. B. Schutgens, R. J. Wanders, C. W. van Roermund, M. J. van Wijland, A. W. Schram, et al. 1988. A new peroxisomal disorder with enlarged peroxisomes and a specific deficiency of acyl-CoA oxidase (pseudo-neonatal adreno leukodystrophy). *Am.J.Hum.Genet.* 42.3: 422-34.

Preisig-Muller, R., G. Muster, and H. Kindl. 1994. Heat shock enhances the amount of prenylated Dnaj protein at membranes of glyoxysomes. *Eur. J. Biochem.* 219:57-63.

Pringle, J. R., A. E. M. Adams, D. G. Drubin, and B. K. Haarer. 1991. Immunofluorescence methods for yeasts. *Methods Enzymol.* 194:565-602.

Purdue, P. E., and P. B. Lazarow. 2001. Peroxisome biogenesis. *Annu. Rev. Cell Dev. Biol.* 17:701-752.

Purdue, P. E., J. W. Zhang, M. Skoneczny, and P. B. Lazarow. 1997. Rhizomelic chondrodysplasia punctata is caused by deficiency of human PEX7, a homologue of the yeast PTS2 receptor. *Nat. Genet.* 15:381-384.

Purdue, P. E., X. Yang, and P. B. Lazarow. 1998. Pex18p and Pex21p, a novel pair of related peroxins essential for peroxisomal targeting by the PTS2 pathway. *J. Cell Biol.* 143:1859-1869.

Rachubinski, R. A., and S. Subramani. 1995. How proteins penetrate peroxisomes. *Cell.* 83:525-528.

Rapaport, D. 2003. Finding the right organelle. Targeting signals in mitochondrial outer-membrane proteins. *EMBO Rep.* 4:948-952.

Reddy, J. K., and T. Hashimoto. 2001. Peroxisomal β-oxidation and peroxisome proliferator-activated receptor α: an adaptive metabolic system. *Annu. Rev. Nutr.* 21:193-230.

Reguenga, C., M. E. Oliveira, A. M. Gouveia, C. Sa-Miranda, and J. E. Azevedo. 2001. Characterization of the mammalian peroxisomal import machinery: Pex2p, Pex5p, Pex12p, and Pex14p are subunits of the same protein assembly. *J. Biol. Chem.* 276:29935-29942.

Rehling, P., M. Marzioch, F. Niesen, E. Wittke, M. Veenhuis, and W. H. Kunau. 1996. The import receptor for the peroxisomal targeting signal 2 (PTS2) in *Saccharomyces cerevisiae* is encoded by the PAS7 gene. *EMBO J.* 15:2901-2913.

Rhodin, J. 1954. Correlation of Ultrastructural Organization and Function in Normal and Experimentally Changed Convoluted Tubule Cells of the Mouse Kidney. *Karolinska Institute*, Ph.D. Thesis.

Robinson, C., and R. B. Klosgen. 1994. Targeting of proteins into and across the thylakoid membrane-a multitude of mechanisms. *Plant Mol. Biol.* 26:15-24.

Romisch, K., N. Collie, N. Soto, J. Logue, M. Lindsay, W. Scheper, and C. H. Cheng. 2003. Protein translocation across the endoplasmic reticulum membrane in cold-adapted organisms. *J. Cell Sci.* 116:2875-2883.

Rose, M. D., F. Winston, and P. Heiter. 1988. Laboratory Course Manual for Methods in Yeast Genetics. *Cold Spring Harbor Laboratory*, Cold Spring Harbor, NY.

Rottensteiner, H., A. Hartig, B. Hamilton, H. Ruis, R. Erdmann, and A. Gurvitz. 2003a. *Saccharomyces cerevisiae* Pip2p-Oaf1p regulates *PEX25* transcription through an adenine-less ORE. *Eur. J. Biochem.* 270:2013-2022.

Rottensteiner, H., A. Kramer, S. Lorenzen, K. Stein, C. Landgraf, R. Volkmer-Engert, and R. Erdmann. 2004. Peroxisomal membrane proteins contain common Pex19p-binding sites that are an integral part of their targeting signals. *Mol. Biol. Cell.* 15:3406-3417.

Rottensteiner, H., A. J. Kal, M. Filipits, M. Binder, B. Hamilton, H. F. Tabak, and H. Ruis. 1996. Pip2p: a transcriptional regulator of peroxisome proliferation in the yeast *Saccharomyces cerevisiae*. *EMBO J.* 15:2924-2934.

Rottensteiner, H., L. Palmieri, A. Hartig, B. Hamilton, H. Ruis, R. Erdmann, and A. Gurvitz. 2002. The peroxisomal transporter gene *ANT1* is regulated by a deviant oleate response element (ORE): characterization of the signal for fatty acid induction. *Biochem. J.* 365:109-117.

Rottensteiner, H., K. Stein, E. Sonnenhol, and R. Erdmann. 2003b. Conserved function of Pex11p and the novel Pex25p and Pex27p in peroxisome biogenesis. *Mol. Biol. Cell.* 14:4316-4328.

Rout, M. P., J. D. Aitchison, A. Suprapto, K. Hjertaas, Y. Zhao, and B. T. Chait. 2000. The yeast nuclear pore complex: composition, architecture, and transport mechanism. *J. Cell Biol.* 148:635-651.

Sabatini, D. D., G. Kreibich, T. Morimoto, and M. Adesnik. 1982. Mechanisms for the incorporation of proteins in membranes and organelles. *J. Cell Biol.* 92:1-22.

Sacksteder, K. A., and S. J. Gould. 2000. The genetics of peroxisome biogenesis. *Annu. Rev. Genet.* 34:623-652.

Sacksteder, K. A., J. M. Jones, S. T. South, X .Li, Y. Liu, and S. J. Gould. 2000. PEX19 binds multiple peroxisomal membrane proteins, is predominantly cytoplasmic, and is required for peroxisome membrane synthesis. *J. Cell Biol.* 148:931-944.

Saiki, R. K. 1990. Amplification of genomic DNA. *In* PCR Protocols: A Guide to Methods and Applications. M. A. Innis, D. H. Gelfand, J. J. Sninsky, and T. J. White, editors. *Academic Press*, San Diego, CA, pp. 13-21.

Sakai, Y., P. A. Marshall, A. Saiganji, K. Takabe, H. Saiki, N. Kato, and J. M. Goodman. 1995. The *Candida boidinii* peroxisomal membrane protein Pmp30 has a role in peroxisomal proliferation and is functionally homologous to Pmp27 from *Saccharomyces cerevisiae*. *J. Bacteriol.* 177:6773-6781.

Salomons, F. A., I. J. van der Klei, A. M. Kram, W. Harder, and M. Veenhuis. 1997. Brefeldin A interferes with peroxisomal protein sorting in the yeast *Hansenula polymorpha*. *FEBS Lett.* 411:133-139.

Sanger, F., S. Nicklen, and A. R. Coulson. 1977. DNA sequencing with chain-terminating inhibitors. *Proc. Natl. Acad. Sci. U. S. A.* 74:5463-5467.

Santos, M. J., T. Imanaka, H. Shio, G. M. Small, and P. B. Lazarow. 1988. Peroxisomal membrane ghosts in Zellweger syndrome-aberrant organelle assembly. *Science.* 239:1536-1538.

Schatz, G., and B. Dobberstein. 1996. Common principles of protein translocation across membranes. *Science.* 271:1519-1526.

Schell-Steven, A., K. Stein, M. Amoros, C. Landgraf, R. Volkmer-Engert, H. Rottensteiner, and R. Erdmann. 2005. Identification of a novel, intraperoxisomal Pex14-binding site in Pex13: association of Pex13 with the docking complex is essential for peroxisomal matrix protein import. *Mol. Cell. Biol.* 25:3007-3018.

Schliebs, W., and W. H. Kunau. 2004. Peroxisome membrane biogenesis: the stage is set. *Curr. Biol.* 14:R397-R399.

Scholz, O., A. Thiel, W. Hillen, and M. Niederweis. 2000. Quantitative analysis of gene expression with an improved green fluorescent protein. *Eur. J. Biochem.* 267:1565-1570.

Schrader, M., B. E. Reuber, J. C. Morrell, G. Jimenez-Sanchez, C. Obie, T. A. Stroh, D. Valle, T. A. Schroer, and S. J. Gould. 1998. Expression of Pex11β mediates peroxisome proliferation in the absence of extracellular stimuli. *J. Biol. Chem.* 273:29607-29614.

Schutgens, R. B., H. S. Heymans, R. J. Wanders, H. van den Bosch, and J. M. Tager. 1986. Peroxisomal disorders: a newly recognised group of genetic diseases. *Eur. J. Pediatr.* 144:430-440.

Schwarz, E., and W. Neupert. 1994. Mitochondrial protein import: mechanisms, components and energetics. *Biochim. Biophys. Acta.* 1187:270-274.

Seeley, E. S., M. Kato, N. Margolis, W. Wickner, and G. A. Eitzen. 2002. Genomic analysis of homotypic vacuole fusion. *Mol. Biol. Cell.* 13:782-794.

Shaw, J. M., and J. Nunnari. 2002. Mitochondrial dynamics and division in budding yeast. *Trends Cell Biol.* 12:178-184.

Sherman, F., and J. Hicks. 1991. Micromanipulation and dissection of asci. *Methods Enzymol.* 194:21-37.

Shibata, H., Y. Kashiwayama, T. Imanaka, and H. Kato. 2004. Domain architecture and activity of human Pex19p, a chaperone-like protein for intracellular trafficking of peroxisomal membrane proteins. *J. Biol. Chem.* 279:38486-38494.

Shimozawa, N., T. Tsukamoto, Y. Suzuki, T. Orii, and Y. Fujiki. 1992. Animal cell mutants represent two complementation groups of peroxisome-defective Zellweger syndrome. *J. Clin. Invest* 90:1864-1870.

Shimozawa, N., Y. Suzuki, Z. Zhang, A. Imamura, K. Ghaedi, Y. Fujiki, and N. Kondo. 2000. Identification of PEX3 as the gene mutated in a Zellweger syndrome patient lacking peroxisomal remnant structures. *Hum. Mol. Genet.* 9:1995-1999.

Sichting, M., A. Schell-Steven, H. Prokisch, R. Erdmann, and H. Rottensteiner. 2003. Pex7p and Pex20p of *Neurospora crassa* function together in PTS2-dependent protein import into peroxisomes. *Mol. Biol. Cell.* 14:810-821.

Sikorski, R. S., and P. Hieter. 1989. A system of shuttle vectors and yeast host strains designed for efficient manipulation of DNA in *Saccharomyces cerevisiae*. *Genetics.* 122:19-27.

Slawecki, M. L., G. Dodt, S. Steinberg, A. B. Moser, H. W. Moser, and S. J. Gould. 1995. Identification of three distinct peroxisomal protein import defects in patients with peroxisome biogenesis disorders. *J. Cell Sci.* 108:1817-1829.

Smith, J. J. 2000. Maintenance of Peroxisomes in the Yeast *Yarrowia lipolytica*. 2000. *University of Alberta,* Ph.D. Thesis.

Smith, J. J., and R. A. Rachubinski. 2001. A role for the peroxin Pex8p in Pex20p-dependent thiolase import into peroxisomes of the yeast *Yarrowia lipolytica*. *J. Biol. Chem.* 276:1618-1625.

Smith, J. J., T. W. Brown, G. A. Eitzen, and R. A. Rachubinski. 2000. Regulation of peroxisome size and number by fatty acid β-oxidation in the yeast *Yarrowia lipolytica*. *J. Biol. Chem.* 275:20168-20178.

Smith, J. J., M. Marelli, R. H. Christmas, F. J. Vizeacoumar, D. J. Dilworth, T. Ideker, T. Galitski, K. Dimitrov, R. A. Rachubinski, and J. D. Aitchison. 2002. Transcriptome profiling to identify genes involved in peroxisome assembly and function. *J. Cell Biol.* 158:259-271.

Snyder, W. B., K. N. Faber, T. J. Wenzel, A. Koller, G. H. Luers, L. Rangell, G. A. Keller, and S. Subramani. 1999. Pex19p interacts with Pex3p and Pex10p and is

essential for peroxisome biogenesis in *Pichia pastoris*. *Mol. Biol. Cell.* 10:1745-1761.

Snyder, W. B., A. Koller, A. J. Choy, and S. Subramani. 2000. The peroxin Pex19p interacts with multiple, integral membrane proteins at the peroxisomal membrane. *J. Cell Biol. 149*, 1171-1178.

South, S. T., and S. J. Gould. 1999. Peroxisome synthesis in the absence of preexisting peroxisomes. *J. Cell Biol. 144*, 255-266.

Subramani, S. 1998. Components involved in peroxisome import, biogenesis, proliferation, turnover, and movement. *Physiol. Rev.* 78:171-188.

Subramani, S. 2002. Hitchhiking fads en route to peroxisomes. *J. Cell Biol.* 156:415-417.

Subramani, S., A. Koller, and W. B. Snyder. 2000. Import of peroxisomal matrix and membrane proteins. *Annu. Rev. Biochem.* 69:399-418.

Swinkels, B. W., S. J. Gould, A. G. Bodnar, R. A. Rachubinski, and S. Subramani. 1991. A novel, cleavable peroxisomal targeting signal at the amino-terminus of the rat 3-ketoacyl-CoA thiolase. *EMBO (Eur. Mol. Biol. Organ.) J.* 10:3255-3262.

Swinkels, B. W., S. J. Gould, and S. Subramani. 1992. Targeting efficiencies of various permutations of the consensus C- terminal tripeptide peroxisomal targeting signal. *FEBS Lett.* 305:133-136.

Szilard, R. K., V. I. Titorenko, M. Veenhuis, and R. A. Rachubinski. 1995. Pay32p of the yeast *Yarrowia lipolytica* is an intraperoxisomal component of the matrix protein translocation machinery. *J Cell Biol.* 131:1453-1469.

Tam, Y. Y. C., and R. A. Rachubinski. 2002. *Yarrowia lipolytica* cells mutant for the *PEX24* gene encoding a peroxisomal membrane peroxin mislocalize peroxisomal proteins and accumulate membrane structures containing both peroxisomal matrix and membrane proteins. *Mol. Biol. Cell.* 13:2681-2691 2002.

Tam, Y. Y. C., J. C. Torres-Guzman, F. J. Vizeacoumar, J. J. Smith, M. Marelli, J. D. Aitchison, and R. A. Rachubinski. 2003. Pex11-related proteins in peroxisome

dynamics: a role for the novel peroxin Pex27p in controlling peroxisome size and number in *Saccharomyces cerevisiae*. *Mol. Biol. Cell 14*, 4089-4102.

Tan, X., H. R. Waterham, M. Veenhuis, and J. M. Cregg. 1995. The *Hansenula polymorpha PER8* gene encodes a novel peroxisomal integral membrane protein involved in proliferation. *J. Cell Biol. 128*, 307-319.

Tanaka, A., K. Okumoto, and Y. Fujiki. 2003. cDNA cloning and characterization of the third isoform of human peroxin Pex11p. *Biochem. Biophys. Res. Commun.* 300:819-823.

Tanaka, A., M. Osumi, and S. Fukui. 1982. Peroxisomes of alkane-grown yeast: fundamental and practical aspects. *Ann N Y Acad Sci*. 386:183-199.

Tang, H. Y., A. Munn, and M. Cai. 1997. EH domain proteins Pan1p and End3p are components of a complex that plays a dual role in organization of the cortical actin cytoskeleton and endocytosis in Saccharomyces cerevisiae. *Mol.Cell Biol.* 17.8 1997: 4294-304.

Terlecky, S. R., and M. Fransen. 2000. How peroxisomes arise. *Traffic*. 1:465-473.

Terlecky, S. R., W. M. Nuttley, D. McCollum, E. Sock, and S. Subramani. 1995. The *Pichia pastoris* peroxisomal protein PAS8p is the receptor for the C- terminal tripeptide peroxisomal targeting signal. *Embo J.* 14:3627-3634.

Titorenko, V. I. and R. A. Rachubinski. 2000. Peroxisomal membrane fusion requires two AAA family ATPases, Pex1p and Pex6p. *J. Cell Biol.* 150:881-886.

Titorenko, V. I. and R. A. Rachubinski. 2004. The peroxisome: orchestrating important developmental decisions from inside the cell. *J. Cell Biol.* 164:641-645.

Titorenko, V. I., and R. A. Rachubinski. 2001. The life cycle of the peroxisome. *Nat. Rev. Mol. Cell Biol.* 2:357-368.

Titorenko, V. I., D. M. Ogrydziak, and R. A. Rachubinski. 1997. Four distinct secretory pathways serve protein secretion, cell surface growth, and peroxisome biogenesis in the yeast *Yarrowia lipolytica*. *Mol. Cell Biol.* 17:5210-5226.

Titorenko, V. I., H. Chan, and R. A. Rachubinski. 2000. Fusion of small peroxisomal vesicles in vitro reconstructs an early step in the in vivo multistep peroxisome assembly pathway of *Yarrowia lipolytica*. *J. Cell Biol.* 148:29-44.

Titorenko, V. I., J. M. Nicaud, H. Wang, H. Chan, and R. A. Rachubinski. 2002. Acyl-CoA oxidase is imported as a heteropentameric, cofactor-containing complex into peroxisomes of *Yarrowia lipolytica*. *J. Cell Biol.* 156:481-494.

Titorenko,V. I. and R. A. Rachubinski. 1998a. Mutants of the yeast Yarrowia lipolytica defective in protein exit from the endoplasmic reticulum are also defective in peroxisome biogenesis. *Mol. Cell Biol. 18*, 2789-2803.

Towbin, H., T. Staehelin, and J. Gordon. 1979. Electrophoretic transfer of proteins from polyacrylamide gels to nitrocellulose sheets: procedure and some applications. *Proc. Natl. Acad. Sci. U. S. A* 76:4350-4354.

Tsukamoto, T., S. Yokota, and Y. Fujiki. 1990. Isolation and characterization of Chinese hamster ovary cell mutants defective in assembly of peroxisomes. *J. Cell Biol.* 110:651-660.

Urquhart, A. J., D. Kennedy, S. J. Gould, and D.I.Crane. 2000. Interaction of Pex5p, the type 1 peroxisome targeting signal receptor, with the peroxisomal membrane proteins Pex14p and Pex13p. *J. Biol. Chem.* 275:4127-4136.

van den Bosch, H., R. B. H. Schutgens, R. J. A. Wanders, and J. M. Tager. 1992. Biochemistry of peroxisomes. *Annu. Rev. Biochem.* 61:157-197.

van der Klei, I. J., R. E. Hilbrands, G. J. Swaving, H. R. Waterham, E. G. Vrieling, V.I. Titorenko, J. M. Cregg, W. Harder, and M. Veenhuis. 1995. The *Hansenula polymorpha* PER3 gene is essential for the import of PTS1 proteins into the peroxisomal matrix. *J Biol Chem.* 270:17229-17236.

van der Leij, I., M. M. Franse, Y. Elgersma, B. Distel, and H. F. Tabak. 1993. PAS10 is a tetratricopeptide-repeat protein that is essential for the import of most matrix proteins into peroxisomes of *Saccharomyces cerevisiae*. *Proc Natl Acad Sci USA.* 90:11782-11786.

van Roermund, C. W. T., H. F. Tabak, M. van den Berg, R. J. A. Wanders, and E. H. Hettema. 2000. Pex11p plays a primary role in medium-chain fatty acid oxidation,

a process that affects peroxisome number and size in *Saccharomyces cerevisiae*. *J. Cell Biol.* 150:489-497.

Veenhuis, M. and d. K. van, I. 2002. Peroxisomes: surprisingly versatile organelles. *Biochim. Biophys. Acta* 1555:44-47.

Veenhuis, M. and der Klei van, I. 2002. Peroxisomes: surprisingly versatile organelles. Biochim.Biophys.Acta 1555.1-3 2002: 44-47.

Veenhuis, M. and W. Harder. 1987. Metabolic significance and biogenesis of microbodies in yeasts. *In* Peroxisomes in Biology and Medicine. H. D. Fahimi and H. Sies, editors. *Springer-Verlag, Berlin*. 436-458.

Veenhuis, M., A. Douma, W. Harder, and M. Osumi. 1983. Degradation and turnover of peroxisomes in the yeast *Hansenula polymorpha* induced by selective inactivation of peroxisomal enzymes. *Arch Microbiol.* 134:193-203.

Veenhuis, M., and J. M. Goodman. 1990. Peroxisomal assembly: membrane proliferation precedes the induction of the abundant matrix proteins in the methylotrophic yeast Candida boidinii. *J Cell Sci.* 96:583-590.

Vida, T. A. and S. D. Emr. 1995. A new vital stain for visualizing vacuolar membrane dynamics and endocytosis in yeast. J.Cell Biol. 128.5 1995: 779-92.

Vizeacoumar, F. J., J. C. Torres-Guzman, Y. Y. C. Tam, J. D. Aitchison, and R. A. Rachubinski. 2003. *YHR150w* and *YDR479c* encode peroxisomal integral membrane proteins involved in the regulation of peroxisome number, size, and distribution in *Saccharomyces cerevisiae*. *J. Cell Biol. 161,* 321-332.

Vizeacoumar, F. J., J. C. Torres-Guzman, D. Bouard, J. D. Aitchison, and R. A. Rachubinski. 2004. Pex30p, Pex31p, and Pex32p form a family of peroxisomal integral membrane proteins regulating peroxisome size and number 7in Saccharomyces cerevisiae. *Mol. Biol. Cell 15*, 665-677.

Voorn-Brouwer, T., A. Kragt, H. F. Tabak, and B. Distel. 2001. Peroxisomal membrane proteins are properly targeted to peroxisomes in the absence of. *J. Cell Sci.* 114:2199-2204.

Walton, P. A., M. Wendland, S. Subramani, R. A. Rachubinski, and W. J. Welch. 1994. Involvement of 70-kD heat-shock proteins in peroxisomal import. *J. Cell Biol.* 125:1037-1046.

Walton, P. A., P. E. Hill, and S. Subramani. 1995. Import of stably folded proteins into peroxisomes. *Mol. Biol. Cell.* 6:675-683.

Walton, P. A., S. J. Gould, J. R. Feramisco, and S. Subramani. 1992. Transport of microinjected proteins into peroxisomes of mammalian cells: inability of Zellweger cell lines to import proteins with the SKL tripeptide peroxisomal targeting signal. *Mol. Cell. Biol.* 12:531-541.

Wang, X., Unruh, M. J., and Goodman, J. M. 2001. Discrete targeting signals direct Pmp47 to oleate-induced peroxisomes in *Saccharomyces cerevisiae*. *J. Biol. Chem. 276,* 10897-10905.

Wang, X., M. A. McMahon, S. N. Shelton, M. Nampaisansuk, J. L. Ballard, and J. M. Goodman. 2004. Multiple targeting modules on peroxisomal proteins are not redundant: discrete functions of targeting signals within Pmp47 and Pex8p. *Mol. Biol. Cell* 15, 1702-1710.

Ward, W. W. 1998. Green Fluorescent Protein: Properties, Applications, and Protocols. *Wiley, New York*. 45-75 pp.

Warren, D. T., P. D. Andrews, C. W. Gourlay, K. R. Ayscough. 2002. Sla1p couples the yeast endocytic machinery to proteins regulating actin dynamics. *J.Cell Sci.* 115.Pt 8 1703-15.

Waterham, H. R., V. I. Titorenko, P. Haima, J. M. Cregg, W. Harder, and M. Veenhuis. 1994. The *Hansenula polymorpha PER1* gene is essential for peroxisome biogenesis and encodes a peroxisomal matrix protein with both carboxy- and amino-terminal targeting signals. *J. Cell Biol.* 127:737-749

Weibel, E. R., and P. Bolender. 1973. Stereological techniques for electron microscopic morphometry. *In* Principles and Techniques of Electron Microscopy. Vol. 3. M. A. Hayat, editor. *Van Nostrand Reinhold*, New York. 237-296.

Will, G. K., M. Soukupova, X. Hong, K. S. Erdmann, J. A. Kiel, G. Dodt, W. H. Kunau, and R. Erdmann. 1999. Identification and characterization of the human orthologue of yeast Pex14p. *Mol Cell Biol.* 19:2265-2277.

Yu, X. and M. Cai. The yeast dynamin-related GTPase Vps1p functions in the organization of the actin cytoskeleton via interaction with Sla1p. *J.Cell Sci.* 117.Pt 17 2004: 3839-53.

Zomer, A. W., B. B. van Der, G. A. Jansen, R. J. Wanders, Poll-The BT, and P. T. van Der Saag. 2000. Pristanic acid and phytanic acid: naturally occurring ligands for the nuclear receptor peroxisome proliferator-activated receptor alpha. *J. Lipid Res.* 41:1801-1810.